Investigation of ACE overexpression in Myeloid Cell Lines through Whole-Proteome Analysis

by

DELIA OOSTHUIZEN

OSTDEL002

Submitted to the University of Cape Town

In fulfilment of the requirements for the degree

MSc (Med) in Chemical Biology

Faculty of Health Sciences

University of Cape Town

April 2023

Supervisor: Professor Edward Sturrock, **Co-Supervisor:** Dr Tariq Ganief

Integrative Biomedical Sciences, University of Cape Town

DECLARATION

I, ……**Delia Oosthuizen**……, hereby declare that the work on which this dissertation/thesis is based is my original work (except where acknowledgements indicate otherwise) and that neither the whole work nor any part of it has been, is being, or is to be submitted for another degree in this or any other university.

I empower the university to reproduce for the purpose of research either the whole or any portion of the contents in any manner whatsoever.

Signature: … Signed by candidate

Date: ……21 April 2023

Abstract

Angiotensin converting enzyme (ACE) plays an important role in blood pressure regulation and is a key component of the renin-angiotensin aldosterone system (RAAS). A dipeptidyl carboxypeptidase, ACE also hydrolyses many different substrates across its N- and C-domain. This substrate variability has uncovered novel ACE function in other biological systems and disease. In the immune system, ACE and angiotensin II influence inflammation and wound repair. Independently of angiotensin II, ACE overexpression in murine macrophages (ACE 10/10) and neutrophils (NeuACE) has shown remarkable enhanced immune phenotypes with the ability to improve murine survival against B16 melanoma, methicillin-resistant *Staphylococcus aureus* (MRSA) and *Listeria monocytogenes*. Current literature points to the C-domain as the main proponent. The myeloid cells have enhanced reactive oxygen species (ROS) generation, pro-inflammatory cytokine production and phagocytosis with increased ATP and TCA cycle intermediate production. ACE overexpressing macrophages also improve cognitive ability in murine Alzheimer's models by amyloid-β (1-42) protein cleavage and degradation. Despite lengthy characterization of ACE overexpression and the enhanced immune phenotype of ACE 10/10 macrophages and NeuACE neutrophils, the mechanism, and substrate(s) by which it occurs is unknown. Understanding the biological processes influenced by ACE overexpression may provide alternative therapies where standard medicine is no longer effective including resistant bacterial infections and tumours. Importantly, ACE inhibition in human and murine neutrophils, and ACE 10/10 macrophages has shown reduced extracellular and intracellular microbicidal function. This and the immune benefit associated with ACE overexpression has prompted interest in the mechanism responsible. This project aimed to identify differentially expressed and significantly dysregulated biological pathways and proteins in ACE overexpressing murine (ACE 10/10 PTM) and human macrophages (ACE +/+ THP-1) whilst also analysing global proteomic changes with respects to ACE inhibition using discovery mass spectrometry (MS).

ACE overexpressing murine and human macrophage whole cell protein lysates underwent label-free discovery MS to identify proteomic shifts in comparison to control macrophages. Using data-independent methodology, 270 and 442 differentially expressed proteins were identified in murine and human ACE overexpressing macrophages, respectively. Functional

enrichment for several immune processes including phagocytosis, ROS generation, and antigen processing and presentation were identified whilst metabolic enrichment for TCA, fatty acid oxidation, electron transport chain (ETC) and glucose was present in murine ACE 10/10 macrophages. Human ACE +/+ THP-1 macrophages saw similar ETC, ATP synthase and glucose protein up-regulation and cytokine signalling, antigen processing and presentation functional enrichment. Unique to ACE +/+ human macrophages was neutrophil degranulation whereupon ACE C-domain inhibition by Lis-Trp dysregulated these proteins. Both murine and human ACE overexpression identified KEGG peroxisome proliferator-activated receptor (PPAR) signalling as significantly enriched, providing a possible target pathway for future mechanistic validation studies. ACE C-domain inhibition following Lis-Trp treatment led to a general down-regulation of the functionally enriched ETC, TCA and ATP synthase components identified as up-regulated in the literature and our own murine MS results. Murine phosphoproteomic analysis identified ERK2/MAPK1 and PKA kinase-substrate enrichment with ACE overexpression.

Using the human cell line, THP-1, Lis-Trp uptake was quantified through MS and ACE enzymatic activity assays over two hours. Minimal internalization took place for both 10 µM and 100 µM with < 1% intracellular Lis-Trp detected. However, partial ACE inhibition was achieved for both treatments despite low intracellular concentrations. To study the impact of this partial inhibition, the role of ACE in phagocytosis was explored. Using elastomeric micropattern contraction as a proxy for phagocytic uptake, ACE C- and N-domain inhibition both led to significant reduction in micropattern contraction in comparison to uninhibited control THP-1 macrophages. ACE +/+ THP-1 macrophages showed enhanced phagocytosis as observed in murine ACE 10/10 macrophage literature by means of increased micropattern contraction. Following ACE domain inhibition by 10 µM Lis-Trp (C-domain) and 10 µM RXP407 (N-domain) a statistically significant decrease in contraction measurements was observed, implying that both the N- and C-domain of ACE play a role in phagocytosis. Partial ACE inhibition may therefore be sufficient in reducing macrophage microbicidal function as observed in NeuACE and human neutrophils, increasing the potential risk of dangerous infection in immunocompromised patients.

This work demonstrated an altered proteomic profile in ACE overexpressing murine and human macrophages, and confirmed findings on ACE 10/10 murine macrophages, whilst

providing a novel and deeper understanding of ACE +/+ human macrophages. Furthermore, ACE C-domain inhibition likely negatively impacts macrophage function including phagocytosis whilst increasing neutrophil degranulation, but further biochemical characterization is required. Importantly, novel lipid metabolism and PPAR signalling were functionally enriched in both species, providing an exciting path for future studies in ACE overexpression and enhanced immunity.

Acknowledgements

Completing this degree has been a momentous task and at times I was close to giving up. I must thank so many for their support and guidance throughout the entire process.

To the ACE lab: Lizelle, Vinasha, Siya, Liam, Anna, Sasha, Sedzani; I want to thank you all for the laughs, chats, your encouragement, and ideas when I was in dire need of it. To Sylva, thank you for your willingness to help, always. I appreciate you all so much and it was wonderful to work with all of you. To Anca, I want to give a special thank you as you have been my greatest supporter and a wonderful colleague and friend in the process. It was an absolute pleasure to have worked with you. Thank you for being such a great 'hype man' for me. To our collaborator, Dr Kenneth Bernstein thank you for the opportunity to work with and participate in your work.

To my supervisor Ed, thank you for the opportunity to join your lab. I have learnt and grown so much, and it is all thanks to you believing in my abilities. Thank you for your keen reading and editing of my thesis and your ear whenever I had ideas and questions. Thanks to my co-supervisor, Tariq and members of the Blackburn lab for their keen minds, edits and recommendations in all things mass spectrometry.

To my parents, Vaughan, and Helena, thank you for mopping up the tears and giving me hope for the future. Thank you for your endless dedication to fulfil my dreams, your endless love and support. I love you both and I can never thank you enough. To my best friends, the three musketeers we were, Michaela and Chanté. You two were my rocks in so many ways and I treasure the phone calls and group conversations we've had. I love you both so very much like the sisters I never had. Thank you for your support and hype all the way to the end! To Arad, the friend I wished I had since day one I have to dedicate some thanks to you, for our coffee chats and adventures on campus. I'm so glad to have met you and to have had you as a supporter on this journey! To Keegan, a dear friend, thank you for your understanding and your invites for cake and sweet treats or games whenever I needed a break.

Most importantly, I thank my partner and soon-to-be husband, Byron. Thank you for being there, always. For supporting me and loving me so much that I always felt like I had an army

behind me on the worst of days. I cannot put into words how much your patience and love have meant to me all these years. You are my greatest ally and confidante.

And lastly, I want to dedicate this work to my grandparents Andries-Pieter, Vivian, Virginia, and Helena. Although all but one of you are no longer with me, you were always supportive of my dreams wherever I went and made me into the person I am today. I hope I have made you proud.

List Of Abbreviations & Acronyms

ABC: Ammonium Bicarbonate

ACE: Angiotensin Converting Enzyme

ACE2: Angiotensin Converting Enzyme 2

ACEi: ACE Inhibitor

ACN: Acetonitrile

AD: Alzheimer's Disease

AGC: Automatic Gain Control

AGT: Angiotensinogen

ALDH2: Aldehyde Dehydrogenase 2

Ang II: Angiotensin II

APCs: Antigen Presenting Cells

aPKC: Atypical PKC

APOE: Apolipoprotein E

ARB: Angiotensin Receptor Blocker

AT1R: AT_1 Receptor

AT2R: AT_2 Receptor

ATR4: AT_4 Receptor

BH_4: Tetrahydrobiopterin

BiNGO: Biological Networks Gene Ontology Tool

BK: Bradykinin

BLQ: Below Limit Of Quantitation

BMDMs: Bone Marrow-Derived Macrophages

BSA: Bovine Serum Albumin

CAR: Chimeric Antigen Receptor

CBP1: Cellular Retinol-Binding Protein 1

CD: Cluster Of Differentiation

cGMP: Cyclic GMP

CM: Cell Membrane

COX-1: Cyclooxygenase 1

COX-2: Cyclooxygenase 2

CT: C-Terminus

CTGF: Connective Tissue Growth Factor

DC: Dendritic Cell

DDA: Data-Dependent Acquisition

DE: Differentially Expressed

DIA: Data-Independent Acquisition

DIA-NN: Data Independent Acquisition Neural Network

DLST: Dihydrolipoyllysine-Residue Succinyltransferase

DPI: Diphenyleneiodonium

DTT: Dithiothreitol

EDTA: Ethylenediaminetetraacetic Acid

EEA1: Early Endosome Antigen 1

ELISA: Enzyme-linked immunosorbent assay

eNOS: Endothelial Nitric Oxide Synthase

ER: Endoplasimic Reticulum

ESI: Electrospray Ionisation (ESI)

ETC: Electron Transport Chain

FA: Formic Acid

FDR: False Discovery Rate

GO: Gene Ontology

GSH: Glutathione

GSOT1: Glutathione-Dependent Dehydroascorbate Reductase

GWAS: Genome-Wide Association Study

HEPES: 4-(2-Hydroxyethyl)-1-Piperazineethanesulfonic Acid

HL: His-Leu

hMDMs: Human Monocyte-Derived Macrophages

HPLC: High-Performance Liquid Chromatography

IAA: Iodoacetamide

ICAM-1: Intercellular Cell Adhesion Modecule 1

IFN: Interferon

IL: Interleukin

IMAC: Immobilised Metal Affinity Chromatography

Inpp5d/SHIP: Phosphatidylinositol 3,4,5-Trisphosphate 5-Phosphatase 1

IRAP: Insulin-Regulated Aminopeptidase

K: Lysine

KEGG: Kyoto Encyclopaedia Of Genes And Genomes

KKS: Kallikrein-Kinin System

LC: Liquid Chromatography

Lis-Trp: Lisinopril-Tryptophan

LPS: Lipopolysaccharide

LR: Linker Sequence

LTB_4: Leukotriene B4

m/z: Mass-To-Charge Ratios

mAbs: Monoclonal Antibodies

MAPK: Mitogen-Activated Protein Kinase

Mas: Mas Receptor

MCP-1: Monocytic Chemotactic Protein 1

Mdh2: Mitochondrial Malate Dehydrogenase

MDSC: Myeloid Suppressor Cell

Me: Malic Acid Enzyme

MeOH: Methanol

MHC: Major Histocompatibility Complex

MIP-2: Macrophage Inflammatory Protein 2

MMP: Matrix Metalloproteinase

MOAC: Metal Oxide Affinity Chromatography

MPO: Myeloperoxidase

MR: Mineralocorticoid Receptor

MRM: Multiple Reaction Monitoring

MRSA: Methicillin-Resistant *Staphylococcus Aureus*

MS: Mass Spectrometry

mU: Milliunits

NEP: Neprilysin

NET: Neutrophil Extracellular Trap

NGAL: Neutrophil-Gelatinase-Associated Lipocalin

NO: Nitric Oxide

NT: N-Terminus

OVA: Ovalbumin

oxLDL: Oxidized Low Density Lipoprotein

PAMPs: Pathogen-Associated Molecular Patterns

PEPT: Peptide Carrier-Mediated Transporters

PGM2: Glucose Phosphomutase 2

PI3K: Phosphatidylinositol 3-kinase

Pkn1: Protein Kinase N1

PMA: Phorbol 12-Myristate 12 Acetate

PMNs: Polymorphonuclear Neutrophils

PPAR: Peroxisome Proliferator-Activated Receptor

PRDX6: Acidic Calcium-Independent Phospholipase A2

PRR: (Pro)Renin Receptor

PSP: Phosphositeplus

PWAS: Proteome-Wide Association Study

QE: QExactive^{tm} Orbitrap Mass Spectrometer

R: Arginine

RA: Rheumatoid Arthritis

RAAS: Renin-Angiotensin-Aldosterone System

ROS: Reactive Oxygen Species

RT: Room Temperature

S: Serine

sACE: Somatic ACE

SBI: Systems Biosciences

SD: Standard Deviation

SNV: Single Nucleotide Variation

SPD: Sample Per Day

STRING: Search Tool For The Retrieval Of Interacting Genes/Proteins

SWATH: Sequential Window Acquisition Of All Theoretical Fragment Ion Spectra

T: Threonine

tACE: Testicular ACE

TALDO1: Transaldolase 1

TCA: Tricarboxylic Acid

TFA: Trifluoroacetic Acid

TGF: Transforming Growth Factor

Tg-KO: Transgenic Knockout

Th: T Helper Cell

TIMP: Tissue Inhibitors Of Metalloproteinase

TKT: Transketolase

TM: Transmembrane Domain

TNF: Tumour Necrosis Factor

TOF: Time-Of-Flight

TPM: Tumour-Bearing Peritoneal Macrophages

TPSA: Total Polar Surface Area

T_{regs}: T Suppressor Cells

TTOF: Triple-TOF

VCAM-1: Vascular Cell Adhesion Molecule 1

VEGF: Vascular Endothelial Growth Factor

VSMC: Vascular Smooth Muscle Cells

WT: Wild Type

Y: Tyrosine

ZFHL: Z-Phenylalanine-L-Histidyl-L-Leucine

Table of Contents

List of Figures xv

List of Tables xix

1. Literature Review 1

1.1. Introduction 1

1.1.1. An Overview of the Renin-Angiotensin -Aldosterone System (RAAS) 1

1.1.2. ACE Structure, Specificity & Expression 5

1.1.3. Substrate Specificity & Binding 7

1.1.4. ACE Substrate Specificity 8

1.1.5. ACE Localisation & Expression 9

1.2. ACE in Immunity 9

1.2.1. Ang II-dependent Immune Effects 10

1.2.2. Ang II-independent Immune Effects 17

1.3. ACE Overexpression Conveys Enhanced Immunity 20

1.3.1. Phenotypes of ACE Overexpression 21

1.3.2. Mechanistic Pathways in ACE Overexpression 24

1.4. Implications of RAAS & ACE Manipulation in Humans 27

1.5. Aims & Objectives 27

1.5.1. Objectives 28

2. The Effect of ACE Overexpression & Inhibition in the Murine Macrophage Proteome ..29

2.1. Introduction 29

2.1.1. An Introduction to Mass Spectrometry 29

2.1.2. Triple-TOF-Based SWATH Proteomics 30

2.1.3. Phosphoproteomics 32

2.1.4. The Basal Proteome & Cell Signalling in ACE 10/10 Murine Macrophages 33

2.2. Methodology 34
2.2.1. Cell Culture & Treatment 36
2.2.2. Mass Spectrometry Sample Preparation 37
2.2.3. Mass Spectrometry 40
2.2.4. Data Processing & Analysis 41
2.3. Results 42
2.3.1. Identified Proteins & Phosphoproteins 42
2.3.2. Mouse Proteome & Phosphoproteome Quality Checks & Quantification 43
2.3.3. The Effect of ACE Overexpression on the Murine Macrophage Proteome 44
2.3.4. The Effect of ACE Overexpression & Inhibition on the Murine Macrophage Phosphoproteome 45
2.3.5. Network Signalling in the ACE 10/10 Macrophage Proteome 47
2.3.6. Network & Functional Enrichment of ACE C-domain inhibition on ACE 10/10 Macrophages 51
2.3.7. Network & Functional Enrichment Analysis of Lis-Trp-treated WT Murine Macrophages 53
2.4. Discussion 55
3. Lisinopril-Tryptophan Uptake in Human THP-1 Monocyte/Macrophage-like Cells 62
3.1. Introduction 62
3.1.1. Lisinopril versus Lisinopril-Tryptophan (Lis-Trp) 63
3.1.2. Inhibitor Uptake in Immune Cells 64
3.1.3. Aims & Objectives 64
3.2. Methodology 65
3.2.1. Cell Culture Conditions 65
3.2.2. Lisinopril-Tryptophan Treatment 66
3.2.3. Mass Spectrometric Analysis of Intracellular Lisinopril-Tryptophan 67

3.2.4. ACE Activity 68
3.2.5. Statistical Analysis 69
3.3. Results 69
3.3.1. Intracellular Lis-Trp Quantification 69
3.3.2. ACE Activity Measurement 71
3.4. Discussion 73
4. The Effects of ACE Overexpression & Inhibition in Human THP-1 Macrophages 76
4.1. Introduction 76
4.1.1. Investigating the Human ACE Overexpressing Macrophage Proteome 76
4.2. Methodology 77
4.2.1. Cell Culture & Treatment 77
4.2.2. Sample Preparation 78
4.2.3. Mass Spectrometry 78
4.2.4. Data Analysis 78
4.3. Results 79
4.3.1. Peptide & Protein Identifications 79
4.3.2. Quality assessments 79
4.3.3. Differential Analysis 80
4.3.4. Network & Functional Analysis of Human THP-1 Macrophages 82
4.4. Discussion 95
5. The Role of ACE in Phagocytosis in Human THP-1 Monocyte/Macrophages 102
5.1. Introduction 102
5.1.1. An Overview of Phagocytosis 102
5.1.2. Aim & Objectives 106
5.2. Methodology 107
5.2.1. ACE +/+ & WT THP-1 Cell Culture 109

5.2.2. Elastomeric Micropatterns for Measuring Single Cell Mechanical Force 109
5.2.3. Statistical Analysis 112
5.3. Results 112
5.3.1. WT THP-1 ACE Inhibition & Phagocytic Measurement 112
5.3.2. ACE Overexpression & Inhibition Alters THP-1 Macrophage Phagocytic Contraction 115
5.4. Discussion 116
6. Conclusions, Limitations & Future Directions 121
6.1. Conclusions 121
6.2. Limitations 124
6.3. Future Directions 125
7. References 127
8. Appendix 170
8.1. Bio-Rad Bradford Rapid Quantification Standard Curve 170
8.2. Mouse Proteomic & Phosphoproteomic Analysis 171
8.3. HL Standard Curve – ACE Activity Assay 173
8.4. Triple-TOF SWATH-MS of Human ACE Overexpressing & WT THP-1 Macrophages 174
8.4.1. Hierarchical Clustering Output 174
8.4.2. ACE Overexpression Confirmation 175

List of Figures

Figure 1.1: An overview of the RAAS pathway showing the classical products and newly identified secondary products from ACE2 cleavage along with their known receptors. 3

Figure 1.2: Schematic of the domain structure of both ACE isoforms, somatic and testicular.7

Figure 1.3: Overview of Ang II-induced inflammatory actions. 10

Figure 1.4: Ang II-induced vascular inflammation and crosstalk mediation under the control of transcription factors, NF-κB and Est-1. 13

Figure 1.5: The roles of Ang II in innate and adaptive immunity.....16

Figure 1.6: Additional ACE-mediated cleavage increases the MHC Class I and II peptide repertoire. 18

Figure 1.7: ACE overexpression enhances key immune and metabolic pathways in murine overexpression models. 22

Figure 2.1: Principle of TOF. 31

Figure 2.2: SWATH-MS isolation window scan scheme and eluted precursor detection. 32

Figure 2.3: Phosphorylation and dephosphorylation of proteins. 33

Figure 2.4: Mass spectrometry sample preparation.. 35

Figure 2.5: Data were processed in Perseus to remove false hits and contaminants. 43

Figure 2.6: Pearson correlations between ACE 10/10 and WT TPM replicate samples. 44

Figure 2.7: Volcano plots comparing differentially expressed (DE) proteins of murine macrophages. 45

Figure 2.8: Volcano plots comparing differentially expressed (DE) phosphoproteins/phospho-sites (p-sites) of murine macrophages. 47

Figure 2.9: STRING interaction network between differentially expressed proteins of ACE 10/10 and WT macrophage controls.. 48

Figure 2.10: Enlarged protein clusters present in ACE 10/10 macrophages. 49

Figure 2.11: Biological process GO term enrichment analysis of ACE 10/10 macrophages. ..50

Figure 2.12: Network generated from ACE 10/10 and ACE 10/10 Lis-Trp treatment comparison. 51

Figure 2.13: Enlarged functional clusters in Lis-Trp-treated ACE 10/10 macrophages. 52

Figure 2.14: ACE C-domain inhibition by Lis-Trp impacts several ACE 10/10 macrophage biological processes. 53

Figure 2.15: Network analysis of dysregulated proteins between Lis-Trp WT TPMs and control WT TPMs.....54

Figure 2.16: Functionally enriched GO biological processes in WT macrophages with ACE C-domain inhibition. 55

Figure 3.1: Structural schematic of lisinopril and lisinopril-tryptophan. 63

Figure 3.2: A schematic showing the experimental design for determining the uptake of the Lis-Trp by THP-1 macrophages using LC-MS. 68

Figure 3.3: A representative chromatogram for Lis-Trp (analyte) and Verapamil (internal standard). 70

Figure 3.4: Intracellular uptake of Lis-Trp by THP-1 macrophages as measured by LC-MS/MS. 71

Figure 3.5: ACE activity in differentiated THP-1 macrophages and THP-1 monocytes. 72

Figure 3.6: Total THP-1 macrophage ACE activity after Lis-Trp treatments decreases within 1-hour post-treatment. 73

Figure 4.1: Pearson correlation co-efficients of the human ACE +/+ and WT THP-1 macrophage proteomes.....80

Figure 4.2: Volcano plots showing between-group comparisons in human THP-1 macrophages.....81

Figure 4.3: Human ACE +/+ THP-1 macrophage STRING network with dysregulated proteins in relation to WT THP-1 macrophages. 83

Figure 4.4: Enlarged frame of ACE +/+ THP-1 macrophage network with ATP synthase and ETC components. 84

Figure 4.5: Significantly enriched GO biological processes in ACE +/+ THP-1 macrophages. .85

Figure 4.6: Enriched Reactome and KEGG Ontology pathways in ACE +/+ THP-1 macrophages in comparison to WT THP-1 macrophages. 86

Figure 4.7: Network of dysregulated proteins in Lis-Trp ACE +/+ THP-1 macrophages in relation to ACE +/+ THP-1 macrophages. 87

Figure 4.8: Functionally enriched biological processes in ACE +/+ THP-1 macrophages treated with Lis-Trp.....88

Figure 4.9: KEGG and Reactome-enriched terms in ACE +/+ THP-1 macrophages after Lis-Trp treatment. 89

Figure 4.10: Lis-Trp-treated human WT THP-1 macrophage network in relation to WT THP-1 macrophages.....91

Figure 4.11: Enlarged network frame focusing on down-regulated ATP synthase components in WT THP-1 macrophages after Lis-Trp treatment. 92

Figure 4.12: Functionally enriched biological processes in WT THP-1 macrophages treated with Lis-Trp.....93

Figure 4.13: Enriched pathways in Reactome and KEGG databases for Lis-Trp-treated WT THP-1 macrophages. 94

Figure 5.1: The early and late stages of phagocytosis in professional phagocytic cells. A summary of the phagocytic process sampling receptor-mediated endocytosis.....104

Figure 5.2: Experimental design using elastomeric micropatterns to assess the role of ACE in phagocytosis and the impact of ACE inhibition on WT and ACE +/+ THP-1 macrophages. ..108

Figure 5.3: FLECS combination technology schematic. 110

Figure 5.4: Mechanical force, including phagocytosis was measured on single cells that were adhered to elastomeric micropatterns. 113

Figure 5.5: WT THP-1 macrophages exhibit cellular contraction on micropatterns both with and without ACE inhibition. 114

Figure 5.6: The impact of ACE overexpression & inhibition on THP-1 macrophage phagocytosis. 115

Figure 5.7: ACE overexpression aids phagocytic contraction whilst ACE inhibition negatively affects contraction in THP-1 macrophages. 116

Figure 8.1: BSA Standard Curve 170

Figure 8.2: Hierarchical clustering analysis of TTOF proteome and QE phosphoproteome. 171

Figure 8.3: HL Standard Curve used to calculate ACE activity. 173

Figure 8.4: Hierarchical Euclidean clustering of human macrophage proteomic samples. ..174

Figure 8.5: ACE overexpression in ACE +/+ THP-1 macrophages after PMA treatment and before cell lysate harvest. 175

Figure 8.6: ACE activity results of monocytic state ACE +/+ THP-1 macrophages. 176

List of Tables

Table 2.1: Experimental groups of mouse macrophage lysate samples 36

Table 3.1: Recorded inhibitory constants (Ki) of lisinopril and lisinopril-tryptophan using testis ACE (C-domain) and N-domain mutants. 64

Table 4.1: Experimental groups of human THP-1 cell lysate samples 78

Table 5.1: Stellar Vision fluorescent channels. 112

Table 8.1: Identified PhosphoSitePlus (PSP) phosphorylation sites and their corresponding kinases within the differentially expressed phosphoproteins of ACE 10/10 and WT TPM lysates. 172

1. Literature Review

1.1. Introduction

The pressing need for the development of effective treatments against antibiotic resistant infections, aggressive cancers and increasing cases of neurodegenerative diseases including Alzheimer's has led to the re-investigation of physiological systems. Most human biological systems have been described in depth, however new research avenues, including those concerning promiscuous enzymes, are constantly discovered in these systems. It is these creative directions that may lead medical science to new solutions to modern medical problems.

Since its discovery in 1954 by Skeggs *et al*., diverse biological roles of angiotensin converting enzyme (ACE) have continued to emerge [1]. Interestingly, ACE was discovered a second time in 1966 with bradykinin-degrading enzymatic activity, leading to further understanding of its function, discussed in Sections 1.1.1 and 1.2.

Originally, ACE was seen as an important component of the renin-angiotensin-aldosterone system (RAAS) [2]. However, it also plays an important role in several different physiological systems [3–6]. Of growing interest is the use of ACE manipulation and its overexpression in enhancing the immune response against common diseases such as cancer, resistant bacterial infections, and Alzheimer's disease (AD) [5].

1.1.1. An Overview of the Renin-Angiotensin-Aldosterone System (RAAS)

To begin with, the RAAS is an important regulator of blood pressure and fluid electrolyte homeostasis [7]. Activation of the RAAS potentially results in hypertension, renal and heart failure. The classical circulating system has endocrine function in addition to the local RAAS which has autocrine (cellular) and paracrine (tissue) functions depending on the physiological role in action [7,8]. This cardiac regulatory system exists in several tissues, with key effector molecules and components produced in the kidneys and liver. An important local tissue system is the intrarenal RAAS which functions independently of the systemic RAAS [7].

Classically, the RAAS pathway begins with the enzymatic activity of renin cleaving its substrate angiotensinogen (AGT), produced in the liver, into angiotensin I (Ang I) **(Figure 1.1)**. Renin is released from the renal juxtaglomerular cells as stimulated via hypotension and diminished sodium delivery [2,9]. Following this rate-limiting step, ACE removes the carboxy-terminal dipeptide from Ang I, generating angiotensin II (Ang II) [2,10]. Up-regulated Ang II binding through the AT_1 receptor (AT1R) sees increased collecting duct renin expression, secretion, and formation into the distal nephron [7]. Ang II acts as a strong effector molecule in the local RAAS, altering the action of circulating RAAS molecules, including inhibition of renin secretion to limit system activity or long-term activation by upregulating renin, prorenin, AGT and ACE [7]. Regarding the cardiovascular system, Ang II stimulates aldosterone production, favouring vasoconstriction.

Additionally, Ang II functions independently by stimulating vasoconstriction of blood vessels and salt retention in the kidneys. However, Ang II can also stimulate vasodilation through binding the AT_2 receptor (AT2R) over AT1R [2,11–13]. Aside from its main purpose in the cardiovascular system, Ang II has several effects on other physiological processes through binding the AT_1 receptor [5,14,15]. Other products of ACE cleavage in the RAAS include Ang (1-7) and Ang (1-5) **(Figure 1.1)** [10,16].

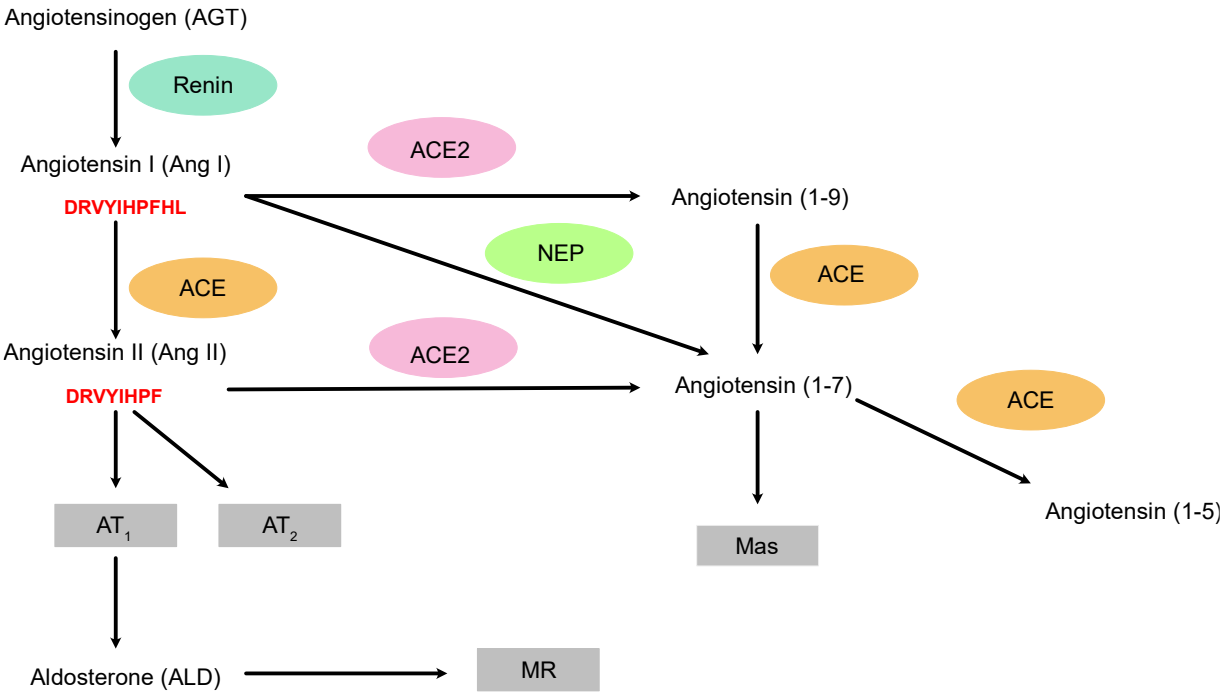

Figure 1.1: An overview of the RAAS pathway showing the classical products and newly identified secondary products from ACE2 cleavage along with their known receptors. Sequences for Ang I and Ang II are included as the best described substrate-product pair of ACE cleavage. Coloured ovals represent enzymes: renin (cyan), ACE (orange), ACE2 (pink) or NEP (green). Grey rectangles represent receptors. Abbreviations: ACE – angiotensin converting enzyme, ACE2 – angiotensin converting enzyme 2, MR- mineralocorticoid receptor, Mas- Mas receptor and NEP- neprilysin (Adapted from: Bader *et al.*, Fournier *et al.* [2,10]).

In addition to the tissue RAAS, a subcellular RAAS within the mitochondria and nucleus of many different cells exists. Within the nuclear compartment, three receptors may bind Ang II: AT_1, AT_2 and *Mas* receptors [7]. Ang II-bound AT_1 is coupled to the production of reactive oxygen species (ROS) through protein kinase C and phosphoinositol-3 kinase whilst AT_2 and *Mas* are involved in nitric oxide (NO) production. The mitochondrial Ang II system is coupled to AT_2-induced activation of NO production and regulating mitochondrial respiration [7,17,18].

1.1.1.1. Additional RAAS Pathways

Historically renin was responsible for catalysing the conversion of AGT into Ang I through a rate-limiting step and prorenin was considered an inactive precursor molecule [7,8]. Active renin is produced through Cathepsin B cleavage of prorenin. However, prorenin and active renin directly bind the (pro)renin receptor (PRR) to increase catalytic conversion of AGT into Ang I [2]. PRR is expressed in the apical membrane of intercalated cells within kidney

collecting ducts, glomerular mesangial cells, and the sub-endothelium of renal arteries. Its expression and activation induce the ERK1/2 pathways to acidify intracellular compartments such as lysosomes through increased V-ATPase activity [7]. PRR potentially favours tissue fibrosis via production of transforming growth factor (TGF)-β.

The ACE2/Ang (1-7)/ *Mas* receptor pathway is a regulatory counter-arm of the RAAS by opposing Ang II/AT_1 actions. Ang (1-7) is formed through removal of phenylalanine from Ang II by the ACE homolog, ACE2 **(Figure 1.1)**. It then binds the *Mas* receptor [2,12] inducing the phosphatidylinositol 3-kinase/Akt (PI3K) pathway and endothelial NO synthase. These downstream pathways result in vasodilation and a decrease in blood pressure. Ang (1-7) is generated in the kidney proximal tubules but can be rapidly degraded by ACE and neprilysin without inhibition of the classical RAAS pathway. The true biological role of the ACE2/ Ang (1-7)/ *Mas* pathway is expanding, with substantial evidence of its intrarenal effects showing involvement in cancer and heart failure amongst others [7,12,19]. Also under investigation are the alamandine/ *Mas* and the Ang I/ Ang (1-9) pathways. Decarboxylation of Ang (1-7) produces the heptapeptide alamandine with a C-terminal alanine. Converted via an unknown enzyme, the function of the pathway is to induce antifibrotic activity along with NO-dependent vasorelaxation via the *MrgD* receptor. Lastly, Ang (1-9) is also an angiotensin peptide generated via ACE2 activity and potentially counter-regulates the classic RAAS activity as noted for Ang (1-7) and Ang II/ AT_2 receptor interactions [7,12].

Additional products absent from **Figure 1.1** include Ang (2-7), Ang (3-7) and Ang (2-10) which have no known receptors [8,10,20]. Angiotensin III (2-8) (Ang III, sequence: RVYIHPF) and angiotensin IV (3-8) (Ang IV, sequence: DRVYIHP) also accompany the RAAS. For Ang III to induce a natriuretic response, Ang II must be transformed by aminopeptidase A in the kidney and bind AT_2 expressed in the renal proximal tubule, glomeruli, or intrarenal vasculature [7,21]. Once activated, AT_2 induces renal production of bradykinin, cyclic GMP (cGMP) and NO, and the translocation of receptors to the plasma membrane.

Separate to peripheral RAAS functions, Ang IV forms part of the brain RAAS. Aminopeptidase N cleaves Ang III into Ang IV. The mechanism of angiotensin receptor blockers (ARBs) improving AD outcomes, is thought to be mediated through Ang IV and its receptor, AT_4 (ATR4), otherwise known as insulin-regulated aminopeptidases (IRAPs) [22]. Ang IV improves cognitive ability and memory function in the brain by mediating anti-

inflammatory benefits in Alzheimer's patients as it inhibits the proteolytic nature of its receptor when bound. These effects are independent of blood pressure and oxidative stress, allowing accumulation of neuropeptides that aid memory formation [22].

With a rich angiotensin derivative library, it follows that ACE, and its functions are wide-ranging due to its previously identified substrate promiscuity. Following the AT_1 and AT_2 pathways alone, Ang II and ACE are postulated as important molecules within the immune system and ongoing research strives to uncover its function with regards to ACE substrate specificity, structure, and expression within the body.

1.1.2. ACE Structure, Specificity & Expression

The RAAS has several different arms affecting various processes within the body. This system diversity leads one to conclude that with the various aspects of each arm, come different physiologic functions aside from the control and regulation of electrolyte fluids or blood pressure. Within the RAAS ACE and Ang II have important roles in other pathways, including that of the immune response [3,11]. ACE therapeutic strategies utilize its substrate promiscuity stemming from its structural properties. The overarching aim of the treatment dictates how ACE is to be manipulated through its activity and expression. Lubbe and colleagues have published high resolution structures of fully glycosylated somatic ACE and its homodimers, providing insight into its flexible structure [23]. Ongoing investigation using computer modelling, cryo-electron microscopy and crystallography has shown the complex nature of ACE and how there is a vast area of knowledge still to be uncovered.

1.1.2.1. Structure of ACE

ACE (EC 3.4.15.1) belongs to the M2 zinc metallopeptidase family with two isoforms, somatic ACE (sACE) and testicular ACE (tACE). Both are similarly structured but not entirely identical [24]. A heavily glycosylated dipeptidyl carboxypeptidase, ACE functions through the cleavage of dipeptides from the C-terminal of substrates [25,26].

1.1.2.2. ACE Genetic Properties

sACE is encoded by a single gene located on human chromosome 17. It consists of 26 exons, splicing exon 13 and is translated as a 140-170 kDa protein, with 1306 residues [27,28]. It is thought that sACE underwent a gene duplication leading to the existence of two homologous domains, the N- and C-domains [10,24]. tACE is expressed through an

intragenic promoter of the sACE gene but gives rise to a single domain that is identical to the C-domain of sACE barring 36 unique encoded amino acid residues in the N-terminus of tACE [9,26].

1.1.2.3. ACE Protein Structural Properties

Mature tACE is 701-residues in length with a leader sequence and 36-residue serine and threonine rich N-terminus that is heavily O-glycosylated [29]. Its tertiary structure is comprised mostly of alpha helices, with seven alpha-helices and six beta strands [29]. tACE is less glycosylated than sACE with six potential glycosylation sites, three shown to always be glycosylated and three partially glycosylated. The glycosylation sites of tACE help to shape and form the mature protein during folding, aid localisation and stability [26,28]. An additional feature found in the crystal structure of tACE was the presence of two chloride (Cl^-) ions within distinct binding pockets. The importance of chloride presence in the binding pockets is known to influence ACE inhibitor binding and ACE hydrolytic activity on different substrates [28,30].

Within the single sACE polypeptide, the N-terminal signalling sequence is 29 residues and a hydrophobic transmembrane sequence for anchorage is present towards the C-terminus [9]. sACE is a monomeric enzyme with two homologous domains, the N- and C-domains, each holding a single zinc cation (Zn^{+2}) in their active sites [27]. The active sites contain a zinc-binding-motif (HExxH) with histidine on either side to facilitate zinc ion co-ordination [24,25]. The structure of mature sACE **(Figure 1.2)**, begins at the N-terminus with an ectodomain comprised of both domains, a 36-residue juxtamembrane region followed by a 17-hydrophobic-residue transmembrane region and the 30-residue long C-terminal region within the cell cytoplasm [28]. Along with these regions are posttranslational glycosylation sites. sACE shares the same six glycosylation sites as tACE, additionally holding another ten glycosylation sites on the N-domain. Eight of these sites are glycosylated in the folded protein with increased glycosylation aiding thermal stability of the N-domain and altering its substrate selection [28,31]. For sACE, the N-domain is known to be less dependent on chloride ion availability, and able to function normally under low chloride conditions in comparison to the C-domain [28,30,32–34].

Both tACE and sACE ectodomains can be removed from their transmembrane anchors through truncation by an as yet unknown sheddase, which cleaves the arginine-serine bond in the juxtamembrane region or domain [28].

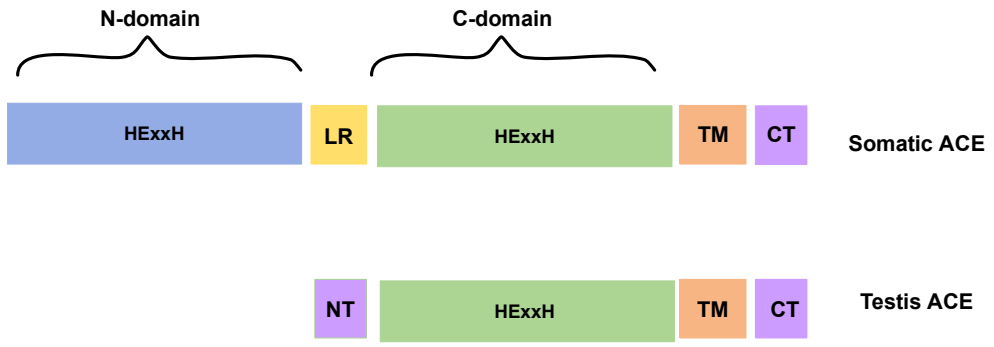

Figure 1.2: Schematic of the domain structure of both ACE isoforms, somatic and testicular. Somatic ACE contains two similarly structured domains, the N- and C-domain whilst testicular ACE has one domain almost identical to the somatic C-domain, only lacking 36 residues. Abbreviations: HExxH – zinc-binding motif active site, LR- linker sequence, TM – transmembrane domain, CT – C-terminus, and NT- N-terminus. (Adapted from: Harrison *et al*. [26]).

Crystal structures of sACE and tACE have shown a channel within the C-domain and a cleft within the N-domain. tACE, identical to the C-domain, is composed of two subdomains separated by a central 30Å groove covered with various charged residues located in three N-terminal alpha helices. The charged residues around the channel prevent tACE and the sACE C-domain from hydrolysing large, folded polypeptides [23,25,28,30]. The N-domain is also divided into two subdomains with a central groove separating them [34]. A short linker (residues 602 – 612), has been visualised between the two domains. The first eight residues remain rigid in their conformation, held in place by hydrogen bonds between tyrosine and glutamine, whilst the remaining four are flexible and suggest interactions between the N- and C-domains of sACE may occur [34]. Cryo-electron microscopy structures of full length, glycosylated sACE were published by Lubbe *et al.* in 2022 providing further evidence that ACE is capable of dimerization when exposed to certain inhibitors, causing increased membrane expression [23,35–37].

1.1.3. Substrate Specificity & Binding

Schechter and Berger (1967) nomenclature assign specific subsite identities (S^n/S'^n) to each residue within the protease active site where *n* represents the position number [38].

Directionally, S' positions are towards the C-terminus and S positions move towards the N-terminus. Both substrate binding and catalytic activity of a protease are via its active site [39,40]. An active site has subsites which bind substrate residues in the correct sequence position, denoted as P^n or P'^n. The scissile bond is located between P^1 and P'^1 [39]. Substrate specificity and binding strength is attributed to the different residues within active site pockets [38,40]. Interactions between the substrate and the subsites within the ACE active sites influence how well it is held in position. Incoming substrates optimise their positions at the S_2, S_1, S_1' and S_2' subsites through the displacement of zinc-bound water towards a glutamate residue [25]. Based on the catalytic mechanism of thermolysin, a zinc metalloprotease and structural analogue of ACE, a general-base mechanism was proposed [25,28,41].

1.1.4. ACE Substrate Specificity

ACE acts on a variety of substrates with different chloride-dependencies and specificities for each one, highlighting the similar but unidentical N- and C-domain specificities [42]. It can cleave tripeptides or peptides up to 40 residues in length [43]. These characteristics are well described but currently poorly understood. ACE also favours action on unfolded peptides rather than fully formed proteins and shows both ectopeptidase and endopeptidase activity [25,28].

The most celebrated substrates of ACE include Ang I, generating the active vasopressor Ang II, and bradykinin, a vasodilator which is inactivated through the removal of two carboxy dipeptides [25,28]. The C-domain hydrolyses Ang I preferentially over the N-domain despite having equal binding affinities and similar domain homology [28,44]. Acetyl-SDKP and amyloid β (1-42) are also well studied and preferentially cleaved by the N-domain [45]. The promiscuity of ACE in macrophages and other myeloid cells is discussed in Sections 1.2.2 and 1.3.2. However, it is worth noting that these new substrates were identified in mouse plasma of an ACE overexpressing myeloid model [46]. The novel substrates and products exist under normal circumstances but may not necessarily be cleaved in hypertensive or homeostatic conditions nor human tissues.

1.1.5. ACE Localisation & Expression

sACE is widely distributed throughout the body as endothelial ACE, whilst tACE is solely expressed by developing spermatids within the testes [25,26]. Additionally, ACE is produced in the kidney, brain, gastrointestinal tissues, the prostate, and lungs [25,47,48]. Along with its wide expression, differences between tissue/cell-specific ACE have been observed through 'ACE conformational fingerprinting' procedures using monoclonal antibodies (mAbs) for different ACE epitopes on either domain [49–51]. The different epitopes provide evidence of slight conformational changes in ACE that may lead to identifying the origins of increased ACE levels within the body [49].

Importantly, human ACE has both a signalling sequence to direct it towards extracellular localisation and a carboxy-terminal hydrophobic sequence to anchor it in the cellular membrane [24]. However, sACE can also exist as plasma ACE in addition to tissue ACE, due to proteolytic cleavage in the juxtamembrane region to create a soluble form [52–54]. Furthermore, ACE is constitutively expressed on the surface of epithelial, neuroepithelial and immune cells (macrophages, neutrophils, and dendritic cells) as reviewed by Bernstein *et al.* [3,9]. The ubiquitous presence of ACE across human tissues provides evidence of its role in other physiological processes [5,9].

1.2. ACE in Immunity

The effects of ACE on the immune response have not been well researched despite the observation of elevated serum ACE in active sarcoidosis patients and its association with other granulomatous diseases [55]. However, various review articles exist noting the putative roles of ACE within the immune system [3,5,56–59].

With the discovery of elevated serum ACE levels in sarcoidosis and atherosclerotic plaques, its use as a biomarker to observe disease progression has been considered [49,51]. ACE has been designated a cluster of differentiation marker (CD) known as CD143 with numerous reviews and publications noting its use as a predictive biomarker in several diseases, including liver fibrosis and Gaucher's disease [49,60–62]. Through cell and tissue-specific ACE expression studies, localised ACE has been found in myeloid cell lines, namely macrophages, monocytes, and dendritic cells [9,49,63]. The expression of RAAS components

in immune cell lines and their peptide/enzymatic effects on the inflammatory response have been quite diverse [64].

1.2.1. Ang II-dependent Immune Effects

Immune benefits or disadvantages observed due to Ang II have been thoroughly investigated as compared to other ACE substrates. Ang II-AT_1 receptor interaction has been observed to encourage pro-inflammatory responses and macrophage activation [5]. When the AT_2 receptor is bound by Ang II, anti-inflammatory and tissue repair responses are favoured by activated myeloid cells [5].

Inflammation is composed of three stages: vascular permeability, leukocyte recruitment and activation of tissue repair processes. All stages are influenced by Ang II through its interactions with the AT_1 and AT_2 receptors **(Figure 1.3)** [65,66].

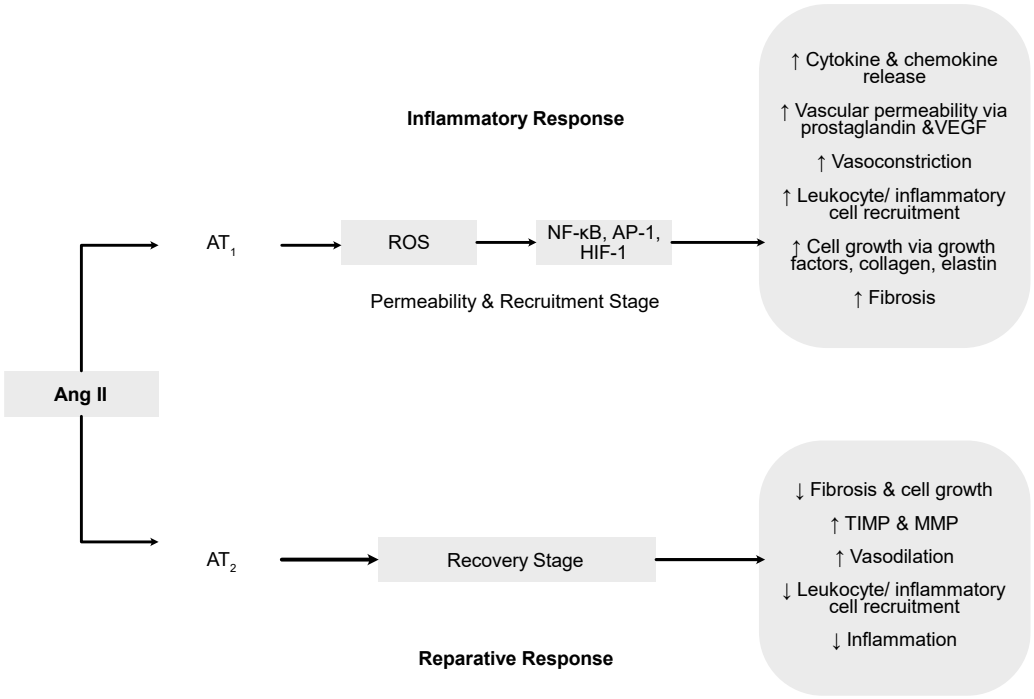

Figure 1.3: Overview of Ang II-induced inflammatory actions. The effects of Ang II-induced inflammation within the vasculature and globally, influencing all stages of the inflammatory response. Ang II either decreases or increases ROS-related inflammatory responses and the resulting transcriptional factor regulation based on AT_1 or AT_2 interaction. Abbreviations: VEGF – vascular endothelial growth factor, TIMP – tissue inhibitors of metalloproteinase, MMP – matrix metalloproteinase (Adapted from: Touyz [67]).

Ang II stimulates prostaglandin, and vascular endothelial cell growth factor (VEGF) production through AT_1, modulating microvascular permeability [65,66]. Vascular smooth

muscle cells (VSMC) secrete VEGF after Ang II induction. VEGF and their tyrosine kinase receptors regulate vascular permeability with the mechanisms being both pressor-dependent and independent. For Ang II, it is postulated to be through cytoskeletal rearrangement [67]. Vascular inflammation and remodelling are controlled through VEGF, independently mediated of Ang II non-haemodynamic actions, and this is further observed in Ang II-infused mice where VEGF inhibition attenuated vascular inflammation [67].

Throughout the second phase, leukocytes including neutrophils and monocytes are recruited to the inflammatory site. During recruitment into the vascular walls, Ang II up-regulates the expression of E-selectins, vascular cell adhesion molecule 1 (VCAM-1), and intercellular cell adhesion molecule 1 (ICAM-1), which are necessary for leukocyte adhesion and diapedesis into the tissues [65,66]. For instance, Ang II levels directly increase endothelial cell E- and P-selectin expression and is mediated through superoxide (ROS) generation and AT_1 [66]. Furthermore, Ang II regulates ICAM-1 and VCAM-1 through a signalling cascade of AT_1 and the mitogen-activated protein kinase (MAPK) pathway that is blood pressure independent [66,67]. Ang II also induces cytokine expression including monocytic chemotactic protein (MCP-1) and interleukin (IL)-8, which function in macrophage recruitment to the vascular walls [65]. Ang II favours increased macrophage-produced cytokines including TGF-β, IL-1, interferon (IFN) and tumour necrosis factor (TNF)-α [67]. These cytokines favour monocyte differentiation, polarization and improve macrophage phagocytosis through the direct influence of Ang II [3,5,66].

When RAAS inhibitors (ACE and AT_1) are administered to murine atherosclerotic lesions, the pro-inflammatory effects of Ang II are prevented and there is decreased MCP-1 [65]. Experimental atherosclerosis and hypertension studies have decreased monocytic infiltration into lesions and aortic tissues along with MCP-1 and CD11b attenuation on circulating monocytes, benefitting patient outcome [66]. *In vitro* studies have shown that ACE inhibitor (ACEi) treatment diminishes cell proliferation of myeloid progenitor cells [66].

Multiple mechanisms of Ang II-induced vascular inflammation exist. One such mechanism is through the highly pro-inflammatory ROS, which is active in each stage of inflammation **(Figure 1.4)**. ROS activates multiple inflammatory signalling pathways including MAPK, transcription factors (NF-κB), protein tyrosine phosphatases and tyrosine receptor and non-receptor kinases.

In terms of NF-κB and Ang II, it can stimulate the expression of the AGT gene, thereby increasing Ang I and its subsequent products [65]. Within the vascular smooth muscle cells, Ang II enhances NF-κB activation through crosstalk with IL-18, a pro-inflammatory cytokine responsible for interaction with the NLRP3 and NLRP6 inflammasomes [65,68]. The NLRP3 inflammasome is recognised as a key contributor to cardiovascular fibrogenesis and controls the release of not only IL-18 but also IL-1ß [69]. This inflammasome functions through activation of myocardial injury and subsequent inflammation which promotes cytokine release as an attempt at tissue repair. Chronic inflammasome activation shift mechanisms remain elusive [69]. Consequently, Ang II signalling largely acts through NF-κB activation via AT_1 to cause the subsequent production of chemokines, cytokines and cell adhesion molecules that amplify the pro-inflammatory response [70]. During inhibition of both ACE and NF-κB, a study reported reduced expression of IL-6, VCAM-1, and MCP-1, reducing inflammation in the vasculature and leukocyte recruitment to the vascular walls [65].

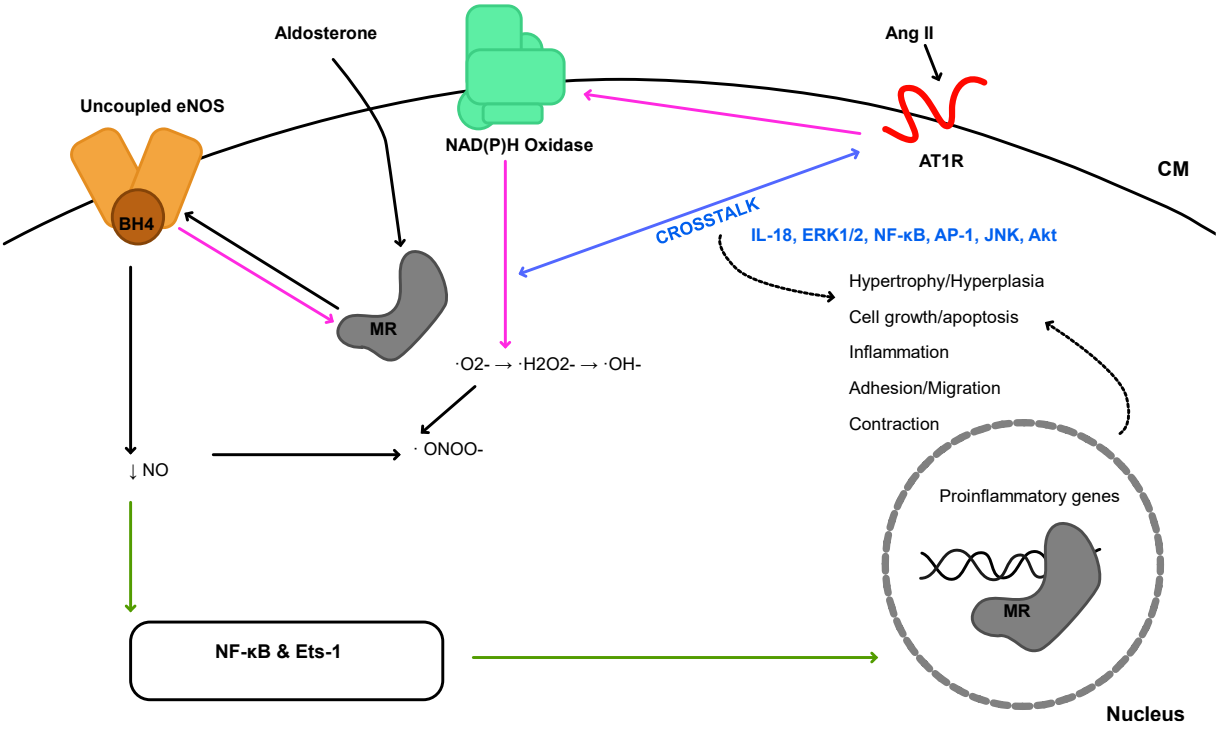

Figure 1.4: Ang II-induced vascular inflammation and crosstalk mediation under the control of transcription factors, NF-κB and Est-1. Both Ang II and aldosterone act on enhancing transcription mediator control over various signalling pathways to influence the three stages of inflammation. These effects are non-haemodynamic. Ang II binds to AT_1R to induce oxidative stress as mediated by NAD(P)H oxidase. Production of superoxide oxidizes tetrahydrobiopterin (BH_4), a nitric oxide synthase cofactor. This reduces BH_4 availability, and the NOS reaction uncouples to increase superoxide production. Increased ROS then causes activation of the transcription factors NF-κB and Est-1 to up-regulate inflammatory reactions and proinflammatory genes. IL-18 and NF-κB crosstalk also influence Ang II-induced effects. Abbreviations: MR – mineralocorticoid receptor, eNOS – endothelial nitric oxide synthase, CM – cell membrane, AT1R – Angiotensin type 1 receptor, Ang II – angiotensin II (Adapted from: Marchesi *et al*. [65]).

Crosstalk between several pathways and Ang II amplifies vascular injury **(Figure 1.4)**. NAD(P)H oxidase, expressed in the vascular wall, endothelial cells, and macrophages, generates oxygen radicals through uncoupled NO synthase to amplify the inflammatory response, increase vascular contractility, and impair the relaxation process [65]. The oxidative stress caused by Ang II may also be from other ROS sources such as the mitochondria and xanthine oxidase. However, it is unclear whether Ang II-induced vascular injury primarily involves inflammation or oxidative stress [65]. A second downstream mediator of Ang II-induced oxidative stress and inflammation is the transcriptional regulator Ets-1 **(Figure 1.4)**. Ets-1 is expressed in the VSMCs and blocking this mediator results in decreased NAD(P)H oxidase, vascular remodelling, and ROS production [65].

Aldosterone, a further inflammatory mediator of the RAAS, binds to the mineralocorticoid receptor (MR) and causes vascular injury within the brain, heart, and kidneys. Aldosterone, as with Ang II, induces oxidative stress and inflammation through crosstalk between several pathways as depicted in **Figure 1.4**. Ang II induces aldosterone secretion from the adrenal glomerulosa and both molecules induce inflammation through their non-haemodynamic effects. Furthermore, Ang II is degraded by ACE2 into Ang (1-7), regulating vascular inflammation through a conversion of vasoconstriction to vasodilation, providing protection to the vasculature over injury [65].

Lastly, Ang II may be profibrotic or antifibrotic in the recovery stage. This is dependent on whether it is bound to AT_1 or AT_2 [67]. Firstly, Ang II induces fibrosis via the TGF-β dependent and independent Smad-signalling pathways. It also stimulates fibrosis by increasing connective tissue growth factor (CTGF) production in the vasculature and inducing abnormal vascular repair. Ang II therefore influences extracellular matrix deposition, growth factor and collagen deposition within the vascular walls [65]. When bound to AT_1, Ang II induces hyperplasia and hypertrophy through cellular growth factors [65,67]. The antifibrotic action of AT_2 occurs via blockade of AT_1 and subsequent up-regulation of AT_2. This receptor being bound also inhibits vascular inflammation, thus favouring vascular recovery [65].

Ang II is capable of modulating both the innate and adaptive immune system, as summarised in **Figure 1.5** [70]. In innate immunity, monocytes/macrophages, natural killer cells and neutrophils are all known to produce the full complement of RAAS components. Monocytes, once activated by Ang II, produce MCP-1, and increase their NF-κB activity for migration to inflammatory sites. In addition, natural killer cells can induce monocyte maturation and differentiation into macrophages and dendritic cells through production of IFN-γ via Ang II stimulation [70]. In neutrophils, Ang II aids their migration and infiltration through increased leukocyte-endothelial interactions. They enhance CXC chemokines, IL-8, and macrophage inflammatory protein-2 (MIP-2) required for further macrophage activation and pro-inflammatory function [70,71].

T lymphocytes, particularly $CD4^+$ T lymphocytes, experience the majority of Ang II modulation in adaptive immunity by modulating their proliferation and differentiation **(Figure 1.5)**. Chronic Ang II expression, both *in vivo* and *in vitro,* up-regulates early activation

markers including CD44, CD69 and CCR5 [70]. Locally produced Ang II favours T helper (Th1 and Th17) proliferation by stimulating increased IFN-γ, IL-17 and decreased IL-4 production [70,72]. Transfer of T regulatory/ T suppressor cells (T_{regs}) in chronic Ang II-infused mice prevents macrophage and T lymphocyte tissue infiltration demonstrating Ang II-mediated attenuation of the inflammatory response and its influence on T_{regs} [70,72].

AT_1 also exercises a protective role when expressed in myeloid cells and T lymphocytes in comparison to hypertensive-related cells [64]. In T lymphocytes, $CD4^+$ Th1 differentiation is driven by the T-bet transcription factor. In mice lacking AT_1, Th1 differentiation is elevated and pro-inflammatory cytokines including IFN-γ and TNF-α are abundant. However, when the AT_1 is present, Th1 differentiation and pro-inflammatory cytokine release is suppressed [64]. In macrophages, a suppression of proinflammatory M1 polarization is also seen when AT_1 is activated. Once activated, AT_1 results in reduced TNF and IL-1β levels, two potent pro-inflammatory cytokines [64]. The exact AT_1 modulation pathway interactions of the myeloid and lymphoid pro-inflammatory populations are under investigation and may aid in reversing or preventing degradative hypertensive and renal fibrotic consequences [64].

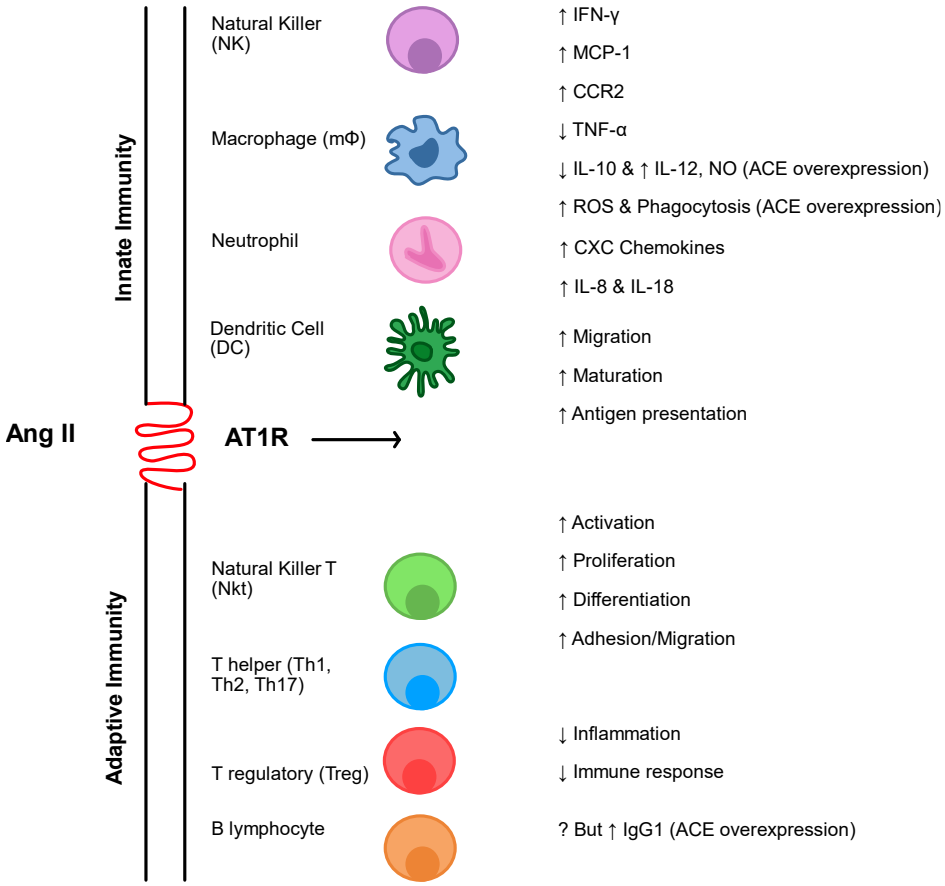

Figure 1.5: The roles of Ang II in innate and adaptive immunity. These functions are mediated through the AT_1 receptor signalling cascade in different immune cell lineages, some roles are enhanced through ACE overexpression and mediated via Ang II (Adapted from: Chang *et al*. [70]).

Bridging the adaptive and innate response are dendritic cells (DCs). When exposed to Ang II, DCs mature faster and are stimulated to migrate and present antigens **(Figure 1.5)** [70,73]. However, their proliferation and phagocytic activity is suppressed by Ang II [73]. DC activation up-regulates and mediates T lymphocyte activation through the activation of the STAT1, ERK1/2, p65 and NF-κB pathways, of which some were highlighted in **Figure 1.4** [73].

From these innate and adaptive immune Ang II-induced observations, it is postulated to play a potential role in mediating autoimmunity. Animal model studies have shown immune benefits from inhibiting Ang II production or binding of AT_1, particularly in rheumatoid arthritis (RA) research. In human studies, elevated AT_1 and Ang II have been observed along with increased ACE activity within arthritic patients. The potential use of tissue-specific ACE inhibitors may prove beneficial to these patients in alleviating the onset of arthritis as a prophylactic drug or further damage by the ongoing condition [56,70].

Ongoing investigations of the therapeutic benefits involving AT_1 blockade and ACE inhibitor treatment on autoimmunity, arthritis and other pathologies will lead to further understanding the implications of Ang II-dependent immune responses [56]. In closing, ACE was thought to mediate inflammation through Ang II and RAAS-like functions within macrophages or through bradykinin inactivation of its active form [9]. However, the recent upsurge in investigating its role within immunity has shown that there are Ang II-independent effects as well [5,9].

1.2.2. Ang II-independent Immune Effects

Ang II-independent immunity has been investigated to a lesser extent, but introduces important results [5,70]. An early example of Ang II-independent immune enhancement is through the different RAAS components which elicit effects on target tissues as discovered by Nguyen *et al*. during their cloning of the PRR [74]. Renin and prorenin were able to activate the ERK1/2 signalling cascade independently of Ang II by binding the PRR and promoting inflammation. As monocytes, macrophages and T lymphocytes express the RAAS components, PRR is required for $CD4^+$ and $CD8^+$ requisition during thymic selection and maturation of T lymphocytes. Renin also induces IL-6 and cyclooxygenase 2 (COX-2) secretion in macrophages through this kinase signalling pathway [64,74]. However, the extent of renin and prorenin mediation of the inflammatory response or immune cell marker expression is yet to be fully clarified [64].

ACE immune modulation is complicated by its broad substrate specificity. As mentioned in Section 1.1.4, Semis *et al*. established a novel ACE substrate peptide library from mouse plasma. Peptides ranged from 3 to several amino acids in length [42]. However, earlier studies have also characterised the substrate promiscuity of ACE and observed Ang II-independent effects, particularly in the adaptive and innate immune response [64]. Furthermore, ACEi reduce inflammatory cytokines supporting a partial role in mediating the immune response. ACE inhibition reduces cardiovascular and renal damage but its expression in immune cells specifically results in their altered cellular actions [64].

1.2.2.1. ACE partakes in Major Histocompatibility Complex Antigen Presentation

ACE participates in antigen presentation and processing and T lymphocyte activation [14,43]. ACE provides additional peptide cleavage after proteasomal degradation

during Major Histocompatibility Complex (MHC) Class I peptide preparation as indicated in **Figure 1.6** [64].

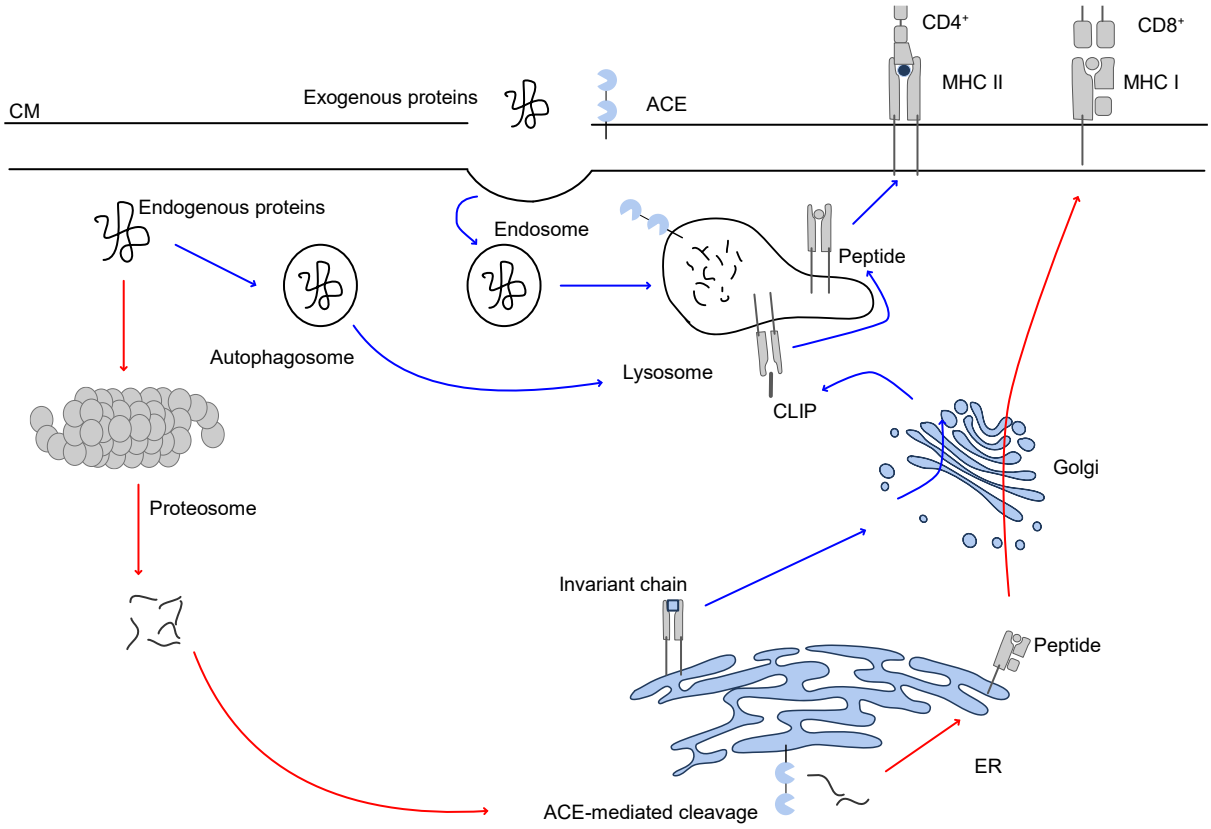

Figure 1.6: Additional ACE-mediated cleavage increases the MHC Class I and II peptide repertoire. ACE provides further peptide processing in the ER after proteosomal degradation in the MHC Class I pathway for $CD8^+$ T cells. During MHC Class II preparation, ACE may process peptides within the endosome, lysosome, and ER before antigen presentation for $CD4^+$ T cells. Both pathways have increased peptide libraries for antigen presentation due to ACE involvement. Abbreviations: ER – endoplasmic reticulum, CLIP – Class II-associated invariant chain peptide, MHC – major histocompatibility complex, CM – cell membrane, CD – cluster of differentiation (Adapted from: Oosthuizen & Sturrock [56]).

During peptide loading of MHC molecules, peptides are chosen for surface presentation based on their length and sequence. The peptide pool is altered through aminopeptidases for trimming of the N-termini, whilst the C-termini were accepted to be cleaved through the proteasome [75–77] before moving to the endoplasmic reticulum (ER). Functional ACE in the ER of antigen presenting cells (APCs), namely macrophages and dendritic cells, can digest and modify the MHC Class I peptide repertoire [14]. Though ACE overexpression identified this functionality, subsequent studies showed ACE altered the C-termini of antigenic peptides under physiologic conditions [14,15]. In mice, other carboxy peptidases

cannot correct for a lack of ACE during MHC peptide digestion and presentation [15]. ACE therefore contributes to the specialised adaptive response through additional MHC peptide processing [5,15,64].

Additionally, ACE adds to the MHC Class II repertoire **(Figure 1.6)**. As with MHC Class I, ACE can increase or decrease certain types of peptide presentations, depending on how well it binds to the peptide [43]. MHC Class II endosomal/lysosomal ACE involvement has been recorded in both ACE overexpressing and wild type (WT) mice. Murine ACE overexpression has been associated with increased B16 melanoma resistance, partially attributed to the altered MHC Class II peptide processing pathway [43,78]. However, ACE involvement in antigen presentation is still dependent on the peptide amino acid positions in the sequence, favouring one array over another as described in Section 1.1.3 [5]. As a result, ACE overexpression will not always increase peptide immunogenicity and the enhanced immune response seen in overexpressing murine macrophages likely involves several mechanisms [5].

The importance of ACE in MHC Class II peptide processing and whether its inhibition in APCs will influence autoimmunity is still to be investigated. It is worth noting that with ACE inhibitor treatment, no autoimmunity in humans has been observed [79]. However, ACE inhibitor treatment has improved the outcome of certain autoimmune conditions such as multiple sclerosis, lupus, and rheumatoid arthritis by decreasing pro-inflammatory cytokine production. IL-12 and TNF-α cytokines are significantly reduced in autoimmune disease models and when used in conjunction with AT_1 blockers, immune cell activation, cytokine expression and autoantibodies decreased. This is partially due to the lack of Ang II to activate the inflammatory response but as blockade of its receptor also improved disease outcome, an unknown mechanism behind ACE-mediated autoimmunity was also inhibited [70,72,79].

1.2.2.2. The Relationship between ACE & Alzheimer's Disease

Using genome- and proteome-wide association studies (GWAS and PWAS), ACE was identified as a candidate gene in AD. Individuals with the single nucleotide variation (SNV), rs4277405, in the ACE gene have an up to 45-fold increased risk of developing AD when present as a homozygous insertion (I/I) allele [62,80–84]. However, individuals with the

variant D/D allele of ACE have increased plasma levels of the enzyme and a lowered risk of developing AD [80].

Importantly, ACE can cleave β-amyloid derivatives including the 42 sequence-long plaque, amyloid β (1-42) responsible for AD pathogenesis [85]. Neuroprotective macrophages have an increased ability to cleave β-amyloid plaques when recruited to the brain, partially due to ACE expression. Neuroinflammation is regulated by these peripheral macrophages in contrast to resident microglia associated with neurodegenerative disease [80]. In mice, ACE overexpressing macrophages have increased memory retention and cognitive stability unlike WT mouse phenotypes.

Lifelong ACE overexpressing mice with AD had reduced inflammation and pathogenic amyloid-β protein in the brain. This effect was mediated by monocytes and macrophages which had a protective phenotype on the brain and conserved cognitive function in the mice, preserving their synapses [86]. Furthermore, transferring bone marrow-derived ACE overexpressing macrophages had comparable neurocognitive protection in AD mice [80]. ACE 10/10 monocytes and macrophages were effective against both soluble and insoluble forms of the amyloid β (1-42) peptides in the brain, preserving murine cognitive abilities. These results offer an alternative AD treatment for human patients by transferring ACE overexpressing monocytes and macrophages similar to chimeric antigen receptor (CAR) T cell therapy and the novel CAR macrophages [80,87,88].

1.3. ACE Overexpression Conveys Enhanced Immunity

Bernstein and colleagues lead in revealing new roles of ACE and its involvement in the immune response, which provide holistic views on its function in humans and mice [3,5,57]. The role of ACE overexpression in immunity is expanding with numerous reviews highlighting its variable functionality [1,5,56–58,89]

ACE overexpressing murine models have improved resistance to immunological challenges such as bacterial infection and B16 melanoma. The transgenic ACE 10/10 model overexpresses ACE 16- to 25-fold in murine macrophages in comparison to their WT littermates [1,5,6]. In addition, the NeuACE mouse model overexpresses ACE in neutrophils up to 18-fold. Both models have enhanced immune capabilities whilst maintaining normal blood pressure and kidney function.

1.3.1. Phenotypes of ACE Overexpression

Macrophages are now known to have varying phenotypes and greater plasticity or flexibility due to changing microenvironments and variable cytokine secretion [90]. Two main phenotypes are described in response to IFN-γ and IL-4, classically activated M1 (pro-inflammatory) and alternatively activated M2 (anti-inflammatory), respectively [90,91]. Anti-microbial M1 macrophages are essential to the innate immune response whilst M2 macrophages are integral to clearance and tissue repair pathways [90–92]. The emphasis of enhanced immunity in the ACE 10/10 model comes from the tilt toward a classical M1 phenotype of the murine macrophages **(Figure 1.7)**.

ACE 10/10 macrophages exhibit enhanced pathogen-killing and antitumour capabilities, features associated with the M1 phenotype [78]. These macrophages have decreased IL-10 levels and elevated IL-12 and NO levels. ACE 10/10 tumour resistance is attenuated by ACEi but not AT_1 inhibition, suggesting Ang II independent pathways and potentially unidentified ACE substrates [78].

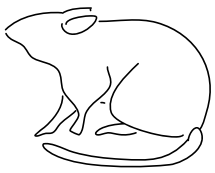

NeuACE & ACE 10/10	↑ NADPH Oxidase & ATP
	↑ NO
	↑ ROS
	↑ Phagocytosis
	↑ TCA Intermediates (malic acid, citric acid, isocitric acid)
ACE 10/10 only	↑ MHC antigen presentation
	↑ Antitumour response
	↑ TNF-α, STAT1, NF-κB
	↑ IgG1 production
	↑ IL-12, NO
	↓ IL-10
NeuACE only	↑ LTB4
	↑ C3 activation to C3b
	↓ Bactericidal ability with ACEi administration *in vivo*

Human Neutrophils	↓ Bactericidal ability with ACEi administration *in vitro*

Figure 1.7: ACE overexpression enhances key immune and metabolic pathways in murine overexpression models. Both NeuACE and ACE 10/10 models show improved clearance of infections and tumours. No overexpression work has been concluded in human immune cell lines whilst ACE inhibition reduces bactericidal ability of both isolated human and murine ACE overexpressing neutrophils (NeuACE model).

It is of interest whether both or one of the catalytically active domains of ACE participate in the enhanced immune response. Alternative C- and N-domain substrates could induce ACE-mediated enhanced immunity, but one domain may be more suited to this role than the other. Secondly, identifying the domain responsible for the enhanced immunity paves the way for the development of domain-specific drugs that could activate or halt this role to treat overactive immune systems. In transgenic knockout (Tg-KO) mouse models, an active C-domain (Tg-NKO) was required for the exaggerated ACE phenotype and slowed tumour growth whilst an active N-domain (Tg-CKO) was unable to replicate the enhanced immunity [93]. The up-regulated inflammatory state of ACE overexpressing macrophages is therefore due to active C-domain overexpression (NKO) rather than the active N-domain (CKO). Myeloid-derived suppressor cell (MDSC) development is also suppressed by the up-

regulated C-domain catalytic activity of the ACE 10/10 macrophages [93,94]. Normally, the immune response is dampened by MDSCs, but they also impact several pathologies including chronic inflammation, sepsis, and cancer [94]. A lack of ACE in murine models results in increased immature myeloid precursor populations (macrophages, granulocytes and DCs) whilst ACE overexpression lowers MDSC populations and favours pro-inflammatory macrophage development [94].

The TNF-α signalling pathways play a role in ACE-mediated tumour resistance as when blocked through TNF-α antibodies, M1 polarization of macrophages is inhibited. M2 markers increase in expression during TNF-α blockade. M1 polarization through TNF-α is further dependent on ROS production and can be prevented through ROS blockade by diphenyleneiodonium (DPI) [93]. Through the different macrophage crosstalk pathways, the net effect of the observed cytokine changes is an increase in immune response beyond that of WT mice [93]. A further indicator of ACE C-domain involvement in enhanced immunity is through experiments that have determined the effect is independent of Ang II, substance P, and bradykinin by utilising receptor inhibitors and transgenic mice incapable of producing angiotensin peptides [78,95,96]. These studies highlight a novel ACE C-domain-mediated pathway utilising an unknown substrate and product above WT macrophage abilities [46,93].

Furthermore, improved immunity continued with lipopolysaccharide (LPS) challenge to bone marrow-derived ACE 10/10 macrophages in culture and their transplantation into WT mice [5,78]. In adaptive immunity, antigen presentation from the macrophages to $CD8^+$ and $CD4^+$ T lymphocytes is also enhanced and required for efficient tumour-specific immune attacks as outlined in Section 1.2.2.1 [78]. In B lymphocytes, macrophage ACE overexpression mediates $CD4^+$ activation and elevates anti-OVA (ovalbumin) antibodies in mice [5,43]. The humoral adaptive branch can also be enhanced by ACE overexpression as a result **(Figure 1.5 &Figure 1.7)** [43]. This finding was particularly true for the IgG1 antibody which was up to 20-fold higher and is an important initial antibody during infection [5].

Listeria monocytogenes and methicillin-resistant *Staphylococcus aureus* (MRSA) immune challenge observe enhanced bactericidal properties in the ACE 10/10 model [97]. MRSA-infected skin lesions of these mice resist bacterial growth, but the macrophages require IFN-γ priming. Furthermore, ACE participates in peptide processing for antigen presentation

aiding adaptive immunity and does not use its catalytic activity for direct bactericidal action. The critical role of ACE overexpression may be enhanced peptide presentation and immune pathway activation rather than a separate hostile microenvironment being created [5,97]. However, heightened iNOS and nitrogen intermediate expression in place of increased ROS production also aid the enhanced ACE 10/10 immunity. Using an iNOS inhibitor, elevated bacterial infection resistance was alleviated as compared to their WT murine counterparts [97]. These observations coincide with ACE/Ang II-mediated vascular inflammation, using elevated NO production as the driver.

In NeuACE neutrophils, bactericidal and oxidative responses are strengthened [4]. In WT neutrophils challenged with MRSA, ACE expression increases. Interestingly, NeuACE neutrophils exercise heightened bactericidal ability emphasising a direct connection between ACE production and bactericidal ability [5,95]. The mechanisms by which neutrophils exercise the bacterial killing ability are enhanced through ACE overexpression. Specifically, phagocytosis (via ROS production) and neutrophil extracellular trap (NET) formation [4,95,98]. Both NAD(P)H oxidase inhibitors and ACE inhibitors inhibit ROS production and alleviate the enhanced immune effect in NeuACE and ACE 10/10 macrophages [5]. In addition, a small human pilot study noted decreased *in vitro* extracellular and intracellular bactericidal abilities of neutrophils when participants were treated with a one-week ramipril regimen [99]. In contrast, the ARB losartan had no impact on murine neutrophil bactericidal ability whilst ramipril reduced ROS production and leukotriene B4 (LTB_4), a key honing molecule in neutrophil migration. This lends itself to the idea that ACE inhibition may negatively impact human immune cell ability, but this is still to be explored in other cell types and diseases [56,99].

1.3.2. Mechanistic Pathways in ACE Overexpression

The exact ACE-mediated mechanism of enhanced immunity is under investigation. Cao *et al*. provided evidence of amplified oxidative metabolism and ATP production in ACE 10/10 macrophages and NeuACE neutrophils [100]. ACE 10/10 macrophages without stimulation did not differ in their ATP levels in comparison to WT macrophages whilst unstimulated neutrophils from NeuACE mice had increased ATP over their WT counterparts. When stimulated, both peritoneal and bone marrow-derived macrophages had 2.4 times more ATP than WT cells [95]. This suggests a sophisticated regulatory control of macrophage

metabolic activity under the influence of ACE overexpression. Within the adaptive immune system, T and B lymphocytes of ACE 10/10 mice had no difference in their oxidative metabolism [95].

No significant difference in glucose nor glucose transporter levels was apparent between WT and ACE 10/10 or NeuACE cells. Glycolytic activity was insignificantly increased whilst oxidative phosphorylation was more active [95]. The mitochondrial size and number in cells remained unchanged despite higher electron transport chain (ETC) complex I and IV expression [95]. However, increased oxygen consumption and cyclooxygenase 1 (COX-1) expression as part of complex IV was observed in ACE 10/10 macrophages. In NeuACE neutrophils, ETC complex I and IV were also up-regulated despite favouring glycolysis over oxidative phosphorylation. Both cell lines had more active cell states as a result [95,98]. Along with the increased oxidative metabolism came an increase in membrane potential up to 24% greater than for WT cells, thus an increase in ATP production could be expected from ATP synthase (complex V) activity.

The relationship between increased ATP production and the immune response is seen with an increase in superoxide production which acts as a bactericidal and phagocytic effector molecule in macrophages [92,95]. The enhanced immune phenotype of ACE 10/10 macrophages has a direct link between increased ATP production and oxidative phosphorylation shown by the enhanced phagocytic ability and superoxide production in these cells when challenged with bacterial infection [95].

ACE overexpressing neutrophils and macrophages also increase TCA cycle intermediate production (succinate, isocitrate, citrate and L-malate) which compensates a glycolytic burst and elevated signalling molecules in other immune cells [92,95]. However, ACE 10/10 macrophages had only a slight glycolytic increase. The overall oxidative metabolism of the ACE 10/10 macrophages was 31% greater than WT macrophages. Overexpressing neutrophils had 27% more oxidative activity than WT neutrophils. These oxidative metabolic alterations suggest bactericidal products aside from superoxide production to enhance their killing ability and that a novel pathway is at work [92].

At present, the peptide(s) responsible for the ACE 10/10 and NeuACE phenotypes are unknown with a new library of potential substrates identified by Semis *et al*. in 2019 [42].

Following this, the bone marrow-derived macrophages of ACE 10/10 mice see no increase in cellular ATP unless stimulated and under tissue culture conditions do not have increased ATP either, possibly due to the novel ACE substrate not being available under culture conditions [95]. Semis *et al*. performed high resolution mass spectrometry for comparative peptidomic analysis through both untreated and ACE-treated mouse plasma, favouring peptides less than 5 kDa. These experiments were performed in ACE knockout/deficient mice as using ACEi-treated mouse plasma would have skewed results due to other competitive peptidases acting on potential ACE substrates. The proteomic data obtained identified 244 novel peptide substrates and products of ACE with 168 substrates and 85 products. Putative substrate/product pairs totalling 36 were identified through the preferential cleavage of two amino acids from the C-terminus of the substrate, the composition favouring polar residues in positions P1-P4 but excluding proline or isoleucine in positions P1' and P1, respectively [38,42].

Additionally, several of the peptides have also been identified in human plasma. Thus, the alternative ACE pathway in enhanced immunity is likely to be present in both humans and mice. Of interest were several complement proteins identified in sera, NeuACE mice enhanced their immune complex uptake in a glomerulonephritis model through increased complement C3b activation. Complement C3 was previously identified in mouse serum as an ACE substrate and provided protection against glomerular damage using NeuACE neutrophils [42,101].

Despite substantial evidence of an increase in ACE expression in both humans and mice when immunologically challenged, the enhanced effect seen in mice may not translate to humans as the differences in ACE expression under normal conditions are stark [5,49]. ACE expression in murine myeloid cells decreases during differentiation of monocytes into macrophages, whereas in humans, ACE expression is low but increases up to 50-fold during monocyte-macrophage differentiation [5,49]. Furthermore, ACE activity in murine blood and tissues is higher than that observed in humans, indicating that the enhanced immune responses may be increased baseline activity over expression levels [49].

These considerations could limit the potential of ACE immunotherapies in humans, but in-depth monocyte/macrophage proteomic studies may lead to explanations on how to utilise these differences and gain the same immune benefits as observed in transgenic mice.

1.4. Implications of RAAS & ACE Manipulation in Humans

Expression of RAAS components in immune cells and their unique actions on immunity should realise the possibility of optimized clinical interventions in humans. New therapies may be personalised and limit both RAAS-dependent inflammation and enhance immunity against common and deadly pathological conditions. Once carefully developed, manipulation of the RAAS components, including ACE and AT_1, could be applied to specific cardiovascular and renal conditions to limit the inflammatory response; particularly negative effects of inhibitor treatment [64]. The use of ACE inhibitors does not induce immunosuppression as can be expected from the numerous pathway overlays and interactions that occur in the immune system [5]. With regards to the PRR, direct renin inhibition has seen clinical improvements in diabetes patients, decreasing IFN-2α and IL-2 urinary excretion, whilst in hypertensive patients, C-reactive protein secretion decreased [64]. These results were not consistent in some groups, requiring a new RAAS-manipulation strategy to be used in a therapeutic setting [64].

RAAS signalling cascades therefore interact with immunity on multiple levels, causing cell-, organ-specific and global changes to the immune system [64]. The complex nature of these interactions requires further analysis to provide new directions for treatment of conditions, be they Ang II-mediated or Ang II-independent RAAS effects [64]. Thus, the importance of ACE as a potential role-player in the immune response cannot be overlooked and its influence could be harnessed as a new therapeutic tool in humans.

1.5. Aims & Objectives

Better understanding and further investigations regarding the mechanism of how ACE affects the immune response are needed before progress in human disease can be made, specifically cancer, Alzheimer's, and autoimmunity [5]. ACE inhibition, although it does not cause immunosuppression, may alter myeloid cell populations in humans which should be investigated along with different myeloid populations in mice and humans [94].

Currently the true effects of ACE overexpression in human myeloid cells are unknown and require further investigation to determine if similar immune benefits are seen in humans as in mice [5]. Therefore, this body of work aims to investigate the mechanism of ACE overexpression in myeloid cells and the associated proteomic changes.

1.5.1. Objectives

1. Perform proteomic analysis of murine and human ACE overexpressing macrophages to investigate changes in the intracellular proteome using mass spectrometry.
2. Identify putative pathway(s) that are active and/or dysregulated during ACE overexpression in myeloid cells.
3. Investigate the effect of domain-specific ACE inhibitors on the intracellular proteome of ACE overexpressing macrophages.

2. The Effect of ACE Overexpression & Inhibition in the Murine Macrophage Proteome

2.1. Introduction

The dynamic functions of cells and biological systems is best described by measuring changes in their proteome rather than genetic makeup. Genes are constant, and change very little if at all over time, while the homeostatic nature of living cells results in constant changes to protein components according to the environment and conditions they find themselves in [102,103]. Proteomics studies types, quantities, and functional interactions of the protein components of a specific cell, tissue, or system [104,105]. It allows for complex relationships to be elucidated and understood in a more holistic manner by conducting large-scale determination of direct cellular function at the protein level [105]. A common method of proteomic analysis is through global mass spectrometry-based techniques, particularly for exploratory analysis with limited protein content in samples. Given ACE's broad physiological functions, a global mass spectrometry study would aid in identifying dysregulated proteins and pathways previously not associated with ACE. It allows for cost-effective wide-scale analysis without prior knowledge in contrast to the need for specific antibodies, protein interactor and modification knowledge, and larger amounts of protein samples used in western blots for protein detection, often exceeding 5 µg.

2.1.1. An Introduction to Mass Spectrometry

Mass spectrometry (MS) relies on molecules ionized in the gas phase detecting and recording their mass-to-charge ratios (*m/z*) and intensities [105]. For complex samples such as plasma or cell lysates, a common ionisation method is electrospray ionisation (ESI), which can be combined with liquid-based separation tools such as liquid chromatography (LC) [105,106]. ESI-MS has been paired with tandem MS and LC in a technique known as LC-MS/MS, an efficient technique capable of whole proteome analysis. LC facilitates deeper real time analysis of samples by analyte separation in time producing smaller ion packets. Two broad proteomic categories exist, data-dependent acquisition (DDA) and data-independent acquisition (DIA).

2.1.1.1. Discovery Proteomics & Proteolytic Digestion

Typical proteomics workflows rely on sample preparation which includes protein purification, predictable digestion into peptides, clean up and MS analysis.

DDA is an untargeted approach which favours high intensity ion identification within its global protein coverage but provides a starting point in finding proteins of interest to explain the murine ACE 10/10 macrophage model's immunological benefits. Importantly, proteolytic digestion increases sample complexity, but also increases the chance of sampling a peptide associated with a low-abundance protein by creating smaller peptides for high confidence sequencing and identification due to the presence of multiple copies of proteins within the sample after digestion [107]. Trypsin, a typically used protease is a serine protease which cleaves proteins at the carboxyl side of lysine (K) and arginine (R) residues. It recognises the sequence K/R-Z where Z is any amino acid residue [102,107]. An important factor includes protein solubilization and unfolding to allow access to cleavage sites [106–108]. However, discovery mass spectrometry and DDA is limited by the MS instrument's capabilities and can have high missing values of low abundance proteins and needs longer analysis times. DIA lends itself to tackling these problems.

2.1.2. Triple-TOF-Based SWATH Proteomics

Sequential window acquisition of all theoretical fragment ion spectra (SWATH) mass spectrometry is an untargeted DIA-based method that allows comprehensive proteome coverage, including low abundance peptides/proteins [102,103,109,110]. With high scan speeds up to 100 Hz, the triple quadrupole Time-of-Flight (TOF) mass spectrometers are known for high throughput and enhanced detection. Quadrupoles Q1 and Q3 act as mass filters, whilst Q2 acts as the collision cell to produce fragment ions. The TOF allows for a full MS scan and accelerates ions based on their *m/z* ratios **(Figure 2.1)**, with smaller fragments accelerating faster than larger fragments [102–104].

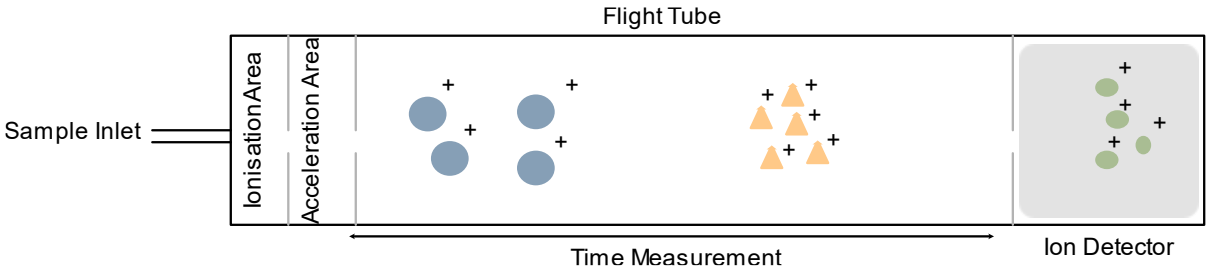

Figure 2.1: Principle of TOF. Ions enter the flight tube and are accelerated with fixed time and at a fixed point with the same potential. Ions separate according to *m/z* ratios with heavier ions travelling slower than light ions towards the detector (Adapted from: Allen *et al*., Andrews *et al*., Comai *et al*. [104–106]).

Briefly, SWATH **(Figure 2.2)** applies cyclical acquisition of precursor ions in a sample across the full *m/z* range. All precursor peptides are fragmented in this method and their respective fragment ion peaks identified across sequential fixed or variable isolation windows [109,111,112]. Those ion species that co-elute at the same point during gradient elution are recorded in the full scan (MS^1), whilst fragment ion spectra are sequentially collected once isolated at the MS^2 level [102,112]. SWATH thus provides the benefit of increased identification reproducibility across replicates, improved proteome coverage because of precursor ion selection independence and precise label-free quantification [102,110,112,113]. Triple-TOF SWATH-MS is therefore a powerful method for the identification of the effects and putative interactors within the ACE overexpressing murine model.

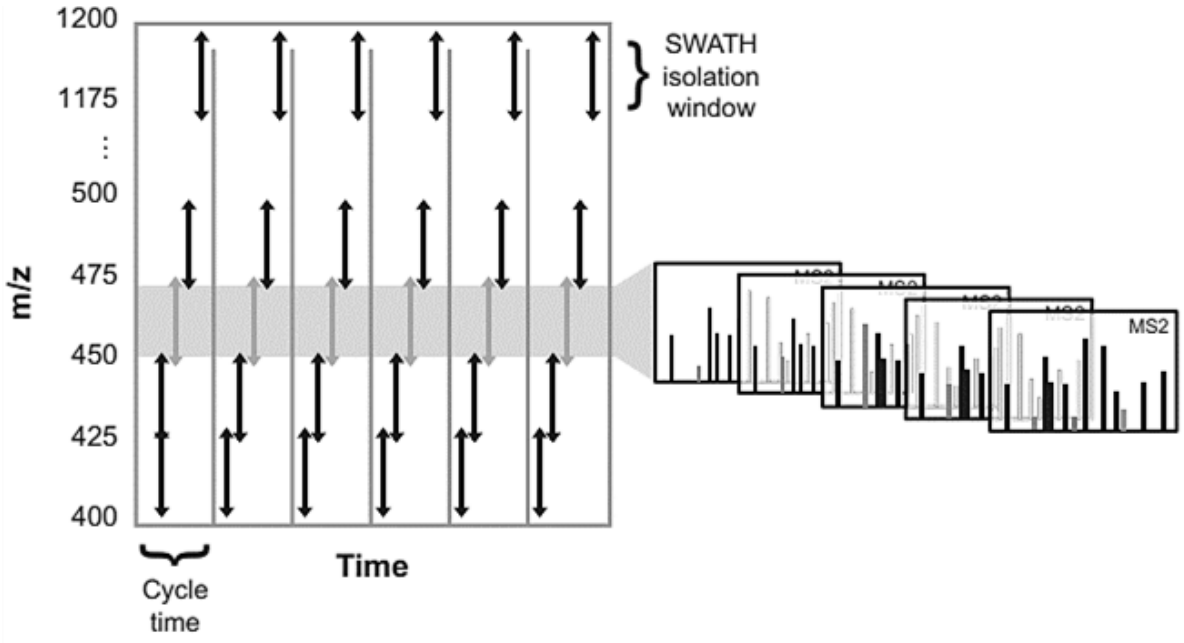

Figure 2.2: SWATH-MS isolation window scan scheme and eluted precursor detection. The mass spectrometer cycles through the *m/z* range in either variable or fixed window sizes as peptides elute. All peptide ions within a window are co-fragmented and their resultant fragment ions recorded in a composite MS^2 scan. For each isolation window, the instrument records fragment ions over time (Adapted from Röst *et al*. [107]).

2.1.3. Phosphoproteomics

Protein phosphorylation **(Figure 2.3)** is important in transient cell signalling systems, where it alters enzyme pathways. Phosphorylation of serine (S), threonine (T) or tyrosine (Y) residues may alter protein activity, localization, and protein interactions in response to stimuli, ultimately changing the internal cellular landscape [108,114,115]. Phosphoproteomics utilizes mass spectrometry to survey the comprehensive landscape of protein phosphorylation sites, characterizing kinase and phosphatase activity [115,116]. Despite their importance in cell signalling phosphorylated proteins are difficult to detect within complex lysates due to low stoichiometry and require enrichment for MS analysis [108,115]. Enrichment methods include immunoaffinity chromatography, metal oxide affinity chromatography (MOAC) and immobilised metal affinity chromatography (IMAC). Ti-IMAC in the form of magnetic bead polymers bound with titanium (Ti^{4+}) ions is currently a popular and affordable enrichment method that provides a selective, fast, and user-friendly experience [108]. Phosphorylated proteins, both multiply and mono-phosphorylated, bind titanium ions well and can be quickly and efficiently separated from

unmodified proteins using a magnetic separator. The beads can be easily washed, and phosphoproteins eluted into separate vessels. Although other phosphoproteomics approaches exist, including microarrays and fluorescent analysis, mass spectrometry requires no prior knowledge or identification of known sequences, an advantage in elucidating putative interactors of ACE 10/10 immune enhancement signalling pathway(s) [5,100].

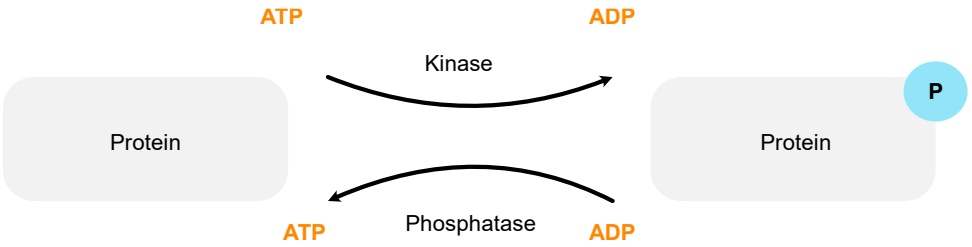

Figure 2.3: Phosphorylation and dephosphorylation of proteins. Both transient processes change system signal networks and their systemic responses. Phosphorylation and dephosphorylation are enacted via the gain or loss of a phosphate group from specific residues (STY) using the energy molecule ATP/ADP, respectively.

2.1.4. The Basal Proteome & Cell Signalling in ACE 10/10 Murine Macrophages

The basal ACE 10/10 macrophage proteome has no external stimulation including cytokine and/or immunological challenge. An overexpression system such as the ACE 10/10 macrophages may still alter cellular signalling and protein function at rest or basal conditions where metabolic changes resulting in increased oxidative metabolism, ATP production and cytokine expression have been recorded with stimulation [117,118]. Global proteomic analysis of ACE 10/10 murine macrophages will serve as a powerful tool for confirming known functional changes and directing research in understanding ACE overexpression-associated immune benefits or mechanisms thereof. Phosphorylation and dephosphorylation studies would contribute to understanding the exaggerated ACE phenotype observed in ACE 10/10 macrophages and may provide regulatory information and protein kinase activity. This study identified the differentially expressed unmodified and phosphorylated proteins in isolated unstimulated murine ACE 10/10 macrophages with and without ACE inhibition.

2.1.4.1. Objectives

- Perform global discovery proteomics analysis using a Sciex 6600 Triple-TOF mass spectrometer to analyse murine ACE 10/10 and WT macrophage cell lysates.
- Compare the murine ACE 10/10 macrophage proteome to the proteome of WT and ACE C-domain inhibited macrophages.
- Identify phosphoproteins and their associated present or dysregulated kinases in murine ACE 10/10 macrophages after phosphopeptide enrichment.

2.2. Methodology

A graphical representation of the standard sample processing and preparation for mammalian mass spectrometry is shown in **Figure 2.4**. Each step is described in further detail in Sections 2.2.2 and 2.2.3. Briefly, proteins were precipitated overnight before resuspension in denaturation buffer **(Figure 2.4A)**. Proteins were then reduced, and dealkylated and the pH was adjusted using ammonium bicarbonate (ABC) before the addition of trypsin. The proteins were digested overnight, and the reaction was stopped by acidification **(Figure 2.4B)**. Peptides were then desalted and eluted into glass vial inserts, dried down and resuspended to the required peptide concentration or eluted from the column directly into the machine for mass spectrometric analysis (**Figure 2.4B-D**). In phosphoproteomics, proteins were enriched for phosphopeptides, and a second aliquot of unmodified protein used as background.

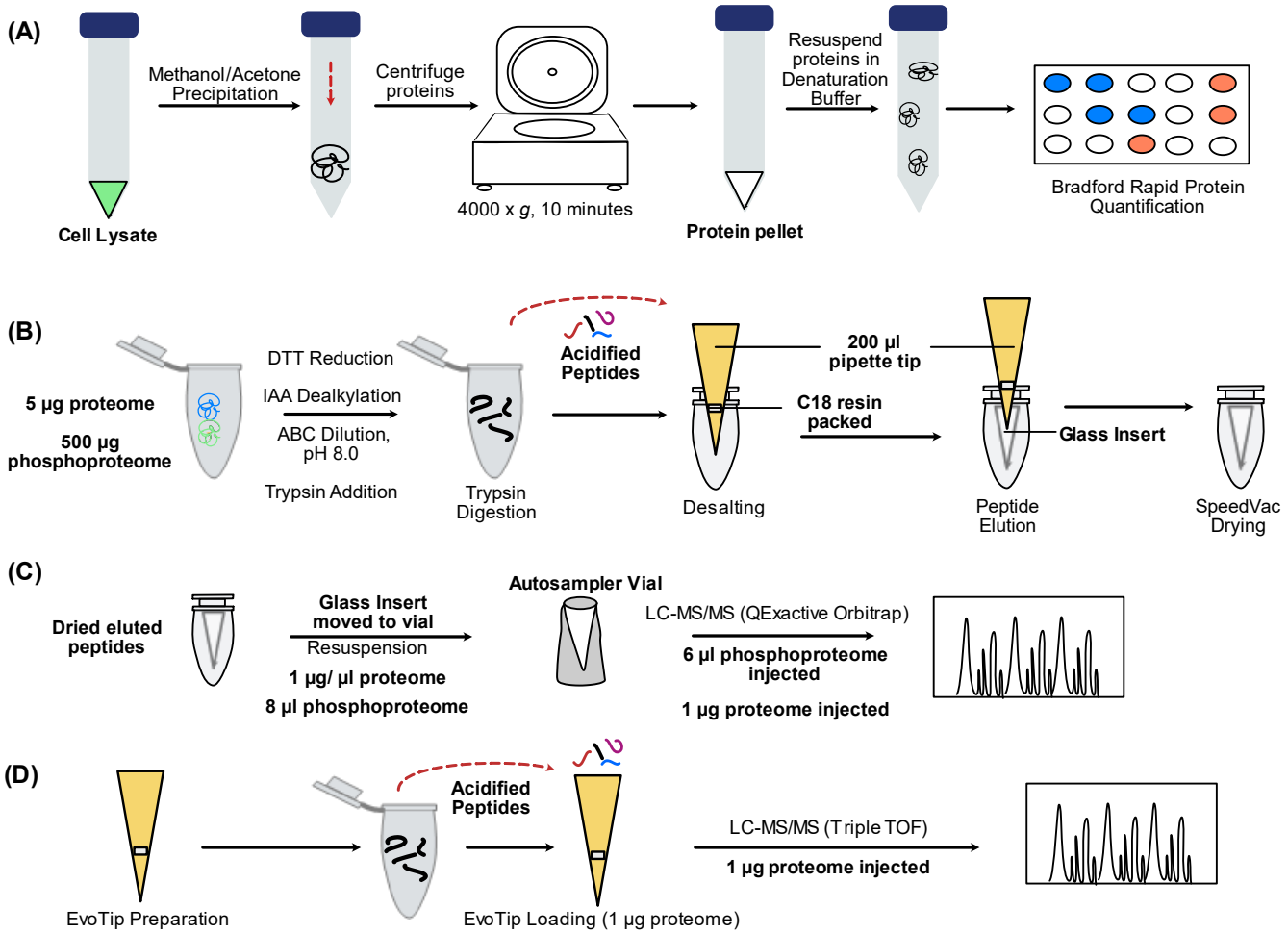

Figure 2.4: Mass spectrometry sample preparation. (A) Protein methanol/acetone precipitation and Bradford [119] quantification from cell lysates. (B) Protein trypsin digestion and desalting in preparation for mass spectrometry analysis. (C) Peptide resuspension and analysis via the relevant mass spectrometer, leading to spectra used for protein identification and differential analysis. (D) Triple TOF digests are acidified, and 1 µg loaded onto EvoTips for offline desalting and elution directly coupled to the mass spectrometer. Abbreviations: DTT – dithiothreitol, IAA-iodoacetamide.

2.2.1. Cell Culture & Treatment

2.2.1.1. ACE 10/10 Transgenic Mouse Model

In mice, Shen and colleagues used homologous recombination to insert both a neomycin resistance cassette and the *c-fms* promoter directly in front of the somatic ACE gene [6,120]. The *c-fms* promoter directly 5' of the ACE gene removes tissue specificity and places ACE tissue expression under control of the *c-fms* promoter instead. In mice this modification removes endothelial ACE expression, but the mice can maintain healthy blood pressure, renal function, and weight. The transgenic mice expressed high levels of ACE in their monocytes and macrophages.

2.2.1.2. Murine Cell Culture & ACE Inhibitor Treatment

Murine ACE 10/10 macrophages and WT tumour-bearing peritoneal macrophages (TPM) were isolated and cultured in 6-well plates at a seeding density of 1 x 10^6 cells/ml. Two experimental conditions were in place for both cell types: untreated macrophages and those treated with 50 µM lisinopril-tryptophan (Lis-Trp), a C-domain selective ACE inhibitor, for 24 hours. Each condition was collected in triplicate, totalling 12 samples **(Table 2.1)**. Cells in each sample were washed with chilled 1x PBS in triplicate and lysed using RIPA buffer containing 4% SDS and a protease inhibitor cocktail to prevent protein degradation. The lysates (gifted by K. Bernstein, Cedars-Sinai Medical Centre, USA) were then frozen and stored at -80°C until use.

Table 2.1: Experimental groups of mouse macrophage lysate samples (gifted by K. Bernstein, USA).

Sample Group	Number of Samples in Group
ACE 10/10	3
ACE 10/10 + Lis-Trp	3
WT TPM	3
WT TPM + Lis-Trp	3

2.2.2. Mass Spectrometry Sample Preparation

2.2.2.1. Protein Precipitation & Quantification

In mass spectrometry, peptide fragments are the molecule of interest. For this purpose, cell lysates were subjected to acetone:methanol precipitation in a ratio of 8:1. All cell lysates were transferred to LoBind® Eppendorf tubes (Eppendorf, Germany), at 9 parts ice-cold acetone:methanol to 1 part lysate. Proteins were precipitated by incubating at -20°C overnight.

The precipitated proteins were centrifuged at 4000 x *g* for 10 minutes, and the pellet washed with ice-cold 80% acetone and left to air-dry. Pellets were then resuspended in denaturation buffer (6 M urea, 2 M thiourea in 10 mM Tris-HCl, pH 8.0).

Protein was quantified using the Bio-Rad Bradford reagent assay (Bio-Rad, USA) [119]. Protein samples were mixed with Bradford reagent (Catalogue #5000006) in a 96-well plate and spectrophotometrically quantified at an absorbance of 595 nm using an iMark™ Microplate Absorbance Reader (Bio-Rad, USA). Samples were prepared in duplicate, whilst the bovine serum albumin (BSA) standard curve was prepared in triplicate over a range of 0 – 2 mg/ml. The resultant standard curve was used to calculate protein concentration in each sample **(Appendix Section 8.1, Figure 8.1)**.

2.2.2.2. Sample Digestion & Enrichment

2.2.2.2.1. Tryptic Digest

Phosphoproteomic analysis requires both phosphopeptide enrichment and a proteomic baseline, 500 µg of digest was used, and these samples were run on the QExactive™ Orbitrap (Thermo Scientific™, USA). Sciex TripleTOF 6600 (Sciex, USA) proteomic analysis used 5 µg total digest.

Samples underwent trypsin digestion overnight at 37°C for optimal enzyme activity. However, denaturation buffer-suspended protein samples need to be prepared before the addition of trypsin. Briefly, reducing agent dithiothreitol (DTT) was added to a final concentration of 3 mM and incubated for 20 minutes at RT. Then alkylating agent iodoacetamide (IAA) was added to the samples at 15 mM and incubated in the dark for 20 minutes at room temperature (RT) due to light sensitivity. Both steps facilitate linearizing protein for protease access in preparation of trypsin addition. Samples were then diluted 5x

using 50 mM ammonium bicarbonate to reach below 1 M urea and pH 8.0. Trypsin was added at a ratio of 1:100 µg protein and left overnight at 30°C. Digestion was halted with the addition of 0.5% formic acid (FA) acidifying the sample and inactivating trypsin.

2.2.2.2.2. Phosphopeptide Enrichment

Phosphopeptide enrichment is required since the phosphoproteome is significantly smaller than the unmodified proteome [114,115]. It is accepted that peptides with lower concentrations in a sample are less likely to be detected unless fractionation or enrichment takes place, this is also dependent on the detection limit of the mass spectrometer in use. To enrich phosphorylated peptides, the MagReSyn Ti-IMAC HP kit (ReSyn Biosciences, RSA) was used as per manufacturer's instructions.

Titanium ions (Ti^{4+}) chelated to polymer microparticles bind phosphopeptides, and a magnetic separator is used to isolate the beads during wash and elution steps. Briefly, to equilibrate the beads, bead suspension was transferred to clean Eppendorf tubes and the shipping solution removed using a magnetic separator. Loading buffer (0.1 M glycolic acid in 80% acetonitrile (ACN), 5% trifluoroacetic acid (TFA)), was then added to the beads for 1 minute and the solution removed using the magnetic separator. Equilibration was performed in triplicate.

Samples were desalted (Section 2.2.2.3.1) using 50 mg Sep-Pak cartridges (Waters Corp, USA) after digest and were resuspended in loading buffer. The samples were then centrifuged at 10 000 x *g* for 5 minutes to remove any insoluble materials and the resultant supernatant transferred into the Eppendorf tubes containing the equilibrated microparticles. To allow maximum interaction with the bead surface, the samples were gently agitated for 20 minutes at RT. Beads were lifted using the magnetic separator and the supernatant removed and kept separately as an unphosphorylated baseline sample. Unbound sample was washed from the beads using loading buffer and agitation for 2 minutes before magnetic separation. Wash buffer 1 (80% ACN, 1% TFA) was then added to remove non-specifically bound peptides, followed by wash buffer 2 (10% ACN, 0.2% TFA) addition and removal using magnetic separation.

In separately labelled LoBind® Eppendorf tubes, phosphopeptides were eluted for 10 minutes and the magnetic beads separated before supernatant collected and transferred

to the clean tubes. This elution step was repeated to a total volume of 400 µl eluent. Elution buffer was composed of 1% ammonium hydroxide (NH_4OH) and all LoBind® Eppendorf tubes contained 50 µl FA per 150 µl elution buffer. Samples were dried using a SpeedVac concentrator (Thermo Scientific™, USA) overnight with no heat before desalting and drying the phosphopeptide samples for MS analysis as outlined in Section 2.2.2.3.1. Phosphopeptide and unmodified peptide background samples were run on the QExactive™ Orbitrap (Thermo Scientific™, USA).

2.2.2.3. Desalting

2.2.2.3.1. QExactive™ Phosphoproteome

Using stage tips or Sep-Pak columns prepared with C18 resin, phosphoproteomic samples were desalted twice. First before phosphopeptide enrichment and second in preparation for MS analysis. Briefly, the resin was activated with 100% methanol and centrifuged slowly at 50 x *g* for 1 minute. Equilibration using 2% ACN, 0.1% FA solution was achieved by centrifuging the columns at 200 x *g* for 1 minute and discarding the flow-through. The acidified samples were then applied to the columns. The columns were slowly centrifuged at 50 x *g* for 5 minutes to allow the proteins to bind the resin. Columns were then washed with 2% ACN, 0.1% FA for 1 minute at 200 x *g*. Before elution, the stage tip columns were moved to a separate Eppendorf tube with a glass insert inside. Peptides could then be eluted using 60% ACN, 0.1% FA and centrifuged slowly at 50 x *g* until dry, approximately 5 minutes. Eluted peptides were dried overnight in a SpeedVac concentrator with no heat.

2.2.2.3.2. Triple-TOF Proteome

Triple-TOF (TTOF) proteomic analysis uses EvoTips (Evosep Biosystems, Denmark), disposable C18 trap columns for offline desalting and elution of peptides directly into the LC-coupled mass spectrometer. Briefly, 1 µg of acidified peptides was loaded onto EvoTips as per manufacturer's instructions. Tips were rinsed using solvent B (ACN, 0.1% FA) and centrifuged at 800 x *g*, 1 minute then conditioned by soaking with propanol until tips were pale white. Solvent A (2% ACN, 0.1% FA) was transferred to each tip and centrifuged at 800 x *g*, 1 minute to equilibrate after which samples were loaded and centrifuged once more. Columns were washed with solvent A and centrifuged again. The prepared tips were preserved by the addition of 100 µl of solvent A and centrifugation (800 x *g*, 10 seconds) prior to MS analysis.

2.2.3. Mass Spectrometry

2.2.3.1. Phosphoproteome as through QExactive™ MS

Eluted, dried peptides and phosphopeptides were resuspended in 2% ACN, 0.1% FA. Proteomic samples were resuspended at 1 µg/µl. Phosphopeptide samples were resuspended in 8 µl of 2% ACN, 0.1% FA. Peptide samples were transferred to labelled autosampler glass vials and run on the QExactive™ Orbitrap (QE) mass spectrometer coupled to a Dionex Ultimate 3500 RSLC nano LC system, via the Blackburn proteomics laboratory (IDM, University of Cape Town, RSA). Digests were loaded on a 20 cm C18 analytical column packed in-house with 1.9 µm, C18 reprosilbeads (Dr Maisch, Germany). Elution was performed using a curved gradient of 10 – 25% ACN and 0.1% FA at a constant flow rate of 300 nl/min over 70 minutes. Data acquisition was through Xcalibur software (Thermo scientific, version 4.1.31.9) in positive ion mode. MS^1 scans were performed at a resolution of 70000 from 300 – 1700 *m/z* with an automatic gain control (AGC) target of $3 \times e^{10}$ in 50 ms. MS^2 scans were performed at a resolution of 15000 with an AGC target of $3 \times e^5$ in 100 ms using a top9 scheme.

2.2.3.2. Proteome as through Triple-TOF SWATH-MS

Liquid chromatography was performed on an Evosep One LC coupled to a Sciex TripleTOF 6600 courtesy of the Blackburn proteomics laboratory. Peptides were separated using the pre-programmed 40 sample per day (SPD) method at a column temperature of 40 °C using the recommended 15 cm, 75 µm column packed with 1.9 µm solid core beads. LC solvent buffer A (2% ACN and 0.1% FA) and buffer B (ACN and 0.1% FA) were used. The OptiFlow source was used with the nanoprobe set to 250°C and a 3000 V spray voltage.

The Sciex 6600 was operated in positive mode using SWATH acquisition comprising a variable window scheme with 120 windows or minimum 3 *m/z* and 1 *m/z* overlap. The MS^1 and MS^2 fill time was set to 250 ms and 15 ms respectively giving an approximately 2 second cycle time.

2.2.4. Data Processing & Analysis

2.2.4.1. Data Processing

2.2.4.1.1. QExactiveTM Phosphoproteome

Raw data was processed through MaxQuant (version 2.1.0.0) [121–123] to identify and quantify peptide intensities across both the proteome baseline and phosphoproteome using the Andromeda search engine [123] and murine UniProtKB database. Default label-free settings were used with variable modifications of oxidation and phosphorylation (STY) selected. A false discovery rate (FDR) of 1% against a reverse decoy database and 2 missed cleavages was allowed.

2.2.4.1.2. Triple-TOF Proteome

Using data independent acquisition neural network (DIA-NN) software (version 1.8.1) [111,124], raw data was processed to identify and normalise label-free quantification values matching against a pre-generated UniProtKB mouse proteome spectral library. The following settings were used as part of the database search: 1 missed cleavage, peptide lengths of 7-30 amino acids and a mass range of 300 – 1150 *m/z* with cysteine as a variable modification.

2.2.4.1.3. Data Clean-up & Statistical Analysis

The resultant phosphoproteomic proteinGroups and STY output tables, and proteomic DIA-NN protein/gene matrices were filtered to remove contaminants and reverse/site only hits. Identified phosphoprotein intensities were normalised against their corresponding unmodified protein intensities measured by the QExactive^{TM} Orbitrap. Quantification data was log2 transformed.

Exploratory data analysis and quality checks involving Pearson correlation, protein identification visualization and hierarchical clustering were performed to identify outliers using Perseus (version 2.0.7.0) and DIA-NN [111,124]. If well correlated and clustered together, samples were allowed to proceed to further analysis. Values were considered valid if two of three replicates were present in any group to account for the overexpression conditions in the ACE 10/10 murine macrophages. A Student's two sample t-test was applied to identify differentially expressed proteins between conditions, taking a p-value ≤ 0.05 as statistically significant.

2.2.4.1.4. Functional Enrichment & Network Analysis

Search tool for the retrieval of interacting genes/proteins (STRING) within Cytoscape (version 3.9.1) [125,126] for network analysis was used amongst those significant differentially expressed proteins. Interaction confidence was set to high (0.7) to account for legibility. Line thickness indicates confidence score of the interaction. The log2(fold-change) or log2FC was continuously mapped to the proteins, blue representing down-regulation and orange representing up-regulation. The shade was attributed to the fold change level where darker indicated a larger fold change.

Following network generation, functional enrichment analysis was performed by Biological Networks Gene Ontology tool (BiNGO) [127] within Cytoscape [126]. Gene Ontology (GO) term enrichment for both molecular function and biological processes using a hypergeometric test with Benjamini-Hochberg FDR correction identified significantly overrepresented proteins ($p \leq 0.05$). Modified proteins were compared against the full phosphoproteome STY list to identify enriched kinases in PhosphoSitePlus [128]. Kyoto Encyclopaedia of Genes and Genomes (KEGG) pathway analysis was included in proteomic functional enrichment analysis [129,130]. Reactome was also utilized for those pathways existing in both mice and humans [131].

2.3. Results

2.3.1. Identified Proteins & Phosphoproteins

Identification using MaxQuant and DIA-NN was mapped against the mouse UniProtKB database. A total of 3378 TTOF protein and 4325 QE phosphoprotein groups were identified across all samples (FDR < 0.01). Upon valid value filtering, keeping those appearing within 2 of 3 replicates in any group (*i.e.*, *ACE 10/10, WT TPM, ACE 10/10 + Lis-Trp* and *WT TPM + Lis-Trp*), 3332 protein and 1044 phosphoprotein groups remained **(Figure 2.5A & B)**. Since multiple phosphorylation sites can exist per protein, a total of 1196 phosphosites were identified for the 1044 valid phosphoproteins. The removal of potential contaminants, site only, and reverse hit identifications did not significantly impact the data resulting in a loss of 15 and 60 identifications in the proteome and phosphoproteome, respectively.

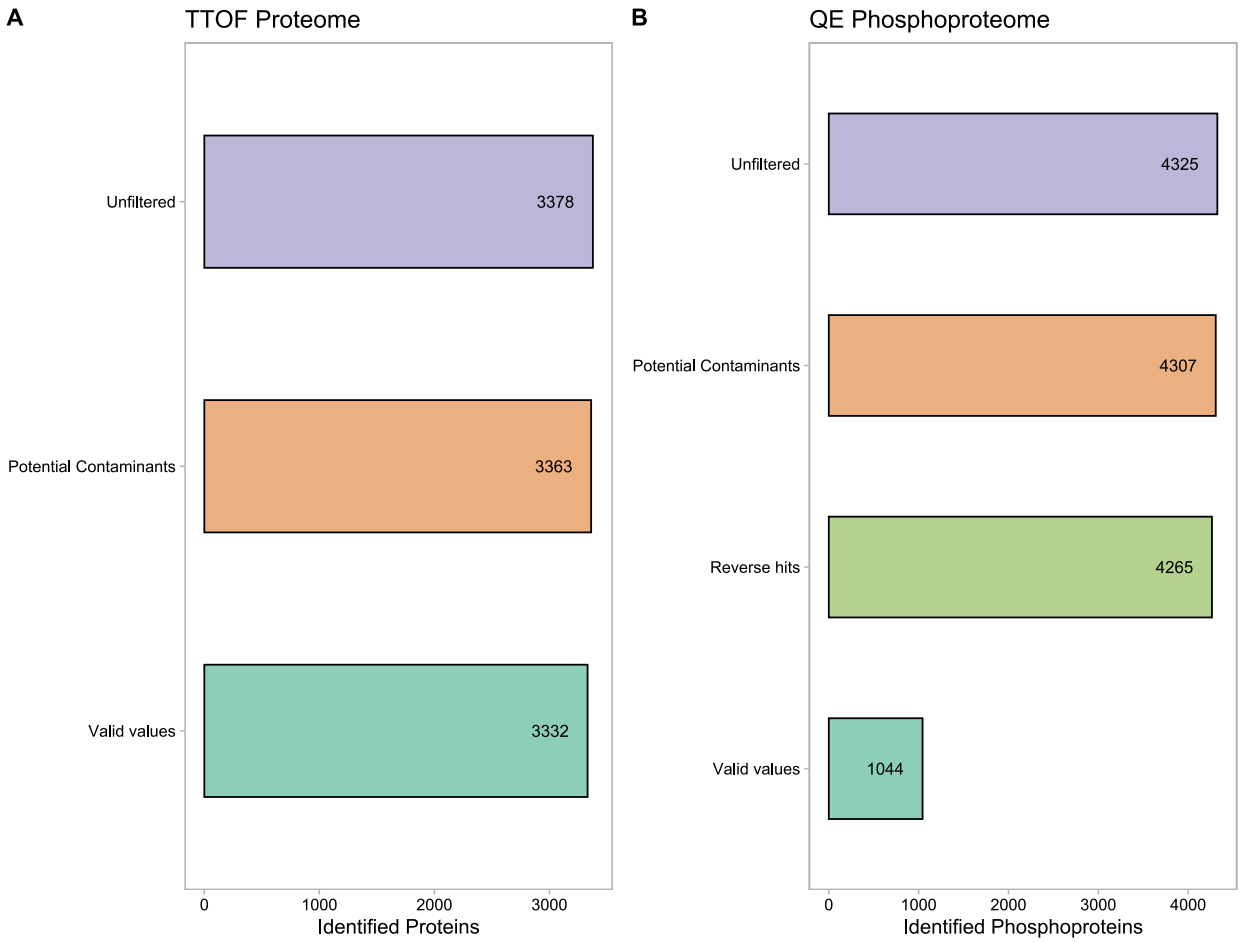

Figure 2.5: Data were processed in Perseus to remove false hits and contaminants. Valid values were selected for by filtering 2 of 3 replicates in any experimental condition having an intensity value. This is inclusive of both the (A) TTOF proteomic and (B) QE phosphoproteomic mouse data after normalisation.

2.3.2. Mouse Proteome & Phosphoproteome Quality Checks & Quantification

Phosphoproteins were normalised against their corresponding unmodified QE protein group intensity values before analysis. To ensure perceived differences in protein expression between ACE 10/10 and WT TPM macrophages were reproducible, the Pearson's co-efficient was determined for group comparisons **(Figure 2.6)**. Overall, a strong correlation between ACE 10/10 and WT murine macrophages was observed across the proteome (0.9 - 0.99) and phosphoproteome (0.7 - 0.94). Despite fewer phosphoprotein identifications and a Pearson's co-efficient ranging from 0.3 - 0.8 for ACE 10/10 Lis-Trp-treated macrophages, the group was maintained for analysis **(Figure 2.6B & Appendix Section 8.2, Figure 8.2)**. The low number of phosphoproteins identified in ACE 10/10 Lis-Trp-treated macrophages may be a biological effect of inhibitor treatment. In addition, some samples

had missing data, as evidenced in hierarchical clustering suggesting some column traps did not bind or elute sample and could not be repeated due to time, cost and sample constraints. Two TTOF proteome and one QE phosphoproteome sample(s) were thus excluded from further analysis, totalling 10 and 11 samples in each dataset, respectively **(Appendix Section 8.2, Figure 8.2)**.

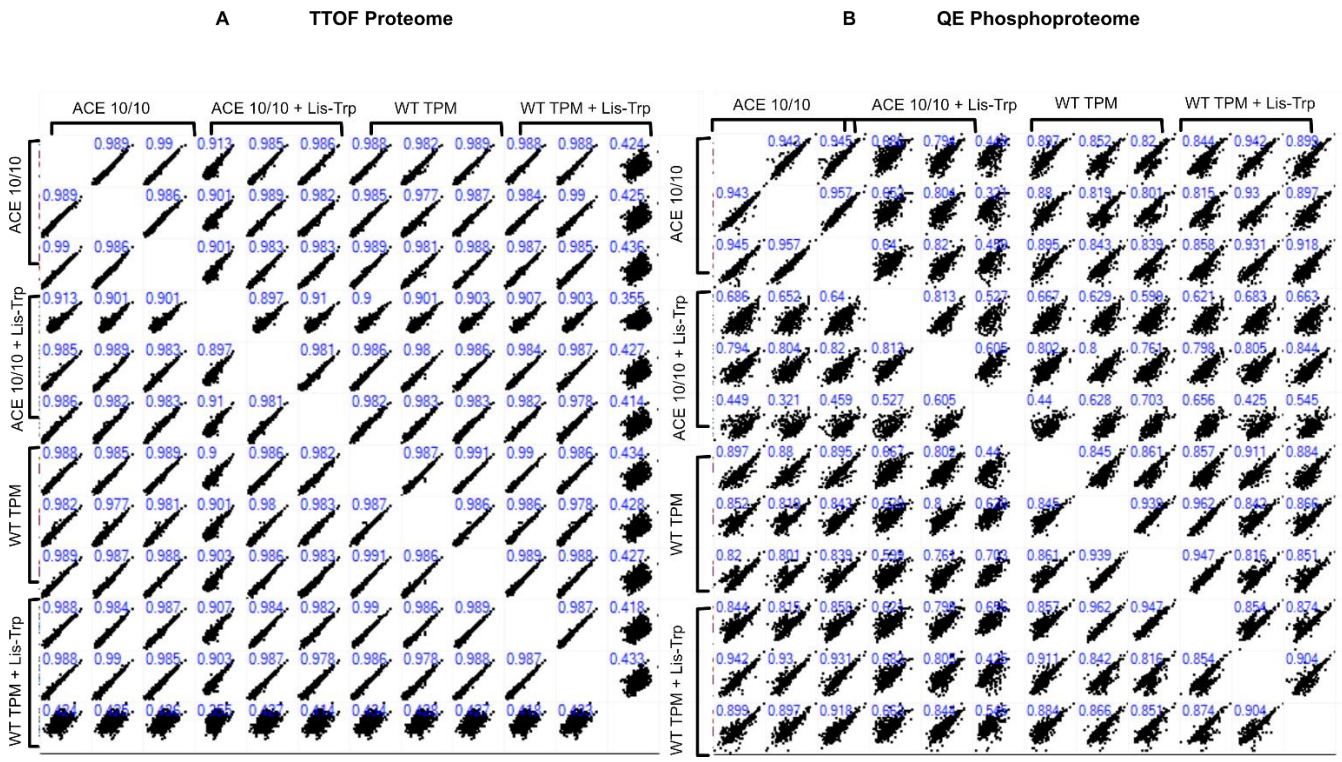

Figure 2.6: Pearson correlations between ACE 10/10 and WT TPM replicate samples. (A) TTOF proteome and (B) the QE phosphoproteome.

2.3.3. The Effect of ACE Overexpression on the Murine Macrophage Proteome

ACE 10/10 macrophages express 16- to 25-fold more ACE than WT macrophages [1,5,6]. After TTOF data clean-up, ACE was detected in only ACE 10/10 samples whilst absent in WT TPM suggesting that it may be below detection in WT samples and evidencing higher expression in ACE 10/10 macrophages.

A Student's t-test identified 270 differentially expressed proteins (p-value ≤ 0.05) across ACE 10/10 and WT TPM proteomes, comprising 118 up-regulated and 152 down-regulated proteins **(Figure 2.7A)**. After Lis-Trp treatment, ACE 10/10 and WT TPM macrophages showed similar proportions of differentially expressed proteins **(Figure 2.7B & C)**; however,

the top 20 differentially expressed proteins were different between treated and untreated macrophages.

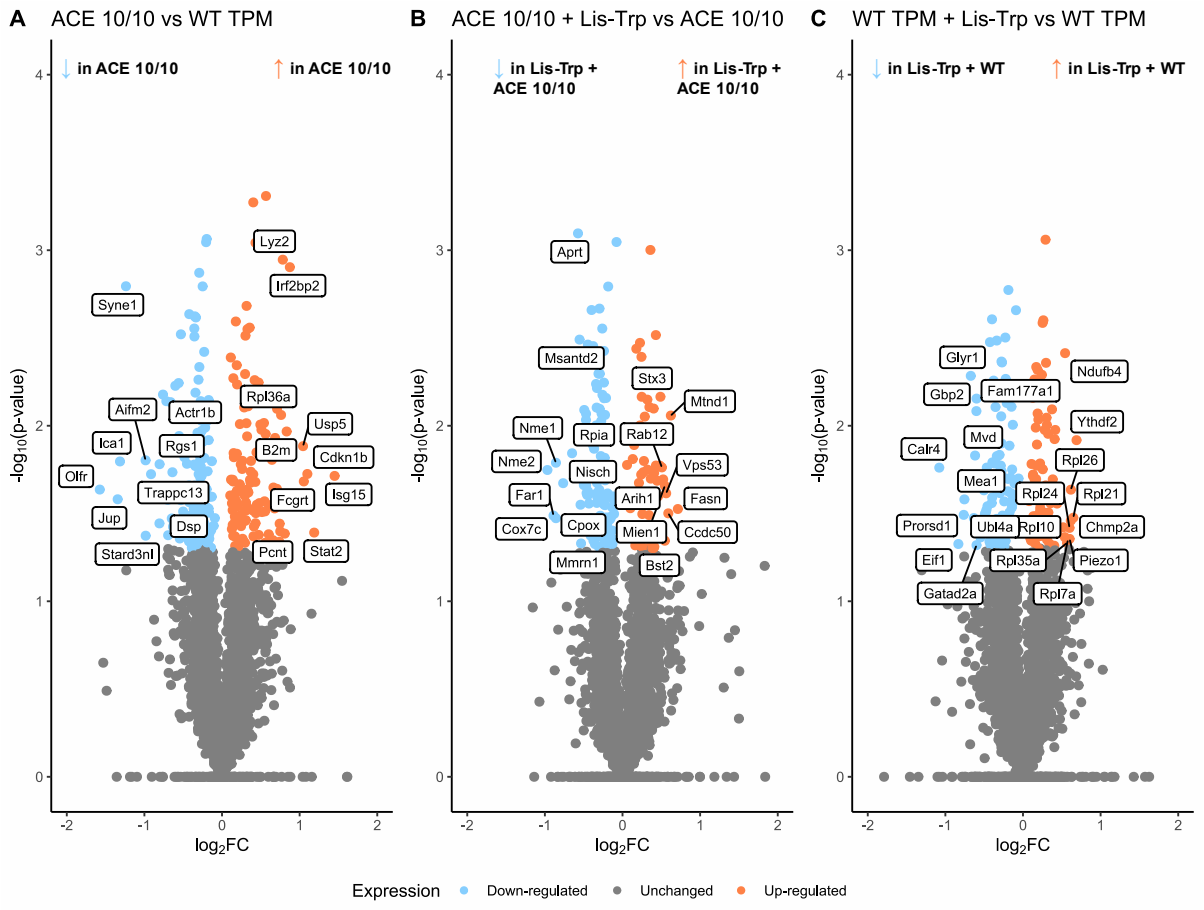

Figure 2.7: Volcano plots comparing differentially expressed (DE) proteins of murine macrophages. Down-regulated proteins are indicated as light blue while up-regulated proteins are indicated in orange. The top 20 differentially regulated proteins are labelled for each comparison. (A) DE ACE 10/10 model proteins in relation to WT TPM control (n = 270). (B) DE proteins of ACE 10/10 Lis-Trp-treated macrophages against ACE 10/10 control (n = 177). (C) DE proteins of WT Lis-Trp-treated macrophages against WT TPM control (n = 190). Analysis using Student's two sample t-test to infer significant differential expression at $p \leq 0.05$. Abbreviations: ACE 10/10 – ACE overexpressing murine macrophage, WT TPM – wild type tumour-bearing peritoneal macrophage, Lis-Trp – lisinopril-tryptophan and FC – fold change.

2.3.4. The Effect of ACE Overexpression & Inhibition on the Murine Macrophage Phosphoproteome

Differential expression is apparent between the ACE 10/10 and WT TPM phosphoproteome **(Figure 2.8A)**. ACE overexpression results in a significant down-regulation (n = 31) of phosphoproteins in comparison to WT murine macrophages, with only one up-regulated

phosphorylated protein (Stx7, an early endosome trafficking protein). Furthermore, protein kinase N1 (Pkn1) and phosphatidylinositol 3,4,5-trisphosphate 5-phosphatase 1 (Inpp5d/SHIP) were down-regulated in ACE 10/10 macrophages. Inpp5d has phosphatase activity and regulates aspects of myeloid cell recruitment, inflammation, cytoskeletal rearrangement, glucose, and lipid metabolism whilst Pkn1 often mediates cell signalling in apoptosis, cytoskeletal rearrangement, and inflammation. Interestingly, a similar response for both Inpp5d and Pkn1 with both ACE overexpression and WT Lis-Trp treatment is observed. However, Inpp5d was phosphorylated at S972 **(Figure 2.8A)**, and S246, S972 and Y1021 **(Figure 2.8C)** whilst Pkn1 was phosphorylated at T778 **(Figure 2.8A)** and S920 **(Figure 2.8C)**. Variable phosphorylation sites may offer an explanation to the altered myeloid immune functions regarding this inflammatory mediating phosphatase and kinase with respects to ACE overexpression. PhosphoSitePlus identified protein kinase A (PKA) substrates within the dataset, including Inpp5d and several mitogen-activated protein kinase 1 (MAPK1/ERK2;p38) substrates **(Appendix Section 8.2, Table 8.1)**.

ACE C-domain inhibition in both ACE 10/10 and WT TPM cells was able to significantly impact phosphoprotein expression. **Figure 2.8C** shows that 24-hour long Lis-Trp treatment in WT TPM cells resulted in down-regulation of phosphoproteins, with only two up-regulated phosphorylated proteins (Hnrnpa1 and Hcfc1) detected. In contrast, Lis-Trp-treated ACE 10/10 cells had 25 up-regulated phosphoproteins **(Figure 2.8B)**. Hnrnpa1 acts as a transporter protein for polyadenylated mRNA molecules across the nuclear membrane into the cytoplasm. It also modulates splice site selection, likely impacting translation, and transcription regulation in the WT Lis-Trp-treated group **(Figure 2.8C)**. Increased significant phosphoproteins in Lis-Trp-treated ACE 10/10 macrophages **(Figure 2.8B)** had functions related to cell structural stability, cell migration and genome organization. Furthermore, phosphorylated Mdh1 (cytoplasmic malate dehydrogenase) was differentially expressed in Lis-Trp-treated ACE 10/10 macrophages, while its substrate, malic acid, was previously found to be increased in untreated ACE 10/10 macrophages [100]. Further work into altered phosphorylation and signalling of ACE 10/10 macrophages is required as many ACE-mediated immune functions are unknown or poorly understood.

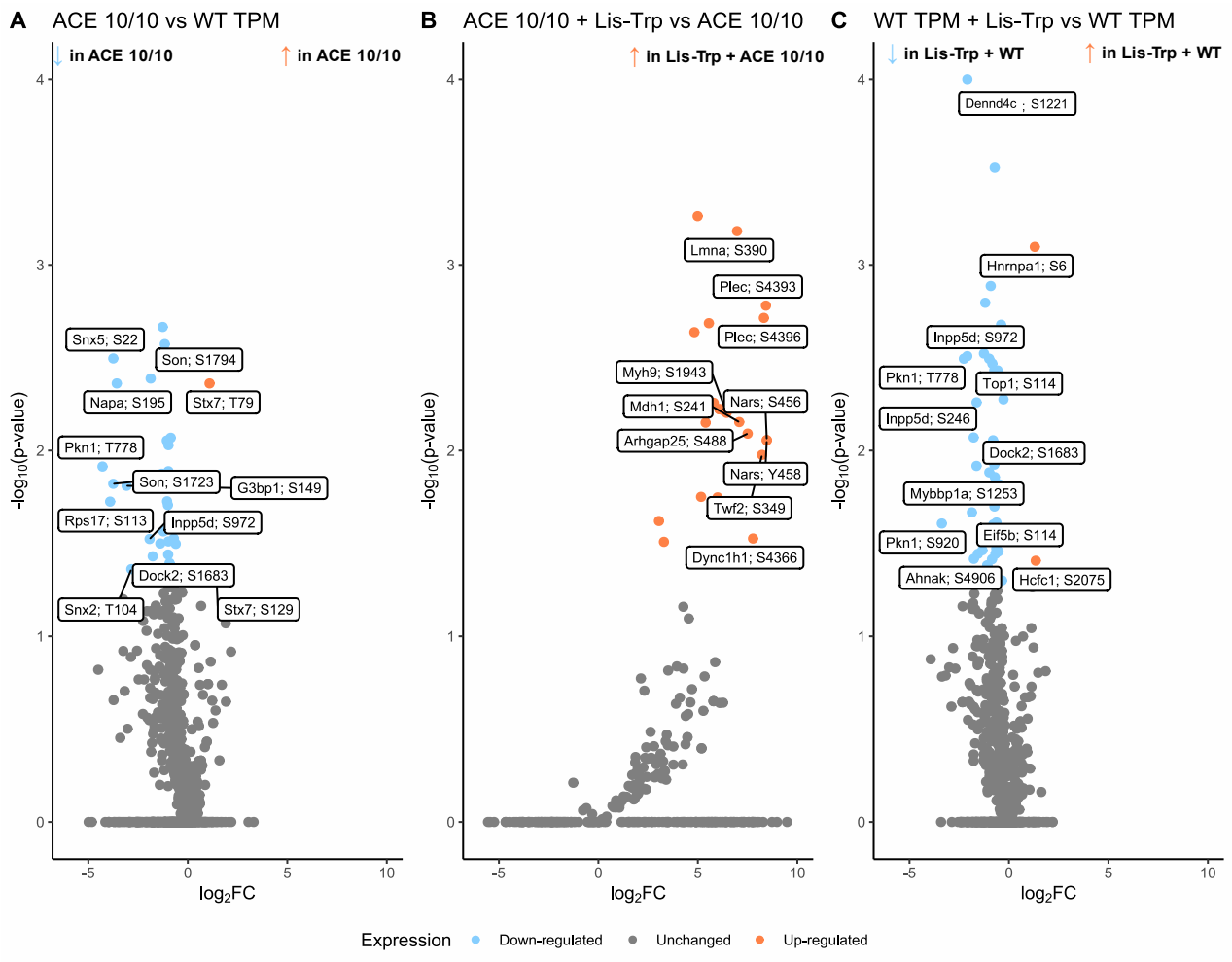

Figure 2.8: Volcano plots comparing differentially expressed (DE) phosphoproteins/phospho-sites (p-sites) of murine macrophages. The top 10 significantly expressed phosphoproteins including those with multiple phosphorylation sites are labelled, down-regulated phosphoproteins are light blue and up-regulated phosphoproteins are orange. (A) The DE phosphoproteins between ACE 10/10 macrophages and WT TPM (n = 33). (B) Differential p-sites between ACE 10/10 Lis-Trp-treated macrophages and ACE 10/10 control (n = 25). (C) DE of WT Lis-Trp-treated macrophages analysed against WT TPM control (n = 53). Analysis using Student's two sample t-test to infer significant differential expression at $p \leq 0.05$. Abbreviations: ACE 10/10 – ACE overexpressing murine macrophage, WT TPM – wild type tumour-bearing peritoneal macrophage, Lis-Trp – Lisinopril-tryptophan and FC – fold change.

2.3.5. Network Signalling in the ACE 10/10 Macrophage Proteome

Network and functional cluster analysis revealed several enriched processes highlighting diverse roles for ACE. Several lipid transport and lipid droplet or oxidation proteins are enriched within the ACE 10/10 model potentially suggesting a novel metabolic and potentially mechanistic factor for ACE involvement in immunity. **Figure 2.9** shows a complex

interaction network with clusters highlighting RNA metabolism, TCA intermediates and their respective enzymes such as mitochondrial malate dehydrogenase (Mdh2).

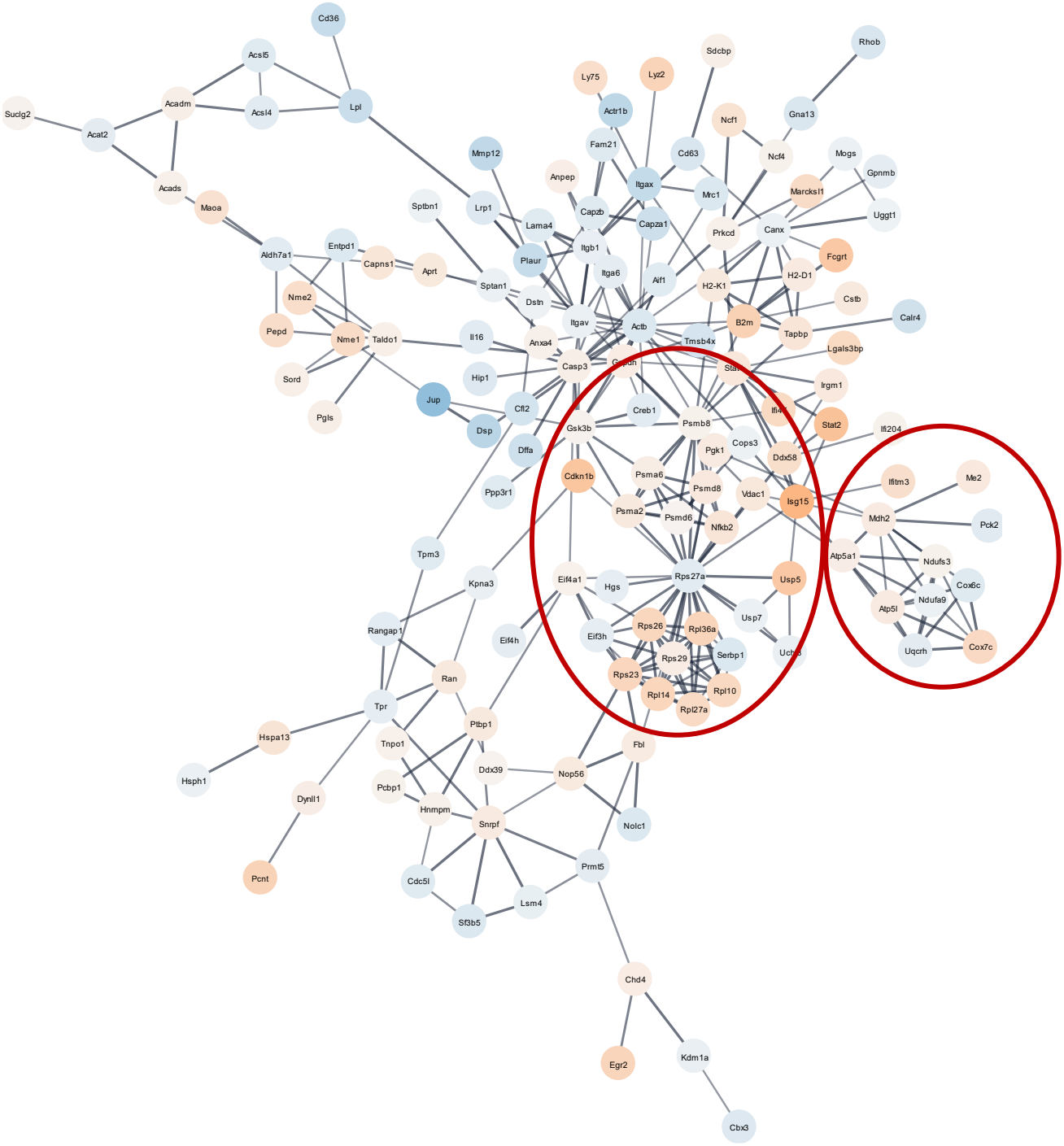

Figure 2.9: STRING interaction network between differentially expressed proteins of ACE 10/10 and WT macrophage controls. Set to 0.7 confidence score, line thickness set as confidence score. Orange nodes are up-regulated proteins and blue nodes are down-regulated proteins. Red circles are clusters of interest.

The clusters in **Figure 2.9** with high evidence for interactions, contain several components involved in proteasomal degradation and ribosomal assembly. Importantly, the NF-κB transcription factor (Nfkb2) is present indicating some regulatory control over proteasome and ribosome assembly, which is likely influenced by pro-inflammatory responses of ACE 10/10 macrophages. **Figure 2.10B** highlights a smaller TCA and ETC-linked cluster where ATP synthase (Atp5a1 and Atp5l) is up-regulated in ACE 10/10 macrophages alongside Mdh2 and Me2 (malic acid enzyme). However, this cluster does not clearly indicate ETC and TCA up-regulation in ACE 10/10 macrophages, as some components of the respiratory chain were up-regulated (Cox7c and Ndufs3) whilst others were down-regulated (Cox6c, Ndufa9 and Uqcrh). Both clusters also have immune links, particularly due to the presence of Stat1, Stat2, Isg15, Ifitm3, Pkg1 and Ifi47 as members of interferon-activated inflammatory responses.

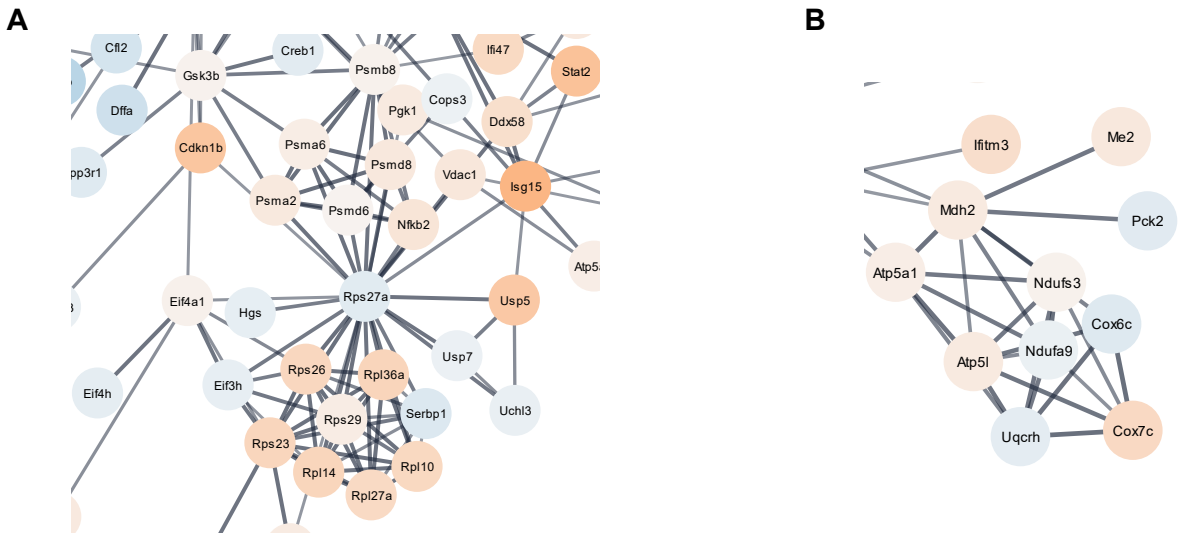

Figure 2.10: Enlarged protein clusters present in ACE 10/10 macrophages. (A) Proteasomal and ribosomal component clusters and (B) TCA, ATP synthase and respiratory chain cluster. Orange nodes are up-regulated proteins and blue nodes are down-regulated proteins compared to WT macrophages.

2.3.5.1. Functional GO Term Enrichment Analysis in ACE 10/10 Macrophages

Biological process functional enrichment between ACE 10/10 and WT TPM macrophages was broad. Importantly, several glycolysis- and immune-related proteins within these functionally enriched clusters were up-regulated in support of previously published data on the ACE 10/10 murine model. Overarching enriched terms such as lipid metabolic processes (GO:0006629), NADP metabolism (GO:0006739), RNA-metabolism (GO:0016070) and actin

cytoskeleton organisation (GO:0030036) are roles that have not yet been explored in ACE 10/10 macrophages **(Figure 2.11)**. The presence of Inpp5d/SHIP and Pkn1 within the phosphoproteomic data can also be linked to the actin cytoskeletal enrichment of ACE 10/10 macrophages. Interestingly, KEGG analysis highlighted lipid metabolism mediator peroxisome proliferator-activated receptor (PPAR) signalling (mmu03320) enrichment and had down-regulation of the following participating proteins: Cd36, Lpl, Acsl4 and Acsl5.

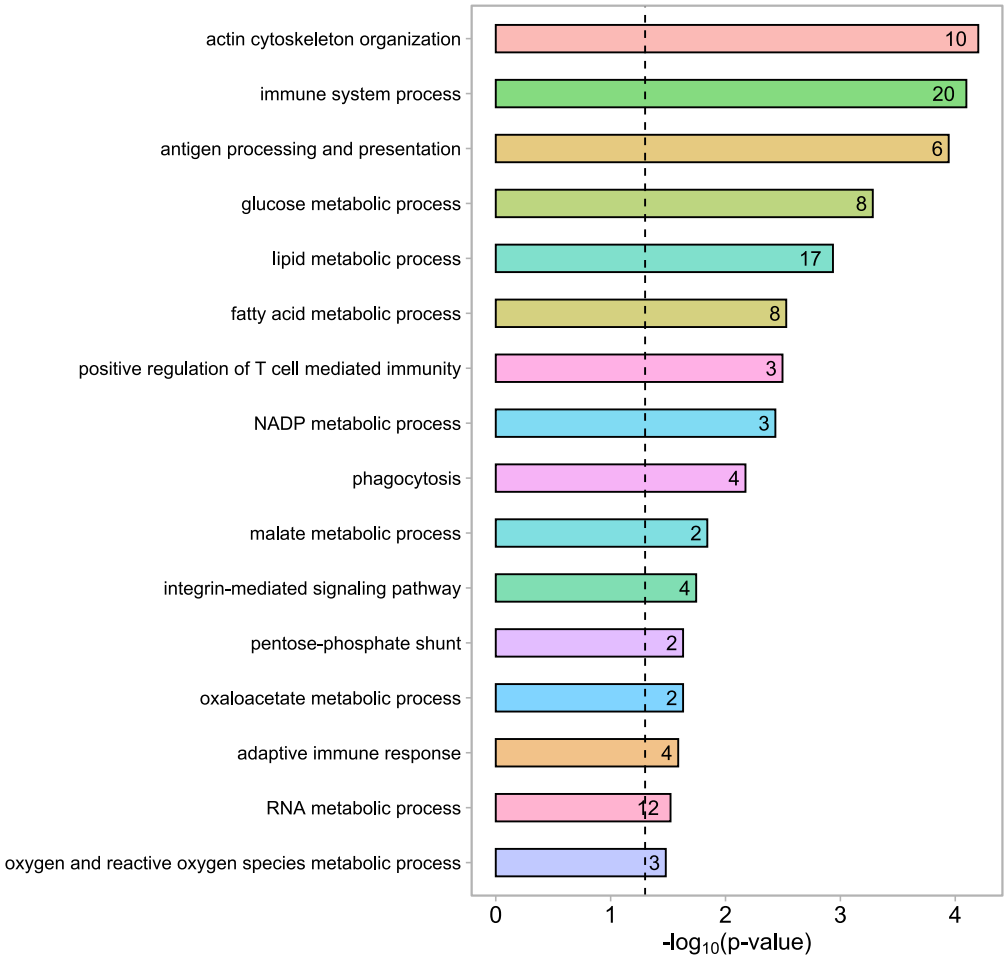

Figure 2.11: Biological process GO term enrichment analysis of ACE 10/10 macrophages. Dashed line indicates significance threshold where $p \leq 0.05$. The number of proteins identified in each functional cluster is shown.

In unstimulated ACE 10/10 macrophages, using STRING and functional enrichment analysis, it can be concluded that ACE overexpression regulates immune-related processes such as antigen processing and presentation, and leukocyte activation and migration. Their immunoreactive state, practicing sophisticated regulation and conservation of energy pools.

2.3.6. Network & Functional Enrichment of ACE C-domain inhibition on ACE 10/10 Macrophages

After 24-hours of ACE inhibitor (Lis-Trp) treatment, ACE 10/10 macrophages had reduced proteasomal complex and mitochondrial respiratory chain expression, particularly NADH dehydrogenase proteins. These interactors were thus significantly affected by ACE C-domain inhibition **(Figure 2.12 &Figure 2.13)**.

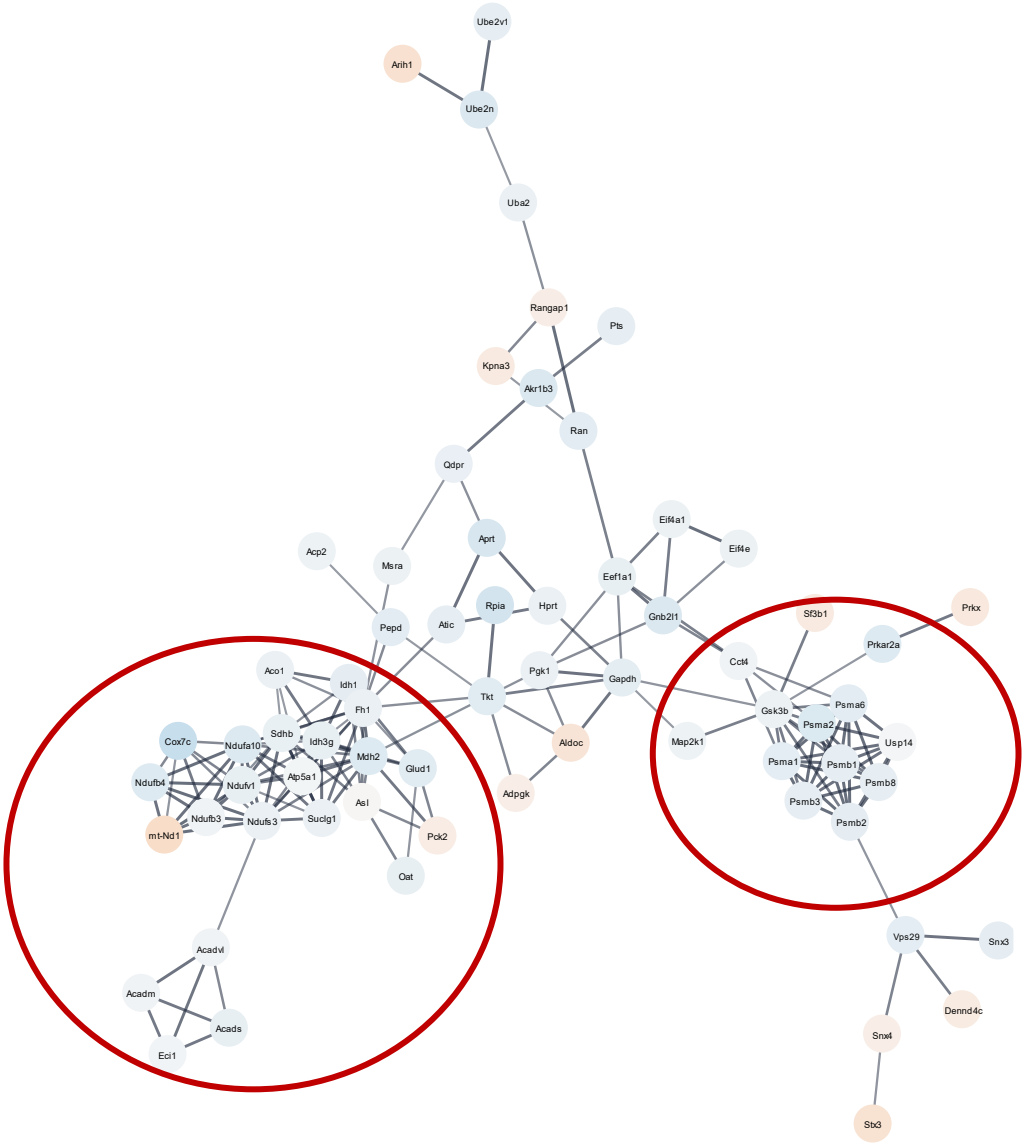

Figure 2.12: Network generated from ACE 10/10 and ACE 10/10 Lis-Trp treatment comparison. The interaction network was generated with a confidence score of 0.7. Orange nodes are up-regulated proteins and blue nodes are down-regulated proteins. The two circled areas show functional clusters.

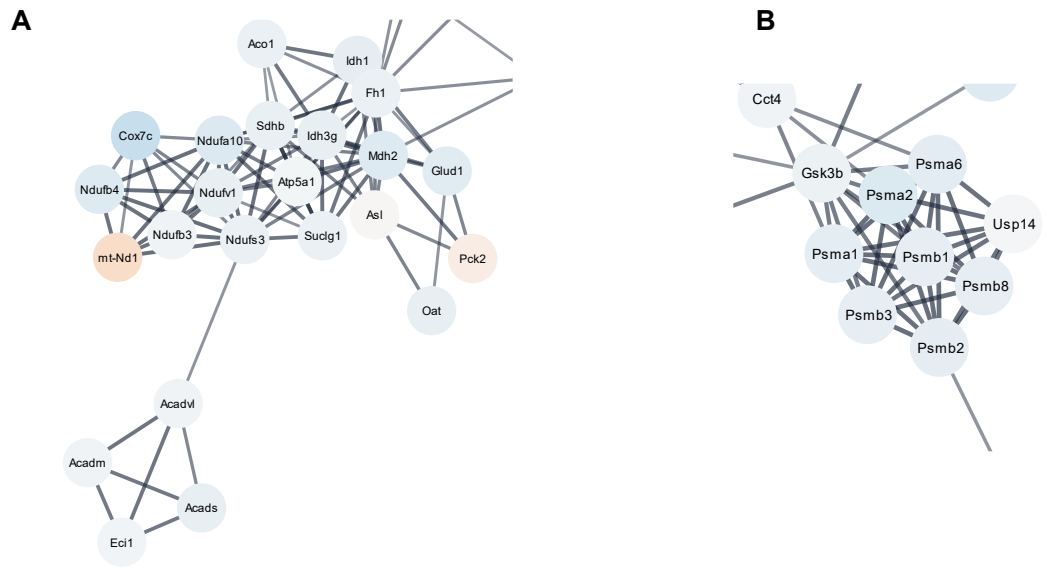

Figure 2.13: Enlarged functional clusters in Lis-Trp-treated ACE 10/10 macrophages. (A) Cluster of mainly respiratory and energy producing protein components. (B) The proteasomal cluster. Confidence score is at 0.7 and proteins are coloured according to expression levels as up-regulated (orange) and down-regulated (blue) with reference to control ACE 10/10 macrophages.

ACE C-domain inhibition in ACE overexpressing macrophages resulted in cellular respiration and glycolysis (GO:0006096), non-oxidative shunts (GO:0009052) and aerobic respiration (GO:0009060) enrichment **(Figure 2.14)**. Once more, actin cytoskeletal organisation, lipid metabolism and RNA metabolism enrichment was present, and the proteins in these biological pathways were largely down-regulated following Lis-Trp treatment. The TCA cycle and intermediate component metabolism for oxaloacetate, succinate and malate were also functionally enriched but were significantly down-regulated in comparison to untreated ACE 10/10 macrophages.

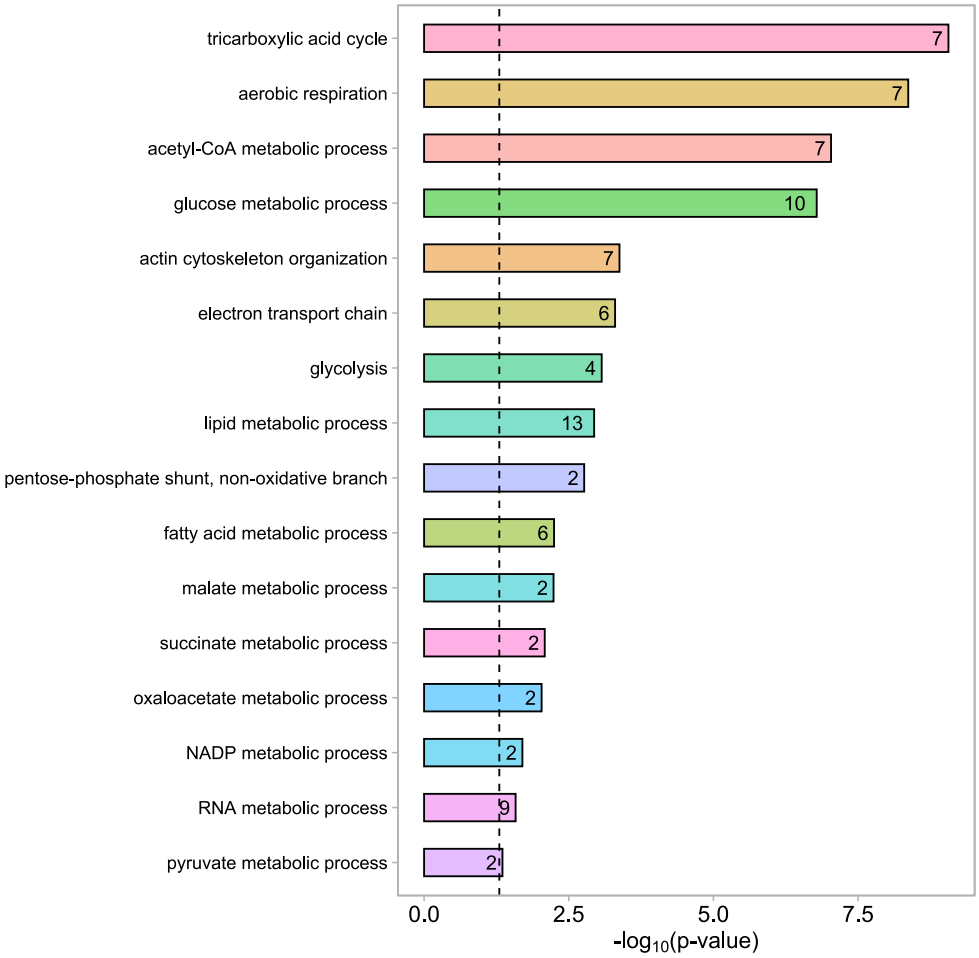

Figure 2.14: ACE C-domain inhibition by Lis-Trp impacts several ACE 10/10 macrophage biological processes. Dashed line indicates significance threshold with p-value ≤ 0.05, proteins present in each cluster are indicated.

2.3.7. Network & Functional Enrichment Analysis of Lis-Trp-treated WT Murine Macrophages

A network of the significantly dysregulated proteins between control WT TPMs and Lis-Trp-treated TPMs has a notable increase in ribosomal component expression with Lis-Trp treatment **(Figure 2.15)**. ATP synthase proteins were elevated in control ACE 10/10 macrophages in comparison to WT, but ATP synthase components were down-regulated in Lis-Trp-treated ACE 10/10 macrophages and Lis-Trp-treated WT macrophages **(Figure 2.9 &Figure 2.13)**. Importantly, Lis-Trp treatment also decreased the expression of Golgi-ER and vesicle trafficking proteins.

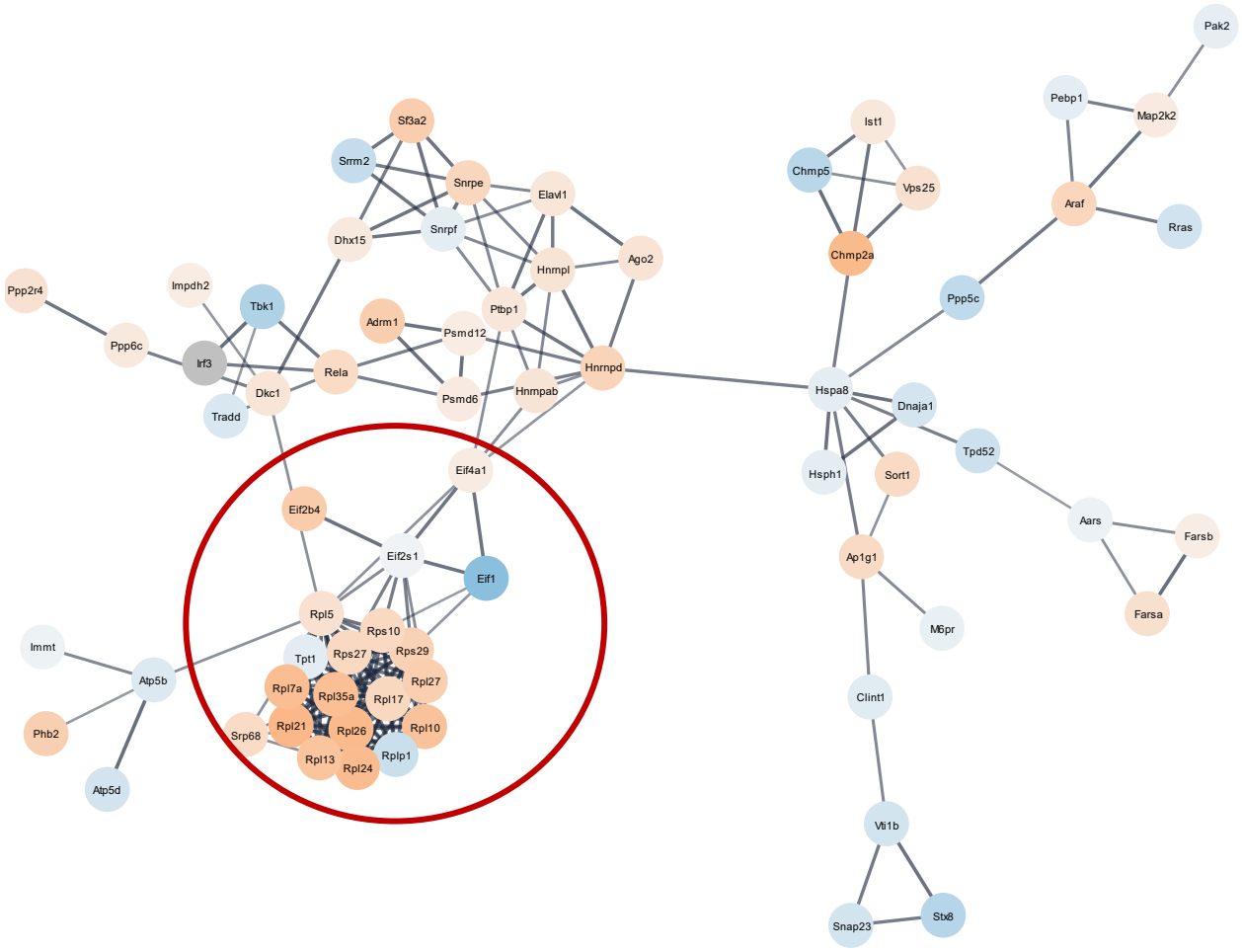

Figure 2.15: Network analysis of dysregulated proteins between Lis-Trp WT TPMs and control WT TPMs. Confidence score of 0.7. Blue nodes are down-regulated, and orange nodes are up-regulated proteins in Lis-Trp WT TPMs.

WT Lis-Trp treatment had PPAR signalling enrichment in contrast to Lis-Trp-treated ACE 10/10 macrophages. ACE C-domain inhibition in WT macrophages had overrepresented and up-regulated ribosomal and RNA modification networks **(Figure 2.15 &Figure 2.16)**. Lis-Trp treatment had only negative actin cytoskeleton regulation functional enrichment, suggesting decreased cell movement and phagocytic abilities in WT macrophages after ACE C-domain inhibition.

Noting significantly dysregulated Pkn1 and Inpp5d/SHIP with Lis-Trp treatment of WT macrophages, ACE C-domain inhibition likely disrupts several signalling pathways and affects protein synthesis or trafficking through its influence on cytoskeletal-, phosphorylation- and RNA-associated functions. The altered phosphorylation and activity of these kinases and phosphatases also influences immune regulation particularly as SHIP negatively mediates

inflammation and inhibits myeloid cell recruitment that is activated by ACE. ACE 10/10 and WT macrophages may experience immune disruption with Lis-Trp treatment, as the IL-12 and IL-1 cytokine activation pathways were overrepresented in the inhibitor-treated lysates with down-regulation of the identified proteins.

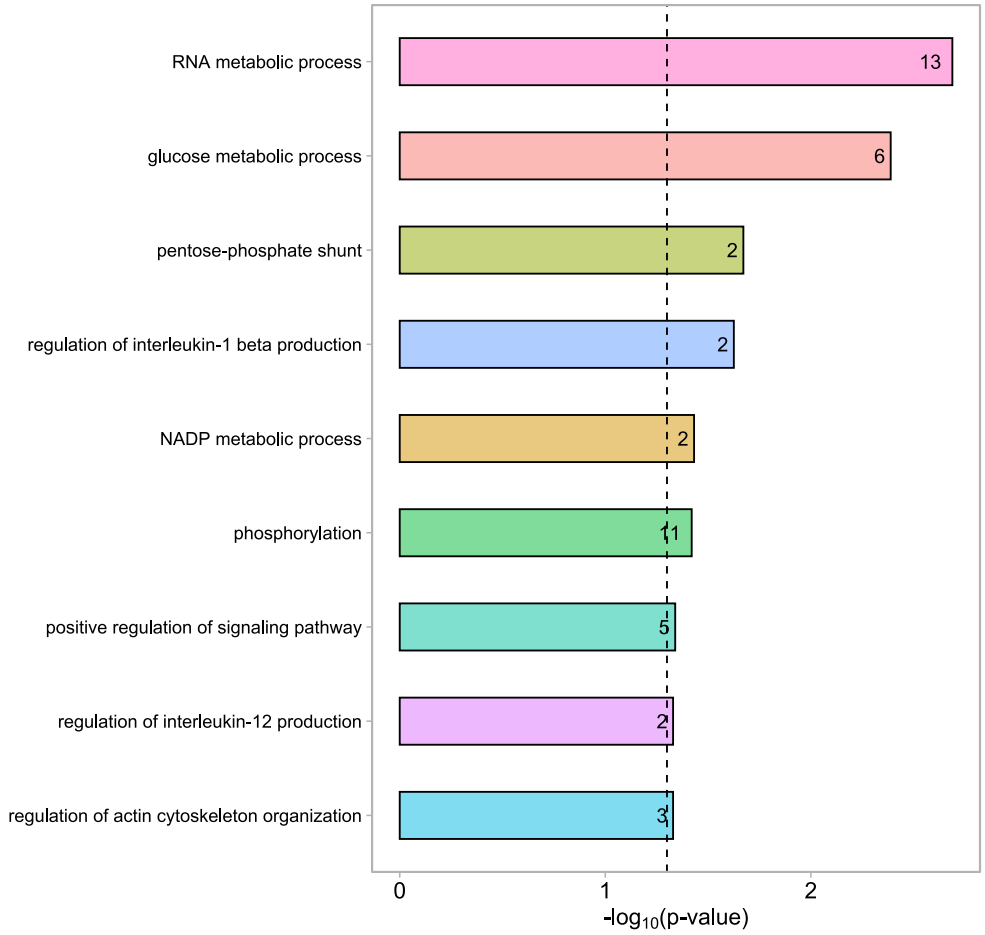

Figure 2.16: Functionally enriched GO biological processes in WT macrophages with ACE C-domain inhibition. Dashed line indicates significance threshold of $p \leq 0.05$. The number of proteins in each cluster is shown.

2.4. Discussion

In this study, MS-based global discovery analysis of the basal murine ACE 10/10 macrophage proteome and phosphoproteome was used to identify a wider range of pathways and proteins regulated by ACE overexpression. The impact of ACE C-domain inhibition was also assessed. Enrichment of lipid metabolism was observed, including transport, catabolism, storage, and oxidation processes that have not yet been studied in the context of macrophage ACE overexpression. Importantly, the study also confirmed the presence of

significantly expressed ATP synthase, TCA enzymes, and antigen processing and presentation proteins as previously identified in ACE 10/10 macrophages through targeted MS and *in vivo* and *in vitro* assays [15,100,132]. ACE inhibition down-regulated, and thus likely disrupted, several immune-related pathways but increased the levels of ribosomal proteins. Within the phosphoproteome, proinflammatory ERK2/MAPK1 and PKA substrates were significantly enriched whilst the phosphatase, Inpp5d/SHIP, and kinase Pkn1 were significantly down-regulated with both ACE overexpression and Lis-Trp treatment of WT macrophages.

ACE overexpression is beneficial in immune-challenged murine macrophages, which remain under strict immunological control. However, certain functions and pathways are more active in basal ACE 10/10 macrophages [6,100]. At baseline, unstimulated ACE 10/10 macrophages may have a proteome that resembles a primed immune phenotype, which is ready to respond accordingly when required.

ACE 10/10 macrophages had a distinctive differential proteome and phosphoproteome to WT murine macrophages. In support of Cao *et al.* [100], the ATP synthase complex proteins Atp5a1 and Atp5l were significantly up-regulated in ACE 10/10 macrophages as well as TCA-related proteins Suclg2 and Mdh2. The resulting increase in the production of ATP and TCA intermediates after stimulation provides energy and potential antimicrobial building blocks for the enhanced immune phenotype [64,92]. In the present study, several other significantly expressed proteins of interest were identified including the transcription factors NF-κB, Stat1 and Stat2, which were up-regulated in ACE 10/10 macrophages when compared to their WT counterparts. The classical M1 macrophage phenotype has greater NF-κB and Stat1/Stat2 activation regulating pro-inflammatory pathway expression, and this can be confirmed via in depth phosphoproteomic and western blot analysis. Both increased NF-κB and Stat1 activation are thought to act in ACE overexpression by driving the M1 phenotype after melanoma stimulation [6,133]. These transcription factors are likely related to the observed enriched interferon (GO:0060338) and integrin-mediated pathways (GO:0007229) which favour glycolysis and inflammatory responses [134]. Previously observed processes, including antigen presentation (GO:0019882), ROS metabolism (GO:0006800), phagocytosis (GO:0006909), NADH metabolism (GO:0006739) and glucose metabolic processes (GO:0006006) were overrepresented in ACE 10/10 macrophages. From

these MS results, ACE overexpression appears to strongly dysregulate multiple immune-related pathways and has increased ATP synthase and ribosomal expression for improved protein synthesis, MHC processing via proteasomal degradation and MHC Class I antigen presentation. Furthermore, actin cytoskeletal organization (GO:0030036) is under sophisticated control in relation to cell migration and movement, and the observed down-regulation of several actin and tubulin protein components suggests that ACE 10/10 peritoneal macrophages require stimulation before enhanced phagocytic and leukocyte migration is available [5,100].

Additionally, lipid transport (GO:0006869) and metabolism (GO:0006629), specifically the acetyl-CoA oxidative branch (GO:0033539) are influenced by ACE overexpression as evidenced by their functional enrichment. Acads & Acadm, fatty acid oxidation proteins, were elevated in the ACE 10/10 macrophages compared to in WT macrophages and may potentiate macrophage differentiation and specialization in murine and human macrophages [135]. M1 macrophages require lipid and acetyl-CoA synthesis as precursors of inflammatory molecules and for inflammasome activation, whilst M2 macrophages favour fatty acid oxidation as a means of activating anti-inflammatory responses to down-regulate NO and ROS production [136–138]. However, several studies have countered that macrophage polarization is dually regulated by lipids, where both M1 and M2 macrophages require both glycolysis and fatty acid oxidation to function properly [138]. In bone marrow-derived macrophages (BMDMs), Huang *et al.* stunted M2 marker expression via glycolytic inhibition. External fatty acid sources were ignored in favour of glucose when present in the culture medium [139,140]. Furthermore, NLRP3 inflammasome activation, an M1-defined property, requires fatty acid oxidation via CPT1 and ROS generation [138,141]. ACE overexpression may be utilizing mixed lipid metabolism, mediated by PPAR. PPAR strongly regulates both inflammatory macrophage responses and lipid metabolism [142–144]. Additionally, ACE 10/10 macrophages may increase ATP synthesis to maintain their TCA cycle components for acetyl-CoA production, where fatty acids are precursors of inflammatory mediators when activated or protectors of the resting state and their oxidation will reduce inflammatory molecules [135,136,138–141].

In the phosphoproteome, ACE 10/10 macrophages and WT macrophages appear to differ mostly through MAPK1/ERK2 phosphorylation sites across multiple proteins. Ang II mediates

dendritic cell maturation via the NF-κB and ERK1/ERK2 signalling pathways and induces ACE up-regulation and ACE2 down-regulation through MAPK/ERK signalling [145–148], but current ACE 10/10 studies have not identified participating kinase(s) in the enhanced phenotype. Since ERK2/MAPK1 and PKA targets were identified in the differentially expressed phosphoproteome of ACE 10/10 macrophages, it follows that targeting these kinases could result in reduced immunity to certain challenges, but these may be Ang II-dependent signalling. This is particularly important for the MAPK/ERK pathways which regulate pro-inflammatory activation in macrophages [149,150]. ERK2 may favour activation over inhibition, based on the up-regulation of pro-inflammatory transcription factors and innate immunity proteins [133,149]. PKA is also associated with positive regulation of macrophage differentiation and activation and acts by direct activation of the ERK1/ERK2 signalling cascade [151].

ACE overexpression had reduced phosphoproteins in comparison to WT macrophages apart from Stx7, an endosomal trafficking protein. The down-regulated phosphatase, Inpp5d and kinase Pkn1 in ACE 10/10 macrophages fall under cytoskeletal rearrangement in agreement with the ACE 10/10 proteome where cytoskeletal organization is negatively regulated but also negatively modulate inflammatory responses as part of the PI3K signalling pathway. For instance, Inpp5d prevents myeloid cell recruitment in contrast to ACE which activates this process [152,153]. Inpp5d phosphorylation of S440 by PKA increases its activity [154] whilst ACE inhibition may promote the immunosuppressive function of Inpp5d tyrosine phosphorylation and its association with the Shc adaptor protein as evidenced by the Y1021 phosphosite in Lis-Trp-treated WT macrophages which also promotes its proteasomal degradation and reduces its expression [155,156]. Our data did not identify the S440 phosphosite in ACE 10/10 and WT macrophages. The S246 Inpp5d phosphosite in WT macrophages and S972 identified in both ACE 10/10 and WT macrophages does not have functional changes associated with it, however Ser/Thr SHIP phosphorylation does control its targeting and is correlated to B cell receptor signalling which could be enhanced with ACE up-regulation [157–159]. Pkn1 is a fatty acid and phospholipid-activated kinase in the Rho GTPase family. It is highly expressed in lymphoid tissues and its absence results in spontaneous autoimmune-like conditions in mice. It is therefore vital to lymphocyte, including macrophage, trafficking, and its activation by the T778 and S920 phosphosites is

required [160]. These sites were identified in our dataset for Lis-Trp-treated WT macrophages and was lower in comparison to WT macrophages. Pkn1 may be less active with ACE inhibitor treatment resulting in dampened lymphocyte trafficking and macrophage adherence and recruitment. Only the T778 phosphosite was present in the ACE 10/10 macrophage dataset and was also lower in comparison to WT macrophages, here Pkn1 is likely not fully active in ACE 10/10 macrophages.

The combination of ACE overexpression and Lis-Trp inhibition resulted in a distinctive phosphoproteome with only up-regulated proteins. Prior investigations have identified a phosphorylation site, Ser^{1270} within the ACE cytoplasmic tail. This site is phosphorylated by serine kinase CK2 and ACE phosphorylation is doubled with ACE inhibitor interaction, also known to increase ACE expression [161–164]. ACE is therefore both directly and indirectly involved in the ACE signalling cascade associated with MAPK7, STAT activation and AP1 transcription factor binding [29]. Unexpectedly, no CK2 enrichment or ACE Ser^{1270} phosphorylation was present with ACE inhibitor treatment, but this pathway activation has only been recorded in endothelial and adipocyte cells and not immune cells [165,166]. The ACE 10/10 macrophage phosphoproteomic data in the present study suggests that there is increased phosphorylation signalling related to MAPK and PKA. However, PKA has not been known to interact with the ACE cytoplasmic tail despite the presence of a theoretical phosphorylation site and requires further study [162,163]. ACE phosphosite data such as Ser^{1270} may be in low abundance despite enrichment and targeted analysis could identify novel sites.

The ACE 10/10 proteome was also significantly altered with Lis-Trp treatment. Previously, ACE C-domain inhibition or knockout in ACE overexpressing murine macrophages and neutrophils was associated with a reduction of ATP, TCA cycle intermediates and cytokines to WT levels [100,133,167]. In the present study, the TCA cycle (GO:0006099), glycolysis (GO:0006096), and the ETC (GO:0022900) were enriched in the ACE 10/10 proteome under Lis-Trp treatment, with significant down-regulation in these pathways in comparison to untreated ACE 10/10 macrophages. These results support an active C-domain requirement for the enhanced immune phenotype associated with ACE overexpression in mice and suggest that a 50 μM Lis-Trp treatment was sufficient to disrupt this [5,99,100,133]. In WT macrophages, the proteomic changes were lower in magnitude with different functional

enrichment to those of ACE 10/10 macrophages. However, as with ACE 10/10 macrophages, C-domain inhibition also caused down-regulation of Atp5b and Atp5d (ATP synthase complex V), which supports a decrease in ATP production. With Lis-Trp treatment, WT macrophages up-regulated their ribosomal and RNA metabolic proteins (GO:0016070) and phosphorylation (GO:0016310) indicating altered spliceosome and PTM patterns. Reactome pathway analysis provides an interesting hypothesis for ACE C-domain inhibition and ribosomal component up-regulation in WT macrophages. The overrepresentation of L13a-mediated translational silencing (Reactome: MMU-156827) is a pathway identified in humans and mice that is highlighted during inflammatory regulation [168,169]. In atherosclerosis, L13a deficiency results in aggravating sclerotic plaque generation and worsens symptoms [170,171]. Thus, in WT macrophages the translational control exerted by L13a may be reducing inflammation and preventing cytokine production during ACE C-domain inhibition, thus providing some protection in autoimmunity and risk in healthy individuals [170]. However, the role ACE inhibition plays in downstream signal cascades is poorly understood, and the changes presented here require further exploration [5,163].

Previous publications have identified several ETC and TCA proteins that were absent from the current dataset. Their absence suggests that a deeper compartmental discovery proteomic approach is needed [5,57,100,153,172]. To remedy this, lysates could be fractionated into nucleus, mitochondrial and cytoplasmic portions. Taking one step further, macrophage populations are heterogeneous in the absence of stimulation or polarizing cytokines and protein expression may not be the only mechanism by which ACE overexpression alters macrophage function. Therefore, single-cell proteomics could facilitate further understanding of ACE 10/10 macrophage specialization, and spatial proteomics would add to the 3D landscape of where proteins are localised, and their functional specialisation as has been previously investigated in THP-1 macrophages [173–175]. Spatial analysis, i.e., identifying protein migration patterns, if any, in ACE 10/10 macrophages may present a new component of the puzzle that is enhanced immunity from ACE overexpression [175]. This could also resolve the issue of poor protein overlap between conditions that was observed in the present study. Furthermore, the phosphoproteomic profile recovered represents long-term phosphorylation and does not reflect the dynamic changes that occur within minutes of treatment. To fully understand the phosphoproteome

and altered signalling cascades of Lis-Trp treatment, future experiments should focus on isolating an immediate snapshot within an hour of inhibitor addition to allow intracellular uptake.

In summary, ACE C-domain inhibition decreased immune regulatory, ETC and ATP synthase-related proteins, which could ultimately lead to a reduction in the pro-inflammatory immune responses in both WT and ACE 10/10 macrophages. Furthermore, WT macrophages appear to up-regulate translational silencing as an anti-inflammatory mechanism upon Lis-Trp treatment. Phosphoproteomic studies identified MAPK1 and PKA pathways, the phosphatase Inpp5d and Pkn1 kinase as proteins of interest in downstream signalling of the ACE 10/10 phenotype particularly as all practice some form of immune regulation. Mass spectrometric analysis of ACE overexpressing murine macrophages confirmed ATP synthase up-regulation suggesting subsequent ATP production and increased TCA cycle activity. Furthermore, innate immune pathways such as IFN and integrin-mediated cytokine expression were also up-regulated alongside MHC Class I production, stressing a basal M1-leaning polarization. Of great interest is the observation that ACE overexpression also seems to have an impact on lipid metabolism, particularly fatty acid oxidation, which possibly provides ACE 10/10 macrophages with the necessary precursors for improved immunological ability when stimulated. With functional enrichment confirmation of these characteristics in the murine ACE 10/10 macrophages, investigating if human ACE overexpressing macrophages show similar properties is of interest.

3. Lisinopril-Tryptophan Uptake in Human THP-1 Monocyte/Macrophage-like Cells

3.1. Introduction

Angiotensin converting enzyme inhibitors (ACEi) and angiotensin receptor blockers (ARBs) are commonly prescribed to treat heart failure and cardiovascular disease. ACE is vital for maintaining sodium retention and blood pressure as part of the RAAS. Most ACE-related effects occur via Ang II and its interaction with AT_1 and AT_2. Ang II-AT_1 causes vasoconstriction, increased blood pressure and increased sodium retention [59,176,177]. ACE inhibitors prevent this interaction and allow vasodilation to occur. However, current ACE inhibitors also inhibit bradykinin (BK) breakdown as they bind both ACE N- and C-domains. Bradykinin is a member of the Kallikrein-Kinin System (KKS) which exerts natriuretic control over the body [178]. When BK is metabolized by the ACE N-domain, it favours vasodilation through NO production and tubular effects. Therefore, when BK is not degraded by ACE, vasodilatory control is lost. The design of ACE inhibitors should therefore be targeted towards the C-domain for effective control of hypertension while preventing unwanted effects.

Several domain-specific ACE inhibitors or dual ARB/ACEi and NEP inhibitor combination therapies are in development and undergoing safety trials [179–182]. A domain-specific ACE inhibitor of interest is lisinopril-tryptophan (Lis-Trp), a derivative of lisinopril designed to favour the C-domain of ACE over the N-domain **(Figure 3.1)**.

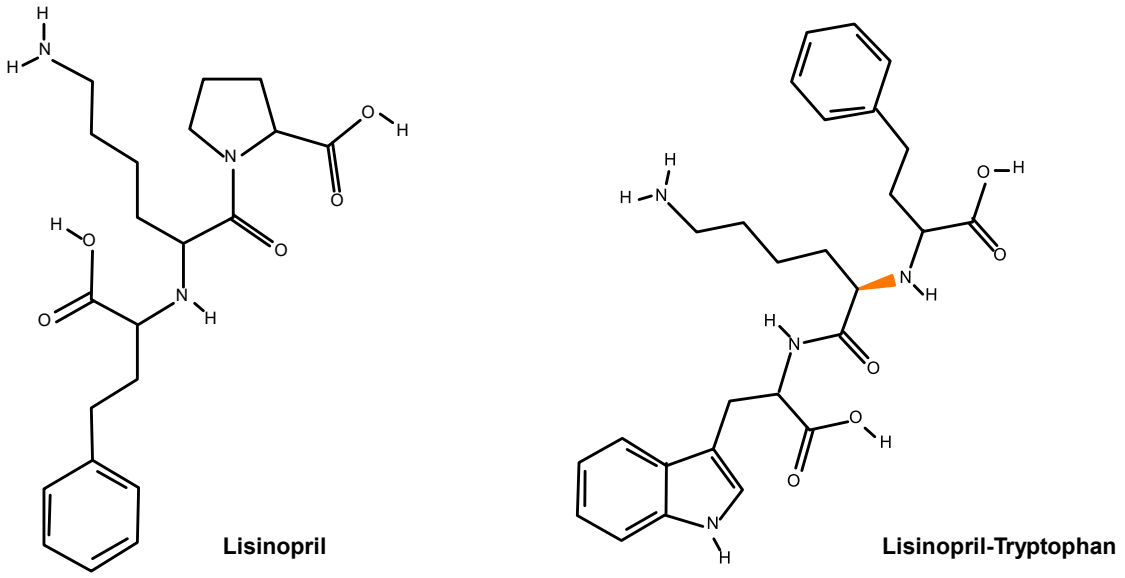

Figure 3.1: Structural schematic of lisinopril and lisinopril-tryptophan. The indole group of Lis-Trp is thought to provide domain selectivity that lisinopril lacks.

3.1.1. Lisinopril versus Lisinopril-Tryptophan (Lis-Trp)

In drug design, important aspects include safety, selectivity, and the associated pharmacokinetics. Although all ACEi are designed to target ACE, their pharmacokinetics and structures differ. Chemically, ACE inhibitors are 2-methylpropionyl-L-proline analogues that bind to the zinc moiety of ACE to exert their inhibitory function [183].

Lisinopril and Lis-Trp both share a carboxylate functional group for binding, but the addition of the tryptophan indole group in Lis-Trp adds domain specificity, allowing the N-domain to retain functionality [183,184]. Both inhibitors share a similar binding mode, however the P_1' and P_2' moieties interact co-operatively with the S_1 and S_2 binding pocket side chains allowing for closer interaction and domain specificity as seen with other C-domain selective inhibitors such as RXP380A [185]. Both are not prodrugs, and are thus minimally processed in the liver, if at all [186–188]. Domain specificity is observed with the different K_i constants shown in **Table 3.1**.

Table 3.1: Recorded inhibitory constants (Ki) of lisinopril and lisinopril-tryptophan using testis ACE (C-domain) and N-domain mutants.

Domain	Lisinopril	Lisinopril-Tryptophan
C (tACE)	1.2 nM	6.6 nM
N	4.8 nM	1700 nM

The domain specificity of Lis-Trp is important as Ang I is mainly cleaved by ACE C-domain whilst BK is cleaved by both domains and contributes to natriuresis and vasodilation. Lisinopril prevents BK metabolism, which in turn causes life-threatening angioedema and a chronic cough associated with ACE inhibitors. These side effects could be avoided by designing a C-domain selective inhibitor, such as Lis-Trp.

3.1.2. Inhibitor Uptake in Immune Cells

There is a lack of research on the bioavailability and uptake of ACE inhibitors in cells. Internal lisinopril concentrations have been measured in Caco-2 cells but ACEi are largely studied in the context of plasma or serum ACE [189]. Although ACE is mainly present in the serum or on endothelial surfaces, it is also intrinsically expressed throughout the body. Therefore, studying how much of these drugs or prodrugs enter other cell types is of interest and necessary for the ongoing safety monitoring of these medications [183,190].

As macrophages and other myeloid-derived cells modulate inflammation, understanding if blood pressure medication affects their activity is important [176,191]. The interaction between ACE inhibition and the immune system is presently unclear, but its impact on autoimmune conditions and infections has been outlined in multiple studies and reviews [56,82,192–194].

3.1.3. Aims & Objectives

In 2021, Cao *et al*. published a pilot study on humans and mice that identified ACEi as a potential risk in post-operative conditions where nosocomial infections are possible [99]. In neutrophils the common ACE inhibitor ramipril has no antimicrobial activity and could decrease extracellular and intracellular bactericidal metabolism in both mice and humans

after a one-week administration [99]. Although this previous study gave a recommended dosage for both ramipril and the ARB losartan (mice only), the intracellular concentration was not measured. The intracellular ACE activity and expression were also not measured within the neutrophils, and it would be interesting to determine if all or partial ACE activity is inhibited.

This information will clarify whether it takes partial or total ACE inhibition to detrimentally impact the function of neutrophils and other immune cells during immune challenge. The aim of the present study was to confirm and quantify the intracellular uptake of Lis-Trp in human THP-1 monocyte/macrophage-like cells.

3.1.3.1. Objectives

- To confirm Lis-Trp entry into THP-1 macrophages using LC-MS/MS.
- To ascertain the intracellular concentration of Lis-Trp in THP-1 macrophages using two different treatment quantities (10 µM and 100 µM) and LC-MS/MS.

3.2. Methodology

3.2.1. Cell Culture Conditions

The human cell line THP-1 was used. Cells that had less than 20 passages were used to prevent genetic or phenotypic variation that could negatively affect results.

The THP-1 cell line is derived from a year-old male suffering from acute monocytic leukaemia and by isolating monocytes from peripheral blood (TIB-202^{TM}, ATCC). THP-1 monocytes are a suspension cell line that requires high density and cell-to-cell contact to proliferate and differentiate into functional macrophages once treated with phorbol 12-myristate-12-acetate (PMA). THP-1 monocytes are widely used in drug interaction and mechanistic studies of human macrophages, resembling peripherally derived macrophages in the human body under specific conditions [91,195–198].

3.2.1.1. THP-1 Monocyte Subculture

An aliquot of THP-1 monocytes was thawed and centrifuged in 10 ml RPMI containing 20% FBS for 5 minutes at 300 x *g* to remove the cryoprotectant, DMSO. The supernatant was discarded, and the cell pellet resuspended in 5 ml of RPMI 1640 supplemented with 20% (v/v) FBS, 1% (v/v) penicillin/streptomycin antibiotic, 10 mM HEPES (4-(2-hydroxyethyl)-

1-piperazineethanesulfonic acid) and 0.2 mM L-glutamine for the initial 24-hour incubation period. Once resuscitated, THP-1 cells were cultured in 5 ml of complete medium (RPMI 1640, 10% FBS, 0.2 mM L-glutamine, and 10 mM HEPES) at a high seeding density of between 5 x 10^5 and 1 x 10^6 cells/ml. If the density exceeded 1 x 10^6 cells/ml, the cells were split. The medium was changed every 2 - 3 days. Standard culturing conditions at 37°C and 5% CO_2 were used for all cultures in a humidified incubator to maintain a constant physiological pH of 7.2 - 7.5.

3.2.1.2. THP-1 Differentiation into Macrophages

To differentiate monocytes into macrophages, standard PMA (Sigma, USA) treatment was used. Cells were centrifuged (300 x *g*) and resuspended in RPMI (10% FBS) at 2 x 10^5 - 1 x 10^6 cells/ml. Following this, 2 ml of cell suspension was transferred to each well in a six well culture plate or 10 ml was transferred into a 10 cm culture dish for Lis-Trp uptake analysis and ACE activity measurement, respectively. PMA (25 ng/ml) was added to differentiate monocytes into macrophages over 24 - 48 hours. Cells were then used for downstream experiments and treated as described in Section 3.2.2.

3.2.2. Lisinopril-Tryptophan Treatment

Following PMA differentiation, an adapted method of Chen *et al.* [199] was used for THP-1 ACE inhibition, cell lysis, and inhibitor quantification. Adherent THP-1 macrophages were washed with cold 1x PBS three times before the addition of PMA-free 10% RPMI media. Each well received 2 ml of media and the plates were incubated for 24 hours to allow for cell recovery and for gene expression to be regulated free of PMA stimulation.

3.2.2.1. Lis-Trp Uptake Time Point Assessment

Intracellular inhibitor concentration differs from that in serum. Over time, intracellular concentration should increase and then decrease as excretion and cell metabolism continues. Three time points were recorded for the analysis of intracellular Lis-Trp uptake: zero-time, one hour, and two hours. Lis-Trp (2 mM stock) was added to each well in a 6-well plate at either 10 µM or 100 µM final concentration and left to incubate for the relevant time points before lysis.

3.2.2.2. Cell Lysis & Bulk Culture Collection

Lysis was carried out on ice to minimize protease activity. Cells were washed with cold 1x PBS three times and 1 ml of 5 mM EDTA (ethylenediaminetetraacetic acid) was used to gently lift and lyse cells from the plate. After 15 minutes of incubation with EDTA, the remaining cells were scraped from the plate and the resulting cell lysate collected into 2 ml Eppendorf tubes on ice. These samples were then frozen and stored at -20°C until analysis. During EDTA incubation, a Trypan Blue cell count was performed within five minutes to quantify cell numbers and evaluate cell viability. A separate 15 µl cell lysate aliquot was collected for protein quantification as described in Section 2.2.2.1.

As a background for protein complexity during analysis, a 50 ml bulk culture of THP-1 macrophages was prepared at a density of 1 x 10^6 cells/ml. Cells were centrifuged at 300 x *g* and washed three times with cold 1xPBS. Gentle lysis in 50 ml of 5 mM EDTA was performed, and the lysate stored at -20°C.

3.2.3. Mass Spectrometric Analysis of Intracellular Lisinopril-Tryptophan

A schematic of the experimental design is shown in **Figure 3.2**. Separate plates were used for each time point and treatment concentration to minimize sample variance. Each experimental condition was cultured in triplicate, and each cell lysate was analysed in triplicate using an AB Sciex 5500 QTrap® mass spectrometer (H3D, UCT, South Africa).

3.2.3.1. Sample Preparation & Extraction

Lysed samples were stored at -20°C until analysis, whereupon samples were thawed at room temperature and vortexed to ensure homogeneity. ACN extraction was carried out using 100 µl cell lysate and 200 µl ice-cold ACN containing 5 nM Verapamil, as an internal standard. To a 96-well plate, each sample supernatant was added for LC-MS/MS analysis, including calibration and quality control standards. Standards consisted of bulk macrophage lysate spiked with Lis-Trp over a range of 1 - 3125 ng/ml. Standards were analysed together with samples after ACN extraction to create a standard curve.

3.2.3.2. LC-MS/MS Analysis

The Sciex 5500 QTrap® mass spectrometer was equipped with an ESI source in positive ionization mode and an Agilent 1290 Rapid Resolution HPLC. Multiple reaction monitoring (MRM) mode was used to measure transitions of the protonated molecular ion of Lis-Trp at

495 *m/z* and its product ions. Product ions for Lis-Trp were 84 *m/z* (quantifier) and 291 *m/z* (qualifier) whilst Verapamil transition was at 455>303 *m/z*. The HPLC separation was carried out on a Poroshell C18 (50 x 4.6 mm, 2.6 µm) column (Agilent, USA), with 0.1% FA as the aqueous mobile phase (A) and 0.1% FA in ACN as the organic mobile phase (B). Elution was achieved with a linear 10 – 100% solvent B gradient over 1.8 minutes at a flowrate of 0.7 ml/min, starting 0.2 minutes after sample injection. The gradient was held at 100% B for one minute before re-equilibration of the column at 10% B for 2.9 minutes. A 6-minute needle wash was performed between each sample, consisting of water, ACN, methanol (MeOH) and isopropanol at a 30:30:30:10 ratio.

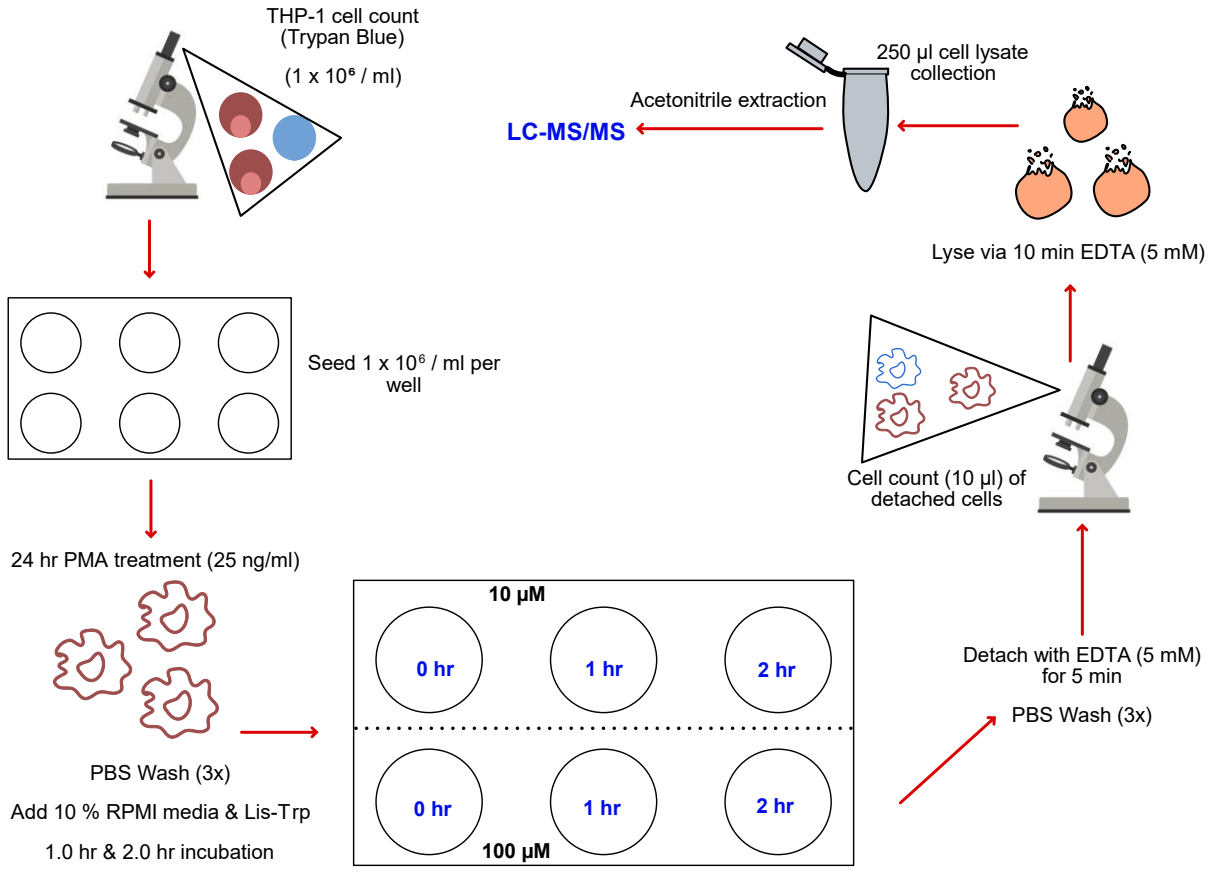

Figure 3.2: A schematic showing the experimental design for determining the uptake of the Lis-Trp by THP-1 macrophages using LC-MS. Each treatment and time point were performed in triplicate.

3.2.4. ACE Activity

ACE inhibition results in a decrease in catalytic ability and therefore a decrease in ACE activity. To quantify these changes, the enzymatic Z-phenylalanine-L-histidyl-L-leucine (ZFHL) (Bachem, Switzerland) assay was used. ZFHL yields an HL peptide upon cleavage and

forms a fluorescent adduct with *o*-phthaldialdehyde (Sigma, USA). The assay was conducted using the protocol of Schwager *et al*. [200]. Briefly, 5 µl of cell lysate was incubated in 30 µl of 2 mM ZFHL at 37°C for 15 minutes. The adduct was created by the addition of 0.28 M NaOH-7mM-*o*-pthaldialdehyde solution and incubated at room temperature for 10 minutes. The solution turned yellow when ZFHL was cleaved and an adduct was formed. The addition of 3 M hydrochloric acid halted the reaction, and fluorescence was measured using a $\lambda_{excitation}$ of 360 nm and $\lambda_{emission}$ of 485 nm (Varian Cary Eclipse, Agilent, USA). To convert fluorescent units to milliunits (mU) ACE activity, an His-Leu (HL) (Sigma, USA) standard curve was generated. One unit of ACE activity is defined as 1 nmole of HL produced/minute/ml by ACE at 37°C **(Appendix Section 8.3, Figure 8.3)**.

3.2.5. Statistical Analysis

Data analysis was carried out in Excel (version 2301, Microsoft, USA) and RStudio (version 2022.12.0+353, RStudio, USA). ACE activity and protein quantification, in triplicate, were recorded as mean values and standard deviation (SD) as part of total cell lysate samples. Cell counts for Lis-Trp quantitation and protein quantitation were also performed and recorded in triplicate. Measured intracellular Lis-Trp concentrations were normalised against cell counts for each time point and treatment concentration, with outliers greater than 2xSD excluded. Lis-Trp concentrations were normalised to cell count, as cells may express different levels of protein and protein recovery is not 100%.

3.3. Results

3.3.1. Intracellular Lis-Trp Quantification

To determine the intracellular concentration of Lis-Trp, samples were analysed using HPLC and the Lis-Trp peak was observed at approximately 2.45 minutes. The internal standard, Verapamil, closely followed at 2.64 minutes. A representative chromatogram is shown in **Figure 3.3**, demonstrating clear resolution of the target and internal standard peaks, as well as low background levels.

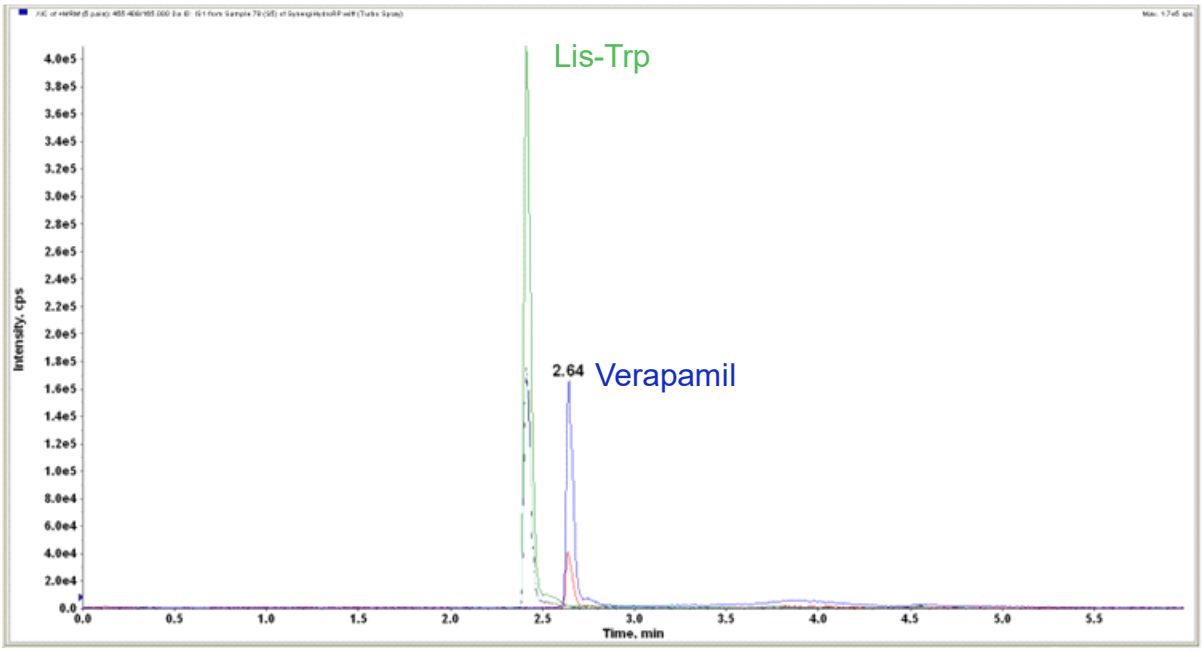

Figure 3.3: A representative chromatogram for Lis-Trp (analyte) and Verapamil (internal standard). Lis-Trp eluted at 2.45 minutes, while Verapamil eluted at 2.64 minutes. Gradient separation was achieved using a C18 column, 0.1% FA aqueous mobile phase (A) and 0.1% FA in ACN organic mobile phase (B) at a flow rate of 0.7 ml/min.

Cellular uptake was quantified in THP-1 macrophages **(Figure 3.4)**. Peak intracellular Lis-Trp (0.036 µM, **Figure 3.4A**) was reached after one hour at 10 µM treatment, whereas 100 µM Lis-Trp treatment resulted in sustained uptake after two hours (0.757 µM), with decreasing intracellular Lis-Trp observed over time with the 10 µM treatment. As expected, a higher treatment concentration resulted in higher uptake by the cells.

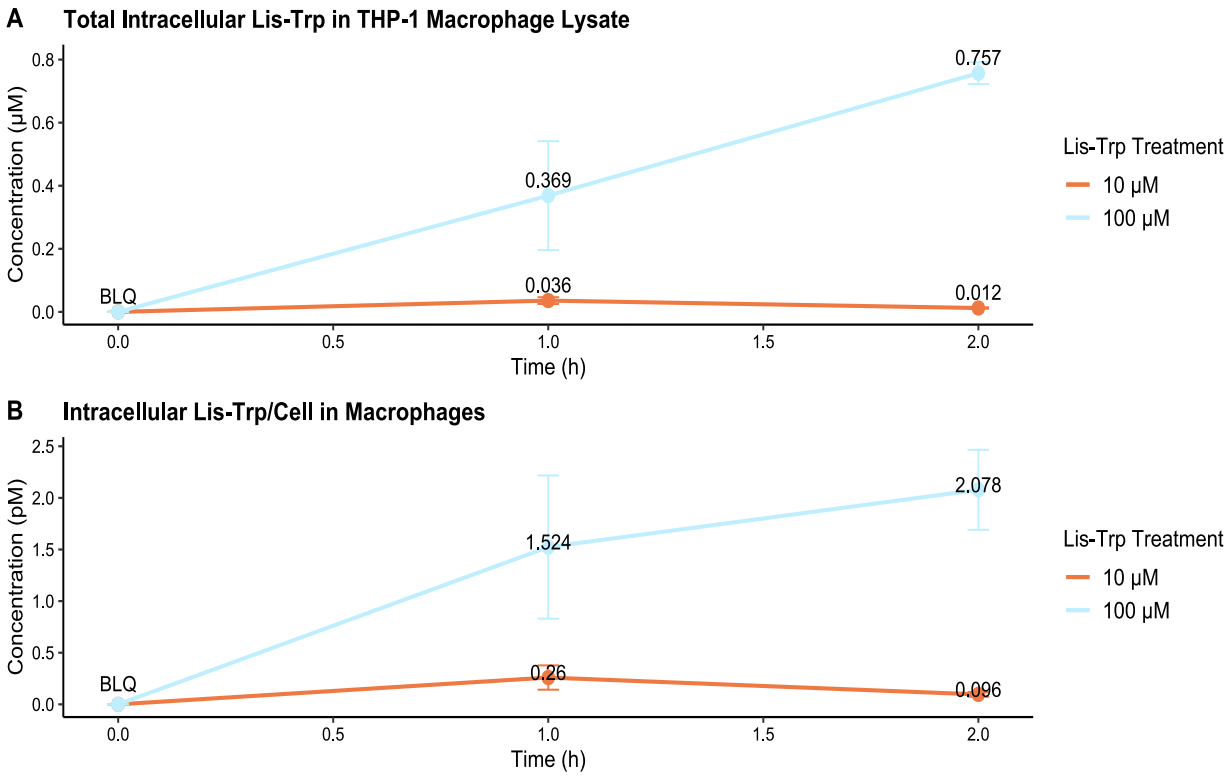

Figure 3.4: Intracellular uptake of Lis-Trp by THP-1 macrophages as measured by LC-MS/MS. Differentiated THP-1 macrophages were able to take up Lis-Trp at both 10 and 100 µM over a period of 2 hours. (A) The total intracellular uptake in THP-1 macrophage cell lysate. (B) Lis-Trp intracellular concentrations normalised to total cell number. *BLQ – Below Limit of Quantitation, 0.00625 µM.

Intracellular Lis-Trp was detected at picomolar levels after normalization to cell count **(Figure 3.4B)**. The standard deviation between samples increased after normalization due to differences in cell counts between samples, but the same trend was observed for both normalised and non-normalised intracellular Lis-Trp at each time point.

3.3.2. ACE Activity Measurement

Differentiated THP-1 macrophages had low intracellular ACE activity in comparison to sACE-CHO cells (positive control) **(Figure 3.5)**. No ACE activity was detected in undifferentiated THP-1 monocytes, but upon PMA treatment the ACE activity increased by approximately 10-fold [174].

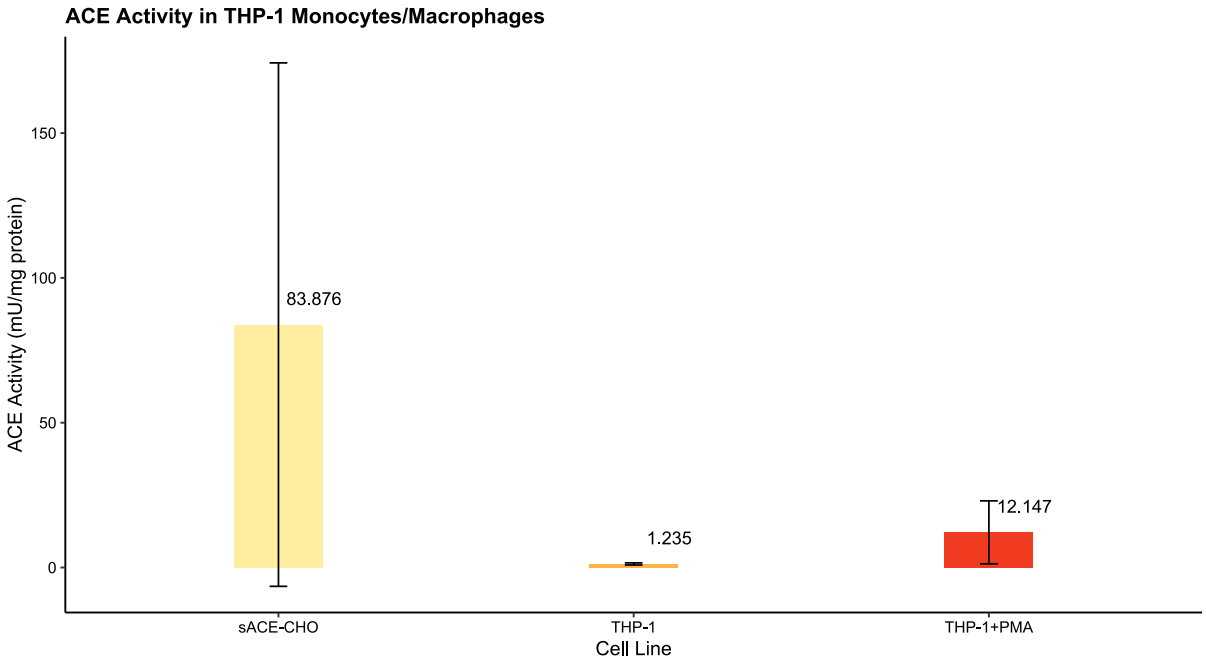

Figure 3.5: ACE activity in differentiated THP-1 macrophages and THP-1 monocytes. After PMA differentiation, THP-1 macrophages exhibited increased ACE activity. sACE-CHO acts as a positive control (Adapted from: Jellema-Butler, Hons 2022 [174]). Total ACE activity normalised by total mg protein in lysate.

THP-1 macrophage lysate ACE activity after Lis-Trp treatment was significantly reduced following 1-hour Lis-Trp exposure but activities remained similar following 2-hours and 24-hours post-treatment. ACE activity was thus partially inhibited in both 10 µM and 100 µM Lis-Trp-treated THP-1 macrophages **(Figure 3.6)**.

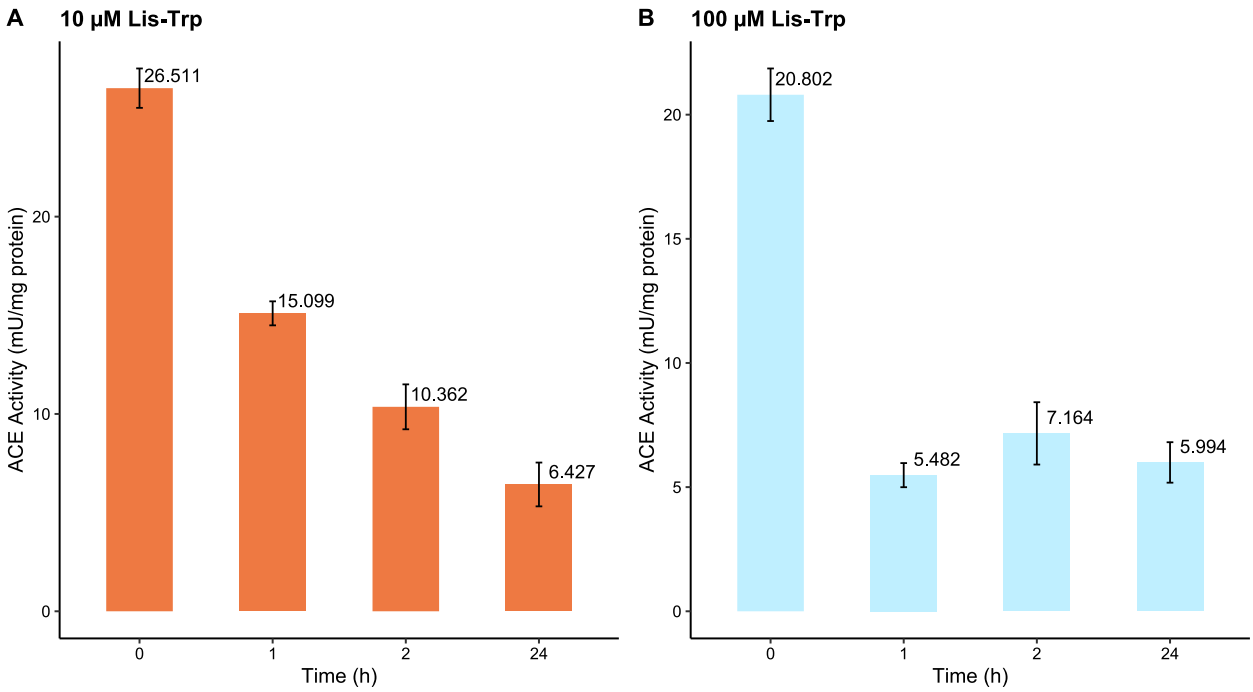

Figure 3.6: Total THP-1 macrophage ACE activity after Lis-Trp treatments decreases within 1-hour post-treatment. Standard deviation showed a large variance amongst samples with one statistical outlier excluded in the 100 µM treatment group. Activity remained similar throughout the time points once Lis-Trp had been added. Total ACE activity (mU) was normalised against lysate mg protein.

In summary, ACE activity increased with PMA treatment of THP-1 monocytic cell lines, but a high cell density is required for its quantification in comparison to the positive control cell line, sACE-CHO. Lis-Trp was detected in THP-1 macrophage cell lysate for both 10 µM and 100 µM treatments for up to 2 hours, but only resulted in partial ACE inhibition.

3.4. Discussion

Catalytically active ACE expression as well as ACE inhibitor entry (Lis-Trp) into differentiated THP-1 macrophages, was confirmed in the present study. Treatment with 10 µM Lis-Trp resulted in detectable intracellular levels of Lis-Trp after 1 hour, before decreasing at 2 hours post-treatment, whereas an increasing quantity of intracellular Lis-Trp was detected throughout the 2-hour incubation period with 100 µM Lis-Trp treatment.

Prior research using the Caco-2 cell line and the ACE inhibitor lisinopril recorded 1 µM intracellular levels from 10 µM treatment, a 10% uptake [189]. In the present study < 1% Lis-Trp was detected in THP-1 macrophages. The structure of Lis-Trp reveals its low lipophilicity (cLogP = -80, ChemDraw version 16) and high total polar surface area

(TPSA = 154, ChemDraw version 16), which result in limited passive diffusion through biological membranes [201]. In this case, it is plausible that, similarly to lisinopril, Lis-Trp is more susceptible to active uptake via proton-coupled oligopeptide transporters or peptide carrier-mediated transport and would also have a low bioavailability as a result (5.4% orally in rats) [202–204].

Importantly, lisinopril is not metabolized in the body and is entirely excreted in the urine requiring transporters for removal from target cells or systems [204]. Lisinopril requires active absorption through intestinal peptide carrier-mediated transporters, typically PEPT1 and PEPT2 but a mix of both active and passive methods have been reported with an oral bioavailability of 25% [201,204–206]. This same mechanism may be applied to Lis-Trp uptake in immune cells. However, THP-1 macrophages only express PEPT2, PHT1 and PHT2 [207]. PEPT2 is a peptide carrier, whilst peptide/histidine transporters PHT1 and PHT2 mediate histidine and di/tripeptide transport [208–210]. These transporters actively move amino acids and other hydrophilic molecules across cell boundaries, so high doses of Lis-Trp could quickly exhaust energy reserves and slow antiport transport dramatically [206,207,211–213]. In the present study, increasing inhibitor concentration resulted in increased detection within the THP-1 cells. Saturation was not reached at 1-hour post-treatment for 100 µM as observed with 10 µM treatment. Instead, the cells treated with 100 µM of Lis-Trp continued to increase their cellular uptake after 2 hours. This may indicate that at lower concentrations (10 µM), Lis-Trp is sufficiently removed from cells via efflux/transporters in the membrane. This system is then overwhelmed at 100 µM and is unable to maintain equilibrium, similar to the observations of Dumont *et al*. in *Escherichia coli* expressing AcrAB efflux pumps at high ciprofloxacin doses [211,213–215]. Alternatively, it is possible that Lis-Trp slowly moves into the THP-1 macrophages due to poor permeability, causing an increase over time at high concentrations. Lis-Trp may also be degraded and/or partially metabolised once internalised by macrophages owing to the presence of high hydrolase levels, resulting in the observed decrease in intracellular Lis-Trp levels. As with efflux pumps, high drug doses result in a maximum rate of enzymatic degradation and compound accumulation within a cell. Lis-Trp may therefore require more time to reach its saturation point within macrophages, which is supported by our observation of higher intracellular levels at higher doses.

In agreement with prior literature, in the current study ACE expression increased upon differentiation of monocytes into macrophages [174,216–218]. Furthermore, after treatment with Lis-Trp, partial ACE inhibition was observed, which was expected since Lis-Trp is C-domain selective. The modified ZFHL ACE assay by Schwager *et al*. measures ACE activity regardless of domain [200,219]. The residual ACE activity observed for both 10 (≈ 31%) and 100 µM (≈ 43%) Lis-Trp treatments suggests that the N-domain remains active and capable of cleaving the Ang I analogue, ZFHL. Future work would benefit from using the Cushman and Chang method, which uses HHL cleavage to only indicate the activity of the C-domain [219,220]. This selective measurement of ACE activity would provide insight into how much Lis-Trp is required to fully inhibit the ACE C-domain of THP-1 macrophages and corroborate the established pharmacokinetics.

In the present study, successful Lis-Trp uptake and absorption was reported for differentiated THP-1 macrophages, a model cell line of human peripheral macrophages. Based on these results, the subsequent chapters will explore the impact of ACE inhibition in human macrophages and related-immune pathways. Although partial ACE inhibition took place, previous studies indicated that partial inhibition, particularly of the C-domain, may negatively impact ACE-related immune function [99]. These effects should therefore be carefully considered in cases where patients are particularly vulnerable to infection or are immunosuppressed.

4. The Effects of ACE Overexpression & Inhibition in Human THP-1 Macrophages

4.1. Introduction

Macrophages are vitally important cells that are responsible for the control, mitigation, and propagation of inflammatory and autoimmune disease, and the control and eradication of pathogenic bacteria from the host [221]. The murine ACE 10/10 model has shown great promise in alleviating immune challenge through ACE overexpression in macrophages [5,57,89,172,222]. These mice also exhibit normal blood pressure and cardiovascular function, despite having no epithelial ACE expression [59,223]. Additionally, mechanisms by which ACE inhibition acts on immune cell populations remain unclear, with most preliminary research having been done between 1980 and 2000 [224–236]. An overarching theme, despite some contradictory findings, was suppression of immune regulation and responses by ACE inhibitors. These studies commonly used enalapril, captopril and lisinopril as ACE inhibitors. In 2021, Cao *et al*. analysed the ACE inhibitors ramipril and lisinopril in NeuACE mice and a small human cohort [99]. Ramipril and lisinopril reduced intracellular and extracellular bactericidal activity in NeuACE neutrophils but not the ARB, losartan. Furthermore, in humans, ramipril retarded neutrophil killing action in blood and intracellularly, while reducing ROS production. Both animal and human neutrophils had suppressed immune function following ACEi treatment.

Chapter 2 described the identification of proteins and pathways that were significantly enriched in ACE 10/10 murine macrophages using MS. There were also significant decreases in ATP synthase and TCA cycle components with ACE C-domain inhibitor treatment. Mouse models such as ACE 10/10 and NeuACE require confirmation in humans and cell cultures are an important step in this process. Based on these revelations, an exploration of ACE overexpression in a suitable human cell culture model, i.e., macrophages and other myeloid-derived cells was undertaken.

4.1.1. Investigating the Human ACE Overexpressing Macrophage Proteome

Only targeted metabolomic analysis of murine macrophages and neutrophils and discovery MS analysis of mouse plasma have been carried out in the murine ACE overexpressing

models [42,100]. The impact of ACE overexpression on human macrophages is unknown. In undifferentiated WT THP-1 cells, little to no ACE has been detected via western blot [237–240]. However, the level of ACE increases in differentiating macrophages and those polarized to M1 and M2 states [241,242]. Proteomic comparison of ACE overexpressing and unmodified human macrophage cell lines will prove helpful in determining if similar immune benefits exist as in mice [42,100]. Secondly, the data collected from the WT cell line will add to our current database of the human macrophage proteome, as well as contributing to our growing understanding of how ACEi impact immune cell function.

4.1.1.1. Objectives

- Perform discovery Triple-TOF SWATH analysis on the ACE overexpressing and WT human THP-1 macrophage lysates.
- Identify significantly differentially expressed proteins in Lis-Trp-treated and untreated ACE overexpressing THP-1 macrophages.
- Identify significantly differentially expressed proteins in Lis-Trp-treated and untreated WT THP-1 macrophages.
- Analyse the functional enrichment of differentially expressed proteins across comparisons and their associated biological processes.

4.2. Methodology

4.2.1. Cell Culture & Treatment

4.2.1.1. ACE Overexpressing (ACE +/+) THP-1 Macrophage Cell Line Synthesis

The human THP-1 cell line usually expresses undetectable to very little ACE until differentiation, when ACE is up-regulated [218]. The ACE +/+ cell line was created using a lentivirus vector system by Systems Biosciences (SBI), USA and gifted by the K. Bernstein laboratory (Cedars-Sinai Medical Centre, USA).

4.2.1.2. Human THP-1 Cell Culture & ACE Inhibitor Treatment

Human THP-1 monocytes were cultured and differentiated into macrophages as described in Section 3.2.1. Experimental conditions and cell lysis were as described in Section 2.2.1.2 and the number of samples per group shown in **Table 4.1**.

Table 4.1: Experimental groups of human THP-1 cell lysate samples (gifted by K. Bernstein, USA).

Sample Group	Number of Samples in Group
ACE +/+ THP-1	3
ACE +/+ THP-1 + Lis-Trp (C)	3
WT THP-1	3
WT THP-1 + Lis-Trp (C)	3

4.2.2. Sample Preparation

4.2.2.1. Protein Precipitation & Quantification

Protein precipitation and quantification were performed as outlined in Section 2.2.2.1.

4.2.2.2. Protein Digestion & Desalting

Samples were prepared and digested using trypsin as outlined in Section 2.2.2.2.1. Desalting was offline using EvoTips as described in Section 2.2.2.3.2.

4.2.3. Mass Spectrometry

Mass spectrometry analysis was performed as outlined in Section 2.2.3.2.

4.2.4. Data Analysis

4.2.4.1. Data Processing

A human UniProtKB library for label-free identification and quantification was created for database searching. Data was processed as described in Section 2.2.4.1.2.

4.2.4.2. Data Clean-up & Statistical Analysis

The resultant protein groups matrix was analysed using Perseus as described in Section 2.2.4.1.3 to produce a list of log2 transformed valid protein identifications for differential expression analysis. Once more a Student's t-test comparison was performed taking a p-value ≤ 0.05 as significant.

4.2.4.3. Functional Enrichment & Network Analysis

Both functional enrichment and network analysis were performed as described in Section 2.2.4.1.4. However, STRING interaction confidence was set to medium (0.4) to account for lower protein identification in human macrophages. High confidence (0.7) was

used for the WT and Lis-Trp-treated WT network due to complexity and excessive node overlapping at medium confidence scores.

4.3. Results

4.3.1. Peptide & Protein Identifications

Roughly 20 000 precursors and 2641 protein groups were identified in the human THP-1 samples. Maintaining valid values in 2 of 3 replicates in any condition, 2308 unique proteins remained after filtration and log2 transformation.

4.3.2. Quality assessments

The human ACE +/+ THP-1 and WT THP-1 macrophage proteomes correlated well with their Lis-Trp-treated counterparts according to their Pearson's correlation coefficients **(Figure 4.1)**. There was strong agreement between both ACE overexpressing cell replicates ranging from 0.9 - 1.0 and between WT replicates (0.8 - 0.95). ACEC1 and WT2 had lesser Pearson correlations (0.5 - 0.7) and, had very few protein identifications due to the EvoTip not eluting well, losing sample. These two replicates were excluded from downstream analysis and could not be repeated due to poor protein recovery either during lysis or precipitation. Following hierarchical clustering, no further replicates were excluded from analysis **(Appendix Section 8.4.1**Error! Reference source not found.**, Figure 8.4)**.

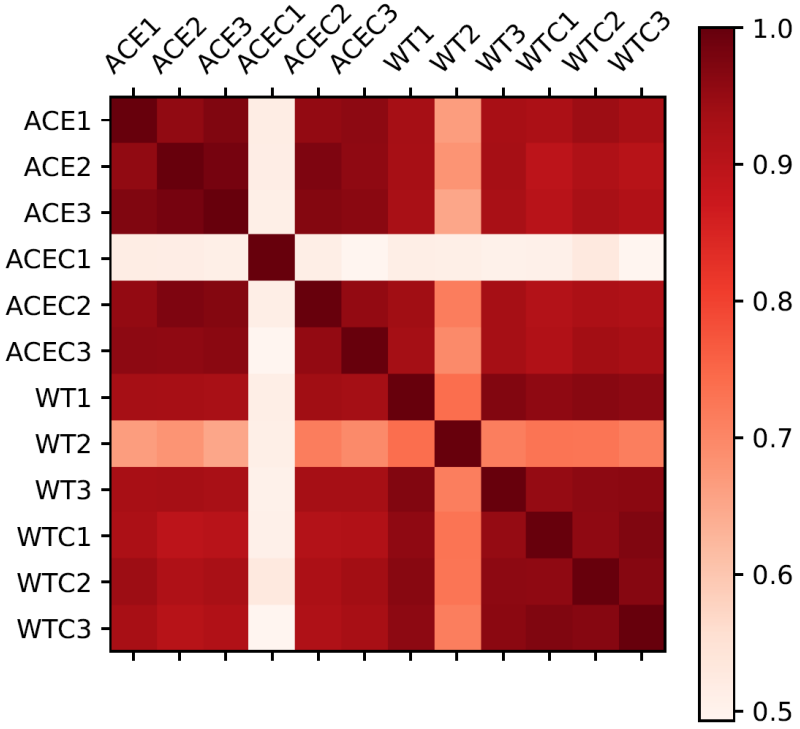

Figure 4.1: Pearson correlation co-efficients of the human ACE +/+ and WT THP-1 macrophage proteomes. Samples denoted with a C represent Lis-Trp treatment and those without are controls/untreated.

4.3.3. Differential Analysis

The ACE inhibitor (50 µM Lis-Trp , 24 hours)-treated ACE +/+ and WT groups were compared to their untreated control groups, while the ACE +/+ control was compared to the WT THP-1 control **(Figure 4.2)**. The ACE and WT THP-1 comparison had 442 differentially expressed proteins, of which 215 were up-regulated and 227 down-regulated **(Figure 4.2A)**. Unexpectedly, ACE was detected at similar levels in WT and ACE +/+ THP-1 samples and was not significantly overexpressed in ACE +/+ THP-1 macrophages. Only 2 ACE-derived peptides were detected during MS analysis out of a possible 75 at low abundance relative to the dataset, possibly resulting in poor quantification, likely from incomplete digestion and rich glycosylation of fragments impairing MS analysis. ACE overexpression was confirmed by our collaborator before treatment and cell lysis via western blot and ACE activity assays **(Appendix Section 8.4.2, Figure 8.6 &Figure 8.5)**.

Lis-Trp-treated ACE overexpressing THP-1 macrophages (ACE +/+) and Lis-Trp-treated WT THP-1 macrophages had 68 and 197 differentially expressed proteins, respectively, in comparison to their untreated controls **(Figure 4.2B & C)**.

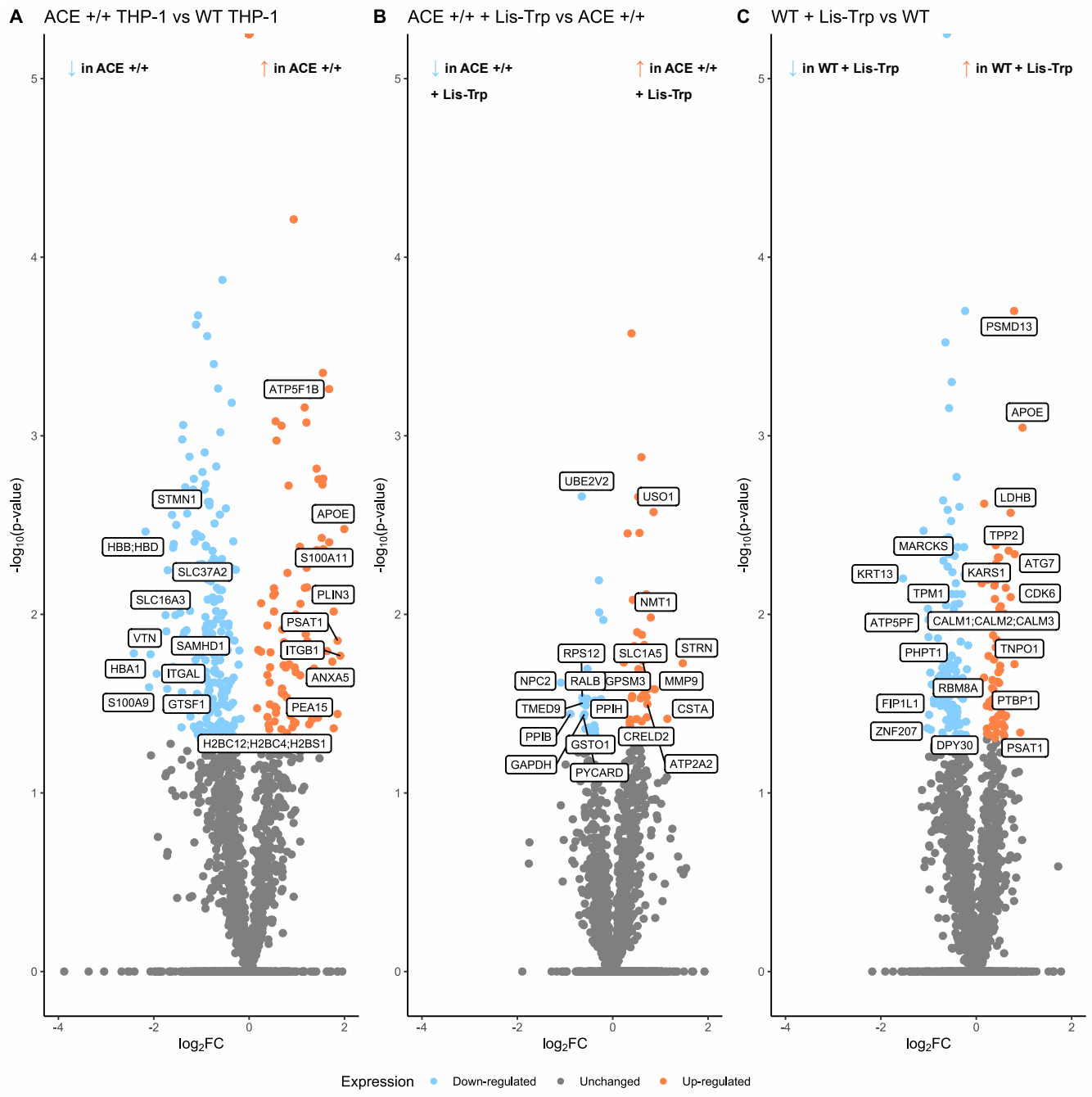

Figure 4.2: Volcano plots showing between-group comparisons in human THP-1 macrophages. (A) Differentially expressed (DE) proteins in ACE +/+ THP-1 macrophages compared to in WT THP-1 macrophages (n = 442). (B) DE proteins in Lis-Trp-treated ACE +/+ THP-1 macrophages as compared to ACE +/+ THP-1 macrophages (n = 68). (C) DE proteins in WT + Lis-Trp THP-1 macrophages compared to in WT THP-1 macrophages (n = 197). Significant proteins are coloured as light blue (down-regulated) or orange (up-regulated). The top 20 significant proteins are labelled. Analysis via Student's t-test, with $p \leq 0.05$ considered statistically significant.

4.3.4. Network & Functional Analysis of Human THP-1 Macrophages

4.3.4.1. Network & Functional Enrichment Analysis of ACE +/+ THP-1 Macrophages

The full set of dysregulated proteins between ACE +/+ THP-1 macrophages and WT THP-1 macrophages was used to generate a STRING network **(Figure 4.3)**, biological process GO enrichment terms **(Figure 4.5)**, KEGG and Reactome analyses **(Figure 4.6)** were performed. Medium interaction confidence (0.4) was used to account for the lower protein identifications (2641) in human THP-1 macrophages in comparison to the prior murine macrophage (3378) proteomic analysis (Section 2.3.1). Similar to murine macrophages, human ACE overexpressing macrophages had increased ATP5B expression and proton-transport associated genes (VDAC1, VDAC2 and NDUFS3) suggesting increased ATP synthesis **(Figure 4.4)**.

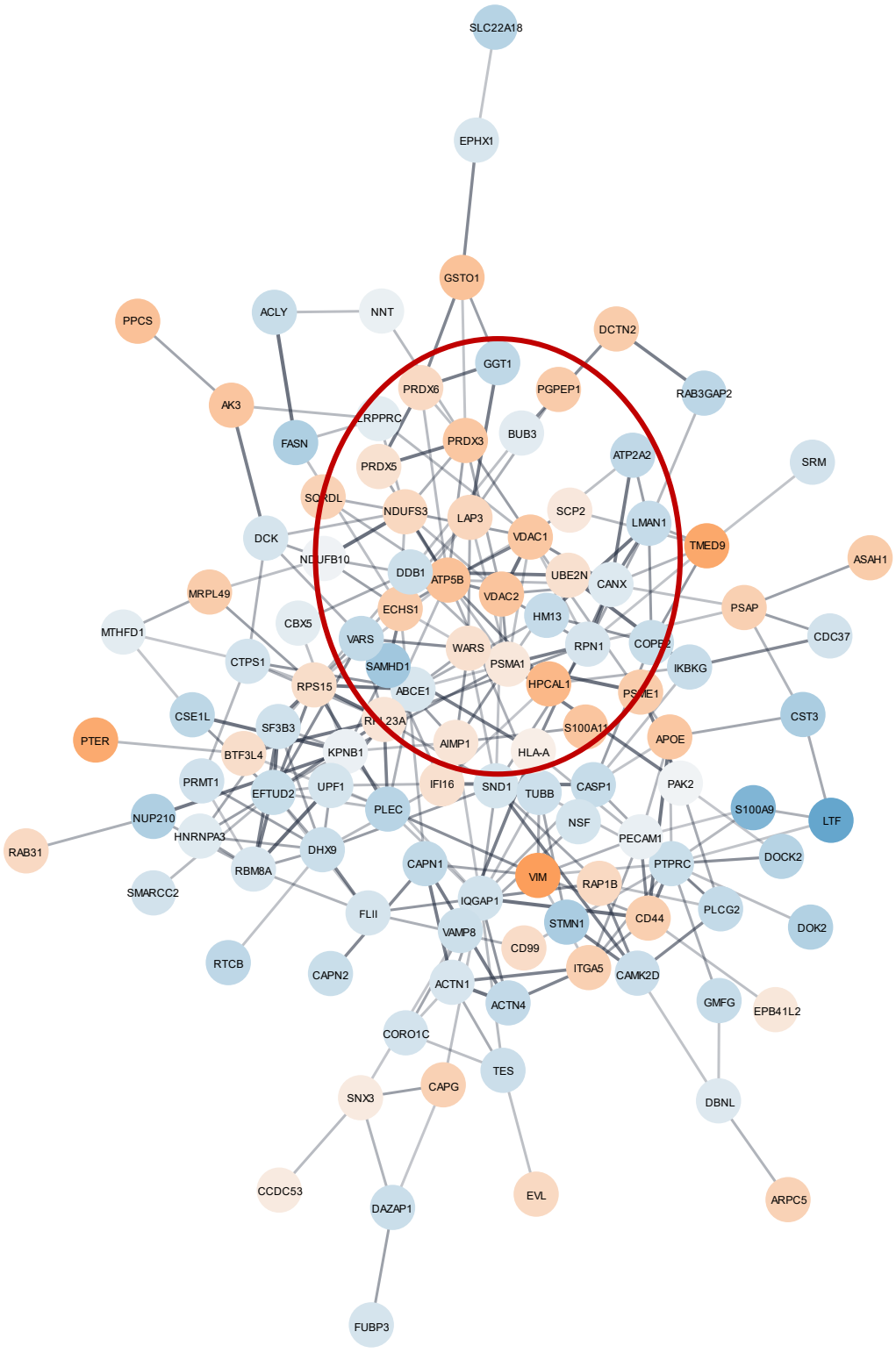

Figure 4.3: Human ACE +/+ THP-1 macrophage STRING network with dysregulated proteins in relation to WT THP-1 macrophages. Confidence of interactions was set to 0.4 and proteins are coloured according to down- (blue) or up-regulation (orange) in ACE +/+ THP-1 macrophages. Line thickness indicates the confidence score of the interaction.

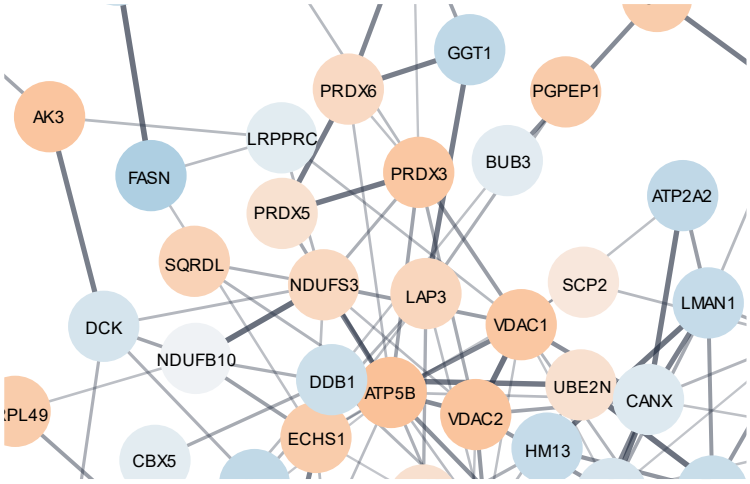

Figure 4.4: Enlarged frame of ACE +/+ THP-1 macrophage network with ATP synthase and ETC components. Blue nodes are down-regulated in ACE +/+ THP-1 macrophages and orange nodes are up-regulated.

Furthermore, several actin cytoskeletal proteins were down-regulated in ACE overexpressing macrophages similar to in murine ACE 10/10 macrophages (ACTN4, ACTN1, CAPN1 and CAPN2), suggesting strong regulation of cellular migration and organisation (GO:0007015).

Cellular lipid catabolism (GO:0044242) was functionally enriched in ACE +/+ THP-1 macrophages **(Figure 4.5)**. The proteins associated with this process were APOE, PSAP, ASAH1, PRDX6, ECHS1, SCP2 and PLCG2. All of these proteins were up-regulated in ACE +/+ THP-1 macrophages except for PLCG2, which is a key signalling factor in lipid metabolism of microglia [32]. No fatty acid oxidation, synthesis, or catabolism was functionally enriched in the ACE overexpressing macrophages as it was in the murine ACE 10/10 macrophages. However, KEGG analysis **(Figure 4.6)** revealed enriched glutathione metabolism (hsa00480). Importantly, innate immune activation (GO:0002218) and cytokine signalling pathways (GO:0019221) were also significantly enriched, which would be expected if ACE overexpression provide an enhanced immune response in human macrophages. Specifically enriched immune pathways were neutrophil degranulation (GO:0043312), T cell receptor signalling pathway (GO:0050852), leukocyte activation (GO:0045321), antigen processing and presentation, specifically MHC Class I (GO:0019882 and GO:0002474).

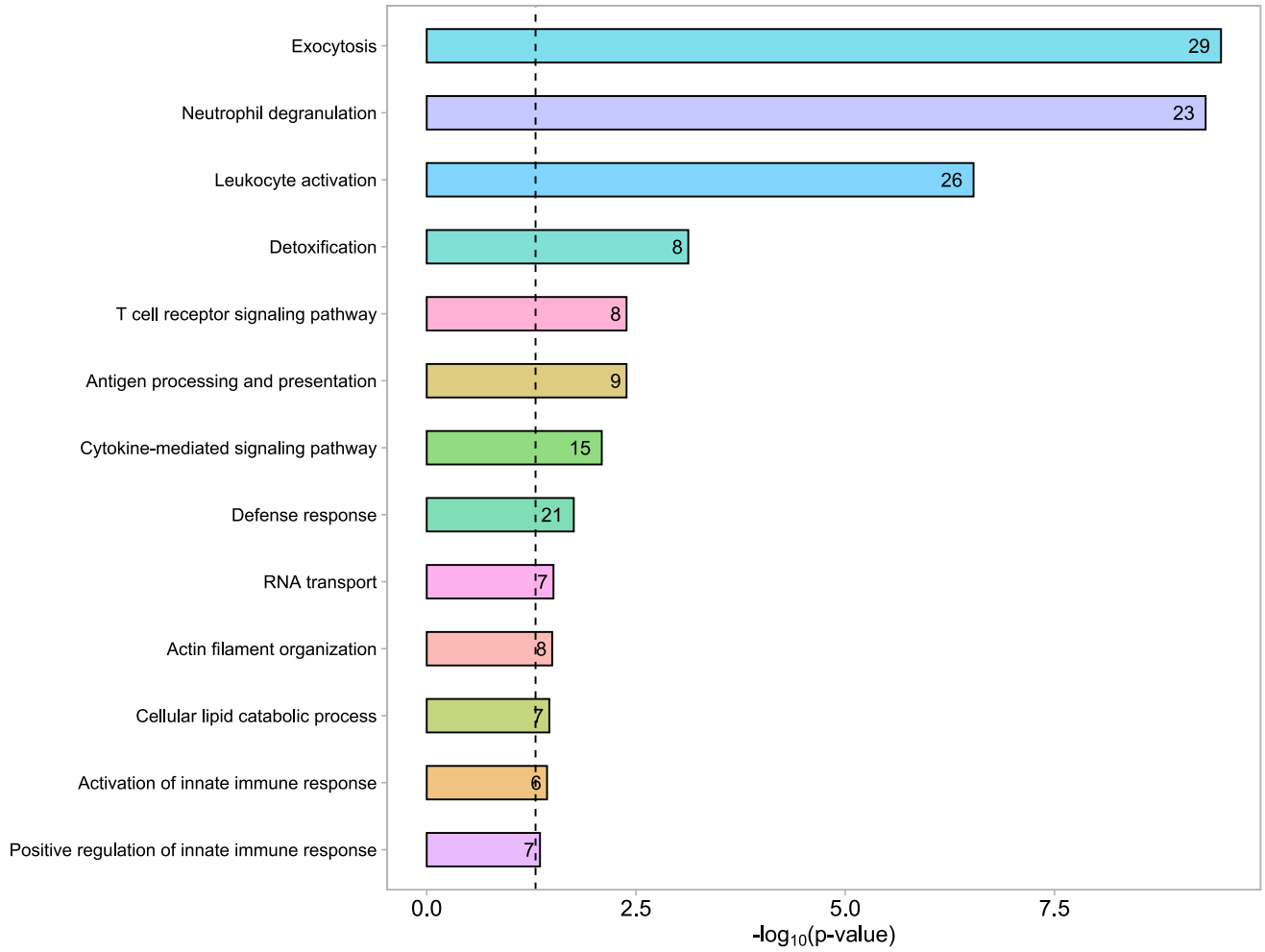

Figure 4.5: Significantly enriched GO biological processes in ACE +/+ THP-1 macrophages. The number of proteins in each process is shown. The dotted line is the significance threshold of $p \leq 0.05$, number of proteins shown in bar.

The term 'Host interactions of HIV factors' (HSA-162909) suggests the presence of lentiviral vector **(Figure 4.6)**. This exploratory analysis highlights differences between mice and human cell culture models and provides an important starting point in that several identical pathways are dysregulated in both human and mouse ACE overexpressing macrophage systems.

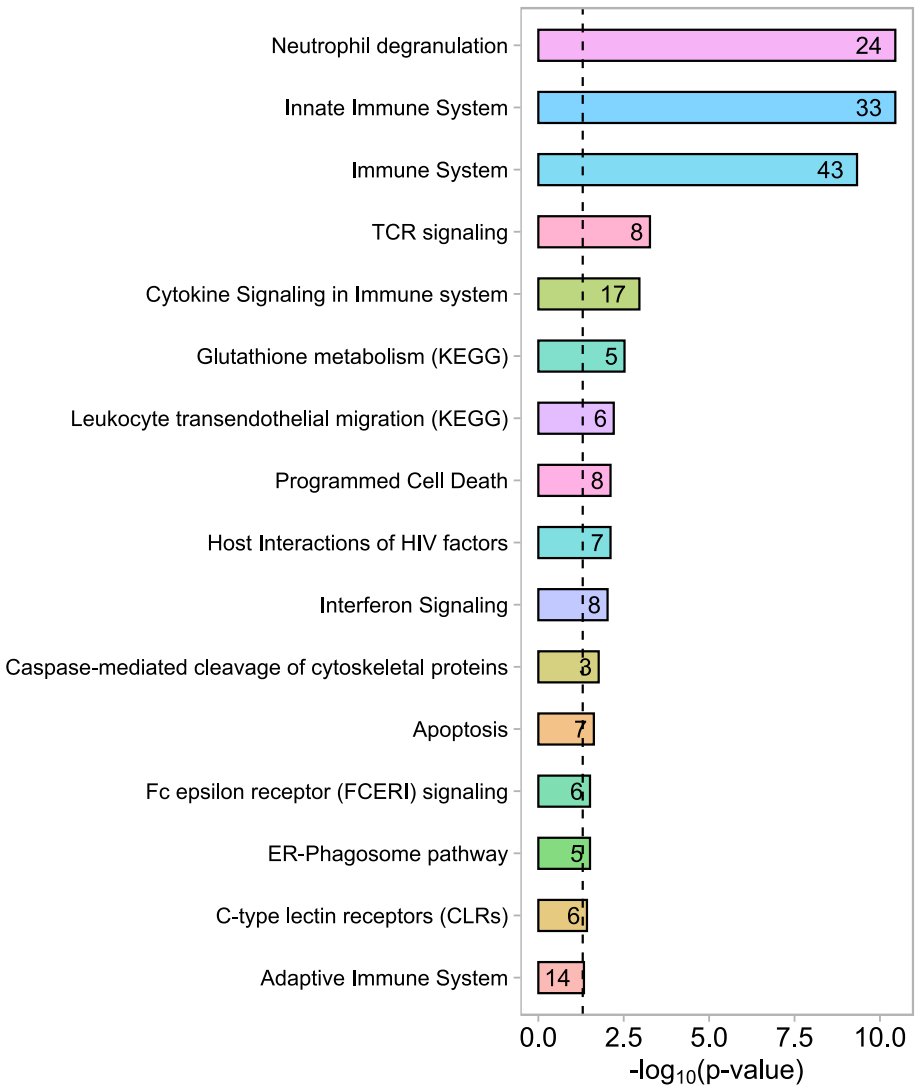

Figure 4.6: Enriched Reactome and KEGG Ontology pathways in ACE +/+ THP-1 macrophages in comparison to WT THP-1 macrophages. Dashed line is significance threshold of $p \leq 0.05$ and number of dataset proteins in cluster is shown in each bar.

4.3.4.2. Lis-Trp-treated ACE +/+ THP-1 Macrophages Network Analysis & Functional Enrichment

Interestingly, Lis-Trp treatment in ACE overexpressing THP-1 macrophages resulted in an increase in the levels of ion-transporting ATPase proteins: ATP6V1H, ATP2A2 and ATP1A1 compared to in untreated ACE +/+ THP-1 macrophages. No significant difference in ATP synthase components was noted after ACE C-domain inhibition **(Figure 4.7)**. Despite no lipid or fatty acid catabolism enrichment **(Figure 4.8)**, acyl-CoA synthetase (ACSL1) was up-regulated after Lis-Trp treatment **(Figure 4.7)**. TCA cycle protein aconitate hydratase (ACO2) and gluconeogenesis protein phosphoenolpyruvate carboxykinase (PCK2) were also up-

regulated, but NADH dehydrogenase subunit and ETC Complex 1 component NDUFA5 was down-regulated. Glyceraldehyde-3-phosphate dehydrogenase (GAPDH) was down-regulated following Lis-Trp treatment, and is known to modulate immune responses, cytoskeletal organization and participate in glycolysis [243].

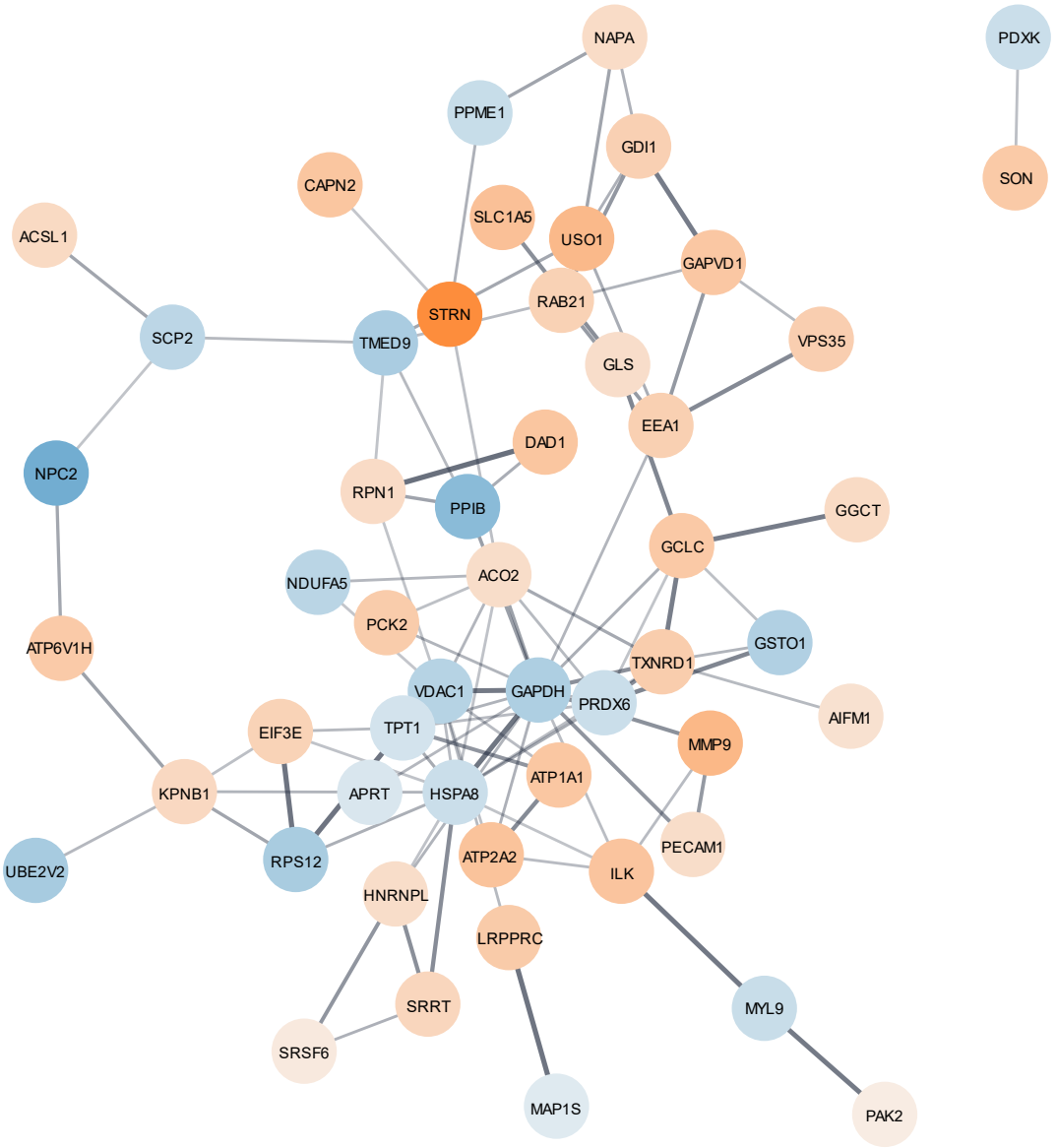

Figure 4.7: Network of dysregulated proteins in Lis-Trp ACE +/+ THP-1 macrophages in relation to ACE +/+ THP-1 macrophages. Confidence score was set to 0.4. Up- or down-regulation is indicated as orange and blue nodes, respectively. Line thickness indicates confidence of interactions.

C-domain inhibition in ACE +/+ cells resulted in fewer significantly different proteins compared to other comparisons. Of interest was neutrophil degranulation (GO:003312) and mRNA splicing **(Figure 4.8)** in Lis-Trp-treated ACE +/+ THP-1 macrophages. Localization (GO:0051649) and vesicle transport proteins (GO:0016192) were mostly up-regulated and were enriched after Lis-Trp treatment, potentially altering the membrane composition and localization of protein pools within vesicles of ACE +/+ THP-1 macrophages. This is inclusive of ATP1A1 and ATP2A2 which aid in active transport using ATPase activity.

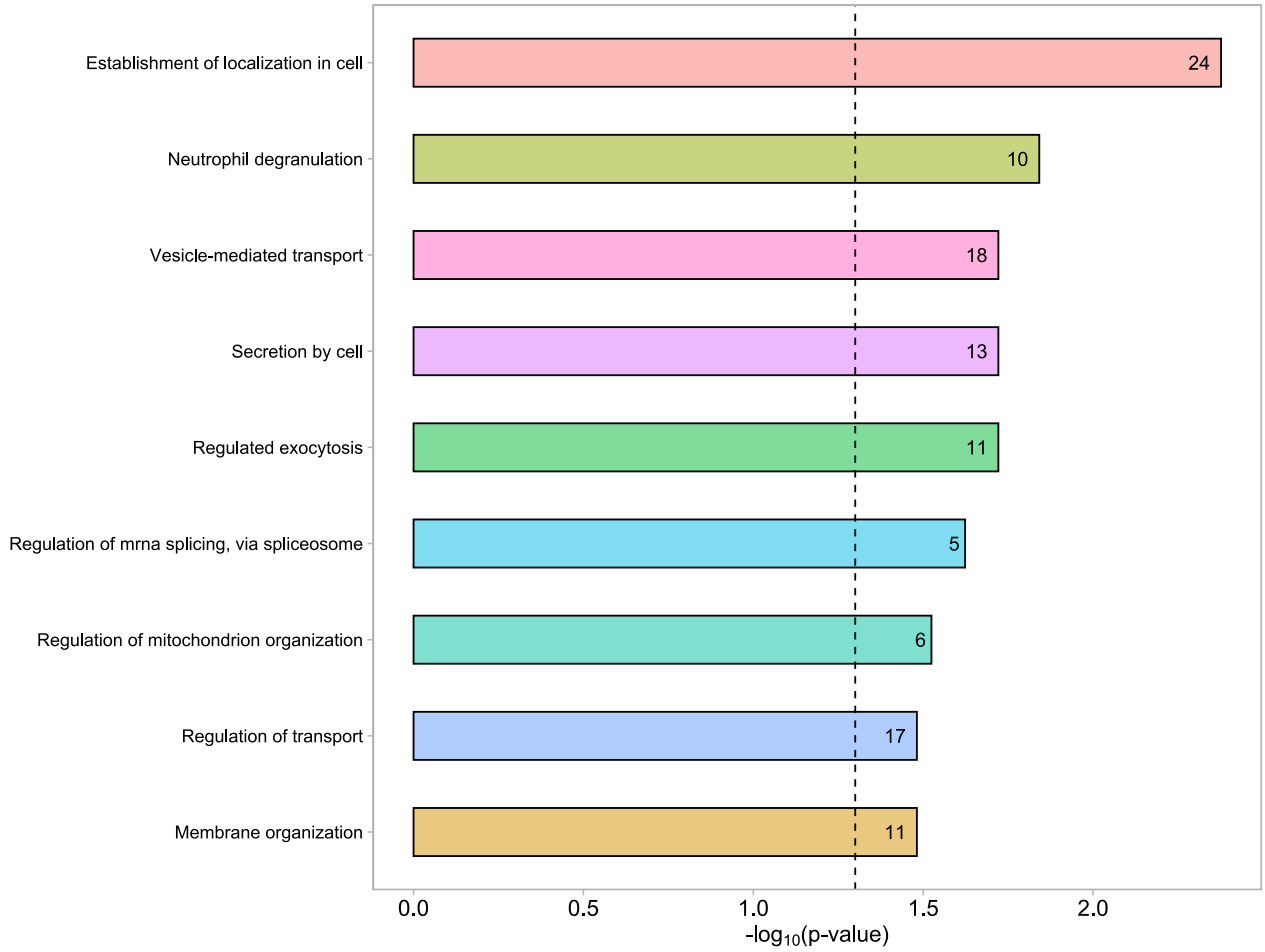

Figure 4.8: Functionally enriched biological processes in ACE +/+ THP-1 macrophages treated with Lis-Trp. Number of proteins in each process is shown. The dotted line represents the significance threshold of $p \leq 0.05$.

According to the Reactome database, innate immunity (HSA-168249) and neutrophil degranulation (HSA-6798695) were enriched. A PPAR signalling pathway (hsa03320) was identified via KEGG, which is an important signalling node within several macrophage killing functions as well as lipid metabolism **(Figure 4.9)**. Glutathione metabolism (hsa00480) was also enriched, and is involved in trained immunity induction and ROS detoxification.

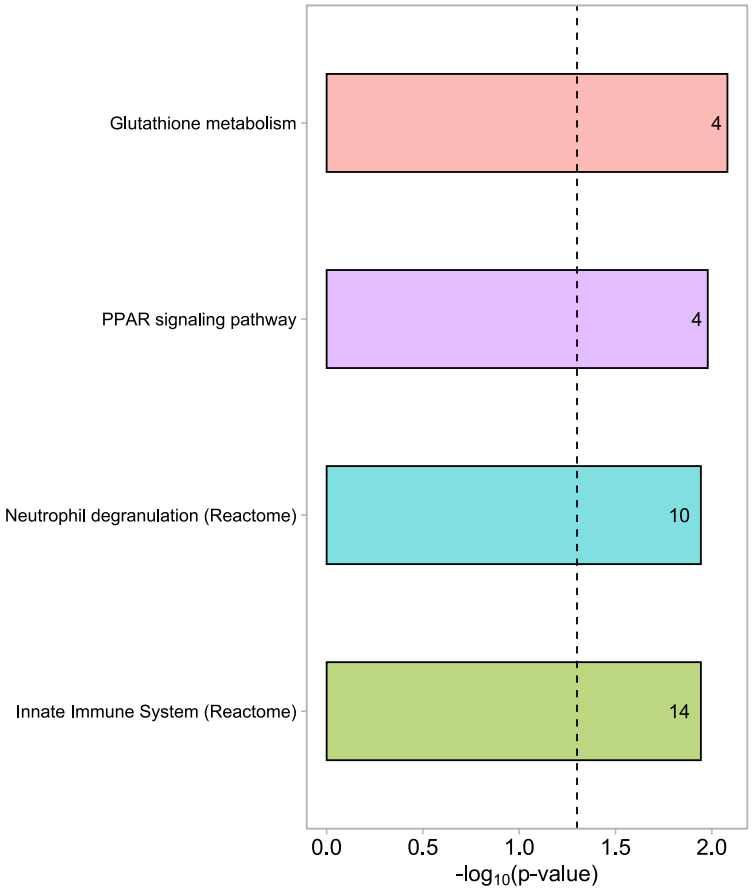

Figure 4.9: KEGG and Reactome-enriched terms in ACE +/+ THP-1 macrophages after Lis-Trp treatment. KEGG and Reactome terms were combined as only two pathways were identified as enriched in Reactome. The dashed line represents the significance threshold of $p \leq 0.05$, and the number of genes per cluster are indicated.

4.3.4.3. Network & Functional Enrichment Analysis of Lis-Trp-treated WT THP-1 Macrophages

More proteins were identified in WT THP-1 macrophages treated with Lis-Trp than in Lis-Trp-treated ACE overexpressing macrophages. Importantly, a significant decrease in ATP synthase proteins ATP5J, ATP5I and ATP5D was observed, which is expected with ACE inhibition, and several ATP metabolic processes were also down-regulated **(Figure 4.10 &Figure 4.11)**. Actin cytoskeletal organization proteins were dysregulated, but this may be a result of PMA differentiation and cell adherence rather than inhibitor treatment.

Neutrophil degranulation and leukocyte activation proteins were up-regulated in WT THP-1 macrophages with Lis-Trp treatment **(Figure 4.12)**. Spliceosome proteins were significantly down-regulated, and several DNA biosynthesis proteins, such as heat shock protein 90 kDa alpha (HSP90AA1), were up-regulated in comparison to untreated cells. In contrast, precursor metabolite generation, including ATP synthase and aldehyde dehydrogenase 2 (ALDH2), were decreased. TCA cycle participants MDH1 and ME2 were up-regulated with Lis-Trp treatment, but dihydrolipoyllysine-residue succinyltransferase, a component of 2-oxoglutarate dehydrogenase complex (DLST), was down-regulated. DLST acts in 2-oxoglutarate to succinyl-CoA conversion, suggesting that Lis-Trp treatment results in reduced succinate and acetyl-CoA production. Importantly, MHC Class I proteins were down-regulated with C-domain inhibition, including the ER-phagosome pathway **(Figure 4.10 &Figure 4.12)**.

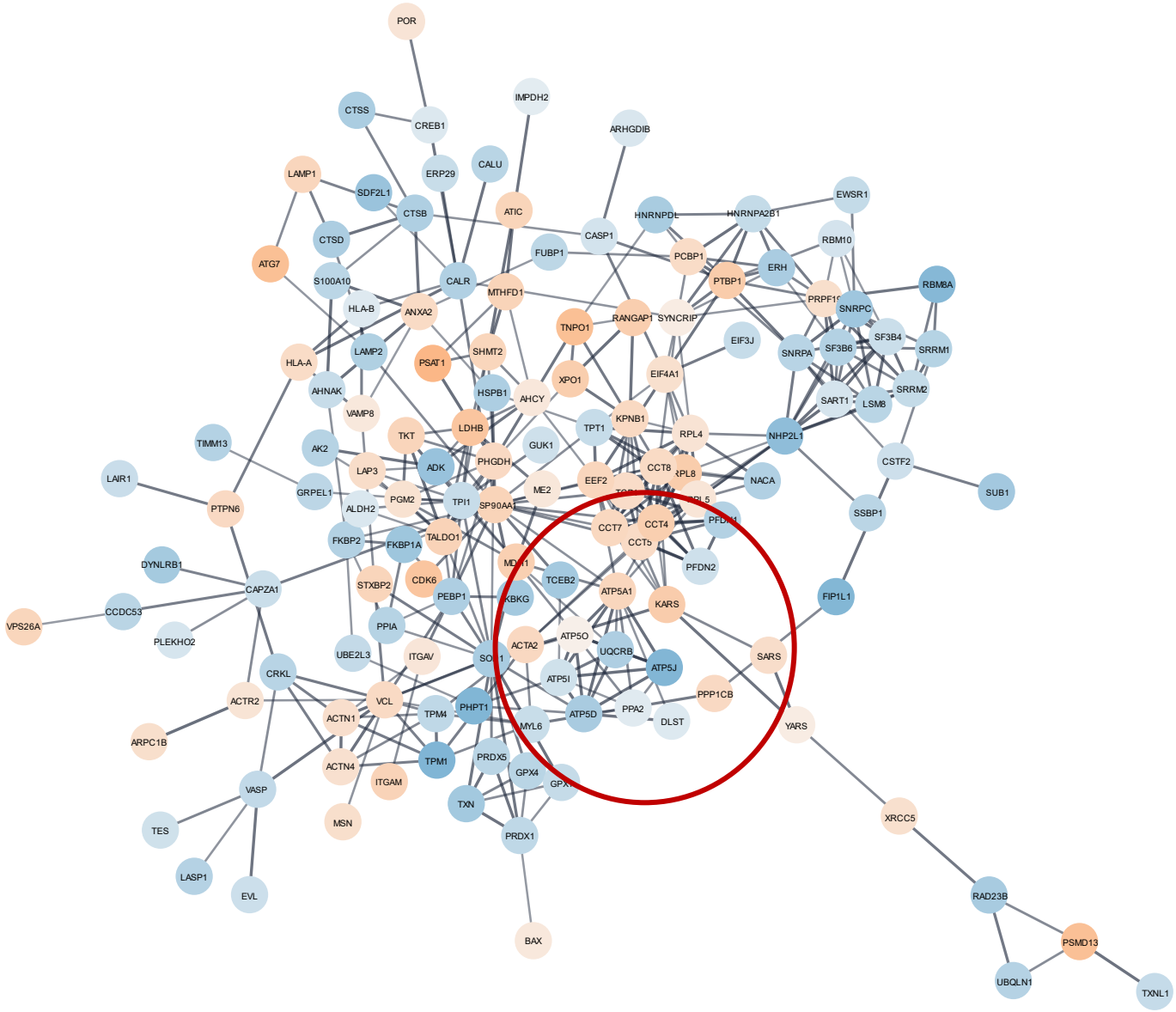

Figure 4.10: Lis-Trp-treated human WT THP-1 macrophage network in relation to WT THP-1 macrophages.

Confidence set to 0.7, blue corresponds to down-regulation and orange corresponds to up-regulation.

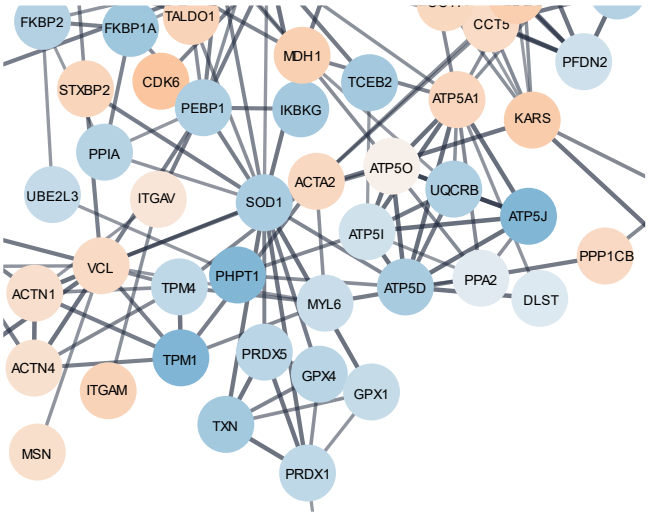

Figure 4.11: Enlarged network frame focusing on down-regulated ATP synthase components in WT THP-1 macrophages after Lis-Trp treatment. Blue nodes are down-regulated and orange nodes up-regulated with line thickness indicating increasing confidence score.

Antigen processing and presentation (GO:0002474) was down-regulated with Lis-Trp treatment, despite leukocyte activation (GO:0045321) proteins being up-regulated and enriched. Furthermore, the IL-12 mediated signalling pathway (GO:0035722) was significantly enriched after Lis-Trp treatment, with down-regulation of nine participating proteins: CAPZA1, SOD1, TCP1, TALDO1, ANXA2, HNRNPDL, HNRNPA2B1, PPIA and MSN. As determined with functional enrichment and DE analysis **(Figure 4.2 &Figure 4.12)**, Lis-Trp-treated WT THP-1 macrophages had increased secreted proteins compared to untreated WT THP-1 macrophages. Several of these proteins are linked to cellular transport and RNA metabolism. RNA processing (GO:0016070) ribosomal components increased following Lis-Trp treatment, but spliceosome component expression decreased, impacting mRNA processing (GO:0006397).

NADP metabolic processes (GO:0006739) were enriched and the associated proteins up-regulated, including oxoacid proteins (GO:0043436). The pentose phosphate pathway proteins transketolase (TKT), glucose phosphomutase 2 (PGM2) and transaldolase 1 (TALDO1) were up-regulated and are part of macrophage inflammatory responses for the regeneration of $NADP^+$ and NAD(P)H, including xylulose biosynthesis (GO:0005999) where TKT and TALDO1 participate **(Figure 4.10)**. However, these biological processes were not as significantly enriched in comparison to neutrophil degranulation and exocytosis owing to lesser protein identification within the cluster.

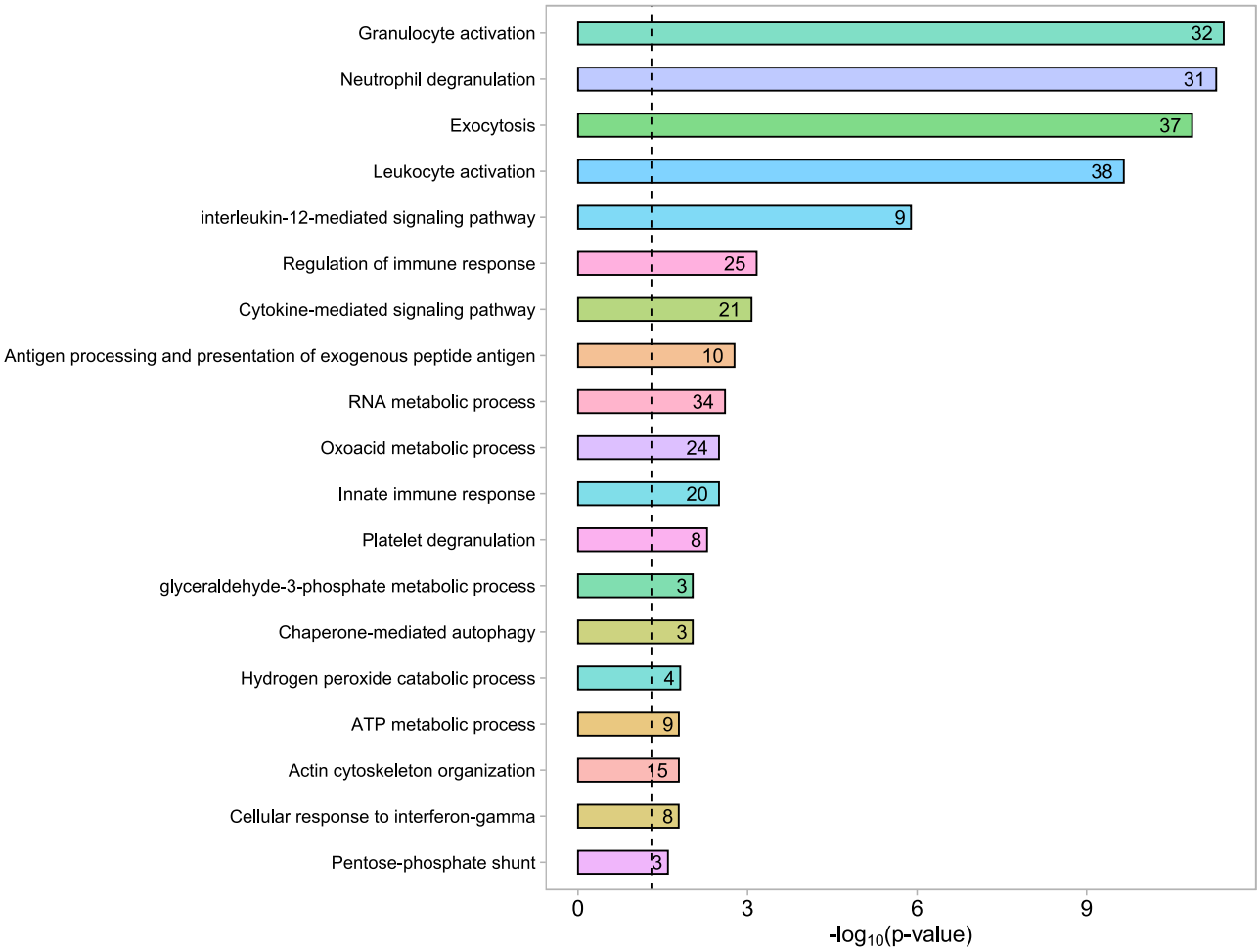

Figure 4.12: Functionally enriched biological processes in WT THP-1 macrophages treated with Lis-Trp. Significance threshold shown as dotted line (p-value ≤ 0.05) and number of genes present per process displayed in its respective bar.

According to the Reactome database **(Figure 4.13A)**, several biological pathways were enriched, including the TCA cycle (HSA-1428517) and ETC surrounding ATP synthesis (HAS-163210). KEGG pathways that were enriched following Lis-Trp treatment included pyruvate metabolism (hsa00620), which is partially connected to the functionally enriched GO terms glyceraldehyde-3-phosphate metabolism (GO:0019682) and pentose phosphate shunt (GO:0006098) **(Figure 4.12 &Figure 4.13B)**. Lis-Trp treatment may contribute to cellular stress levels and cause activation of chaperone-mediated autophagy (GO:0061684). Furthermore, WT THP-1 macrophages had a reduced response to ROS (GO:0000302) following Lis-Trp treatment, with a decrease in TPM1, GPX1, PRDX5, PRDX1, SOD1 and TX1.

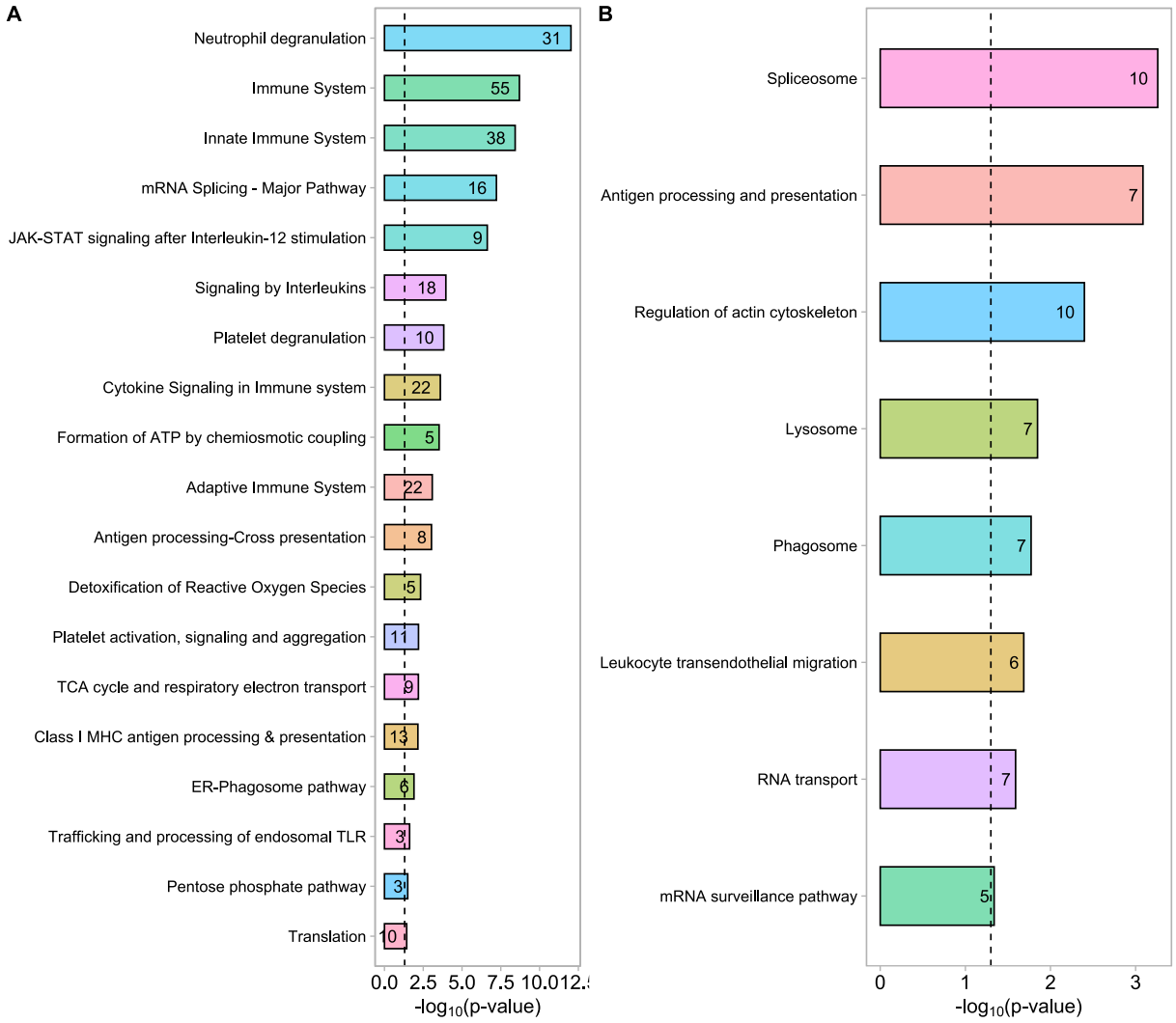

Figure 4.13: Enriched pathways in (A) Reactome and (B) KEGG databases for Lis-Trp-treated WT THP-1 macrophages. Number of genes in each cluster is included within bars and dashed line represents the significance threshold of $p \leq 0.05$.

4.4. Discussion

This study explored the effect of ACE overexpression and its impact on the human THP-1 proteome. The inhibition of the ACE C-domain in macrophages was analysed because previous murine studies have hypothesised that the ACE C-domain plays an important role in neutrophil cytotoxicity [99,244]. To the best of our knowledge, the present study is the first discovery MS analysis of human ACE +/+ macrophages. In these macrophages, ATP synthesis and MHC Class I antigen processing and presentation were up-regulated as in mice [15,100]. The TCA cycle and ETC components were not well detected across samples in human ACE +/+ macrophages, possibly due to their low relative abundance, and may therefore require a targeted proteomics approach. T cell signalling, neutrophil degranulation and leukocyte activation were also functionally enriched in macrophages with ACE overexpression. Overall, the present study confirms that ACE overexpression influences human macrophage immune function and requires further investigation. In contrast, C-domain inhibition appears to encourage neutrophil degranulation and cellular stress response, possibly by increased cellular secretion upon treatment and increased autophagy response. ACE inhibition also led to lowered ATP synthase and ETC complex components in both ACE +/+ and WT THP-1 macrophages. Interestingly, ACE +/+ THP-1 macrophages were functionally enriched for glutathione metabolism and PPAR signalling, which warrants further investigation given the importance of both in macrophage metabolism and function [144,245–247].

ACE overexpression in human macrophages could represent a novel means to improve immune function, as it does in murine macrophages. Through global discovery proteomics, exploratory data could reveal if ACE overexpression is both viable and beneficial in human myeloid cell lines when immunologically challenged. Given that ACE activity and expression is also increased in some autoimmune conditions, its inhibition and impact thereof on immune cell function should be explored further [241,248,249].

Comparison of ACE +/+ and WT THP-1 macrophage proteomes revealed significantly increased ATP5B, a mitochondrial membrane ATP synthase, and NADH dehydrogenase, NDUFS3, a core mitochondrial complex I subunit that functions in electron transfer. The increased levels of these proteins support the hypothesis that ACE overexpression increases ATP production and respiratory bursts, as observed in ACE 10/10 mice [100]. Functional

enrichment analysis did not reveal an increased respiratory or ATP response induced by ACE overexpression; and it is worth noting few of these proteins were identified within the dataset owing to its untargeted approach. To rectify this, cell lysate could be fractionated and enriched for cellular compartments before MS, or a targeted mitochondrial and TCA cycle intermediate enrichment could be adopted. Alternatively, ETC and ATP components could be detected via immunoblotting. This could not be performed on the present samples due to high urea content in the precipitated protein samples and minimal protein recovery from the THP-1 lysates. In contrast, WT THP-1 macrophages had decreased ATP synthase components after Lis-Trp treatment, implying reduced ATP synthesis. Lis-Trp treatment also resulted in enriched NADP metabolism and the pentose phosphate shunt, although relatively few proteins were present in the cluster compared to in Lis-Trp-treated ACE 10/10 murine macrophages (Section 2.3.6). In addition to this, WT THP-1 KEGG ontology identified functional enrichment for the TCA cycle and respiratory electron transport. In ACE +/+ THP-1 macrophages a significant increase in ATPase proteins (such as ATP1A1 and ATP2A2) was recorded with Lis-Trp treatment, and these proteins provide the electrochemical gradient for nutrient transport across membranes.

In mice [250,251], the Kreb's cycle is different in M1 and M2 macrophages. While M2 macrophages have an unbroken cycle, M1 macrophages have one break before citrate to α-ketoglutarate conversion and a second after succinate production which feeds into the argininosuccinate shunt to replenish fumarate and malate needed for citrate production. Citrate accumulation in M1 macrophages is used for antimicrobial itaconic acid and prostaglandin inflammatory responses via fatty acid synthesis [64,251,252]. In unstimulated human ACE +/+ THP-1 macrophages, neither an M1 or M2 phenotype was apparent based on the functional enrichment analysis; however, the glycolytic enzyme GAPDH was significantly down-regulated with Lis-Trp treatment, which implies some form of glycolysis and TCA cycle disruption by ACE inhibitor treatment. Alternatively, and supported by GO and KEGG enrichment analyses, the non-metabolic functions of GAPDH were impacted. These include ER-Golgi vesicle shuttling and transport regulation independent of ATP generation and catalytic activity [253–255]. These changes are dependent on PTM of GAPDH in vesicles of the early secretory pathway, namely phosphorylation by atypical PKC (aPKC) or Akt [253,256]. Analysing the phosphorylation pattern of GAPDH and other phosphoproteins

in ACE +/+ THP-1 macrophages may therefore serve an additional mechanistic understanding of the proteome perturbance caused by ACE overexpression. Comparing the human THP-1 macrophage phosphoproteome with the murine phosphoproteome (Section 2.3.4) could implicate specific kinases in the ACE-induced signalling cascades.

Importantly, other similarities in functional enrichment between murine ACE 10/10 and human ACE +/+ macrophages were present. Human ACE +/+ macrophage actin cytoskeletal organization was functionally enriched and significantly decreased in comparison to WT macrophages as observed in ACE 10/10 mice. ACE overexpressing macrophages likely require stimulation to effect cytoskeletal rearrangement for enhanced phagocytosis and cellular migration [100,257]. At rest, human ACE +/+ macrophages had enriched immune pathways, including T cell signalling, leukocyte activation, positive regulation of the innate immune response and antigen processing and presentation. This is particularly important for the ACE-associated immune phenotype, since both T cell activation and antigen presentation are significantly enhanced in murine ACE 10/10 macrophages [5,15,132,167]. However, T cell signalling and TCR proteins were largely decreased in ACE +/+ macrophages implying down-regulation of leukocyte activation and adaptive immunity without a form of stimulation. In ACE 10/10 macrophages, the same hypothesis exists in that macrophages required stimulation to induce enhanced phagocytosis unlike NeuACE neutrophils which showed improved function at rest [100]. Although antigen processing and presentation was enriched, only the MHC Class I pathway was up-regulated. ACE aids in MHC Class I processing in mice and lack thereof cannot be accounted for by other proteases [5,15,57]. Thus, differentiated but non-polarized human ACE +/+ macrophages favour enhanced MHC Class I processing as observed in mice. In WT macrophages a significant reduction in adaptive and innate immune proteins was seen with Lis-Trp treatment. The IL-12 signalling pathway was functionally enriched and down-regulated with inhibitor treatment, alongside decreased ATP synthase expression. Similar suppression in human PBMCs was observed by Constantinescu *et al*. in 1998 using enalapril and lisinopril [258]. Normally, IL-12 acts in Th1 responses and is produced by activated macrophages [259,260]. It also induces IFN-γ production in T and NK cells, and stimulates inflammation [261]. With reduced production or signalling by IL-12, ACE inhibition may allow successful intracellular bacterial infection as with tuberculosis [261]. Functionally enriched antigen presentation and processing was also

significantly reduced with ACE C-domain inhibition in WT macrophages, which would also negatively impact the antigenic repertoire during infection.

Similar to the murine ACE 10/10 macrophages, lipid catabolism proteins were detected in human macrophages both with and without Lis-Trp treatment. However, in human macrophages, ACE overexpression did not result in fatty acid oxidation and catabolism enrichment. Rather, apolipoprotein E (APOE), a ligand for LDL, was significantly up-regulated and aids in lipoprotein binding and internalization [262–264]. APOE is known to protect against atherosclerosis and stimulates macrophages to move from the M1 to M2 phenotype, serving an anti-inflammatory function [262]. ACE overexpression could promote a baseline anti-inflammatory phenotype in this manner. In addition, PRDX6, ECHS1, SCP2, ASAH1, PSAP, and NAGA were all up-regulated in human ACE +/+ macrophages, and play a role in phospholipid, sphingolipid and glycolipid breakdown and transport, and also in the cellular stress responses and detoxification. APOE up-regulation may therefore form part of a protective arm for ACE overexpression in human macrophages, but increased lipid catabolism will also enhance energy production and provide precursors for antimicrobial pathways. However, since no fatty acid enrichment was observed in human ACE +/+ macrophages, and the fatty acid oxidation protein SCP2 was present and up-regulated, these results remain inconclusive and require more in-depth investigation. Linked to lipid catabolism is the PPAR signalling cascade which was functionally enriched after Lis-Trp treatment of ACE +/+ THP-1 macrophages [142]. PPAR signalling was also functionally enriched in murine untreated ACE 10/10 macrophages and Lis-Trp-treated WT TPMs.

There are three PPAR transcription factors, denoted α, δ and γ, each having its own pathway and downstream effects. PPARs are all activated by fatty acids and their derivatives, and are important regulators of macrophage function [144]. Four PPARγ splice variants exist and are cell/tissue-specific [245]. In macrophages, PPARγ exists as PPARγ1 exclusively owing to alternative splicing [245]. mRNA splicing and spliceosome enrichment was observed in ACE +/+ THP-1 macrophages, with PPARγ1 as a possible product. Interestingly, both ACEi [265,266] and ARBs [267–269] provide protection from type 2 diabetic onset via PPARγ agonism, and ramipril, captopril and lisinopril are thought to alter lipid and glucose metabolism to provide this protection [265,266]. Fogari *et al*. established that the non-selective ACEi lisinopril provided some protection in non-hypertensive patients, whilst

Storka and colleagues provided evidence of PPARγ stimulation and affinity by lisinopril, leading to PPARγ-mediated phosphorylation and adipocytokine release [265,270]. Lis-Trp being selective for the ACE C-domain but still a structural derivative of lisinopril was able to functionally enrich PPAR signalling in ACE +/+ macrophages. Furthermore, ACEi increase adiponectin expression via cellular retinol-binding protein 1 (CRBP1) in adipocytes contributing to anti-inflammatory protections in patients [166]. Hence, PPARγ signalling is likely to play a role in ACE +/+ THP-1 macrophages and its dysregulation by Lis-Trp may offer the same anti-inflammatory benefits. Importantly, Storka *et al.* caution that lisinopril plasma levels and lipophilicity would impact these results in humans, and that the potent PPARγ modulation may not be observed to the same extent as *in vitro* [270]. However, the action of RAS inhibition agents including ARBs and ACEi is not limited to blood pressure, and off-target effects are likely [265,266,268,270].

A pilot study by Cao *et al*. described reduced neutrophil cytotoxicity to bacterial infection in isolated human and mouse neutrophils [99]. The reduced bactericidal ability was assigned to reduced LTB_4 function and ROS production. Given that no clear PPAR pathway is enriched in ACE +/+ macrophages, PPARα may also be implicated in ACE +/+ THP-1 function in contrast to PPARγ activation via CD36 in ACE 10/10 macrophages. PPARα is activated by exposure to oxidized low density lipoprotein (oxLDL) or LTB_4, and negatively mediates inflammatory responses in macrophages. However, PPARα in humans also positively regulates NAD(P)H oxidase and myeloperoxidase (MPO) to increase ROS production [143,271]. PPARα activation in ACE +/+ THP-1 macrophages would thus occur via two pathways. First, intracellular ROS generation would induce NAD(P)H oxidase activation, causing a respiratory burst. Second, NAD(P)H induction would favour oxLDL formation which also binds PPARα to produce anti-inflammatory signals such as iNOS inhibition [143]. Since APOE was also up-regulated, oxLDL exposure could be higher with ACE overexpression and PPARα activation possible; resulting in enhanced immune abilities such as increased ROS and NAD(P)H but with self-regulating abilities to prevent prolonged inflammation [144]. Lastly, glutathione metabolism was functionally enriched in both untreated and treated ACE +/+ THP-1 macrophages. Glutathione (GSH) is primarily responsible for antioxidant defence, and regulates gene expression and nutrient metabolism [272].

GSH regulates cytokine and immune responses, and can inhibit ACE, whilst its oxidized form GSSG can stimulate ACE activity [273]. With ACE overexpression, acidic calcium-independent phospholipase A2 (PRDX6) and glutathione-dependent dehydroascorbate reductase (GSTO1) are of particular interest since they are directly related to ROS clearance, and glutathione and ascorbic acid production. GSTO1 functions in the ascorbate-glutathione cycle whereby hydrogen peroxide is detoxified. With ACE overexpression GSOT1 was up-regulated and highlights the potential for increased ROS production alongside up-regulated PRDX6 which also reduces H_2O_2. ACE 10/10 and NeuACE mouse models have increased ROS production [100]. However, in ACE +/+ THP-1 macrophages it is unclear if ROS production is increased due to enhanced immune benefits or cellular stress, which may be an unknown stimulant or from the addition of the lentiviral vector that controls ACE expression. Alternatively, ROS production may be enhanced and stored within vesicles of ACE +/+ THP-1 macrophages for rapid response after stimulation and immunological challenge via PPAR signalling. Superoxide production could be assayed in future to determine if ACE +/+ macrophages inherently up-regulate their production and in turn study if this is detrimental to the cell viability. ACE +/+ THP-1 macrophages have reduced GSOT1 and PRDX6 with Lis-Trp treatment and so would not efficiently reduce and clear hydrogen peroxide using the GSH-dependent pathway. In contrast to Lis-Trp treatment, other ACEi such as enalapril and captopril improve and favour glutathione-dependent antioxidation responses in mice [233].

A panel of 23 neutrophil degranulation markers were identified in human, but not mouse, ACE overexpressing macrophages. ACE overexpression does not necessarily lead to increased neutrophil degranulation as 15 of the 23 proteins were significantly down-regulated but strong dysregulation is still apparent. This could be studied in co-culture with neutrophils by quantifying their degranulation products, such as MPO and neutrophil-gelatinase-associated lipocalin (NGAL) [274,275]. In the present study, ACE overexpression may be providing a protective effect on macrophages and preventing induction of neutrophil degranulation, unless required. When the ACE C-domain was inhibited, neutrophil degranulation was enriched in both ACE +/+ and WT THP-1 macrophages. However, the proteins identified were significantly up-regulated in comparison to in the untreated control. ACE inhibitors such as Lis-Trp could thus be activating neutrophil degranulation and apoptosis as observed with lisinopril in polymorphonuclear neutrophils

(PMNs) by Miselis and colleagues [227]. Since there are known differences when ACEi are applied *in vitro* or given orally, ACEi have limited effects on circulating neutrophil function. Wysocki *et al*. [276] noted no H_2O_2 release in unstimulated PMNs, and no impact on ROS and H_2O_2 release in stimulated PMNs. *In vitro*, enalapril inhibited H_2O_2 release but neutrophil chemotaxis was also reduced with the addition of captopril or enalaprilat [226,276]. More recently, Cao *et al.* [99] have provided evidence in support of reduced neutrophilic action with ACE inhibition both *in vivo* and *ex vivo.* Although the focus of this study was macrophages, it appears that ACE inhibition in macrophages could cause enhanced neutrophil degranulation and apoptosis, thus indirectly reducing neutrophil survival and function. Degranulation is central to neutrophil function and macrophages co-operate to attract neutrophils to the site of infection [277]. Although the mechanisms are not clear, it is possible that exocytosis is involved based on its functional enrichment in the present study.

In conclusion, SWATH MS analysis was used to identify proteins and pathways in a human macrophage ACE overexpression THP-1 model, several of which were also previously identified in ACE 10/10 murine macrophages. These shared pathways include MHC Class I antigen processing and presentation and ATP synthase proteins. Increased ROS production is also implicated by means of significantly increased oxidant detoxification and glutathione metabolic proteins which were subsequently down-regulated with Lis-Trp treatment in ACE +/+ macrophages. Furthermore, ACE C-domain inhibition significantly dysregulated the THP-1 proteome, and appears to promote neutrophil degranulation, reduced ATP and NAD(P)H production, antigen presentation, leukocyte activation and intracellular bacterial killing. Of interest was the identification of PPAR signalling functional enrichment. Here, ACE overexpression may increase oxLDL exposure by means of up-regulating APOE expression and activating PPARα, whereas ACE inhibition may alternatively activate PPARγ cascades, thus promoting the protective anti-inflammatory responses in unstimulated differentiated ACE +/+ THP-1 macrophages. Although some differences between mouse and human macrophages were indicated, it would be worthwhile to pursue ACE overexpression investigations in human macrophage cell models further by focusing on functional assays, including phagocytic, cytokine assays, and particularly focusing on how these processes may change following M1- or M2-polarization.

5. The Role of ACE in Phagocytosis in Human THP-1 Monocyte/Macrophages

5.1. Introduction

As ACE has been implicated in MHC I/II display, it follows that it may be active in phagocytosis and cross-presentation of phagocytosed antigens [14,132,278]. ACE overexpression, in mice, results in improved phagocytic ability, which is attenuated by inhibition of the ACE C-domain or in ACE C-domain knockout models [100]. How ACE interacts with the cytoskeleton or participates in phagocytosis is unknown, but analysing this process on a cellular level may aid our understanding.

Cells generate mechanical forces to fulfil biological functions, including movement, cytokinesis, and immune regulation. Phagocytosis utilizes mechanical force to rearrange the cytoskeleton and engulf particles [279,280]. These mechanical forces can often become dysregulated, with abnormal forces causing vasoconstriction in hypertension, and can also exert different forces within the same cell population. Measuring cellular force provides a useful metric for evaluating disease progression and identifying therapeutic targets. However, this would require single cells that are uniform in shape to provide statistically significant data and less variability to uncover new disease-specific patterns [281].

5.1.1. An Overview of Phagocytosis

Phagocytosis is a category of endocytosis and is defined as the uptake of particles > 0.5 µm. Phagocytosis is actin-dependent, but clathrin-independent, unlike receptor-mediated endocytosis and pinocytosis [282–285]. During phagocytosis, mechanical force is used to engulf pathogens or clear cell debris and apoptotic cells, but it also participates in the pathogenesis of autoimmune, metabolic, and malignant disorders [282]. Phagocytes, including macrophages, DCs, and neutrophils are important components of the innate immune system, and allow for antigen presentation through macrophages and DCs to activate the adaptive immune system. This chapter presents a detailed discussion of professional phagocytes, one of which being macrophages, and their involvement with ACE [57].

5.1.1.1. Phagocytosis Pathways

Receptor recognition has evolved to enable separation of self from non-self through multiple receptor interactions and exploitation of conserved microbial components required for pathogen infection and survival [283]. Consequently, the phagocytic process is controlled in a pathogen-dependent manner by numerous pathways via the different receptors capable of inducing it [283]. These pathways include Fc receptor- , complement-, and mannose-receptor-mediated phagocytic pathways. However, each of these pathways follow similar steps: exogenous particle internalization via receptor interactions, polymerization of actin and ingestion of the particle, phagosome maturation through fusion and fission with endocytic pathway components, finally leading to mature phagolysosomes **(Figure 5.1)** [283].

Infection recognition is mediated through conserved features involved in pathogenesis. There are two types of phagocytic particles: apoptotic/necrotic and microbial, which are used for distinguishing between altered self and foreign bodies, respectively.

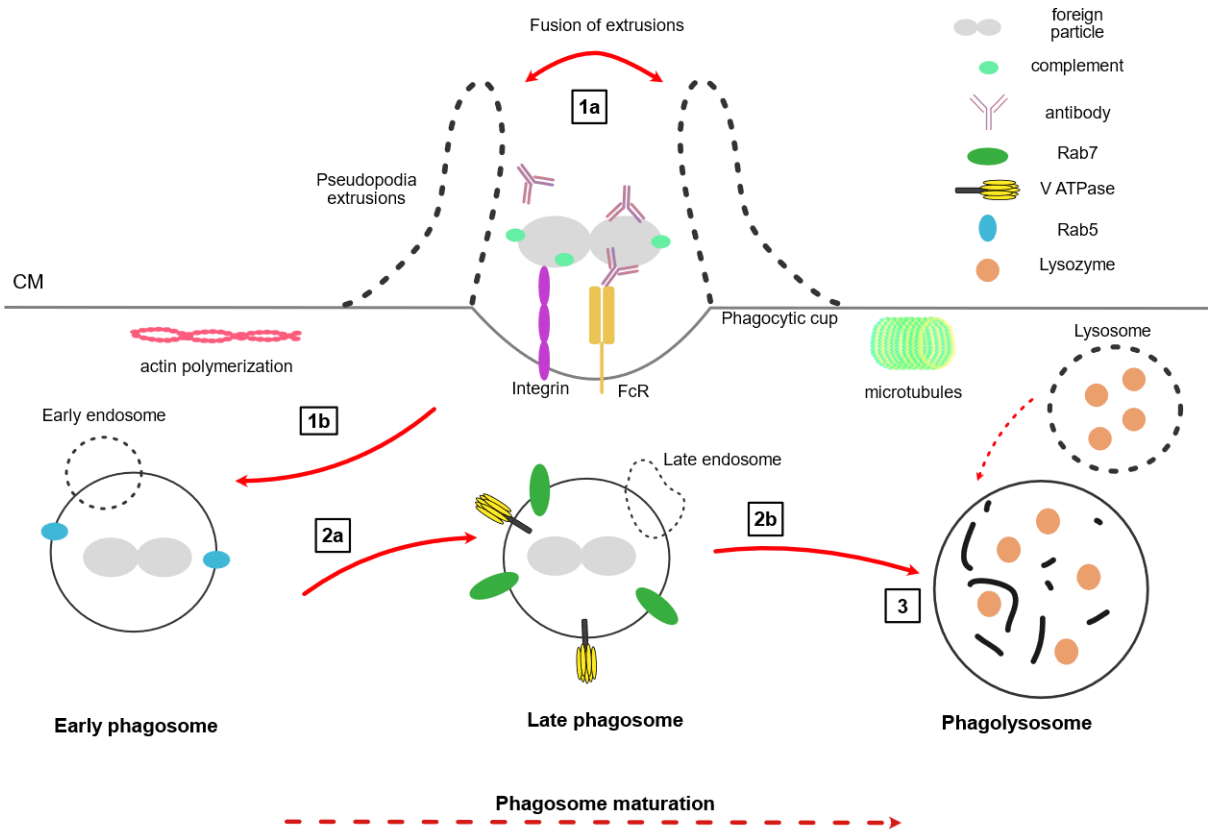

Figure 5.1: The early and late stages of phagocytosis in professional phagocytic cells. A summary of the phagocytic process sampling receptor-mediated endocytosis. The duplicate grey oval represents a phagocytic particle that can either be cellular debris, apoptotic cells, or foreign particulates (e.g., pathogen). The particle is engulfed (1a), and the resultant vesicle is brought into the phagocyte (1b) where it undergoes a series of membrane fusions with endosomal and lysosomal vesicles (2a). If a pathogen is detected, the lysosome fusion will undergo a pH change and degrade the pathogen through acidification and digestion in the phagolysosome (2b & 3). These proteins can then be sampled and displayed for T cell activation. Self-antigens are also sampled and will prevent immune activation. Abbreviations: CM – cell membrane

5.1.1.1. Fc Receptor-Mediated Phagocytosis & Complement-mediated Phagocytosis

Fc receptors recognize immunoglobulin or antibody portions. Antibodies recognize a foreign or self-particle and bind to it and can then opsonize the particle and stimulate phagocytosis through Fc receptor binding. A pathogen may also be opsonized by complement components or antibodies in the humoral response, and via cellular recognition involving pathogen recognition receptors and pathogen-associated molecular patterns (PAMPs), including LPS, mannans, and formylated-peptides. Once the cargo molecule is bound by its receptor, actin filaments assemble to form pseudopods around the antigen. The filaments continue to surround the particle as the phagocytic cup forms and support the plasma

membrane throughout the process. The phagosome then follows a series of fusion events as it matures, with constant antigen sampling to T lymphocytes to differentiate self and non-self. The body enclosed within the phagocytic cup determines the maturation steps that occur [285,286].

5.1.1.2. Mannose Receptor-Mediated Phagocytosis

Mannose receptors are members of the C-type lectin family and bind glycans [283,287,288]. Mannose receptors are PAMPs, and can identify multiple pathogens, including *Mycobacterium tuberculosis* and *Streptococcus pneumoniae*, to the immune system [287]. Glycan recognition also serves as a fungal infection detector, since these sugar molecules are important components of the fungal cell wall, particularly β-glucan [289]. The interactions between pathogen and host glycans with mannose receptors is not well understood, and this is also true in phagocytic macrophages, but the interaction is known to be calcium-dependent [285]. Thus, the phagocytic internalisation pathway is unclear at present, but it is understood to include both pathogenic and macrophage-expressed glycans, which interact with each other to determine the appropriate innate immune response [287].

5.1.1.2. Phagosome Maturation

After internalization, the phagosome and F-actin are depolymerized to allow early endosome access [282,286,290]. The vacuole fuses with endosomes and matures through a series of events and pH changes, ultimately creating phagolysosomes by fusing with lysosomes. The time to reach maturity depends on the receptors activated, ranging from 30 minutes to hours. Rab family GTPases can also determine maturation age, control vesicle fusion and are used as markers for this event [285]. The Rab GTPase family has a characteristic distribution during phagosome maturation. Briefly, Rab5 is displayed by the phagosome promoting early endosome fusion when bound by Early Endosome Antigen 1 (EEA1). Recycling vesicles move to the cellular membrane to balance endosome volume. Rab5 is then exchanged for Rab7, whereupon late endosomes and lysosomes (pH 4.5) fuse together with the early endosomes (pH 6.2) [285,286]. The pH of the resultant phagolysosome changes to between pH 4.5 and 5.0 once fused [282,285]. The phagolysosome then digests the particulate through acidification and degranulation, from which the remaining peptides may be sampled for antigen presentation or destroyed

completely. Cathepsins digest the proteins alongside NAD(P)H oxidase, which initiates ROS production for enhanced pathogen clearance.

Neutrophils activate their powerful microbicidal activity once phagocytosis takes place [282,286]. This allows degranulation and efficient killing of the engulfed particulates or bacteria. Neutrophils also contribute a large oxidative burst to plasma membrane assembly of NAD(P)H oxidase. In contrast, monocytes/macrophages have few granules, but secrete them after phagocytosis [283,286]. This includes generation of free radicals and use of arachidonates and phospholipids from a burst in glycolytic and oxidative/respiratory responses. The macrophages also secrete cytokines and enzymes that aid in inflammation and leukocyte recruitment. The level of acidification in a macrophage differs according to its polarization. M1 macrophages maintain high ROS production and the acidity maintains peptides for MHC activation, while M2 macrophages have lower ROS production and faster acid-mediated peptide degradation for wound healing and resolution of inflammation [285]. As a mixed macrophage phenotype is observed with ACE overexpression in mice, the mechanism of phagocytosis may use a combination of glycolytic/oxidative bursts to encourage enhanced phagocytic clearance with minimal collateral tissue and cell damage [100].

5.1.2. Aim & Objectives

Phagocytic efficiency is improved during ACE overexpression [100]. Although the mechanism is unclear, it is ACE-dependent as knockout and inhibited ACE domains decrease this ability in mice. This bactericidal phenomenon has been observed in macrophages and neutrophils using fluorescent *E.coli* assays and cell population-level neutrophil cytotoxicity assays in mice and humans [99,100]. Single cell methods have not previously been utilized to confirm these population measurements. Furthermore, the C-domain has been implicated in this pathway, but no further work has been done to determine the phagocytotic ability of ACE overexpressing macrophages, to date.

Therefore, the aim of these experiments was to evaluate the effect of ACE overexpression and ACE domain-specific inhibition on human THP-1 macrophage phagocytic ability by applying a novel elastomeric micropattern methodology to measure phagocytic contractions.

5.1.2.1. Objectives

- To ascertain whether THP-1 macrophages could be used on elastomeric micropatterns for measuring their mechanical contraction during phagocytosis.
- To confirm that ACE overexpression enhances phagocytosis at the single cell level using elastomeric micropatterns.
- To determine if treatment with domain-selective ACE inhibitors would have an impact on phagocytosis at the single cell level.

5.2. Methodology

An overview of the experimental design is shown in **Figure 5.2**. Briefly, differentiated THP-1 macrophages were washed and lifted to be seeded onto elastomeric micropattern plates, whereupon ACE domain-selective inhibitor treatments were applied. Phagocytic substrate was added after 30 minutes, and the cells incubated for a total of 3 hours before fluorescent staining and imaging was performed. The phagocytic substrate used was a carboxyl-modified latex bead. Carboxyl modifications are preferrable in phagocytic assays, because carboxyl group microparticles have greater phagocytic efficiency than amine-modified microparticles [291–293].

The domain-selective ACE inhibitors used were RXP380A or Lis-Trp and RXP407 for the C- and N-domain, respectively. RXP380A was chosen as a preliminary inhibitor but was not continued after initial proof of concept experiments as Lis-Trp is more clinically relevant for inhibitor studies and resembles lisinopril [187,294].

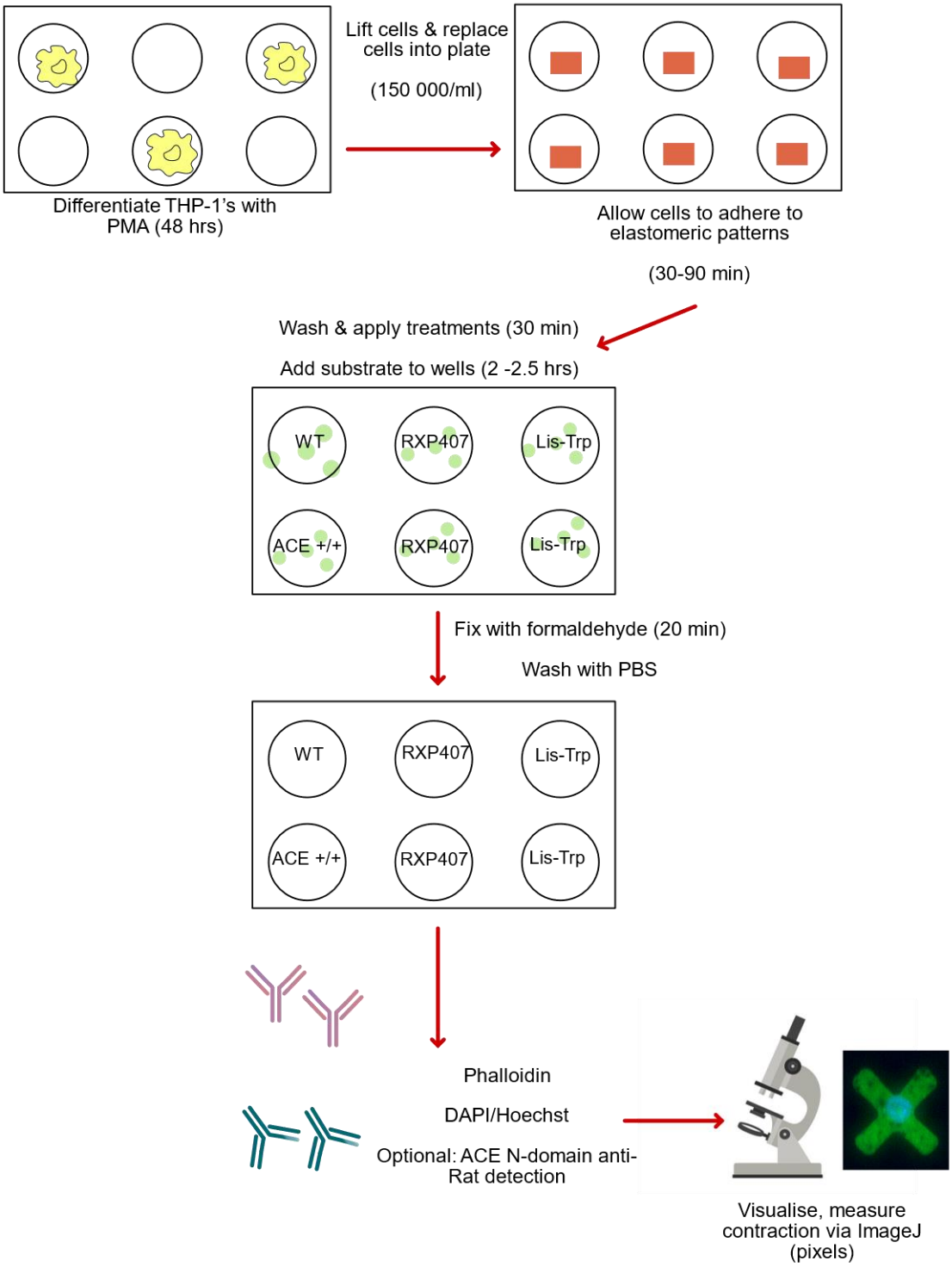

Figure 5.2: Experimental design using elastomeric micropatterns to assess the role of ACE in phagocytosis and the impact of ACE inhibition on WT and ACE +/+ THP-1 macrophages. Contraction was measured and quantified using ImageJ/FiJi [295], and differences between groups were evaluated using the Student's t-test. A red-fluorescently labelled anti-ACE antibody, blue DAPI (nuclei), green micropattern and far-red phalloidin stains (cell contour) were used to visualise distinctive features of the THP-1 macrophages.

5.2.1. ACE +/+ & WT THP-1 Cell Culture

ACE +/+ and WT THP-1 cells were cultured as outlined in Section 3.2.1, but with the addition of 1 μg/ml puromycin for ACE +/+ THP-1 construct selection.

5.2.2. Elastomeric Micropatterns for Measuring Single Cell Mechanical Force

As cells produce mechanical forces to fulfil their function, reliable measurement of these forces becomes important when designing therapeutics which motivate component relaxation, such as in cardiovascular disease [67,176,296]. A biomaterial of Traction Force Microscopy (TFM) and elastomeric micropost array, known as fluorescently labelled elastomeric contractible surfaces (FLECS), allows increased experimental throughput and data acquisition at the single cell level in a multi-well format [281]. Briefly, cells adhere to uniform and fluorescently labelled micropatterns atop an elastomeric film **(Figure 5.3)**. The mechanical forces exerted produce calibrated displacement of the standardized micropatterns that can be quantified using image analysis software.

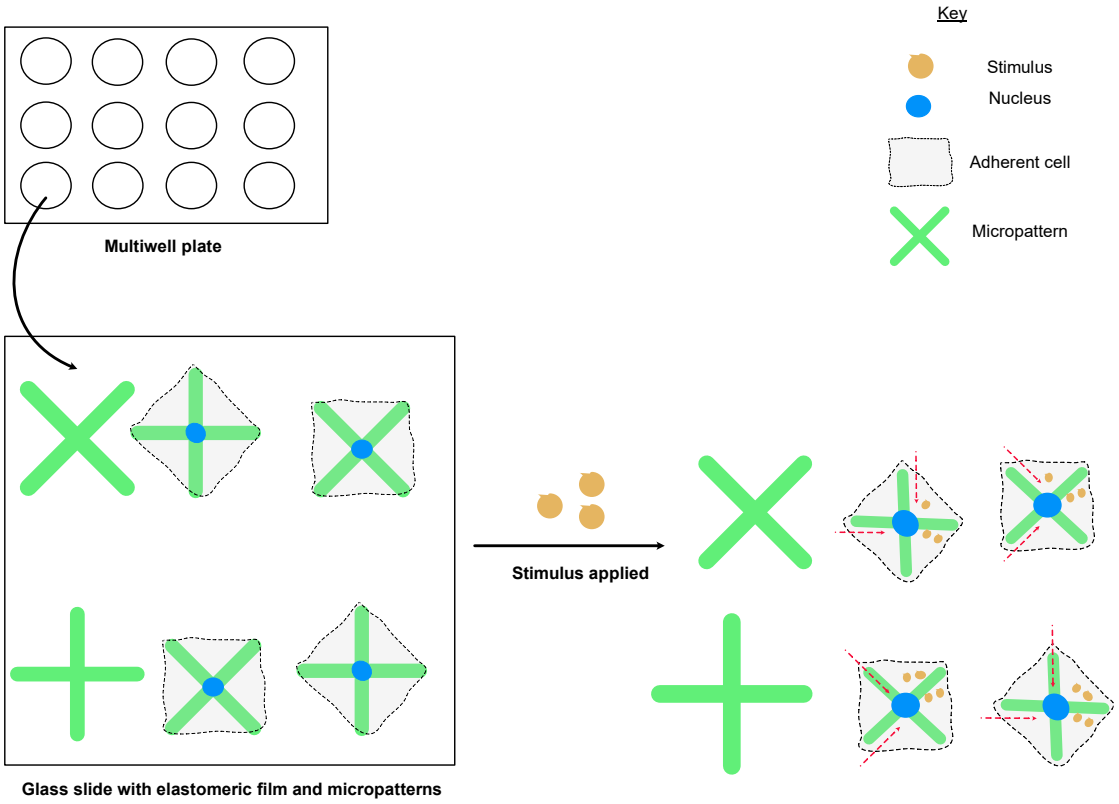

Figure 5.3: FLECS combination technology schematic. A glass support with elastomeric film and adhesive micropatterns is embedded into multi-well plates for high-throughput data acquisition of multiple experimental conditions. Micropatterns without cells remain unchanged despite stimulation, whilst adherent cells are stimulated and exert mechanical forces in the form of contractions (red dotted arrows) which can be measured using image analysis software (Adapted from Pushkarsky *et al*. [281]).

The uniformity imposed on these cells allows one to investigate cell responses in a controlled environment, particularly for macrophages, which are highly plastic and heterogeneously shaped even in cell culture [90,173,297–299]. Using micropatterns can also indicate where subcellular localization, if any, is taking place and this is of interest in protein biochemistry when determining how treatments and stimuli may impact cell movement, degradation, or synthesis [299,300].

5.2.2.1. Elastomeric Micropattern Preparation

WT and ACE +/+ THP-1 monocytes were cultured in 10% RPMI media to a density of 2×10^5 - 1×10^6 cells/ml. Cells were then centrifuged at 300 x *g* for 5 minutes and resuspended in 10% RPMI at 2×10^4 – 1×10^5 cells/ml and seeded at 2×10^4 cells/ml per well in a 6-well plate. PMA differentiation (25 ng/ml) was carried out over 48 hours, with a

24-hour recovery period in PMA-free media. Cells were washed with cold 1x PBS in between media changes and lifted using 0.25% trypsin in EDTA.

For elastomeric micropattern analysis, cells were seeded onto 6- or 12-well plates already prepared with the elastomeric cross-shaped micropatterns. Each well was seeded with 2×10^4 differentiated macrophages, which were then incubated for 60 minutes to allow adherence.

The adherent macrophages were treated with either a C- or N-domain ACE inhibitor (10 µM Lis-Trp or RXP407, respectively). An untreated control group was also prepared. Cells were treated for 30 minutes before addition of the carboxyl-modified latex beads, a phagocytic substrate, followed by a further 2.5-hour incubation period. The media was then removed, and cells were fixed using 4% formaldehyde. The fixed cells were then washed with 1x PBS and permeabilized with 0.25% Triton (20 minutes) to allow fluorescent antibodies and stains entry.

5.2.2.2. Imaging

An ACE rat-derived antibody (4G6, gifted by SM. Danilov, USA) was added to detect the N-domain of ACE, DAPI to visualize the nucleus, and phalloidin to show cell shape. The elastomeric micropatterns were fluorescent green. The latex beads were also fluorescently labelled; however, their fluorescence was not detected because an orange channel was unavailable on the microscope.

Imaging was performed using the Stellar Vision microscope at 20x magnification, utilizing Synthetic Aperture Optic technology (Optical Biosystems, USA). The channels are shown in **Table 5.1**.

Table 5.1: Stellar Vision fluorescent channels. Used to detect specific components of THP-1 macrophages adhered to elastomeric micropatterns and stimulated during phagocytosis.

Channel	Biological Component Detected
532 nm Green (FAMS)	Micropattern
473 nm Blue (DAPI)	Nucleus
660 nm Red (Cy5)	Phalloidin/ACE

5.2.3. Statistical Analysis

Images were analysed using ImageJ/FiJi software (version 1.53q [208,295,301]). A line was drawn from one end of the elastomeric micropattern to the opposite end, and the number of pixels measured. A standard, uncontracted micropattern measures 150 pixels in length. Only singly and correctly adherent cells were chosen for image analysis. The resultant lengths were subtracted from 150 pixels and the mean contraction length calculated along with standard deviations for each experimental group. A Student's t-test was performed to evaluate differences between groups. ACE +/+ data was normalised against WT data. At least 30 cells per experimental condition across all images were analysed. Statistical outliers (>2SD) were removed from experimental groups in downstream processing.

5.3. Results

5.3.1. WT THP-1 ACE Inhibition & Phagocytic Measurement

Representative images of the ACE signal and cell spreading over the elastomeric micropatterns are shown in **Figure 5.4**. Although phagocytosis can be successfully measured using elastomeric micropatterns **(Figure 5.4A)**, the level of THP-1 adherence and the correct ACE antibody for visualization was also tested **(Figure 5.4B & C)**. Cells were seeded at a lower density (2×10^4 - 3×10^4 cells/ml) in future experiments as macrophages tended to clump on micropatterns at higher densities (2×10^5 - 1×10^6 cells/ml) and could not be imaged or quantified. The ACE N-domain selective rat antibody used, 4G6, and fluorescent red anti-rat antibody showed that ACE was dispersed within the cell, and it was therefore necessary to stain for actin filaments using phalloidin in future experiments to ensure correct adherence **(Figure 5.4C)**.

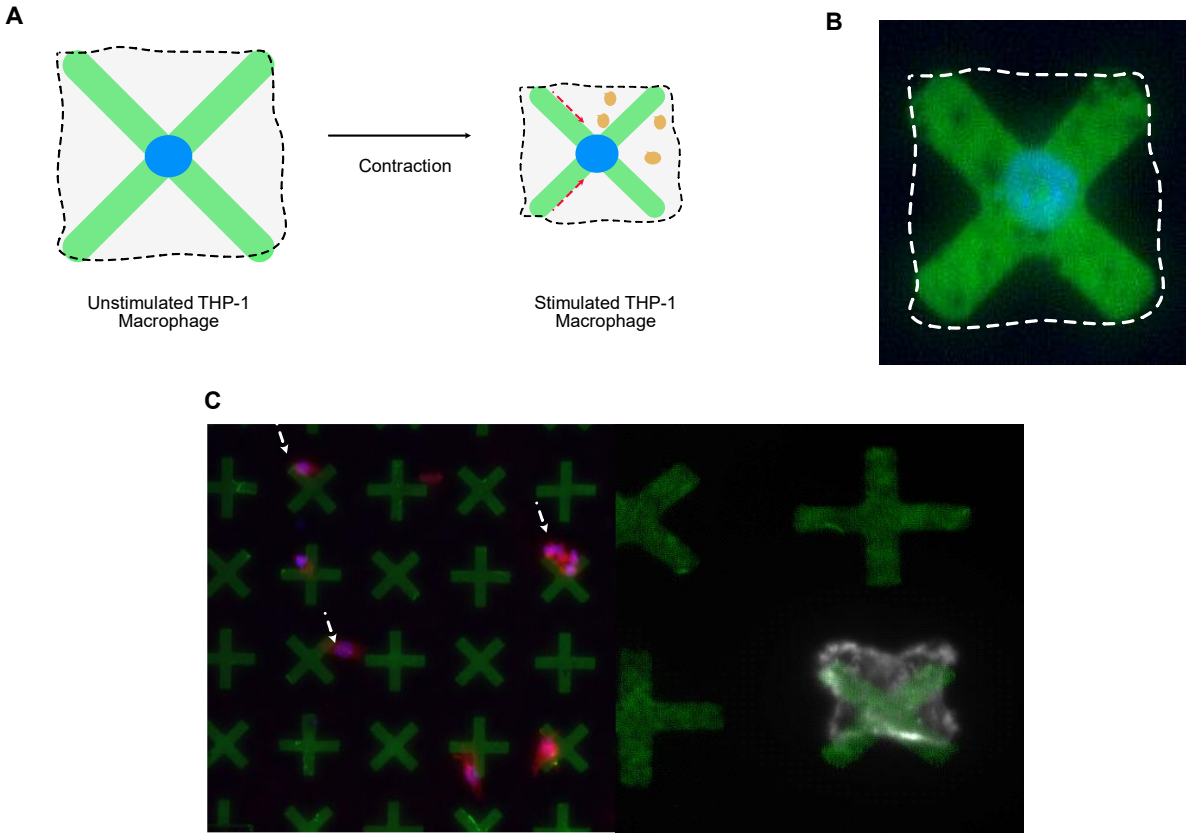

Figure 5.4: Mechanical force, including phagocytosis was measured on single cells that were adhered to elastomeric micropatterns. (A) Schematic of how contraction occurs when cell adheres to a micropattern and is stimulated, in this case with phagocytic latex bead substrate. The cross of the micropattern contracts in size as the cell phagocytoses the substrate. *Red dashed arrows represent contraction, orange circles represent latex beads, blue circle represents nucleus and dashed black line is cell shape with green cross as micropattern. (B) An ideally adherent THP-1 macrophage on an elastomeric micropattern is centrally located on the micropattern indicating maximum mechanistic force would be applied upon stimulation. (C) Sample images of THP-1 cells on elastomeric micropatterns. The left image with white arrows shows clustered or incorrectly adherent THP-1 macrophages. These cells would not contract the micropattern correctly upon stimulation. On the right, the cell contours are shown via phalloidin stain, and the cell is uniform in shape as expected, and will contract the micropattern correctly. The cell cytoskeleton is stained with phalloidin, and nuclei are stained with DAPI.

Importantly, when the phagocytic beads were absent, a lack of micropattern contraction was observed. ACE inhibitors Lis-Trp (or RXP380A) and RXP407 treatments could impact contractile ability in WT THP-1 macrophages. From this proof-of-concept work, WT THP-1 cells showed increased cellular and micropattern contraction when exposed to a phagocytic

substrate and ACE inhibition appeared to cause less cellular contraction and therefore phagocytosis **(Figure 5.5)**.

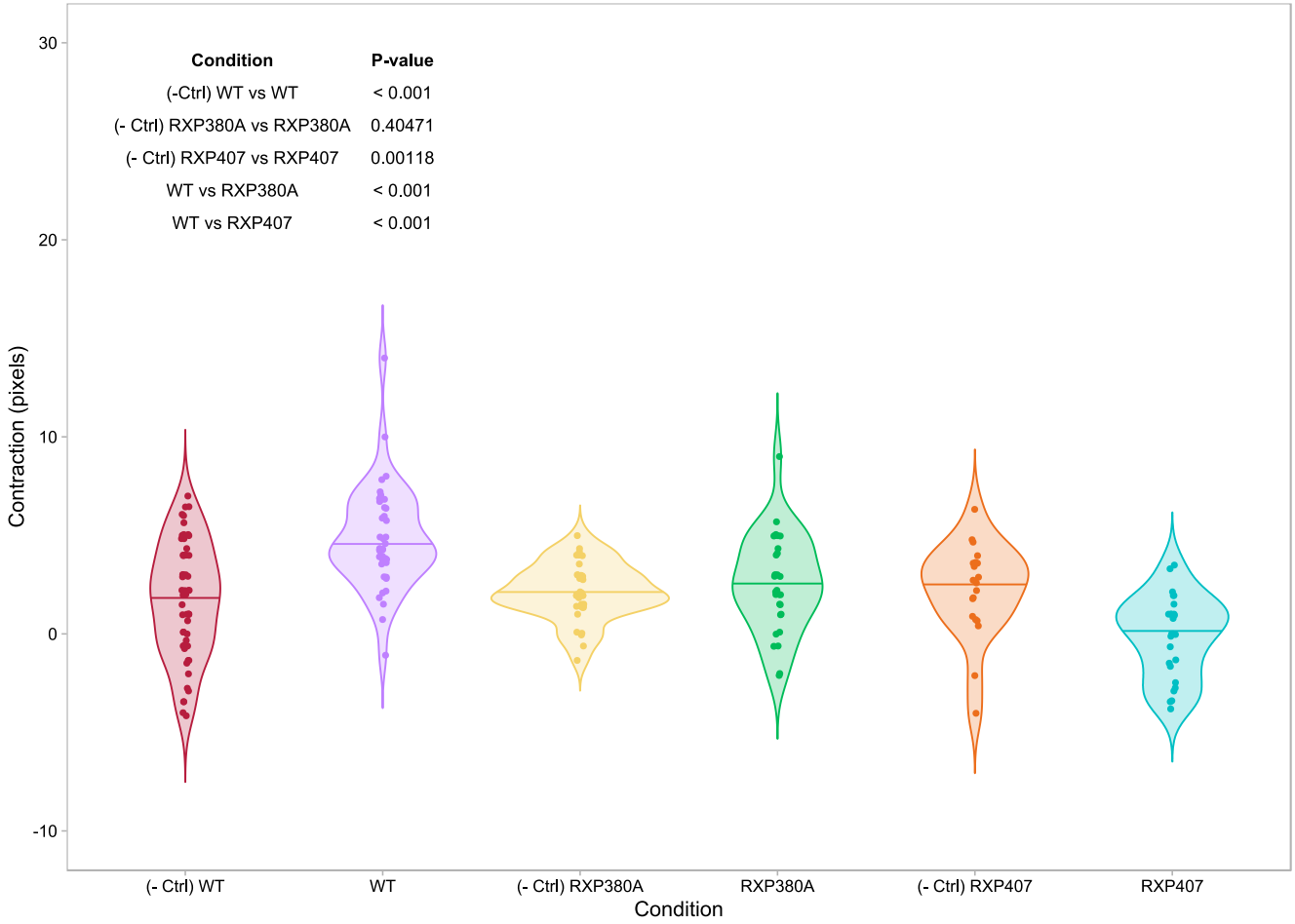

Figure 5.5: WT THP-1 macrophages exhibit cellular contraction on micropatterns both with and without ACE inhibition. A violin plot displays the spread of data for the different experimental conditions with statistical outliers (> ± 2SD) removed. The means are displayed as solid lines in each group. Each group had a minimum of 30 images per condition analysed. RXP380A denotes a C-domain ACE inhibitor and RXP407 denotes an N-domain ACE inhibitor. Differences between groups were evaluated by unpaired Student's t-test, and P-values are shown in the inset. P-values ≤ 0.05 taken as statistically significant. Negative controls (- Ctrl) had no phagocytic substrate present.

Cells receiving RXP407 treatment, both with and without phagocytic substrate, had several outliers, which were removed from further statistical analysis **(Figure 5.5)**. Both C- and N-domain selective ACE inhibition resulted in significantly decreased micropattern contraction compared to WT THP-1 macrophages, suggesting their involvement in the phagocytic behaviour of human macrophages.

5.3.2. ACE Overexpression & Inhibition Alters THP-1 Macrophage Phagocytic Contraction

ACE +/+ THP-1 macrophages showed markedly increased elastomeric micropattern contraction when exposed to a phagocytic substrate in comparison to WT THP-1 macrophages **(Figure 5.6 &Figure 5.7)**.

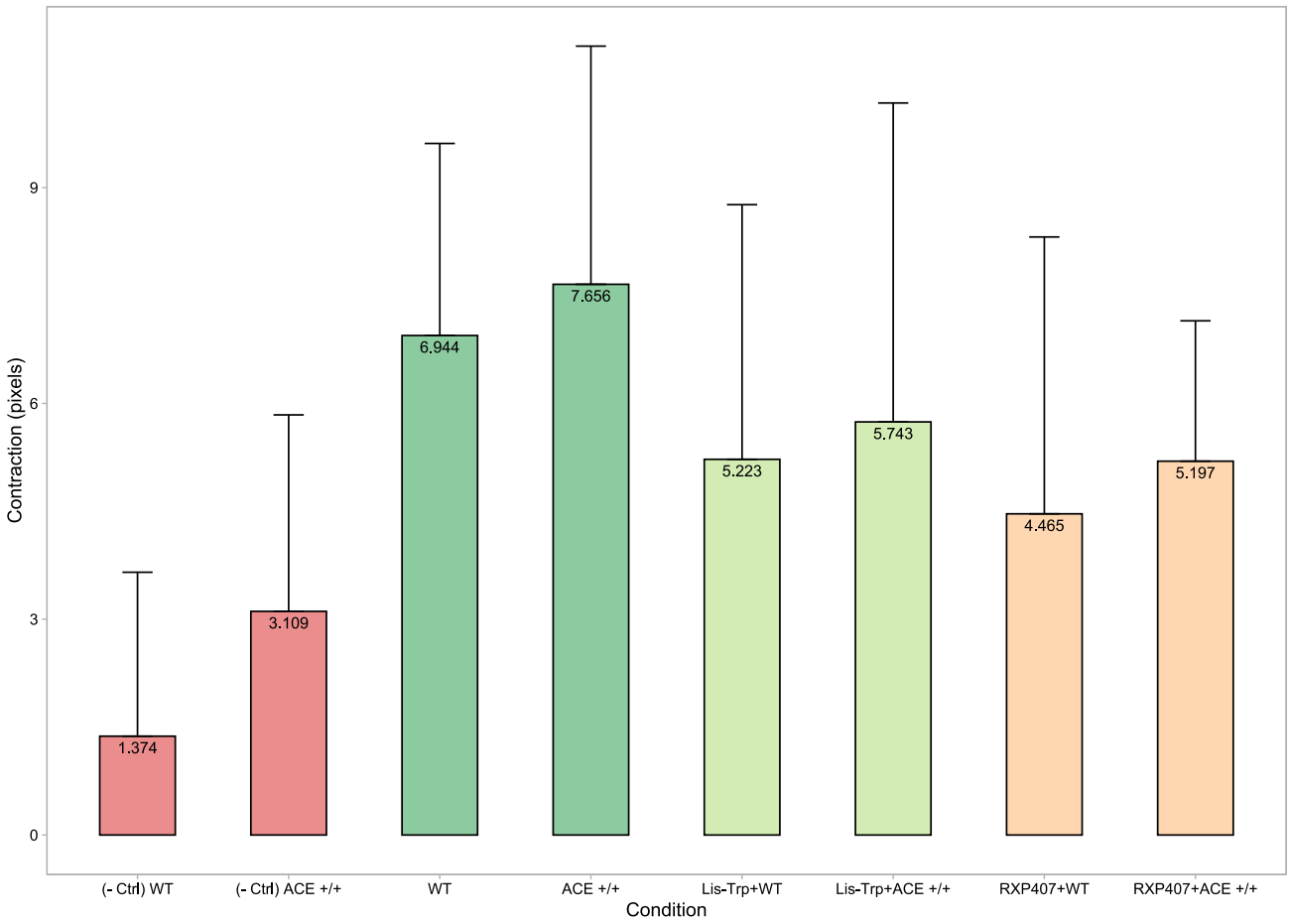

Figure 5.6: The impact of ACE overexpression & inhibition on THP-1 macrophage phagocytosis. WT THP-1 cells were used as a control for normalization purposes. Lis-Trp was used as the C-domain inhibitor, and RXP407 as an N-domain inhibitor. All groups, except for the negative control, received phagocytic substrate. Red – Negative control (- Ctrl), dark green – No inhibitor treatment, light green – Lis-Trp treatment, orange – RXP407 treatment. Data represents the mean contraction and the standard deviation shown as error bars.

Interestingly, both N- and C-domain specific ACE inhibition resulted in a statistically significant decrease in contraction by the ACE +/+ THP-1 macrophages **(Figure 5.7)**. This trend matches that observed for WT macrophages, where a significant reduction in contraction was observed with N- and C-domain specific ACE inhibition **(Figure 5.5)**. ACE overexpression therefore increased human macrophage contractile ability *in vivo*, with both

N-domain and C-domain inhibition significantly decreasing the level of contraction in ACE +/+ THP-1 macrophages.

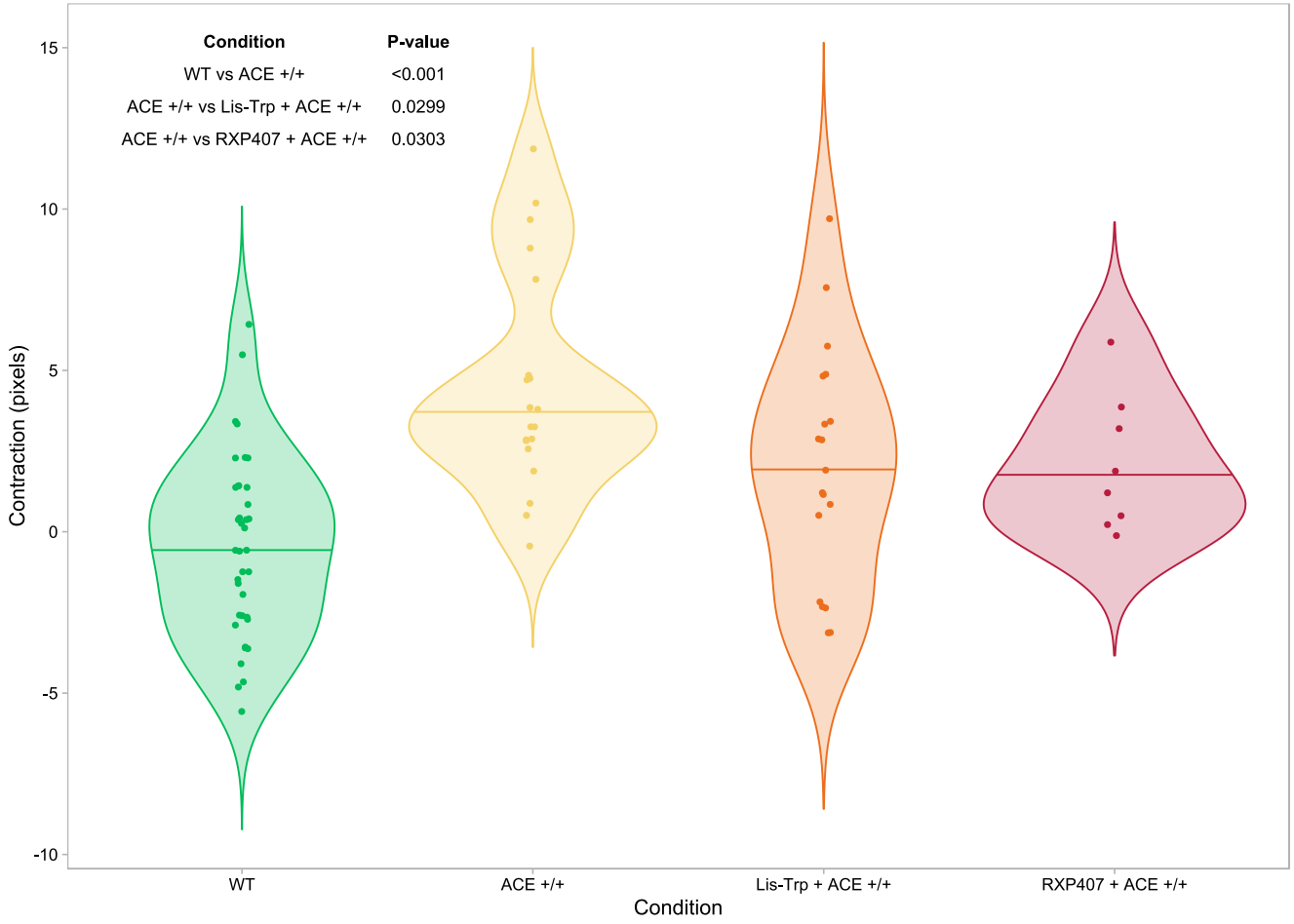

Figure 5.7: ACE overexpression aids phagocytic contraction whilst ACE inhibition negatively affects contraction in THP-1 macrophages. Data are normalised to WT. Contraction was compared in ACE +/+ THP-1 macrophages and WT macrophages with and without ACE inhibitor treatment in the presence of phagocytic substrate. Means displayed as solid lines within each violin plot. P-values ≤ 0.05 taken as statistically significant after an unpaired Student's t-test.

5.4. Discussion

In this chapter, elastomeric micropatterns were used to evaluate cellular contractions of THP-1 macrophages undergoing phagocytosis. ACE overexpression resulted in increased THP-1 contraction compared to WT THP-1 cells, and domain-selective ACE inhibition abrogated this effect. Inhibition of either ACE domain resulted in a statistically significant decrease in cell contraction, suggesting that both domains play a role during phagocytosis.

ACE overexpression in murine macrophages has been studied extensively within these cells and an improved phagocytic ability has been identified using a fluorescent *E. coli* phagocytosis assay [133]. However, this work identified the C-domain as the main player in the enhanced immune abilities of both the murine macrophages (ACE 10/10) and murine neutrophils (NeuACE). In human cell lines, no work has been published, so we aimed to determine if ACE overexpression would have the same effect in human macrophages using the human THP-1 ACE +/+ cell line.

Population level phagocytosis assays, such as the fluorescent *E. coli* assay, tend to give different results with different ligand concentrations, but single-cell measurements may not [302–305]. Macrophage single cell phagocytosis has been previously quantified in macrophages using elastomeric micropatterns and from these studies it was hypothesised that the THP-1 cell line had increased contractions when treated with phagocytic substrates compared to when no substrate was present [281,296]. In the present study, phagocytic substrate was not quantified in the macrophages as the acidic nature of the lysosome has been known to quench fluorescence, and the microscope used did not have an orange channel available (Section 5.2.2.2) [306]. Results could be improved by quantifying the fluorescence of the latex beads as a proxy for latex bead uptake [306]. As this method could be used to assess phagocytic action, it could also be useful for assessing how target proteins impact the signalling pathways leading to cellular response [281].

This novel single cell-level measurement was first used in human monocyte-derived macrophages (hMDMs), utilizing IgG opsonization as the contraction stimulant embedded in a BSA-silicone micropattern [281]. Pushkarsky and colleagues have also assessed which phagocytic stimulant would result in the largest contractile force on these mounted elastomeric micropatterns and if this is directly related to the quantity of stimulant present. Interestingly, there was no significant difference in phagocytic forces exerted by the hMDMs when IgG quantity was altered [281]. This suggests that phagocytic force is independent of opsonin scaling and is either activated or deactivated in single cell hMDMs providing an initial threshold is met. Similarly, cytokine secretion pathways in T cells are activated by the presence of antigens and not their quantity, a process known as ‘digital response’ [302,307]. Digital response is well-characterized in neurons, producing ‘all-or-nothing’ action potentials, but is poorly studied in non-excitable cell types, including immune cells

[281,302,307]. The increased contraction measured in the WT and ACE+/+ cell lines in the present study suggests that digital response may be occurring in human THP-1 macrophages when exposed to varying phagocytic substrate quantities.

Interestingly, cellular contraction was observed despite neither cell line being polarized using cytokines before the addition of latex beads. This suggests that PMA primes THP-1 macrophages for phagocytic stimulation. Although it was not confirmed directly in these experiments, THP-1 macrophages are known to be heterogeneous after PMA differentiation, and still favour an inflammatory phenotype associated with enhanced bacterial clearance [91,196,197,216,308,309]. However, phagocytic forces appear to change in response to opsonin type with immunoglobulins resulting in the greatest contraction and non-opsonized BSA, fibronectin and vitronectin resulting in relatively small displacements [281]. A sub-population within the THP-1 macrophages may have been activated through non-Fc receptors, resulting in some cells having much higher contraction than others within each experimental group [281]. In the present study, there is an overall statistically significant trend towards higher contraction or pixel measurements in the phagocytic substrate-treated WT THP-1 macrophage group compared to in the untreated WT THP-1 macrophages. The mean contraction, which is a proxy for phagocytic movement, was lower in the (-Ctrl) WT (1.655 pixels) than in the WT (4.839 pixels) group, indicating that lesser understood or immunologically important targets can still cause phagocytic stimulation of differentiated THP-1 macrophages [281]. Therefore THP-1 macrophages, both ACE overexpressing and WT, exhibit a downstream signalling convergence that is similar to digital cellular response in T cells via NF-κB and neuronal action potentials [281,302,303,305,307].

Based on the findings of the present study and previous studies; ACE overexpression can increase phagocytic action in THP-1 and murine macrophages, suggesting a role within cytoskeletal rearrangement and movement independent of Ang II. The enhanced phagocytosis is present with ARB but not ACEi treatment or ACE C-domain knockout in mice.

In respect of digital responses, perhaps either Fc or non-Fc receptors require lower activation energy or phosphorylation/dephosphorylation thresholds and fewer pathways to activate phagocytosis, resulting in more cells being activated at any ligand concentration. This should be explored via transcriptomics and proteomics to understand changes in gene

and protein expression, and thus gain insights into this as yet unknown mechanism. Alternatively, ACE may be directly involved in cytoskeletal reorganization and cell migration.

ACE KO and inhibition is detrimental to both human neutrophils and murine ACE 10/10 or NeuACE models in clearing bacterial infections [58,99,100,310]. It is of interest that as little as 10 µM ACE inhibitor treatments are able to significantly impact macrophage contraction, particularly in ACE +/+ THP-1 macrophages since 50 µM Lis-Trp has been deemed necessary for biological impact according to our collaborators [K. Bernstein, personal communications, 27 November, 2021], and 100 µM over two hours also partially inhibited ACE activity (Section 3.3.2). If low ACE inhibitor concentrations can exert this effect with minimal uptake, ACE inhibitor therapy may be detrimental to immunocompromised individuals [99]. The ACE C-domain is thought to be responsible for the enhanced immune phenotype of ACE 10/10 murine macrophages and NeuACE neutrophils. However, our findings suggest that the N-domain is also involved in phagocytic processing as contraction was significantly decreased with RXP407 and Lis-Trp treatment in cells overexpressing ACE. In WT THP-1 macrophages, a significant difference in cellular contraction was observed with both C- and N-domain inhibition. Phosphinic peptides, including RXP407 and RXP380A used here, are highly selective for zinc-metallopeptidases and act as transition state analogues of the enzyme substrates [311]. Dive *et al*. [312] demonstrated a broad substrate specificity for the N-domain, and Semis *et al*. [42] demonstrated broad ACE and more particularly C-domain substrate specificity. In doing so, ACE may be directly involved in phagocytosis through foreign protein degradation as with MHC I/II presentation in murine models [15,132].

In the present study, we confirmed that ACE overexpression increases phagocytosis as measured by elastomeric micropattern contractions in comparison to WT THP-1 macrophages. To improve this high throughput assay, opsonized phagocytic beads or *E. coli* fragments could be used in future to assess whether greater cellular force is associated with different phagocytic substrates. Simultaneously, a greater number of cells should be assessed in future for increased statistical power. To complement the contraction data, the fluorescence of the latex beads should be measured as a proxy for phagocytic uptake. The results of single cell measurements using elastomeric micropatterns implies that both ACE and WT THP-1 macrophages use a digital cellular response when exposed to a threshold of latex beads or phagocytic substrates resulting in more cells being activated and a higher

population responding to the ligand overall. ACE domain inhibition shows a significant decrease in phagocytosis in ACE overexpressing macrophages and is also significantly decreased with both N- and C-domain inhibition in WT human macrophages using phosphinic peptide inhibitors. ACE overexpression therefore shows similar results in respect of phagocytic action in both human and murine macrophages, showing heightened phagocytic ability observed when exposed to non-opsonized phagocytic latex beads, suggesting a direct role for ACE in cytoskeletal rearrangement and phagocytosis that is independent of Ang II. Elastomeric micropatterns are thus suitable for single cell evaluation of phagocytosis in human THP-1 macrophages, with both WT and ACE +/+ cell lines showing contraction when stimulated with a phagocytic substrate.

6. Conclusions, Limitations & Future Directions

6.1. Conclusions

ACE overexpression in macrophages and neutrophils shows promise in treating infections and non-communicable diseases [5]. This enigmatic enzyme participates in an unknown Ang II-independent mechanism that provides enhanced immunity in murine models [6,15,100,133]. Although the substrates and pathways at work remain elusive, global proteomics may provide clues to understanding the ACE overexpression mechanism further and directing future research. This work presents the intracellular proteomic changes in ACE 10/10 murine macrophages and human ACE +/+ THP-1 macrophages. The biological impact of ACE C-domain inhibition on both ACE overexpressing and WT macrophages was also investigated. In Chapter 2, the intracellular murine ACE 10/10 macrophage proteome and phosphoproteome was investigated using untargeted mass spectrometry. Several functional pathways previously identified in the literature as more active, and part of the enhanced immune benefits were enriched and their participating proteins up-regulated. These immune pathways include antigen processing and presentation, T cell activation and signalling, ROS production and phagocytosis. The murine macrophages also have increased TCA cycle activity, ATP production and oxidative respiration all of which were functionally enriched and up-regulated in our dataset. We were thus able to confirm pre-existing literature on the ACE 10/10 macrophages in addition to greater proteome coverage. To gain further insight into active or repressed signalling pathways of ACE overexpressing macrophages, phosphoproteomics was performed. The MAPK1/ERK2 and PKA pathways were highlighted by the presence of their kinase/phosphatase targets including Inpp5d and Pkn1. Although similar phosphoproteomic responses were observed with ACE 10/10 macrophages and WT macrophage C-domain inhibition in comparison to WT macrophages, Inpp5d and Pkn1 had different phosphosites in each comparison. Inpp5d is particularly interesting as it is classically anti-inflammatory and may counteract the immune activation observed with ACE overexpression in macrophages [153,313,314]. ACE also participates in MAPK signalling as observed with ACE inhibitor treatments where it mediates the MAPK and AP1 downstream signalling cascades [165,166]. However, the MAPK/ERK signalling is a known Ang II-mediated pathway that induces ACE up-regulation and ACE2 down-regulation and the addition of an ARB treatment condition may instruct this pathway in conjunction

with ACE overexpression further. Interestingly, lipid metabolism, particularly fatty acid oxidation and PPAR signalling was also enriched in the proteome and presents a novel area of research for ACE overexpression studies as ACE expression is up-regulated with exposure to adipocytes and lipids in conjunction with cytokines [238]. Lipid metabolism in macrophages, both mouse and human, is an important regulator of their activation and differentiation [138,143]. Fatty acids can be used as building blocks of microbicidal molecules and granules but also aid in regulating NO and ROS production through anti-inflammatory signalling [137,138,315]. This emphasises the strict control macrophages, including ACE 10/10 murine macrophages, practice with both M1 and M2-leaning characteristics present until stimulation occurs.

In Chapter 3 the intracellular uptake of Lis-Trp in human THP-1 macrophages was studied in light of recent human and mouse neutrophil studies highlighting a reduced ROS and phagocytic response upon ACE inhibitor treatment [99,244]. ACE activity and intracellular Lis-Trp concentrations were measured using the ZFHL activity assay and MS. Importantly, 10 µM Lis-Trp treatment was sufficient for partial ACE inhibition despite less than 1% uptake into the macrophages and no cytotoxicity was observed; 100 µM treatment provided similar results. Lis-Trp was not capable of easily entering THP-1 macrophages because of poor lipophilicity as has been noted for its structural homologue, lisinopril. However, immune-modulating and off-target effects of Lis-Trp and other ACE inhibitors are still of interest despite minimal uptake. Partial ACE inhibition, particularly the C-domain, is sufficient to alter immune responses in immunocompromised patients [99].

In Chapter 4 the global proteome of ACE overexpressing human THP-1 macrophages was investigated paying particular attention to similar functionally enriched pathways as identified in the ACE 10/10 mouse macrophages. Human ACE +/+ THP-1 macrophages revealed several enriched immune functions, including MHC pathways, T cell, and cytokine signalling. ATP, ETC and TCA cycle enrichment was not present despite up-regulation of ATP synthase and Complex I components in the significantly differentially expressed proteins of ACE +/+ THP-1 macrophages compared to WT THP-1 macrophages. Lipid metabolism was somewhat enriched but not fatty acid oxidation, and interestingly only ACE C-domain inhibition had functional enrichment for PPAR signalling. Previous studies suggest ACE inhibitors, including lisinopril, induce PPARγ signalling through phosphorylation and

adipocytokine release. PPARγ alters lipid metabolism in hypertensive settings to protect against inflammation and diabetic onset [268,270]. However, PPARα activation could also be present with ACE overexpression as APOE was up-regulated and induces oxLDL to provide improved ROS and NAD(P)H oxidase activity. In conjunction with the enriched cytokine and immune cell activation processes was neutrophil degranulation. Current macrophage-neutrophil communication is poorly understood but ACE may be involved by means of increased macrophage recruitment and exocytosis in turn recruiting neutrophils to sites of inflammation and infection. Although fewer protein identifications were present, ACE +/+ THP-1 macrophages still present functional enrichment for immune pathways previously identified in murine ACE 10/10 macrophages and may exhibit similar enhanced immunity to challenges.

In Chapter 5, phagocytosis of latex beads by ACE +/+ and WT THP-1 macrophages treated with ACE C- and N-domain inhibitors was tested. MS analysis revealed functional enrichment for cytoskeletal reorganisation and phagocytosis in both mouse and human ACE overexpressing macrophages. Prior studies have also revealed increased phagocytosis as part of the ACE overexpression phenotype with exposure to fluorescent *E.coli* fragments but stimulation of macrophages was required [100]. As no phagocytic studies had been performed in human macrophages previously, our study provided further insight into ACE +/+ THP-1 characteristics. ACE overexpression had markedly improved contraction of elastomeric micropatterns, a proxy for phagocytic uptake, compared to WT macrophages which was abrogated by both C- and N-domain ACE inhibitor treatments. Additionally, 10 µM treatments were sufficient in reducing micropattern contraction despite the minimal uptake of ACE inhibitors noted in Chapter 3.

Mass spectrometric analysis of human and mouse ACE overexpressing macrophages was able to provide further insight into the potential pathways at work with regards to enhanced immunity whilst also confirming pre-existing literature. This study paves the way for future immunological studies and characterisation of human ACE +/+ THP-1 macrophages and ACE overexpression in select immune cell types may one day act as a powerful and alternative tool in treating drug resistant or autoimmune diseases including cancers, bacterial and fungal infections, diabetes, kidney disease and AD.

6.2. Limitations

To map the proteome of ACE 10/10 murine and ACE +/+ human macrophages, discovery mass spectrometry using TTOF-SWATH was utilised. However, proteomic coverage in our samples was limited due to sample complexity. Fractionation of cell lysates could be employed to remedy this and improve low abundance protein identifications and reproducibility of identifications across samples. There was lower than expected homology between species, and between ACE overexpressing and WT macrophages. Direct parallels of protein expression were therefore limited. Additionally, the reduced homology between species may be a product of inappropriate models being compared. Repeat runs were not possible due to lower-than-expected protein recovery during lysis and it is expected that more cells, particularly human THP-1 macrophages, are required for adequate harvesting. As cell lysates were gifted by our collaborators sample was limited. Finally, ACE detection in MS was contradictory in mouse and human macrophages and would benefit from a targeted RAAS component detection, immunoblotting, and ACE activity assays to confirm its presence and overexpression. However, since protein content was limited, all sample was used for mass spectrometry and high urea content of the denaturation buffer interfered with immunoblotting detection. Although a thorough starting point in characterising ACE overexpressing macrophages; functional assessments including physical protein interaction studies and metabolite measurements (ATP, ROS, and NOS) would strengthen our results.

The deductions from phosphoproteomic analysis are also limited as initial changes from ACE inhibitor treatments were not measured but rather those changes after 24 hours of treatment. Although some modifications were seen, the dynamic nature of the phosphoproteome encourages lysis to be done within minutes or hours of treatment. Based on our initial Lis-Trp uptake in human THP-1 macrophages, phosphoproteomic analysis could be done on lysates collected within 2 hours of treatment.

Furthermore, macrophages exert many of their functions through cytokine and chemokine production. These molecules are excreted into the bloodstream/culture medium and were not directly measured in our cell lysates. Secretome analysis and select cytokine measurements by enzyme-linked immunosorbent assay (ELISA) could be employed but macrophages will first need to be serum-starved to prevent interference with MS analysis. In addition, our study presents proteomic datasets for unstimulated macrophages which are

largely heterogeneous in nature. Differentiation and polarization of macrophages into their classical M1 and M2 states are suspected to have different proteomic properties and one could challenge these ACE overexpressing macrophages with different immunological stimulants to create homogeneous populations. In the case of elastomeric micropattern contraction, greater phagocytic uptake and therefore contraction would be seen with opsonised or microbial phagocytic substrates and imaging should include a fluorescent substrate or adduct that is not sensitive to lysosome acidity.

6.3. Future Directions

Considering the highly glycosylated nature of ACE, targeted RAAS and ACE proteomics would benefit from the inclusion of glycoproteomics. Spatial proteomics would also add to understanding if ACE overexpression is limited to certain subcellular compartments and how or if effector molecules including those for MHC production and T cell signalling are altered as a result. Lastly, lipidomic and pathway analysis of the PPAR alpha and gamma variants presents an interesting link to ACE overexpression and enhanced macrophage function by altering lipid metabolism within the cells and downstream signalling cascades. Lipid-focused studies including functional assays after exposure to lipid-rich culture medium offer a starting point in this respect. Furthermore, macrophages are important effector cells through both direct and indirect actions. In this work we have looked at the intracellular proteome which imparts direct actions such as phagocytosis, leukocyte recruitment and antigen presentation. Future studies could include secretome analysis of ACE overexpressing macrophages to understand changes in cytokine and signalling molecules of a paracrine nature whilst also introducing co-culture models to highlight cellular communications. Noting the influence of ACE overexpression on the tumour response of mice, it may prove interesting to study how human ACE overexpressing macrophages deal with cancerous cells in culture.

Whilst exploratory proteomic data of human ACE +/+ THP-1 macrophages provided some promise of ACE-mediated immune benefit, further study is required. This cell line is however transient and future studies could work on developing a permanently altered macrophage cell line. Furthermore, as ACE overexpressing murine neutrophils also exist a new venture may be to investigate ACE overexpression in human neutrophils.

ACE modulation by ACE inhibitors and ARBs has been well studied, and ACE activity or expression level manipulation presents a future immunotherapy and precision medicine approach [316,317]. However, somatic ACE is expressed throughout the body and use of ACE phenotyping and tissue-specific promoters would be necessary to change expression levels in select cells or tissues [316–319]. Lastly noting ACE inhibitors and their modulation of immune cell function, a human pilot study [99] on neutrophils has identified cause for concern in reduced ROS and extracellular killing abilities but no work has been done in macrophages. The impact of clinically prescribed ACE inhibitors and ARBs should therefore also be applied to isolated human macrophages and other immune cell types.

7. References

[1] K.E. Bernstein, Views of the renin-angiotensin system: Brilling, mimsy, and slithy tove, Hypertension. 47 (2006) 509–514. https://doi.org/10.1161/01.HYP.0000196266.23639.c6.

[2] M. Bader, D. Ganten, Update on tissue renin-angiotensin systems, J Mol Med. 86 (2008) 615–621. https://doi.org/10.1007/s00109-008-0336-0.

[3] K.E. Bernstein, F.S. Ong, W.L.B. Blackwell, K.H. Shah, J.F. Giani, R.A. Gonzalez-Villalobos, X.Z. Shen, S. Fuchs, A modern understanding of the traditional and nontraditional biological functions of angiotensin-converting enzyme, Pharmacol Rev. 65 (2013) 1–46. https://doi.org/10.1124/pr.112.006809.

[4] Z. Khan, X.Z. Shen, E.A. Bernstein, J.F. Giani, M. Eriguchi, T. V. Zhao, R.A. Gonzalez-Villalobos, S. Fuchs, G.Y. Liu, K.E. Bernstein, Angiotensin-converting enzyme enhances the oxidative response and bactericidal activity of neutrophils, Blood. 130 (2017) 328–339. https://doi.org/10.1182/blood-2016-11-752006.

[5] K.E. Bernstein, Z. Khan, J.F. Giani, D.-Y. Cao, E.A. Bernstein, X.Z. Shen, Angiotensin-converting enzyme in innate and adaptive immunity., Nat Rev Nephrol. 14 (2018) 325–336. https://doi.org/10.1038/nrneph.2018.15.

[6] X.Z. Shen, P. Li, D. Weiss, S. Fuchs, H.D. Xiao, J.A. Adams, I.R. Williams, M.R. Capecchi, W.R. Taylor, K.E. Bernstein, Mice with enhanced macrophage angiotensin-converting enzyme are resistant to melanoma, American Journal of Pathology. 170 (2007) 2122–2134. https://doi.org/10.2353/ajpath.2007.061205.

[7] R.M. Carey, The intrarenal renin-angiotensin system in hypertension, Adv Chronic Kidney Dis. 22 (2015) 204–210. https://doi.org/10.1053/j.ackd.2014.11.004.

[8] F. Fyhrquist, O. Saijonmaa, Renin-angiotensin system revisited, J Intern Med. 264 (2008) 224–236. https://doi.org/10.1111/j.1365-2796.2008.01981.x.

[9] M.R.W. Ehlers, J.F. Riordan, Angiotensin-Converting Enzyme: New Concepts Concerning Its Biological Role, Biochemistry. 28 (1989) 5311–5318. https://doi.org/10.1021/bi00439a001.

[10] D. Fournier, F.C. Luft, M. Bader, D. Ganten, M.A. Andrade-Navarro, Emergence and evolution of the renin-angiotensin-aldosterone system, J Mol Med. 90 (2012) 495–508. https://doi.org/10.1007/s00109-012-0894-z.

[11] A. Nguyen Dinh Cat, R.M. Touyz, A new look at the renin-angiotensin system - Focusing on the vascular system, Peptides (N.Y.). 32 (2011) 2141–2150. https://doi.org/10.1016/j.peptides.2011.09.010.

[12] R.A.S. Santos, G.Y. Oudit, T. Verano-Braga, G. Canta, U.M. Steckelings, M. Bader, The renin-angiotensin system: Going beyond the classical paradigms, Am J Physiol Heart Circ Physiol. 316 (2019) H958–H970. https://doi.org/10.1152/ajpheart.00723.2018.

[13] U.M. Steckelings, R.E. Widdop, E.D. Sturrock, L. Lubbe, T. Hussain, E. Kaschina, T. Unger, A. Hallberg, R.M. Carey, C. Sumners, The Angiotensin AT2 Receptor: From a Binding Site to a Novel Therapeutic Target, Pharmacol Rev. 74 (2022) 1051–1135. https://doi.org/10.1124/pharmrev.120.000281.

[14] X.Z. Shen, A.E. Lukacher, S. Billet, I.R. Williams, K.E. Bernstein, Expression of angiotensin-converting enzyme changes major histocompatibility complex class I peptide presentation by modifying C termini of peptide precursors, Journal of Biological Chemistry. 283 (2008) 9957–9965. https://doi.org/10.1074/jbc.M709574200.

[15] X.Z. Shen, S. Billet, C. Lin, D. Okwan-Duodu, X. Chen, A.E. Lukacher, K.E. Bernstein, The carboxypeptidase ACE shapes the MHC class i peptide repertoire, Nat Immunol. 12 (2011) 1078–1085. https://doi.org/10.1038/ni.2107.

[16] C. Höcht, M. Mayer, C.A. Taira, Therapeutic perspectives of angiotensin-(1-7) in the treatment of cardiovascular disease, Open Pharmacology Journal. 3 (2009) 21–31. https://doi.org/10.2174/1874143600903010021.

[17] M. Friederich-Persson, P. Persson, Mitochondrial angiotensin II receptors regulate oxygen consumption in kidney mitochondria from healthy and type 1 diabetic rats, Am J Physiol Renal Physiol. 318 (2020) 683–688. https://doi.org/10.1152/ajprenal.00417.2019.-Exaggerated.

[18] P.M. Abadir, D.B. Foster, M. Crow, C.A. Cooke, J.J. Rucker, A. Jain, B.J. Smith, T.N. Burks, R.D. Cohn, N.S. Fedarko, R.M. Carey, B. O'Rourke, J.D. Walston, Identification and characterization of a functional mitochondrial angiotensin system, Proc Natl Acad Sci U S A. 108 (2011) 14849–14854. https://doi.org/10.1073/pnas.1101507108.

[19] J. Xu, J. Fan, F. Wu, Q. Huang, M. Guo, Z. Lv, J. Han, L. Duan, G. Hu, L. Chen, T. Liao, W. Ma, X. Tao, Y. Jin, The ACE2/angiotensin-(1-7)/Mas receptor axis: Pleiotropic roles in cancer, Front Physiol. 8 (2017) 1–8. https://doi.org/10.3389/fphys.2017.00276.

[20] R. Yang, I. Smolders, A.G. Dupont, Blood pressure and renal hemodynamic effects of angiotensin fragments, Hypertension Research. 34 (2011) 674–683. https://doi.org/10.1038/hr.2011.24.

[21] V.G. Yugandhar, M.A. Clark, Angiotensin III: A physiological relevant peptide of the renin angiotensin system, Peptides (N.Y.). 46 (2013) 26–32. https://doi.org/10.1016/j.peptides.2013.04.014.

[22] J. Royea, L. Zhang, X.K. Tong, E. Hamel, Angiotensin IV receptors mediate the cognitive and cerebrovascular benefits of losartan in a mouse model of Alzheimer's disease, Journal of Neuroscience. 37 (2017) 5562–5573. https://doi.org/10.1523/JNEUROSCI.0329-17.2017.

[23] L. Lubbe, B.T. Sewell, J.D. Woodward, E.D. Sturrock, Cryo-EM reveals mechanisms of angiotensin I-converting enzyme allostery and dimerization , EMBO J. 41 (2022). https://doi.org/10.15252/embj.2021110550.

[24] J.F. Riordan, Angiotensin-I-converting enzyme and its relatives, Genome Biol. 4 (2003). https://doi.org/10.1186/gb-2003-4-8-225.

[25] E.D. Sturrock, R. Natesh, J.M. van Rooyen, K.R. Acharya, Structure of angiotensin I-converting enzyme, Cellular and Molecular Life Sciences. 61 (2004) 2677–2686. https://doi.org/10.1007/s00018-004-4239-0.

[26] C. Harrison, K.R. Acharya, ACE for all – a molecular perspective, J Cell Commun Signal. 8 (2014) 195–210. https://doi.org/10.1007/s12079-014-0236-8.

[27] F. Soubrier, F. Alhenc-Gelas, C. Hubert, J. Allegrini, M. John, G. Tregear, P. Corvol, Two putative active centers in human angiotensin I-converting enzyme revealed by molecular cloning, Proc Natl Acad Sci U S A. 85 (1988) 9386–9390. https://doi.org/10.1073/pnas.85.24.9386.

[28] G. Masuyer, C.J. Yates, E.D. Sturrock, K.R. Acharya, Angiotensin-I converting enzyme (ACE): Structure, biological roles, and molecular basis for chloride ion dependence, Biol Chem. 395 (2014) 1135–1149. https://doi.org/10.1515/hsz-2014-0157.

[29] M.R.W. Ehlers, Y.P. Chen, J.F. Riordan, Mario R. W. Ehlers, Ying-Nan P. Chen, James F. Riordan, Biochem Biophys Res Commun. 183 (1992) 199–205.

[30] R. Natesh, S.L.U. Schwager, E.D. Sturrock, Crystal structure of the human enzyme – lisinopril complex, Nature. 1429 (2003) 1427–1429.

[31] G. Masuyer, S.L.U. Schwager, E.D. Sturrock, R.E. Isaac, K.R. Acharya, Molecular recognition and regulation of human angiotensin-I converting enzyme (ACE) activity by natural inhibitory peptides, Sci Rep. 2 (2012) 1–10. https://doi.org/10.1038/srep00717.

[32] R. Shapiro, J.F. Riordan, Critical Lysine Residue at the Chloride Binding Site of Angiotensin Converting Enzyme, Biochemistry. 22 (1983) 5315–5321. https://doi.org/10.1021/bi00292a010.

[33] C.J. Yates, G. Masuyer, S.L.U. Schwager, M. Akif, E.D. Sturrock, K.R. Acharya, Molecular and thermodynamic mechanisms of the chloride-dependent human angiotensin-I-converting enzyme (ACE), Journal of Biological Chemistry. 289 (2014) 1798–1814. https://doi.org/10.1074/jbc.M113.512335.

[34] H.R. Corradi, S.L.U. Schwager, A.T. Nchinda, E.D. Sturrock, K.R. Acharya, Crystal structure of the N domain of human somatic angiotensin I-converting enzyme provides a structural basis for domain-specific inhibitor design, J Mol Biol. 357 (2006) 964–974. https://doi.org/10.1016/j.jmb.2006.01.048.

[35] J.A. Abrie, W.J.A. Moolman, G.E. Cozier, S.L. Schwager, K.R. Acharya, E.D. Sturrock, Investigation into the mechanism of homo- and heterodimerization of angiotensin-converting enzyme, Mol Pharmacol. 93 (2018) 344–354. https://doi.org/10.1124/mol.117.110866.

[36] K. Kohlstedt, C. Gershome, M. Friedrich, W. Müller-Esterl, F. Alhenc-Gelas, R. Busse, I. Fleming, Angiotensin-converting enzyme (ACE) dimerization is the initial step in the ACE inhibitor-induced ACE signaling cascade in endothelial cells, Mol Pharmacol. 69 (2006) 1725–1732. https://doi.org/10.1124/mol.105.020636.

[37] O.E. Skirgello, I. v. Balyasnikova, P. v. Binevski, Z.L. Sun, I.I. Baskin, V.A. Palyulin, A.B. Nesterovitch, R.F. Albrecht, O.A. Kost, S.M. Danilov, Inhibitory antibodies to human angiotensin-converting enzyme: Fine epitope mapping and mechanism of action, Biochemistry. 45 (2006) 4831–4847. https://doi.org/10.1021/bi052591h.

[38] I. Schechter, A. Berger, On the size of the active site in proteases. I. Papain. 1967., Biochem Biophys Res Commun. 425 (1967) 497–502. https://doi.org/10.1016/j.bbrc.2012.08.015.

[39] J. Song, H. Tan, S.E. Boyd, H. Shen, K. Mahmood, G.I. Webb, T. Akutsu, J.C. Whisstock, R.N. Pike, Bioinformatic approaches for predicting substrates of proteases, J Bioinform Comput Biol. 9 (2011) 149–178. https://doi.org/10.1142/S0219720011005288.

[40] L.B. Arendse, A.H. Jan Danser, M. Poglitsch, R.M. Touyz, J.C. Burnett, C. Llorens-Cortes, M.R. Ehlers, E.D. Sturrock, Novel therapeutic approaches targeting the renin-angiotensin system and associated peptides in hypertension and heart

failure, Pharmacol Rev. 71 (2019) 539–570. https://doi.org/10.1124/pr.118.017129.

[41] B.W. Matthews, Structural Basis of the Action of Thermolysin and Related Zinc Peptidases, Acc Chem Res. 21 (1988) 333–340. https://doi.org/10.1021/ar00153a003.

[42] M. Semis, G.B. Gugiu, E.A. Bernstein, K.E. Bernstein, M. Kalkum, The Plethora of Angiotensin-Converting Enzyme-Processed Peptides in Mouse Plasma, Anal Chem. 91 (2019) 6440–6453. https://doi.org/10.1021/acs.analchem.8b03828.

[43] T. Zhao, K.E. Bernstein, J. Fang, X.Z. Shen, Angiotensin-converting enzyme affects the presentation of MHC class II antigens, Laboratory Investigation. 97 (2017) 764–771. https://doi.org/10.1038/labinvest.2017.32.

[44] S. Fuchs, H.D. Xiao, C. Hubert, A. Michaud, D.J. Campbell, J.W. Adams, M.R. Capecchi, P. Corvol, K.E. Bernstein, Angiotensin-converting enzyme C-terminal catalytic domain is the main site of angiotensin I cleavage in vivo, Hypertension. 51 (2008) 267–274. https://doi.org/10.1161/HYPERTENSIONAHA.107.097865.

[45] K.E. Bernstein, X.Z. Shen, R.A. Gonzalez-Villalobos, S. Billet, D. Okwan-Duodu, F.S. Ong, S. Fuchs, Different in vivo functions of the two catalytic domains of angiotensin-converting enzyme (ACE)., Curr Opin Pharmacol. 11 (2011) 105–11. https://doi.org/10.1016/j.coph.2010.11.001.

[46] M. Semis, G.B. Gugiu, E.A. Bernstein, K.E. Bernstein, M. Kalkum, The Plethora of Angiotensin-Converting Enzyme-Processed Peptides in Mouse Plasma, Anal Chem. 91 (2019) 6440–6453. https://doi.org/10.1021/acs.analchem.8b03828.

[47] D. Harmer, M. Gilbert, R. Borman, K.L. Clark, Quantitative mRNA expression profiling of ACE 2, a novel homologue of angiotensin converting enzyme, FEBS Lett. 532 (2002) 107–110. https://doi.org/10.1016/S0014-5793(02)03640-2.

[48] K.E. Bernstein, S.Y. Shai, T. Howard, R. Balogh, K. Frenzel, K. Langford, Structure and Regulated Expression of Angiotensin-Converting Enzyme and the Receptor

for Angiotensin II, American Journal of Kidney Diseases. 21 (1993) 53–57. https://doi.org/10.1016/0272-6386(93)70075-A.

[49] S.M. Danilov, I. v. Balyasnikova, A.S. Danilova, I.A. Naperova, N.E. Arablinskaya, S.E. Borisov, R. Metzger, F.E. Franke, D.E. Schwartz, I. v. Gachok, I.N. Trakht, O.A. Kost, J.G.N. Garcia, Conformational fingerprinting of the angiotensin I-converting enzyme (ACE). 1. Application in sarcoidosis, J Proteome Res. 9 (2010) 5782–5793. https://doi.org/10.1021/pr100564r.

[50] S.M. Danilov, Conformational Fingerprinting Using Monoclonal Antibodies (on the Example of Angiotensin I-Converting Enzyme-ACE), Mol Biol. 51 (2017) 906–920. https://doi.org/10.1134/S0026893317060048.

[51] S.M. Danilov, E. Sadovnikova, N. Scharenborg, I. V. Balyasnikova, D.A. Svinareva, E.L. Semikina, E.N. Parovichnikova, V.G. Savchenko, G.J. Adema, Angiotensin-converting enzyme (CD143) is abundantly expressed by dendritic cells and discriminates human monocyte-derived dendritic cells from acute myeloid leukemia-derived dendritic cells, Exp Hematol. 31 (2003) 1301–1309. https://doi.org/10.1016/j.exphem.2003.08.018.

[52] Y. Zhao, C. Xu, Structure and function of angiotensin converting enzyme and its inhibitors, Shengwu Gongcheng Xuebao/Chinese Journal of Biotechnology. 24 (2008) 171–176. https://doi.org/10.1016/s1872-2075(08)60007-2.

[53] Z.L. Woodman, S.Y. Oppong, S. Cook, N.M. Hooper, S.L.U. Schwager, W.F. Brandt, M.R.W. Ehlers, E.D. Sturrock, Shedding of somatic angiotensin-converting enzyme (ACE) is inefficient compared with testis ACE despite cleavage at identical stalk sites, Biochemical Journal. 347 (2000) 711–718. https://doi.org/10.1042/0264-6021:3470711.

[54] M.R.W. Ehlers, S.L.U. Schwager, R.R. Scholle, G.A. Manji, W.F. Brandt, J.F. Riordan, Proteolytic release of membrane-bound angiotensin-converting enzyme: Role of the juxtamembrane stalk sequence, Biochemistry. 35 (1996) 9549–9559. https://doi.org/10.1021/bi9602425.

[55] J. Lieberman, Elevation of serum angiotension-converting-enzyme (ACE) level in sarcoidosis, Am J Med. 59 (1975) 365–372. https://doi.org/https://doi.org/10.1016/0002-9343(75)90395-2.

[56] D. Oosthuizen, E.D. Sturrock, Exploring the Impact of ACE Inhibition in Immunity and Disease, Journal of the Renin-Angiotensin-Aldosterone System. 2022 (2022) 1–17. https://doi.org/10.1155/2022/9028969.

[57] D.Y. Cao, S. Saito, L.C. Veiras, D. Okwan-Duodu, E.A. Bernstein, J.F. Giani, K.E. Bernstein, Z. Khan, Role of angiotensin-converting enzyme in myeloid cell immune responses, Cell Mol Biol Lett. 25 (2020). https://doi.org/10.1186/s11658-020-00225-w.

[58] D.Y. Cao, L. Veiras, F. Ahmed, T. Shibata, E.A. Bernstein, D. Okwan-Duodu, J.F. Giani, Z. Khan, K.E. Bernstein, The non-cardiovascular actions of ACE, Peptides (N.Y.). 152 (2022) 170769. https://doi.org/10.1016/j.peptides.2022.170769.

[59] J.F. Giani, L.C. Veiras, J.Z.Y. Shen, E.A. Bernstein, D.Y. Cao, D. Okwan-Duodu, Z. Khan, R.A. Gonzalez-Villalobos, K.E. Bernstein, Novel roles of the renal angiotensin-converting enzyme, Mol Cell Endocrinol. 529 (2021) 111257. https://doi.org/10.1016/j.mce.2021.111257.

[60] S.M. Danilov, V.E. Tikhomirova, R. Metzger, I.A. Naperova, T.M. Bukina, O. Goker-Alpan, N. Tayebi, N.M. Gayfullin, D.E. Schwartz, L.M. Samokhodskaya, O.A. Kost, E. Sidransky, ACE phenotyping in Gaucher disease, Mol Genet Metab. 123 (2018) 501–510. https://doi.org/10.1016/j.ymgme.2018.02.007.

[61] A.S. Miranda, A.C. Simões E Silva, Serum levels of angiotensin converting enzyme as a biomarker of liver fibrosis, World J Gastroenterol. 23 (2017) 8439–8442. https://doi.org/10.3748/wjg.v23.i48.8439.

[62] H.M. Jochemsen, C.E. Teunissen, E.L. Ashby, W.M. van der Flier, R.E. Jones, M.I. Geerlings, P. Scheltens, P.G. Kehoe, M. Muller, The association of angiotensin-converting enzyme with biomarkers for Alzheimer's disease, Alzheimers Res Ther. 6 (2014) 1–10. https://doi.org/10.1186/alzrt257.

[63] O. v. Kryukova, V.E. Tikhomirova, E.Z. Golukhova, V. v. Evdokimov, G.F. Kalantarov, I.N. Trakht, D.E. Schwartz, R.O. Dull, A. v. Gusakov, I. v. Uporov, O.A. Kost, S.M. Danilov, Tissue specificity of human angiotensin I-converting enzyme, PLoS One. 10 (2015) 1–21. https://doi.org/10.1371/journal.pone.0143455.

[64] S.D. Crowley, N.P. Rudemiller, Immunologic effects of the renin-angiotensin system, Journal of the American Society of Nephrology. 28 (2017) 1350–1361. https://doi.org/10.1681/ASN.2016101066.

[65] C. Marchesi, P. Paradis, E.L. Schiffrin, Role of the renin-angiotensin system in vascular inflammation, Trends Pharmacol Sci. 29 (2008) 367–374. https://doi.org/10.1016/j.tips.2008.05.003.

[66] Y. Suzuki, M. Ruiz-Ortega, O. Lorenzo, M. Ruperez, V. Esteban, J. Egido, Inflammation and angiotensin II, International Journal of Biochemistry and Cell Biology. 35 (2003) 881–900. https://doi.org/10.1016/S1357-2725(02)00271-6.

[67] R.M. Touyz, Molecular and cellular mechanisms in vascular injury in hypertension: Role of angiotensin II, Curr Opin Nephrol Hypertens. 14 (2005) 125–131. https://doi.org/10.1097/00041552-200503000-00007.

[68] M.A. Williams, A. O'Callaghan, S.C. Corr, IL-33 and IL-18 in inflammatory bowel disease etiology and microbial interactions, Front Immunol. 10 (2019) 1–6. https://doi.org/10.3389/fimmu.2019.01091.

[69] A.A. Pinar, T.E. Scott, B.M. Huuskes, F.E. Tapia Cáceres, B.K. Kemp-Harper, C.S. Samuel, Targeting the NLRP3 inflammasome to treat cardiovascular fibrosis, Pharmacol Ther. (2020) 107511. https://doi.org/10.1016/j.pharmthera.2020.107511.

[70] Y. Chang, W. Wei, Angiotensin II in inflammation, immunity and rheumatoid arthritis, Clin Exp Immunol. 179 (2015) 137–145. https://doi.org/10.1111/cei.12467.

[71] M. Pacurari, R. Kafoury, P.B. Tchounwou, K. Ndebele, The renin-angiotensin-aldosterone system in vascular inflammation and remodeling, Int J Inflam. 2014 (2014). https://doi.org/10.1155/2014/689360.

[72] A. Benigni, P. Cassis, G. Remuzzi, Angiotensin II revisited: New roles in inflammation, immunology and aging, EMBO Mol Med. 2 (2010) 247–257. https://doi.org/10.1002/emmm.201000080.

[73] Y. Meng, C. Chen, Y. Liu, C. Tian, H.H. Li, Angiotensin II Regulates Dendritic Cells through Activation of NF-κB/p65, ERK1/2 and STAT1 Pathways, Cellular Physiology and Biochemistry. 42 (2017) 1550–1558. https://doi.org/10.1159/000479272.

[74] G. Nguyen, F. Delarue, C. Burcklé, L. Bouzhir, T. Giller, J.D. Sraer, Pivotal role of the renin/prorenin receptor in angiotensin II production and cellular responses to renin, Journal of Clinical Investigation. 109 (2002) 1417–1427. https://doi.org/10.1172/JCI0214276.

[75] N.J. Beekman, P.A. van Veelen, T. van Hall, A. Neisig, A. Sijts, M. Camps, P.-M. Kloetzel, J.J. Neefjes, C.J. Melief, F. Ossendorp, Abrogation of CTL Epitope Processing by Single Amino Acid Substitution Flanking the C-Terminal Proteasome Cleavage Site, The Journal of Immunology. 164 (2000) 1898–1905. https://doi.org/10.4049/jimmunol.164.4.1898.

[76] A.F. Kisselev, T.N. Akopian, K.M. Woo, A.L. Goldberg, The Sizes of Peptides Generated from Protein by Mammalian 26 and 20 S Proteasomes, Journal of Biological Chemistry. 274 (1999) 3363–3371. https://doi.org/10.1074/jbc.274.6.3363.

[77] B. Strehl, K. Textoris-Taube, S. Jäkel, A. Voigt, P. Henklein, U. Steinhoff, P.-M. Kloetzel, U. Kuckelkorn, Antitopes Define Preferential Proteasomal Cleavage Site Usage, Journal of Biological Chemistry. 283 (2008) 17891–17897. https://doi.org/10.1074/jbc.M710042200.

[78] X.Z. Shen, P. Li, D. Weiss, S. Fuchs, H.D. Xiao, J.A. Adams, I.R. Williams, M.R. Capecchi, W.R. Taylor, K.E. Bernstein, Mice with enhanced macrophage

angiotensin-converting enzyme are resistant to melanoma, American Journal of Pathology. 170 (2007) 2122–2134. https://doi.org/10.2353/ajpath.2007.061205.

[79] K. Bernstein, Y. Koronyo, B. Salumbides, J. Sheyn, L. Pelissier, D. Lopes, K. Shah, E. Bernstein, D.-T. Fuchs, J. Yu, M. Pham, K. Black, X. Shen, S. Fuchs, M. Koronyo-Hamaoui, Angiotensin-converting enzyme overexpression in myelomonocytes prevents Alzheimer's-like cognitive decline, Journal of Clinical Investigation. 124 (2014) 1000–1012. https://doi.org/10.1172/JCI66541DS1.

[80] M. Koronyo-Hamaoui, J. Sheyn, E.Y. Hayden, S. Li, D.T. Fuchs, G.C. Regis, D.H.J. Lopes, K.L. Black, K.E. Bernstein, D.B. Teplow, S. Fuchs, Y. Koronyo, A. Rentsendorj, Peripherally derived angiotensin converting enzyme-enhanced macrophages alleviate Alzheimer-related disease, Brain. 143 (2020) 336–358. https://doi.org/10.1093/brain/awz364.

[81] J.S. Miners, E. Ashby, S. Baig, R. Harrison, H. Tayler, E. Speedy, J.A. Prince, S. Love, P.G. Kehoe, Angiotensin-converting enzyme levels and activity in Alzheimer's disease: Differences in brain and CSF ACE and association with ACE1 genotypes, Am J Transl Res. 1 (2009) 163–177.

[82] P.G. Kehoe, H. Katzov, L. Feuk, A.M. Bennet, B. Johansson, B. Wilman, U. de Faire, N.J. Cairns, G.K. Wilcock, A.J. Brookes, K. Blennow, J.A. Prince, Haplotypes extending across ACE are associated with Alzheimer's disease, Hum Mol Genet. 12 (2003) 859–867. https://doi.org/10.1093/hmg/ddg094.

[83] J. Scott Miners, Z. van Helmond, M. Raiker, S. Love, P.G. Kehoe, Ace variants and association with brain aβ levels in alzheimer's disease, Am J Transl Res. 3 (2011) 73–80. https://pubmed.ncbi.nlm.nih.gov/21139807.

[84] X.Y. Xin, Z.H. Lai, K.Q. Ding, L.L. Zeng, J.F. Ma, Angiotensin-converting enzyme polymorphisms and Alzheimer's disease susceptibility: An updated meta-analysis, PLoS One. 16 (2021) 1–21. https://doi.org/10.1371/journal.pone.0260498.

[85] M.L. Hemming, D.J. Selkoe, Amyloid β-protein is degraded by cellular angiotensin-converting enzyme (ACE) and elevated by an ACE inhibitor, Journal of Biological Chemistry. 280 (2005) 37644–37650. https://doi.org/10.1074/jbc.M508460200.

[86] M. Koronyo-Hamaoui, K. Shah, Y. Koronyo, E. Bernstein, J.F. Giani, T. Janjulia, K.L. Black, P.D. Shi, R.A. Gonzalez-Villalobos, S. Fuchs, X.Z. Shen, K.E. Bernstein, ACE overexpression in myelomonocytic cells: Effect on a mouse model of Alzheimer's disease, Curr Hypertens Rep. 16 (2014). https://doi.org/10.1007/s11906-014-0444-x.

[87] M. Klichinsky, M. Ruella, O. Shestova, X.M. Lu, A. Best, M. Zeeman, M. Schmierer, K. Gabrusiewicz, N.R. Anderson, N.E. Petty, K.D. Cummins, F. Shen, X. Shan, K. Veliz, K. Blouch, Y. Yashiro-Ohtani, S.S. Kenderian, M.Y. Kim, R.S. O'Connor, S.R. Wallace, M.S. Kozlowski, D.M. Marchione, M. Shestov, B.A. Garcia, C.H. June, S. Gill, Human chimeric antigen receptor macrophages for cancer immunotherapy, Nat Biotechnol. 38 (2020) 947–953. https://doi.org/10.1038/s41587-020-0462-y.

[88] J.N. Kochenderfer, W.H. Wilson, J.E. Janik, M.E. Dudley, M. Stetler-Stevenson, S.A. Feldman, I. Maric, M. Raffeld, D.-A.N. Nathan, B.J. Lanier, R.A. Morgan, S.A. Rosenberg, Eradication of B-lineage cells and regression of lymphoma in a patient treated with autologous T cells genetically engineered to recognize CD19, Blood. 116 (2010) 4099–4102. https://doi.org/10.1182/blood-2010-04-281931.

[89] J. Cole, D. Ertoy, K.E. Bernstein, Insights derived from ACE knockout mice, JRAAS - Journal of the Renin-Angiotensin-Aldosterone System. 1 (2000) 137–141. https://doi.org/10.3317/jraas.2000.016.

[90] A. Sica, A. Mantovani, Plasticity and Polarization, Journal of Clinical Investigation. 122 (2012) 787–795. https://doi.org/10.1172/JCI59643DS1.

[91] M. Genin, F. Clement, A. Fattaccioli, M. Raes, C. Michiels, M1 and M2 macrophages derived from THP-1 cells differentially modulate the response of

cancer cells to etoposide, BMC Cancer. 15 (2015) 1–14. https://doi.org/10.1186/s12885-015-1546-9.

[92] D.G. Russell, L. Huang, B.C. VanderVen, Immunometabolism at the interface between macrophages and pathogens, Nat Rev Immunol. 19 (2019) 291–304. https://doi.org/10.1038/s41577-019-0124-9.

[93] Z. Khan, D.Y. Cao, J.F. Giani, E.A. Bernstein, L.C. Veiras, S. Fuchs, Y. Wang, Z. Peng, M. Kalkum, G.Y. Liu, K.E. Bernstein, Overexpression of the C-domain of angiotensin-converting enzyme reduces melanoma growth by stimulating M1 macrophage polarization, Journal of Biological Chemistry. 294 (2019) 4368–4380. https://doi.org/10.1074/jbc.RA118.006275.

[94] X.Z. Shen, D. Okwan-Duodu, W.L. Blackwell, F.S. Ong, T. Janjulia, E.A. Bernstein, S. Fuchs, S. Alkan, K.E. Bernstein, Myeloid expression of angiotensin-converting enzyme facilitates myeloid maturation and inhibits the development of myeloid-derived suppressor cells, Laboratory Investigation. 94 (2014) 536–544. https://doi.org/10.1038/labinvest.2014.41.

[95] D.Y. Cao, W.R. Spivia, L.C. Veiras, Z. Khan, Z. Peng, A.E. Jones, E.A. Bernstein, S. Saito, D. Okwan-Duodu, S.J. Parker, J.F. Giani, A.S. Divakaruni, J.E. Van Eyk, K.E. Bernstein, ACE overexpression in myeloid cells increases oxidative metabolism and cellular ATP, Journal of Biological Chemistry. 295 (2020) 1369–1384. https://doi.org/10.1074/jbc.RA119.011244.

[96] X.Z. Shen, H.D. Xiao, P. Li, C.X. Lin, S. Fuchs, K.E. Bernstein, Tissue specific expression of angiotensin converting enzyme: A new way to study an old friend, Int Immunopharmacol. 8 (2008) 171–176. https://doi.org/10.1016/j.intimp.2007.08.010.

[97] D. Okwan-Duodu, V. Datta, X.Z. Shen, H.S. Goodridge, E.A. Bernstein, S. Fuchs, G.Y. Liu, K.E. Bernstein, Angiotensin-converting enzyme overexpression in mouse myelomonocytic cells augments resistance to Listeria and methicillin-resistant Staphylococcus aureus, Journal of Biological Chemistry. 285 (2010) 39051–39060. https://doi.org/10.1074/jbc.M110.163782.

[98] M. Nahrendorf, F.K. Swirski, Neutrophil-macrophage communication in inflammation and atherosclerosis, Science (1979). 349 (2015) 237–238. https://doi.org/10.1126/science.aac7801.

[99] D.Y. Cao, J.F. Giani, L.C. Veiras, E.A. Bernstein, D. Okwan-Duodu, F. Ahmed, C. Bresee, W.G. Tourtellotte, S. Ananth Karumanchi, K.E. Bernstein, Z. Khan, An ACE inhibitor reduces bactericidal activity of human neutrophils in vitro and impairs mouse neutrophil activity in vivo, Sci Transl Med. 13 (2021). https://doi.org/10.1126/scitranslmed.abj2138.

[100] D.Y. Cao, W.R. Spivia, L.C. Veiras, Z. Khan, Z. Peng, A.E. Jones, E.A. Bernstein, S. Saito, D. Okwan-Duodu, S.J. Parker, J.F. Giani, A.S. Divakaruni, J.E. Van Eyk, K.E. Bernstein, ACE overexpression in myeloid cells increases oxidative metabolism and cellular ATP, Journal of Biological Chemistry. 295 (2020) 1369–1384. https://doi.org/10.1074/jbc.RA119.011244.

[101] S. Saito, N. Tatsumoto, D.-Y. Cao, N. Nosaka, H. Nishi, D.N. Leal, E. Bernstein, K. Shimada, M. Arditi, K.E. Bernstein, M. Yamashita, Overexpressed angiotensin-converting enzyme in neutrophils suppresses glomerular damage in crescentic glomerulonephritis, American Journal of Physiology-Renal Physiology. 323 (2022) F411–F424. https://doi.org/10.1152/ajprenal.00067.2022.

[102] C. Ludwig, L. Gillet, G. Rosenberger, S. Amon, B.C. Collins, R. Aebersold, Data-independent acquisition-based SWATH - MS for quantitative proteomics: a tutorial , Mol Syst Biol. 14 (2018) 1–23. https://doi.org/10.15252/msb.20178126.

[103] K. Frederick, P. Ciborowski, SWATH-MS: Data Acquisition and Analysis, Second Edi, Elsevier, 2016. https://doi.org/10.1016/B978-0-444-63688-1.00009-4.

[104] D.R. Allen, B.C. McWhinney, Quadrupole Time-of-Flight Mass Spectrometry: A Paradigm Shift in Toxicology Screening Applications, Clinical Biochemist Reviews. 40 (2019) 135–146. https://doi.org/10.33176/AACB-19-00023.

[105] G.L. Andrews, B.L. Simons, J.B. Young, A.M. Hawkridge, D.C. Muddiman, Performance Characteristics of a New Hybrid Quadrupole Time-of-Flight

Tandem Mass Spectrometer (TripleTOF 5600), Anal Chem. 83 (2011) 5442–5446. https://doi.org/10.1021/ac200812d.

[106] L. Comai, J.E. Katz, P. Mallick, Proteomics Methods and Protocols Methods in Molecular Biology 1550, 2017. http://www.springer.com/series/7651.

[107] H.L. Röst, R. Aebersold, O.T. Schubert, Automated SWATH Data Analysis Using Targeted Extraction of Ion Chromatograms, in: L. Comai, J.E. Katz, P. Mallick (Eds.), Proteomics: Methods and Protocols, Springer New York, New York, NY, 2017: pp. 289–307. https://doi.org/10.1007/978-1-4939-6747-6_20.

[108] E. Dudley, A.E. Bond, Phosphoproteomic techniques and applications, in: Adv Protein Chem Struct Biol, Academic Press Inc., 2014: pp. 25–69. https://doi.org/10.1016/B978-0-12-800453-1.00002-6.

[109] J.M.B. Simbürger, K. Dettmer, P.J. Oefner, J. Reinders, Optimizing the SWATH-MS-workflow for label-free proteomics, J Proteomics. 145 (2016) 137–140. https://doi.org/10.1016/j.jprot.2016.04.021.

[110] Q. Huang, L. Yang, J. Luo, L. Guo, Z. Wang, X. Yang, W. Jin, Y. Fang, J. Ye, B. Shan, Y. Zhang, SWATH enables precise label-free quantification on proteome scale, Proteomics. 15 (2015) 1215–1223. https://doi.org/10.1002/pmic.201400270.

[111] C.B. Messner, V. Demichev, N. Bloomfield, J.S.L. Yu, M. White, M. Kreidl, A.-S. Egger, A. Freiwald, G. Ivosev, F. Wasim, A. Zelezniak, L. Jürgens, N. Suttorp, L.E. Sander, F. Kurth, K.S. Lilley, M. Mülleder, S. Tate, M. Ralser, Ultra-fast proteomics with Scanning SWATH, Nat Biotechnol. 39 (2021) 846–854. https://doi.org/10.1038/s41587-021-00860-4.

[112] Y. Zhang, A. Bilbao, T. Bruderer, J. Luban, C. Strambio-De-Castillia, F. Lisacek, G. Hopfgartner, E. Varesio, The Use of Variable Q1 Isolation Windows Improves Selectivity in LC-SWATH-MS Acquisition, J Proteome Res. 14 (2015) 4359–4371. https://doi.org/10.1021/acs.jproteome.5b00543.

[113] Sciex, Improved data quality using variable Q1 window widths in SWATH acquisition Data independent acquisition (DIA) on SCIEX ZenoTOF, TripleTOF

and X-Series QTOF systems, 2019. http://sciex.com/support/software-downloads.

[114] E.J. Needham, B.L. Parker, T. Burykin, D.E. James, S.J. Humphrey, Illuminating the dark phosphoproteome, 2019. www.chemicalprobes.org/.

[115] K. Sharma, R.C.J. D'Souza, S. Tyanova, C. Schaab, J.R. Wiśniewski, J. Cox, M. Mann, Ultradeep Human Phosphoproteome Reveals a Distinct Regulatory Nature of Tyr and Ser/Thr-Based Signaling, Cell Rep. 8 (2014) 1583–1594. https://doi.org/10.1016/j.celrep.2014.07.036.

[116] S.R. Savage, B. Zhang, Using phosphoproteomics data to understand cellular signaling: A comprehensive guide to bioinformatics resources, Clin Proteomics. 17 (2020). https://doi.org/10.1186/s12014-020-09290-x.

[117] A. Wolf-Yadlin, N. Kumar, Y. Zhang, S. Hautaniemi, M. Zaman, H. Do Kim, V. Grantcharova, D.A. Lauffenburger, F.M. White, Effects of HER2 overexpression on cell signaling networks governing proliferation and migration, Mol Syst Biol. 2 (2006). https://doi.org/10.1038/msb4100094.

[118] J. Pessoa, M. Martins, S. Casimiro, C. Pérez-Plasencia, V. Shoshan-Barmatz, Editorial: Altered Expression of Proteins in Cancer: Function and Potential Therapeutic Targets, Front Oncol. 12 (2022). https://doi.org/10.3389/fonc.2022.949139.

[119] M.M. Bradford, A rapid and sensitive method for the quantitation of microgram quantities of protein utilizing the principle of protein-dye binding., Anal Biochem. 72 (1976) 248–54. https://doi.org/10.1006/abio.1976.9999.

[120] J. Cole, D. Le Quach, K. Sundaram, P. Corvol, M.R. Capecchi, K.E. Bernstein, Mice Lacking Endothelial Angiotensin-Converting Enzyme Have a Normal Blood Pressure, Circ Res. 90 (2002) 87–92. https://doi.org/10.1161/hh0102.102360.

[121] S. Tyanova, T. Temu, J. Cox, The MaxQuant computational platform for mass spectrometry-based shotgun proteomics, Nat Protoc. 11 (2016) 2301–2319. https://doi.org/10.1038/nprot.2016.136.

[122] J. Cox, M. Mann, MaxQuant enables high peptide identification rates, individualized p.p.b.-range mass accuracies and proteome-wide protein quantification, Nat Biotechnol. 26 (2008) 1367–1372. https://doi.org/10.1038/nbt.1511.

[123] J. Cox, N. Neuhauser, A. Michalski, R.A. Scheltema, J. v. Olsen, M. Mann, Andromeda: A peptide search engine integrated into the MaxQuant environment, J Proteome Res. 10 (2011) 1794–1805. https://doi.org/10.1021/pr101065j.

[124] V. Demichev, C.B. Messner, S.I. Vernardis, K.S. Lilley, M. Ralser, DIA-NN: neural networks and interference correction enable deep proteome coverage in high throughput, Nat Methods. 17 (2020) 41–44. https://doi.org/10.1038/s41592-019-0638-x.

[125] D. Szklarczyk, A.L. Gable, D. Lyon, A. Junge, S. Wyder, J. Huerta-Cepas, M. Simonovic, N.T. Doncheva, J.H. Morris, P. Bork, L.J. Jensen, C. von Mering, STRING v11: protein-protein association networks with increased coverage, supporting functional discovery in genome-wide experimental datasets., Nucleic Acids Res. 47 (2019) D607–D613. https://doi.org/10.1093/nar/gky1131.

[126] P. Shannon, A. Markiel, O. Ozier, N.S. Baliga, J.T. Wang, D. Ramage, N. Amin, B. Schwikowski, T. Ideker, Cytoscape: A software Environment for integrated models of biomolecular interaction networks, Genome Res. 13 (2003) 2498–2504. https://doi.org/10.1101/gr.1239303.

[127] S. Maere, K. Heymans, M. Kuiper, BiNGO: A Cytoscape plugin to assess overrepresentation of Gene Ontology categories in Biological Networks, Bioinformatics. 21 (2005) 3448–3449. https://doi.org/10.1093/bioinformatics/bti551.

[128] P. v Hornbeck, B. Zhang, B. Murray, J.M. Kornhauser, V. Latham, E. Skrzypek, PhosphoSitePlus, 2014: mutations, PTMs and recalibrations., Nucleic Acids Res. 43 (2015) D512-20. https://doi.org/10.1093/nar/gku1267.

[129] M. Kanehisa, S. Goto, KEGG: Kyoto Encyclopedia of Genes and Genomes, Nucleic Acids Res. 28 (2000) 27–30. https://doi.org/10.1093/nar/28.1.27.

[130] M. Kanehisa, M. Furumichi, Y. Sato, M. Kawashima, M. Ishiguro-Watanabe, KEGG for taxonomy-based analysis of pathways and genomes, Nucleic Acids Res. 51 (2023) D587–D592. https://doi.org/10.1093/nar/gkac963.

[131] M. Gillespie, B. Jassal, R. Stephan, M. Milacic, K. Rothfels, A. Senff-Ribeiro, J. Griss, C. Sevilla, L. Matthews, C. Gong, C. Deng, T. Varusai, E. Ragueneau, Y. Haider, B. May, V. Shamovsky, J. Weiser, T. Brunson, N. Sanati, L. Beckman, X. Shao, A. Fabregat, K. Sidiropoulos, J. Murillo, G. Viteri, J. Cook, S. Shorser, G. Bader, E. Demir, C. Sander, R. Haw, G. Wu, L. Stein, H. Hermjakob, P. D'Eustachio, The reactome pathway knowledgebase 2022, Nucleic Acids Res. 50 (2022) D687–D692. https://doi.org/10.1093/nar/gkab1028.

[132] T. Zhao, K.E. Bernstein, J. Fang, X.Z. Shen, Angiotensin-converting enzyme affects the presentation of MHC class II antigens, Laboratory Investigation. 97 (2017) 764–771. https://doi.org/10.1038/labinvest.2017.32.

[133] Z. Khan, D.Y. Cao, J.F. Giani, E.A. Bernstein, L.C. Veiras, S. Fuchs, Y. Wang, Z. Peng, M. Kalkum, G.Y. Liu, K.E. Bernstein, Overexpression of the C-domain of angiotensin-converting enzyme reduces melanoma growth by stimulating M1 macrophage polarization, Journal of Biological Chemistry. 294 (2019) 4368–4380. https://doi.org/10.1074/jbc.RA118.006275.

[134] E. Platanitis, T. Decker, Regulatory networks involving STATs, IRFs, and NFκB in inflammation, Front Immunol. 9 (2018). https://doi.org/10.3389/fimmu.2018.02542.

[135] J. Korbecki, K. Bajdak-Rusinek, The effect of palmitic acid on inflammatory response in macrophages: an overview of molecular mechanisms, Inflammation Research. 68 (2019) 915–932. https://doi.org/10.1007/s00011-019-01273-5.

[136] V. Infantino, V. Iacobazzi, F. Palmieri, A. Menga, ATP-citrate lyase is essential for macrophage inflammatory response, Biochem Biophys Res Commun. 440 (2013) 105–111. https://doi.org/10.1016/j.bbrc.2013.09.037.

[137] A.R. Dinasarapu, S. Gupta, M.R. Maurya, E. Fahy, J. Min, M. Sud, M.J. Gersten, C.K. Glass, S. Subramaniam, A combined omics study on activated macrophages - Enhanced role of STATs in apoptosis, immunity and lipid metabolism, Bioinformatics. 29 (2013) 2735–2743. https://doi.org/10.1093/bioinformatics/btt469.

[138] A. Batista-Gonzalez, R. Vidal, A. Criollo, L.J. Carreño, New Insights on the Role of Lipid Metabolism in the Metabolic Reprogramming of Macrophages, Front Immunol. 10 (2020). https://doi.org/10.3389/fimmu.2019.02993.

[139] S.C.C. Huang, B. Everts, Y. Ivanova, D. O'Sullivan, M. Nascimento, A.M. Smith, W. Beatty, L. Love-Gregory, W.Y. Lam, C.M. O'Neill, C. Yan, H. Du, N.A. Abumrad, J.F. Urban, M.N. Artyomov, E.L. Pearce, E.J. Pearce, Cell-intrinsic lysosomal lipolysis is essential for alternative activation of macrophages, Nat Immunol. 15 (2014) 846–855. https://doi.org/10.1038/ni.2956.

[140] S.C.C. Huang, A.M. Smith, B. Everts, M. Colonna, E.L. Pearce, J.D. Schilling, E.J. Pearce, Metabolic Reprogramming Mediated by the mTORC2-IRF4 Signaling Axis Is Essential for Macrophage Alternative Activation, Immunity. 45 (2016) 817–830. https://doi.org/10.1016/j.immuni.2016.09.016.

[141] J.S. Moon, K. Nakahira, K.P. Chung, G.M. DeNicola, M.J. Koo, M.A. Pabón, K.T. Rooney, J.H. Yoon, S.W. Ryter, H. Stout-Delgado, A.M.K. Choi, NOX4-dependent fatty acid oxidation promotes NLRP3 inflammasome activation in macrophages, Nat Med. 22 (2016) 1002–1012. https://doi.org/10.1038/nm.4153.

[142] P. Gervois, I.P. Torra, J.-C. Fruchart, B. Staels, Regulation of Lipid and Lipoprotein Metabolism by PPAR Activators, Cclm. 38 (2000) 3–11. https://doi.org/10.1515/CCLM.2000.002.

[143] E. Teissier, A. Nohara, G. Chinetti, R. Paumelle, B. Cariou, J.C. Fruchart, R.P. Brandes, A. Shah, B. Staels, Peroxisome proliferator-activated receptor α

induces NADPH oxidase activity in macrophages, leading to the generation of LDL with PPAR-α activation properties, Circ Res. 95 (2004) 1174–1182. https://doi.org/10.1161/01.RES.0000150594.95988.45.

[144] E. Rigamonti, G. Chinetti-Gbaguidi, B. Staels, Regulation of macrophage functions by PPAR- α, PPAR- γ, and LXRs in mice and men, Arterioscler Thromb Vasc Biol. 28 (2008) 1050–1059. https://doi.org/10.1161/ATVBAHA.107.158998.

[145] Y. Meng, C. Chen, Y. Liu, C. Tian, H.-H. Li, Angiotensin II Regulates Dendritic Cells through Activation of NF-κB /p65, ERK1/2 and STAT1 Pathways, Cellular Physiology and Biochemistry. 42 (2017) 1550–1558. https://doi.org/10.1159/000479272.

[146] V. Koka, X.R. Huang, A.C.K. Chung, W. Wang, L.D. Truong, H.Y. Lan, Angiotensin II Up-Regulates Angiotensin I-Converting Enzyme (ACE), but Down-Regulates ACE2 via the AT1-ERK/p38 MAP Kinase Pathway, Am J Pathol. 172 (2008) 1174–1183. https://doi.org/https://doi.org/10.2353/ajpath.2008.070762.

[147] Y. Pan, Y. Huang, Z. Wang, Q. Fang, Y. Sun, C. Tong, K. Peng, Y. Wang, L. Miao, L. Cai, Y. Zhao, G. Liang, Inhibition of MAPK-mediated ACE expression by compound C66 prevents STZ-induced diabetic nephropathy, J Cell Mol Med. 18 (2014) 231–241. https://doi.org/10.1111/jcmm.12175.

[148] P.E. Gallagher, C.M. Ferrario, E.A. Tallant, MAP kinase/phosphatase pathway mediates the regulation of ACE2 by angiotensin peptides, American Journal of Physiology-Cell Physiology. 295 (2008) C1169–C1174. https://doi.org/10.1152/ajpcell.00145.2008.

[149] T. Neamatallah, Mitogen-activated protein kinase pathway: A critical regulator in tumor-associated macrophage polarization, J Microsc Ultrastruct. 7 (2019) 53. https://doi.org/10.4103/jmau.jmau_68_18.

[150] K.M. Rao, MAP kinase activation in macrophages., J Leukoc Biol. 69 (2001) 3–10. http://www.ncbi.nlm.nih.gov/pubmed/11200064.

[151] A. Pierce, C.M. Heyworth, S.E. Nicholls, E. Spooncer, T.M. Dexter, J.M. Lord, P.J. Owen-Lynch, G. Wark, A.D. Whetton, An Activated Protein Kinase C Gives a Differentiation Signal for Hematopoietic Progenitor Cells and Mimicks Macrophage Colony-stimulating Factor-stimulated Signaling Events, 1998. http://www.jcb.org.

[152] S. Qin, J. Li, C. Zhou, B. Privratsky, J. Schettler, X. Deng, Z. Xia, Y. Zeng, H. Wu, M. Wu, SHIP-1 Regulates Phagocytosis and M2 Polarization Through the PI3K/Akt–STAT5–Trib1 Circuit in Pseudomonas aeruginosa Infection, Front Immunol. 11 (2020). https://doi.org/10.3389/fimmu.2020.00307.

[153] X.Z. Shen, D. Okwan-Duodu, W.L. Blackwell, F.S. Ong, T. Janjulia, E.A. Bernstein, S. Fuchs, S. Alkan, K.E. Bernstein, Myeloid expression of angiotensin-converting enzyme facilitates myeloid maturation and inhibits the development of myeloid-derived suppressor cells, Laboratory Investigation. 94 (2014) 536–544. https://doi.org/10.1038/labinvest.2014.41.

[154] J. Zhang, K.S. Ravichandran, J.C. Garrison, A key role for the phosphorylation of Ser440by the cyclic AMP-dependent protein kinase in regulating the activity of the Src homology 2 domain-containing inositol 5'-phosphatase (SHIP1), Journal of Biological Chemistry. 285 (2010) 34839–34849. https://doi.org/10.1074/jbc.M110.128827.

[155] J. Ruschmann, V. Ho, F. Antignano, E. Kuroda, V. Lam, M. Ibaraki, K. Snyder, C. Kim, R.A. Flavell, T. Kawakami, L. Sly, A.G. Turhan, G. Krystal, Tyrosine phosphorylation of SHIP promotes its proteasomal degradation, Exp Hematol. 38 (2010) 392—402, 402.e1. https://doi.org/10.1016/j.exphem.2010.03.010.

[156] G.W. Chacko, S. Tridandapani, J.E. Damen, L. Liu, G. Krystal, K.M. Coggeshall, Negative signaling in B lymphocytes induces tyrosine phosphorylation of the 145-kDa inositol polyphosphate 5-phosphatase, SHIP, J Immunol. 157 (1996) 2234—2238. http://europepmc.org/abstract/MED/8805618.

[157] C. Guo, R.R. Mattingly, P.M. Stemmer, A.J. Rosenspire, At low levels, inorganic mercury interference with antigen signaling is associated with modifications to

a panel of novel phosphoserine sites in B cell receptor pathway proteins, Toxicology in Vitro. (2023) 105564. https://doi.org/10.1016/j.tiv.2023.105564.

[158] S.D. Pauls, A.J. Marshall, Regulation of immune cell signaling by SHIP1: A phosphatase, scaffold protein, and potential therapeutic target, Eur J Immunol. 47 (2017) 932–945. https://doi.org/10.1002/eji.201646795.

[159] W.E. Edimo, V. Janssens, E. Waelkens, C. Erneux, Reversible Ser/Thr SHIP phosphorylation: A new paradigm in phosphoinositide signalling?: Targeting of SHIP1/2 phosphatases may be controlled by phosphorylation on Ser and Thr residues, BioEssays. 34 (2012) 634–642. https://doi.org/10.1002/bies.201100195.

[160] R. Mashud, A. Nomachi, A. Hayakawa, K. Kubouchi, S. Danno, T. Hirata, K. Matsuo, T. Nakayama, R. Satoh, R. Sugiura, M. Abe, K. Sakimura, S. Wakana, H. Ohsaki, S. Kamoshida, H. Mukai, Impaired lymphocyte trafficking in mice deficient in the kinase activity of PKN1, Sci Rep. 7 (2017). https://doi.org/10.1038/s41598-017-07936-9.

[161] K. Kohlstedt, R. Busse, I. Fleming, Signaling via the angiotensin-converting enzyme enhances the expression of cyclooxygenase-2 in endothelial cells, Hypertension. 45 (2005) 126–132. https://doi.org/10.1161/01.HYP.0000150159.48992.11.

[162] K. Kohlstedt, F. Shoghi, W. Müller-Esterl, R. Busse, I. Fleming, CK2 phosphorylates the angiotensin-converting enzyme and regulates its retention in the endothelial cell plasma membrane., Circ Res. 91 (2002) 749–56. https://doi.org/10.1161/01.res.0000038114.17939.c8.

[163] K. Kohlstedt, R.P. Brandes, W. Müller-Esterl, R. Busse, I. Fleming, Angiotensin-converting enzyme is involved in outside-in signaling in endothelial cells., Circ Res. 94 (2004) 60–7. https://doi.org/10.1161/01.RES.0000107195.13573.E4.

[164] F. Boomsma, J.H. de Bruyn, F.H. Derkx, M.A. Schalekamp, Opposite effects of captopril on angiotensin I-converting enzyme “activity” and “concentration”;

relation between enzyme inhibition and long-term blood pressure response., Clin Sci (Lond). 60 (1981) 491–8. https://doi.org/10.1042/cs0600491.

[165] K. Kohlstedt, C. Gershome, M. Friedrich, W. Müller-Esterl, F. Alhenc-Gelas, R. Busse, I. Fleming, Angiotensin-converting enzyme (ACE) dimerization is the initial step in the ACE inhibitor-induced ACE signaling cascade in endothelial cells, Mol Pharmacol. 69 (2006) 1725–1732. https://doi.org/10.1124/mol.105.020636.

[166] K. Kohlstedt, C. Gershome, C. Trouvain, W.-K. Hofmann, S. Fichtlscherer, I. Fleming, Angiotensin-Converting Enzyme (ACE) Inhibitors Modulate Cellular Retinol-Binding Protein 1 and Adiponectin Expression in Adipocytes via the ACE-Dependent Signaling Cascade, Mol Pharmacol. 75 (2009) 685–692. https://doi.org/10.1124/mol.108.051631.

[167] L.C. Veiras, D.Y. Cao, S. Saito, Z. Peng, E.A. Bernstein, J.Z.Y. Shen, M. Koronyo-Hamaoui, D. Okwan-Duodu, J.F. Giani, Z. Khan, K.E. Bernstein, Overexpression of ACE in Myeloid Cells Increases Immune Effectiveness and Leads to a New Way of Considering Inflammation in Acute and Chronic Diseases, Curr Hypertens Rep. 22 (2020). https://doi.org/10.1007/s11906-019-1008-x.

[168] D. Poddar, R. Kaur, W.M. Baldwin, B. Mazumder, L13a-dependent translational control in macrophages limits the pathogenesis of colitis., Cell Mol Immunol. 13 (2016) 816–827. https://doi.org/10.1038/cmi.2015.53.

[169] A. Basu, N. Dvorina, W.M. Baldwin, B. Mazumder, High-fat diet-induced GAIT element-mediated translational silencing of mRNAs encoding inflammatory proteins in macrophage protects against atherosclerosis., FASEB J. 34 (2020) 6888–6906. https://doi.org/10.1096/fj.201903119R.

[170] A. Basu, D. Poddar, P. Robinet, J.D. Smith, M. Febbraio, W.M. Baldwin, B. Mazumder, Ribosomal protein L13a deficiency in macrophages promotes atherosclerosis by limiting translation control-dependent retardation of inflammation, Arterioscler Thromb Vasc Biol. 34 (2014) 533–542. https://doi.org/10.1161/ATVBAHA.113.302573.

[171] B. Mazumder, P. Sampath, V. Seshadri, R.K. Maitra, P.E. DiCorleto, P.L. Fox, Regulated Release of L13a from the 60S Ribosomal Subunit as A Mechanism of Transcript-Specific Translational Control, Cell. 115 (2003) 187–198. https://doi.org/10.1016/S0092-8674(03)00773-6.

[172] K.E. Bernstein, Z. Khan, J.F. Giani, T. Zhao, M. Eriguchi, E.A. Bernstein, R.A. Gonzalez-Villalobos, X.Z. Shen, Overexpression of angiotensin-converting enzyme in myelomonocytic cells enhances the immune response, F1000Res. 5 (2016) 1–8. https://doi.org/10.12688/f1000research.7508.1.

[173] A.F. Savulescu, E. Bouilhol, N. Beaume, M. Nikolski, Prediction of RNA subcellular localization: Learning from heterogeneous data sources, IScience. 24 (2021) 103298. https://doi.org/10.1016/j.isci.2021.103298.

[174] A. Jellema-Butler, Characterization of the Subcellular Localization of Angiotensin-Converting Enzyme (ACE), BSc (Hons), University of Cape Town, 2022.

[175] C.M. Mulvey, L.M. Breckels, O.M. Crook, D.J. Sanders, A.L.R. Ribeiro, A. Geladaki, A. Christoforou, N.K. Britovšek, T. Hurrell, M.J. Deery, L. Gatto, A.M. Smith, K.S. Lilley, Spatiotemporal proteomic profiling of the pro-inflammatory response to lipopolysaccharide in the THP-1 human leukaemia cell line, Nat Commun. 12 (2021). https://doi.org/10.1038/s41467-021-26000-9.

[176] A.C. Montezano, A. Nguyen Dinh Cat, F.J. Rios, R.M. Touyz, Angiotensin II and vascular injury, Curr Hypertens Rep. 16 (2014). https://doi.org/10.1007/s11906-014-0431-2.

[177] R.A. Gonzalez-Villalobos, X.Z. Shen, E.A. Bernstein, T. Janjulia, B. Taylor, J.F. Giani, W.L.B. Blackwell, K.H. Shah, P.D. Shi, S. Fuchs, K.E. Bernstein, Rediscovering ACE: Novel insights into the many roles of the angiotensin-converting enzyme, J Mol Med. 91 (2013) 1143–1154. https://doi.org/10.1007/s00109-013-1051-z.

[178] D. Georgiadis, F. Beau, B. Czarny, J. Cotton, A. Yiotakis, V. Dive, Roles of the two active sites of somatic angiotensin-converting enzyme in the cleavage of

angiotensin I and bradykinin insights from selective inhibitors, Circ Res. 93 (2003) 148–154. https://doi.org/10.1161/01.RES.0000081593.33848.FC.

[179] United States Food and Drug Administration, Angiotensin-Converting Enzyme Inhibitor (ACE inhibitor) Drugs | FDA, (2015). https://www.fda.gov/drugs/postmarket-drug-safety-information-patients-and-providers/angiotensin-converting-enzyme-inhibitor-ace-inhibitor-drugs (accessed August 24, 2022).

[180] U. Sharma, G.E. Cozier, E.D. Sturrock, K.R. Acharya, Molecular Basis for Omapatrilat and Sampatrilat Binding to Neprilysin-Implications for Dual Inhibitor Design with Angiotensin-Converting Enzyme, J Med Chem. 63 (2020) 5488–5500. https://doi.org/10.1021/acs.jmedchem.0c00441.

[181] R. Alves-Lopes, A.C. Montezano, K.B. Neves, A. Harvey, F.J. Rios, D.S. Skiba, L.B. Arendse, T.J. Guzik, D. Graham, M. Poglitsch, E. Sturrock, R.M. Touyz, Selective Inhibition of the C-Domain of ACE (Angiotensin-Converting Enzyme) Combined with Inhibition of NEP (Neprilysin): A Potential New Therapy for Hypertension, Hypertension. (2021) 604–616. https://doi.org/10.1161/HYPERTENSIONAHA.121.17041.

[182] E. Uijl, D.C. 't Hart, L.C.W. Roksnoer, M.C.C. van Groningen, R. van Veghel, I.M. Garrelds, R. de Vries, J. van der Vlag, R. Zietse, T. Nijenhuis, J.A. Joles, E.J. Hoorn, A.H.J. Danser, Angiotensin-neprilysin inhibition confers renoprotection in rats with diabetes and hypertension by limiting podocyte injury, J Hypertens. 38 (2020) 755–764. https://doi.org/10.1097/HJH.0000000000002326.

[183] R.W. Piepho, Overview of the angiotensin-converting-enzyme inhibitors, American Journal of Health-System Pharmacy. 57 (2000) S3-7. https://doi.org/10.1093/ajhp/57.suppl_1.s3.

[184] P. Denti, S.K. Sharp, W.L. Kröger, S.L. Schwager, A. Mahajan, M. Njoroge, L. Gibhard, I. Smit, K. Chibale, L. Wiesner, E.D. Sturrock, N.H. Davies, Pharmacokinetic evaluation of lisinopril-tryptophan, a novel C-domain ACE

inhibitor, European Journal of Pharmaceutical Sciences. 56 (2014) 113–119. https://doi.org/10.1016/j.ejps.2014.01.012.

[185] J.M. Watermeyer, W.L. Kröger, H.G. O'Neill, B.T. Sewell, E.D. Sturrock, Characterization of domain-selective inhibitor binding in angiotensin-converting enzyme using a novel derivative of lisinopril, Biochemical Journal. 428 (2010) 67–74. https://doi.org/10.1042/BJ20100056.

[186] P. Denti, S.K. Sharp, W.L. Kröger, S.L. Schwager, A. Mahajan, M. Njoroge, L. Gibhard, I. Smit, K. Chibale, L. Wiesner, E.D. Sturrock, N.H. Davies, Pharmacokinetic evaluation of lisinopril-tryptophan, a novel C-domain ACE inhibitor, European Journal of Pharmaceutical Sciences. 56 (2014) 113–119. https://doi.org/10.1016/j.ejps.2014.01.012.

[187] J.M. Watermeyer, W.L. Kröger, H.G. O'Neill, B.T. Sewell, E.D. Sturrock, Characterization of domain-selective inhibitor binding in angiotensin-converting enzyme using a novel derivative of lisinopril, Biochemical Journal. 428 (2010) 67–74. https://doi.org/10.1042/BJ20100056.

[188] J. Thomas, H. Smith, C.A. Smith, L. Coward, G. Gorman, M. de Luca, P. Jumbo-Lucioni, The angiotensin-converting enzyme inhibitor lisinopril mitigates memory and motor deficits in a drosophila model of alzheimer's disease, Pathophysiology. 28 (2021) 307–319. https://doi.org/10.3390/pathophysiology28020020.

[189] D.T. Thwaites, M. Cavet, B.H. Hirst, N.L. Simmons, Angiotensin-converting enzyme (ACE) inhibitor transport in human intestinal epithelial (Caco-2) cells, Br J Pharmacol. 114 (1995) 981–986. https://doi.org/10.1111/j.1476-5381.1995.tb13301.x.

[190] P.M. Abadir, J.D. Walston, R.M. Carey, Subcellular characteristics of functional intracellular renin-angiotensin systems, Peptides (N.Y.). 38 (2012) 437–445. https://doi.org/10.1016/j.peptides.2012.09.016.

[191] A. Higaki, A. Caillon, P. Paradis, E.L. Schiffrin, Innate and Innate-Like Immune System in Hypertension and Vascular Injury, Curr Hypertens Rep. 21 (2019) 1–9. https://doi.org/10.1007/s11906-019-0907-1.

[192] H. Shimazu, K. Kinoshita, S. Hino, T. Yano, K. Kishimoto, Y. Nagare, Y. Nozaki, M. Sugiyama, S. Ikoma, M. Funauchi, Effect of combining ACE inhibitor and statin in lupus-prone mice, Clinical Immunology. 136 (2010) 188–196. https://doi.org/10.1016/j.clim.2010.03.008.

[193] J. Nestor, Y. Arinuma, T.S. Huerta, C. Kowal, E. Nasiri, N. Kello, Y. Fujieda, A. Bialas, T. Hammond, U. Sriram, B. Stevens, P.T. Huerta, B.T. Volpe, B. Diamond, Lupus antibodies induce behavioral changes mediated by microglia and blocked by ACE inhibitors, Journal of Experimental Medicine. 215 (2018) 2554–2566. https://doi.org/10.1084/jem.20180776.

[194] K.M. Fairbrass, D. Hoshen, D.J. Gracie, A.C. Ford, Effect of ACE inhibitors and angiotensin II receptor blockers on disease outcomes in inflammatory bowel disease, Gut. 70 (2021) 218–219. https://doi.org/10.1136/gutjnl-2020-321186.

[195] W. Chanput, J.J. Mes, H.J. Wichers, THP-1 cell line: An in vitro cell model for immune modulation approach, Int Immunopharmacol. 23 (2014) 37–45. https://doi.org/10.1016/j.intimp.2014.08.002.

[196] M. Daigneault, J.A. Preston, H.M. Marriott, M.K.B. Whyte, D.H. Dockrell, The identification of markers of macrophage differentiation in PMA-stimulated THP-1 cells and monocyte-derived macrophages, PLoS One. 5 (2010). https://doi.org/10.1371/journal.pone.0008668.

[197] E.W. Baxter, A.E. Graham, N.A. Re, I.M. Carr, J.I. Robinson, S.L. Mackie, A.W. Morgan, Standardized protocols for differentiation of THP-1 cells to macrophages with distinct M(IFNγ+LPS), M(IL-4) and M(IL-10) phenotypes, J Immunol Methods. 478 (2020) 1–11. https://doi.org/10.1016/j.jim.2019.112721.

[198] S. Tedesco, F. de Majo, J. Kim, A. Trenti, L. Trevisi, G.P. Fadini, C. Bolego, P.W. Zandstra, A. Cignarella, L. Vitiello, Convenience versus biological significance:

Are PMA-differentiated THP-1 cells a reliable substitute for blood-derived macrophages when studying in vitro polarization?, Front Pharmacol. 9 (2018). https://doi.org/10.3389/fphar.2018.00071.

[199] C. Chen, S. Gardete, R.S. Jansen, A. Shetty, T. Dick, K.Y. Rhee, V. Dartois, Verapamil Targets Membrane Energetics in Mycobacterium tuberculosis., Antimicrob Agents Chemother. 62 (2018). https://doi.org/10.1128/AAC.02107-17.

[200] S.L. Schwager, A.K. Carmona, E.D. Sturrock, A high-throughput fluorimetric assay for angiotensin I-converting enzyme, 1 (2006) 1961–1964. https://doi.org/10.1038/nprot.2006.305.

[201] P. Denti, S.K. Sharp, W.L. Kröger, S.L. Schwager, A. Mahajan, M. Njoroge, L. Gibhard, I. Smit, K. Chibale, L. Wiesner, E.D. Sturrock, N.H. Davies, Pharmacokinetic evaluation of lisinopril-tryptophan, a novel C-domain ACE inhibitor, European Journal of Pharmaceutical Sciences. 56 (2014) 113–119. https://doi.org/10.1016/j.ejps.2014.01.012.

[202] D. Smith, P. Artursson, A. Avdeef, L. Di, G.F. Ecker, B. Faller, J.B. Houston, M. Kansy, E.H. Kerns, S.D. Krämer, H. Lennernäs, H. van de Waterbeemd, K. Sugano, B. Testa, Passive lipoidal diffusion and carrier-mediated cell uptake are both important mechanisms of membrane permeation in drug disposition, Mol Pharm. 11 (2014) 1727–1738. https://doi.org/10.1021/mp400713v.

[203] V. Vermeirssen, J. van Camp, W. Verstraete, Bioavailability of angiotensin I converting enzyme inhibitory peptides, British Journal of Nutrition. 92 (2004) 357–366. https://doi.org/10.1079/bjn20041189.

[204] F. Xie, J. van Bocxlaer, A. Vermeulen, Physiologically based pharmacokinetic modelling of lisinopril in children: A case story of angiotensin converting enzyme inhibitors, Br J Clin Pharmacol. 87 (2021) 1203–1214. https://doi.org/10.1111/bcp.14492.

[205] D.I. Friedman, G.L. Amidon, Passive and carrier-mediated intestinal absorption components of two angiotensin converting enzyme (ACE) inhibitor prodrugs in

rats: enalapril and fosinopril., Pharm Res. 6 (1989) 1043–7. https://doi.org/10.1023/a:1015978420797.

[206] D.I. Friedman, G.L. Amidon, Intestinal absorption mechanism of dipeptide angiotensin converting enzyme inhibitors of the lysyl-proline type: lisinopril and SQ 29,852., J Pharm Sci. 78 (1989) 995–8. https://doi.org/10.1002/jps.2600781205.

[207] D. Sun, Y. Wang, F. Tan, D. Fang, Y. Hu, D.E. Smith, H. Jiang, Functional and molecular expression of the proton-coupled oligopeptide transporters in spleen and macrophages from mouse and human, Mol Pharm. 10 (2013) 1409–1416. https://doi.org/10.1021/mp300700p.

[208] B. Zwarycz, E.A. Wong, Expression of the peptide transporters PepT1, PepT2, and PHT1 in the embryonic and posthatch chick, Poult Sci. 92 (2013) 1314–1321. https://doi.org/10.3382/ps.2012-02826.

[209] H. Oppermann, M. Heinrich, C. Birkemeyer, J. Meixensberger, F. Gaunitz, The proton-coupled oligopeptide transporters PEPT2, PHT1 and PHT2 mediate the uptake of carnosine in glioblastoma cells, Amino Acids. 51 (2019) 999–1008. https://doi.org/10.1007/s00726-019-02739-w.

[210] Y. Wang, P. Li, F. Song, X. Yang, Y. Weng, Z. Ma, L. Wang, H. Jiang, Substrate Transport Properties of the Human Peptide/Histidine Transporter PHT2 in Transfected MDCK Cells, J Pharm Sci. 108 (2019) 3416–3424. https://doi.org/10.1016/j.xphs.2019.06.016.

[211] W.J. Lu, H.J. Lin, P.H. Hsu, H.T.V. Lin, Determination of drug efflux pump efficiency in drug-resistant bacteria using MALDI-TOF MS, Antibiotics. 9 (2020) 1–20. https://doi.org/10.3390/antibiotics9100639.

[212] O. Jensen, L. Gebauer, J. Brockmöller, C. Dücker, Relationships between Inhibition, Transport and Enhanced Transport via the Organic Cation Transporter 1, Int J Mol Sci. 23 (2022). https://doi.org/10.3390/ijms23042007.

[213] X. Gao, D. Aguanno, M. Board, R. Callaghan, Exploiting the metabolic energy demands of drug efflux pumps provides a strategy to overcome multidrug

resistance in cancer, Biochim Biophys Acta Gen Subj. 1865 (2021). https://doi.org/10.1016/j.bbagen.2021.129915.

[214] S.S. Motta, P. Cluzel, M. Aldana, Adaptive resistance in bacteria requires epigenetic inheritance, genetic noise, and cost of efflux pumps, PLoS One. 10 (2015). https://doi.org/10.1371/journal.pone.0118464.

[215] E. Dumont, J. Vergalli, L. Conraux, C. Taillier, A. Vassort, J. Pajović, M. Signgiers, M. Mourez, J.M. Pagès, Antibiotics and efflux: Combined spectrofluorimetry and mass spectrometry to evaluate the involvement of concentration and efflux activity in antibiotic intracellular accumulation, Journal of Antimicrobial Chemotherapy. 74 (2019) 58–65. https://doi.org/10.1093/jac/dky396.

[216] M.E. Lund, J. To, B.A. O'Brien, S. Donnelly, The choice of phorbol 12-myristate 13-acetate differentiation protocol influences the response of THP-1 macrophages to a pro-inflammatory stimulus, J Immunol Methods. 430 (2016) 64–70. https://doi.org/10.1016/j.jim.2016.01.012.

[217] H. Schunkert, J.R. Ingelfinger, A.T. Hirsch, Y. Pinto, W.J. Remme, H. Jacob, V.J. Dzau, Feedback regulation of angiotensin converting enzyme activity and mRNA levels by angiotensin II., Circ Res. 72 (1993) 312–318. https://doi.org/10.1161/01.RES.72.2.312.

[218] A. Okamura, H. Rakugi, M. Ohishi, Y. Yanagitani, S. Takiuchi, K. Moriguchi, P.A. Fennessy, J. Higaki, T. Ogihara, Upregulation of renin-angiotensin system during differentiation of monocytes to macrophages, J Hypertens. 17 (1999). https://journals.lww.com/jhypertension/Fulltext/1999/17040/Upregulation_of_renin_angiotensin_system_during.12.aspx.

[219] S.M. Danilov, I. v Balyasnikova, R.F.A. Ii, O.A. Kost, Simultaneous Determination of ACE Activity with 2 Substrates Provides Information on the Status of Somatic ACE and Allows Detection of Inhibitors in Human Blood, n.d.

[220] D.W. Cushman, H.S. Cheung, Spectrophotometric assay and properties of the angiotensin-converting enzyme of rabbit lung, Biochem Pharmacol. 20 (1971) 1637–1648. https://doi.org/https://doi.org/10.1016/0006-2952(71)90292-9.

[221] A. Dupont, C. Tokarski, O. Dekeyzer, A.L. Guihot, P. Amouyel, C. Rolando, F. Pinet, Two-dimensional maps and databases of the human macrophage proteome and secretome, Proteomics. 4 (2004) 1761–1778. https://doi.org/10.1002/pmic.200300691.

[222] D. Okwan-Duodu, V. Datta, X.Z. Shen, H.S. Goodridge, E.A. Bernstein, S. Fuchs, G.Y. Liu, K.E. Bernstein, Angiotensin-converting enzyme overexpression in mouse myelomonocytic cells augments resistance to Listeria and methicillin-resistant Staphylococcus aureus, Journal of Biological Chemistry. 285 (2010) 39051–39060. https://doi.org/10.1074/jbc.M110.163782.

[223] X.Z. Shen, H.D. Xiao, P. Li, C.X. Lin, S. Billet, D. Okwan-Duodu, J.W. Adams, E.A. Bernstein, Y. Xu, S. Fuchs, K.E. Bernstein, New insights into the role of angiotensin-converting enzyme obtained from the analysis of genetically modified mice, J Mol Med. 86 (2008) 679–684. https://doi.org/10.1007/s00109-008-0325-3.

[224] M.M.G.M. Thunnissen, B. Andersson, B. Samuelsson, C.H. Wong, J.Z. Haeggström, Crystal structures of leukotriene A4 hydrolase in complex with captopril and two competitive tight-binding inhibitors., The FASEB Journal : Official Publication of the Federation of American Societies for Experimental Biology. 16 (2002) 1648–1650. https://doi.org/10.1096/fj.01-1017fje.

[225] A. Tarkowski, H. Carlsten, H. Herlitz, G. Westberg, Differential effects of captopril and enalapril, two angiotensin converting enzyme inhibitors, on immune reactivity in experimental lupus disease, Agents Actions. 31 (1990) 96–101. https://doi.org/10.1007/BF02003227.

[226] M. Clapperton, J. McMurray, A. Fisher, H. Dargie, The effect of angiotensin-converting enzyme inhibitors on human neutrophil chemotaxis in vitro., Br J Clin Pharmacol. 38 (1994) 53–56. https://doi.org/10.1111/j.1365-2125.1994.tb04321.x.

[227] J. Miselis, T. Siminiak, H. Wysocki, Evidence for stimulation of neutrophil degranulation by selected angiotensin converting enzyme inhibitors in vitro, J

Hum Hypertens. 8 (1994) 565–569. http://europepmc.org/abstract/MED/7990082.

[228] V. Petrov, R. Fagard, P. Lijnen, Effect of protease inhibitors on angiotensin-converting enzyme activity in human T-lymphocytes, Am J Hypertens. 13 (2000) 535–539. https://doi.org/10.1016/s0895-7061(99)00236-8.

[229] M.F.R. Martin, F. Mckenna, H.A. Bird, K.E. Surrall, J.S. Dixon, V. Wright, Captopril: a New Treatment for Rheumatoid Arthritis?, The Lancet. 323 (1984) 1325–1328. https://doi.org/10.1016/S0140-6736(84)91821-X.

[230] K. Watanabe, K. Nishimura, M. Shiode, M. Sekiya, S. Ikeda, Y. Inoue, C. Iwanaga, Captopril, an angiotensin-converting enzyme inhibitor, induced pulmonary infiltration with eosinophilia, Internal Medicine. 35 (1996) 142–145. https://doi.org/10.2169/internalmedicine.35.142.

[231] J.F. Delfraissy, P. Galanaud, J.F. Balavoine, C. Wallon, J. Dormont, Captopril and immune regulation, Kidney Int. 25 (1984) 925–929. https://doi.org/10.1038/ki.1984.111.

[232] L. Orning, G. Krivi, G. Bild, J. Gierse, S. Aykent, F.A. Fitzpatrick, Inhibition of leukotriene A4 hydrolase/aminopeptidase by Captopril, Journal of Biological Chemistry. 266 (1991) 16507–16511. https://doi.org/10.1016/s0021-9258(18)55329-1.

[233] E.M. v de Cavanagh, F. Inserra, L. Leo´, L. Ferder, A. Cé, S.G. Fraga, Enalapril and captopril enhance glutathione-dependent antioxidant defenses in mouse tissues, 2000. http://www.ajpregu.org.

[234] C.S. Constantinescu, E. Ventura, B. Hilliard, A. Rostami, Effects of the angiotensin converting enzyme inhibitor captopril on experimental autoimmune encephalomyelitis, Immunopharmacol Immunotoxicol. 17 (1995) 471–491. https://doi.org/10.3109/08923979509016382.

[235] K. Shindo, J.R. Baker, D.A. Munafo, T.D. Bigby, Captopril inhibits neutrophil synthesis of leukotriene B4 in vitro and in vivo, The Journal of Immunology. 153 (1994) 5750–5759.

[236] S.I. Hii, D.L. Nicol, D.C. Gotley, L.C. Thompson, M.K. Green, J.R. Jonsson, Captopril inhibits tumour growth in a xenograft model of human renal cell carcinoma, Br J Cancer. 77 (1998) 880–883. https://doi.org/10.1038/bjc.1998.145.

[237] S.M. Danilov, E. Sadovnikova, N. Scharenborg, I. v Balyasnikova, D.A. Svinareva, E.L. Semikina, E.N. Parovichnikova, V.G. Savchenko, G.J. Adema, Angiotensin-converting enzyme (CD143) is abundantly expressed by dendritic cells and discriminates human monocyte-derived dendritic cells from acute myeloid leukemia-derived dendritic cells, 2003.

[238] K. Kohlstedt, C. Trouvain, D. Namgaladze, I. Fleming, Adipocyte-derived lipids increase angiotensin-converting enzyme (ACE) expression and modulate macrophage phenotype, Basic Res Cardiol. 106 (2011) 205–215. https://doi.org/10.1007/s00395-010-0137-9.

[239] J. Friedland, C. Setton, E. Silverstein, Induction of angiotensin converting enzyme in human monocytes in culture, Biochem Biophys Res Commun. 83 (1978) 843–849. https://doi.org/10.1016/0006-291X(78)91471-7.

[240] M.S. Rohrbach, Metabolism and subcellular localization of angiotensin converting enzyme in cultured human monocytes, Biochem Biophys Res Commun. 124 (1984) 843–849. https://doi.org/10.1016/0006-291X(84)91034-9.

[241] M. Ohishi, M. Ueda, H. Rakugi, T. Naruko, A. Kojima, A. Okamura, J. Higaki, T. Ogihara, Enhanced expression of angiotensin-converting enzyme is associated with progression of coronary atherosclerosis in humans, J Hypertens. 15 (1997) 1295–1302. https://doi.org/10.1097/00004872-199715110-00014.

[242] F. Diet, R.E. Pratt, G.J. Berry, N. Momose, G.H. Gibbons, V.J. Dzau, Increased Accumulation of Tissue ACE in Human Atherosclerotic Coronary Artery Disease, Circulation. 94 (1996) 2756–2767. https://doi.org/10.1161/01.CIR.94.11.2756.

[243] V.F. Lazarev, I. v. Guzhova, B.A. Margulis, Glyceraldehyde-3-phosphate dehydrogenase is a multifaceted therapeutic target, Pharmaceutics. 12 (2020). https://doi.org/10.3390/pharmaceutics12050416.

[244] P. Andersson, J. Bratt, M. Heimbürger, T. Cederholm, J. Palmblad, Inhibition of neutrophil-dependent cytotoxicity for human endothelial cells by ACE inhibitors, Scand J Immunol. 80 (2014) 339–345. https://doi.org/10.1111/sji.12218.

[245] M. Hernandez-Quiles, M.F. Broekema, E. Kalkhoven, PPARgamma in Metabolism, Immunity, and Cancer: Unified and Diverse Mechanisms of Action, Front Endocrinol (Lausanne). 12 (2021). https://doi.org/10.3389/fendo.2021.624112.

[246] A. v. Ferreira, V.A.C.M. Koeken, V. Matzaraki, S. Kostidis, J.C. Alarcon-Barrera, L.C.J. de Bree, S.J.C.F.M. Moorlag, V.P. Mourits, B. Novakovic, M.A. Giera, M.G. Netea, J. Domínguez-Andrés, Glutathione metabolism contributes to the induction of trained immunity, Cells. 10 (2021). https://doi.org/10.3390/cells10050971.

[247] H. Gmünder, H.-P. Eck, B. Benninghoff, S. Roth, W. Dröge, Macrophages regulate intracellular glutathione levels of lymphocytes. Evidence for an immunoregulatory role of cysteine, Cell Immunol. 129 (1990) 32–46. https://doi.org/10.1016/0008-8749(90)90184-S.

[248] M.A. Rabbani, M.S. Mahmood, S.F. Mekan, P.M. Frossard, Association of angiotensin-converting enzyme gene dimorphisms with severity of lupus disease., Saudi J Kidney Dis Transpl. 19 (2008) 761–766.

[249] A. Parsa, E. Peden, R.F. Lum, V.A. Seligman, J.L. Olson, H. Li, M.F. Seldin, L.A. Criswell, Association of angiotensin-converting enzyme polymorphisms with systemic lupus erythematosus and nephritis: analysis of 644 SLE families., Genes Immun. 3 Suppl 1 (2002) S42-6. https://doi.org/10.1038/sj.gene.6363907.

[250] J.T. Noe, R.A. Mitchell, Tricarboxylic acid cycle metabolites in the control of macrophage activation and effector phenotypes, J Leukoc Biol. 106 (2019) 359–367. https://doi.org/10.1002/JLB.3RU1218-496R.

[251] L.A.J. O'Neill, A Broken Krebs Cycle in Macrophages, Immunity. 42 (2015) 393–394. https://doi.org/10.1016/j.immuni.2015.02.017.

[252] M. Akram, Citric Acid Cycle and Role of its Intermediates in Metabolism, Cell Biochem Biophys. 68 (2014) 475–478. https://doi.org/10.1007/s12013-013-9750-1.

[253] E.J. Tisdale, Glyceraldehyde-3-phosphate Dehydrogenase Is Phosphorylated by Protein Kinase Cι/λ and Plays a Role in Microtubule Dynamics in the Early Secretory Pathway, Journal of Biological Chemistry. 277 (2002) 3334–3341. https://doi.org/10.1074/jbc.M109744200.

[254] E.J. Tisdale, Glyceraldehyde-3-phosphate Dehydrogenase Is Phosphorylated by Protein Kinase Cι/λ and Plays a Role in Microtubule Dynamics in the Early Secretory Pathway, Journal of Biological Chemistry. 277 (2002) 3334–3341. https://doi.org/10.1074/jbc.M109744200.

[255] E.J. Tisdale, Glyceraldehyde-3-phosphate Dehydrogenase Is Required for Vesicular Transport in the Early Secretory Pathway, Journal of Biological Chemistry. 276 (2001) 2480–2486. https://doi.org/10.1074/jbc.M007567200.

[256] E.J. Tisdale, N.K. Talati, C.R. Artalejo, A. Shisheva, GAPDH binds Akt to facilitate cargo transport in the early secretory pathway, Exp Cell Res. 349 (2016) 310–319. https://doi.org/10.1016/j.yexcr.2016.10.025.

[257] Z. Khan, X.Z. Shen, E.A. Bernstein, J.F. Giani, M. Eriguchi, T. v. Zhao, R.A. Gonzalez-Villalobos, S. Fuchs, G.Y. Liu, K.E. Bernstein, Angiotensin-converting enzyme enhances the oxidative response and bactericidal activity of neutrophils, Blood. 130 (2017) 328–339. https://doi.org/10.1182/blood-2016-11-752006.

[258] C.S. Constantinescu, D.B.P. Goodman, E.S. Ventura, Captopril and lisinopril suppress production of interleukin-12 by human peripheral blood mononuclear

cells, Immunol Lett. 62 (1998) 25–31. https://doi.org/10.1016/S0165-2478(98)00025-X.

[259] D.A.A. Vignali, V.K. Kuchroo, IL-12 family cytokines: immunological playmakers, Nat Immunol. 13 (2012) 722–728. https://doi.org/10.1038/ni.2366.

[260] S.E. Dorman, S.M. Holland, Interferon-g and interleukin-12 pathway defects and human disease, n.d. www.elsevier.com/locate/cytogfr.

[261] X. Ma, W. Yan, H. Zheng, Q. Du, L. Zhang, Y. Ban, N. Li, F. Wei, Regulation of IL-10 and IL-12 production and function in macrophages and dendritic cells, F1000Res. 4 (2015) 1–13. https://doi.org/10.12688/f1000research.7010.1.

[262] D. Baitsch, H.H. Bock, T. Engel, R. Telgmann, C. Müller-Tidow, G. Varga, M. Bot, J. Herz, H. Robenek, A. von Eckardstein, J.R. Nofer, Apolipoprotein e induces antiinflammatory phenotype in macrophages, Arterioscler Thromb Vasc Biol. 31 (2011) 1160–1168. https://doi.org/10.1161/ATVBAHA.111.222745.

[263] L. Bouchareychas, R.L. Raffai, Apolipoprotein E and atherosclerosis: From lipoprotein metabolism to MicroRNA control of inflammation, J Cardiovasc Dev Dis. 5 (2018). https://doi.org/10.3390/jcdd5020030.

[264] O. Combarros, E. Rodríguez-Rodríguez, I. Mateo, J.L. Vázquez-Higuera, J. Infante, J. Berciano, P. Sánchez-Juan, APOE dependent-association of PPAR-γ genetic variants with Alzheimer's disease risk, Neurobiol Aging. 32 (2011) 547.e1-547.e6. https://doi.org/10.1016/j.neurobiolaging.2009.07.004.

[265] R. Fogari, A. Zoppi, L. Corradi, P. Lazzari, A. Mugellini, P. Lusardi, Comparative effects of lisinopril and losartan on insulin sensitivity in the treatment of non diabetic hypertensive patients, Br J Clin Pharmacol. 46 (1998) 467–471. https://doi.org/10.1046/j.1365-2125.1998.00811.x.

[266] R. Fogari, A. Zoppi, P. Lazzari, P. Preti, A. Mugellini, L. Corradi, P. Lusardi, ACE Inhibition But Not Angiotensin II Antagonism Reduces Plasma Fibrinogen and Insulin Resistance in Overweight Hypertensive Patients, J Cardiovasc Pharmacol. 32 (1998) 616–620. https://doi.org/10.1097/00005344-199810000-00014.

[267] H.A. Pershadsingh, T.W. Kurtz, Insulin-Sensitizing Effects of Telmisartan, Diabetes Care. 27 (2004) 1015–1015. https://doi.org/10.2337/diacare.27.4.1015.

[268] A.J. Scheen, N. Paquot, PPAR-gamma receptors, new therapeutic target in metabolic and cardiovascular diseases., Rev Med Liege. 60 (2005) 89–95.

[269] M. Schupp, J. Janke, R. Clasen, T. Unger, U. Kintscher, Angiotensin Type 1 Receptor Blockers Induce Peroxisome Proliferator–Activated Receptor-γ Activity, Circulation. 109 (2004) 2054–2057. https://doi.org/10.1161/01.CIR.0000127955.36250.65.

[270] A. Storka, E. Vojtassakova, M. Mueller, S. Kapiotis, D.G. Haider, A. Jungbauer, M. Wolzt, Angiotensin inhibition stimulates PPARγ and the release of visfatin, Eur J Clin Invest. 38 (2008) 820–826. https://doi.org/10.1111/j.1365-2362.2008.02025.x.

[271] W.F. Reynolds, A.P. Kumar, F.J. Piedrafita, The human myeloperoxidase gene is regulated by LXR and PPARα ligands, Biochem Biophys Res Commun. 349 (2006) 846–854. https://doi.org/10.1016/j.bbrc.2006.08.119.

[272] G. Wu, J.R. Lupton, N.D. Turner, Y.-Z. Fang, S. Yang, Glutathione Metabolism and Its Implications for Health, J Nutr. 134 (2004) 489–492. https://doi.org/10.1093/jn/134.3.489.

[273] Z. Basi, V. Turkoglu, In vitro effect of oxidized and reduced glutathione peptides on angiotensin converting enzyme purified from human plasma, Journal of Chromatography B. 1104 (2019) 190–195. https://doi.org/10.1016/j.jchromb.2018.11.023.

[274] C.C. Winterbourn, A.J. Kettle, M.B. Hampton, Reactive Oxygen Species and Neutrophil Function, Annu Rev Biochem. 85 (2016) 765–792. https://doi.org/10.1146/annurev-biochem-060815-014442.

[275] S. Bedouhène, P.M.-C. Dang, M. Hurtado-Nedelec, J. El-Benna, Neutrophil Degranulation of Azurophil and Specific Granules, in: 2020: pp. 215–222. https://doi.org/10.1007/978-1-0716-0154-9_16.

[276] H. Wysocki, T. Siminiak, D. Zozulińska, B. Wierusz-Wysocka, Evaluation of the effect of oral enalapril on neutrophil functions: comparison with the in vitro effect of enalapril and enalaprilat., Pol J Pharmacol. 47 (1995) 53–58.

[277] S. Rørvig, O. Østergaard, N.H.H. Heegaard, N. Borregaard, Proteome profiling of human neutrophil granule subsets, secretory vesicles, and cell membrane: correlation with transcriptome profiling of neutrophil precursors, J Leukoc Biol. 94 (2013) 711–721. https://doi.org/10.1189/jlb.1212619.

[278] A.R. Mantegazza, J.G. Magalhaes, S. Amigorena, M.S. Marks, Presentation of Phagocytosed Antigens by MHC Class I and II, Traffic. 14 (2013) 135–152. https://doi.org/10.1111/tra.12026.

[279] C.N. Hall, C. Reynell, B. Gesslein, N.B. Hamilton, A. Mishra, B.A. Sutherland, F.M. Oâ Farrell, A.M. Buchan, M. Lauritzen, D. Attwell, Capillary pericytes regulate cerebral blood flow in health and disease, Nature. 508 (2014) 55–60. https://doi.org/10.1038/nature13165.

[280] M. Yemisci, Y. Gursoy-Ozdemir, A. Vural, A. Can, K. Topalkara, T. Dalkara, Pericyte contraction induced by oxidative-nitrative stress impairs capillary reflow despite successful opening of an occluded cerebral artery, Nat Med. 15 (2009) 1031–1037. https://doi.org/10.1038/nm.2022.

[281] I. Pushkarsky, P. Tseng, D. Black, B. France, L. Warfe, C.J. Koziol-White, W.F. Jester, R.K. Trinh, J. Lin, P.O. Scumpia, S.L. Morrison, R.A. Panettieri, R. Damoiseaux, D. di Carlo, Elastomeric sensor surfaces for high-Throughput single-cell force cytometry, Nat Biomed Eng. 2 (2018) 124–137. https://doi.org/10.1038/s41551-018-0193-2.

[282] S. Gordon, Phagocytosis: An Immunobiologic Process, Immunity. 44 (2016) 463–475. https://doi.org/10.1016/j.immuni.2016.02.026.

[283] A. Aderem, D.M. Underhill, Mechanisms of phagocytosis in macrophages, Annu Rev Immunol. 17 (1999) 593–623. https://doi.org/10.1146/annurev.immunol.17.1.593.

[284] D.M. Richards, R.G. Endres, How cells engulf: A review of theoretical approaches to phagocytosis, Reports on Progress in Physics. 80 (2017). https://doi.org/10.1088/1361-6633/aa8730.

[285] S. Lukácsi, Z. Farkas, É. Saskői, Z. Bajtay, K. Takács-Vellai, Conserved and distinct elements of phagocytosis in human and c. Elegans, Int J Mol Sci. 22 (2021). https://doi.org/10.3390/ijms22168934.

[286] E. Uribe-Querol, C. Rosales, Phagocytosis: Our Current Understanding of a Universal Biological Process, Front Immunol. 11 (2020) 1–13. https://doi.org/10.3389/fimmu.2020.01066.

[287] R.D. Cummings, The mannose receptor ligands and the macrophage glycome, Curr Opin Struct Biol. 75 (2022) 102394. https://doi.org/10.1016/j.sbi.2022.102394.

[288] M.C. Slomianny, A. Dupont, F. Bouanou, O. Beseme, A.L. Guihot, P. Amouyel, J.C. Michalski, F. Pinet, Profiling of membrane proteins from human macrophages: Comparison of two approaches, Proteomics. 6 (2006) 2365–2375. https://doi.org/10.1002/pmic.200500546.

[289] M. Hoenigl, J. Pérez-Santiago, M. Nakazawa, M.F. de Oliveira, Y. Zhang, M.A. Finkelman, S. Letendre, D. Smith, S. Gianella, (1→3)-β-D-Glucan: A biomarker for microbial translocation in individuals with acute or early HIV infection?, Front Immunol. 7 (2016) 1–7. https://doi.org/10.3389/fimmu.2016.00404.

[290] D.M. Richards, R.G. Endres, The mechanism of phagocytosis: Two stages of engulfment, Biophys J. 107 (2014) 1542–1553. https://doi.org/10.1016/j.bpj.2014.07.070.

[291] L. Leclerc, D. Boudard, J. Pourchez, V. Forest, O. Sabido, V. Bin, S. Palle, P. Grosseau, D. Bernache, M. Cottier, Quantification of microsized fluorescent particles phagocytosis to a better knowledge of toxicity mechanisms, Inhal Toxicol. 22 (2010) 1091–1100. https://doi.org/10.3109/08958378.2010.522781.

[292] L. Thiele, H.P. Merkle, E. Walter, Phagocytosis and phagosomal fate of surface-modified microparticles in dendritic cells and macrophages, Pharm Res. 20 (2003) 221–228. https://doi.org/10.1023/A:1022271020390.

[293] M. Claudia, Ö. Kristin, O. Jennifer, R. Eva, F. Eleonore, Comparison of fluorescence-based methods to determine nanoparticle uptake by phagocytes and non-phagocytic cells in vitro, Toxicology. 378 (2017) 25–36. https://doi.org/10.1016/j.tox.2017.01.001.

[294] A.T. Nchinda, K. Chibale, P. Redelinghuys, E.D. Sturrock, Synthesis and molecular modeling of a lisinopril-tryptophan analogue inhibitor of angiotensin I-converting enzyme, Bioorg Med Chem Lett. 16 (2006) 4616–4619. https://doi.org/10.1016/j.bmcl.2006.06.004.

[295] W.S. Rasband, ImageJ, (1997).

[296] I. Pushkarsky, FLECS Technology for High-Throughput Single-Cell Force Biology and Screening, Assay Drug Dev Technol. 16 (2018) 7–11. https://doi.org/10.1089/adt.2017.825.

[297] M. Théry, M. Bornens, Cell shape and cell division., Curr Opin Cell Biol. 18 (2006) 648–657. https://doi.org/10.1016/j.ceb.2006.10.001.

[298] A.F. Savulescu, R. Brackin, E. Bouilhol, B. Dartigues, J.H. Warrell, M.R. Pimentel, S. Dallongeville, J. Schmoranzer, J.-C. Olivo-Marin, E.R. Gomes, M. Nikolski, M. Mhlanga, DypFISH: Dynamic Patterned FISH to Interrogate RNA and Protein Spatial and Temporal Subcellular Distribution, SSRN Electronic Journal. (2019). https://doi.org/10.2139/ssrn.3323373.

[299] A.F. Savulescu, C. Jacobs, Y. Negishi, L. Davignon, M.M. Mhlanga, Pinpointing Cell Identity in Time and Space, Front Mol Biosci. 7 (2020) 1–12. https://doi.org/10.3389/fmolb.2020.00209.

[300] M. Théry, Micropatterning as a tool to decipher cell morphogenesis and functions, J Cell Sci. 123 (2010) 4201–4213. https://doi.org/10.1242/jcs.075150.

[301] C.A. Schneider, W.S. Rasband, K.W. Eliceiri, NIH Image to ImageJ: 25 years of image analysis, Nat Methods. 9 (2012) 671–675. https://doi.org/10.1038/nmeth.2089.

[302] F. Wertek, C. Xu, Digital response in T cells: To be or not to be, Cell Res. 24 (2014) 265–266. https://doi.org/10.1038/cr.2014.5.

[303] S. Tay, J.J. Hughey, T.K. Lee, T. Lipniacki, S.R. Quake, M.W. Covert, Single-cell NF-B dynamics reveal digital activation and analogue information processing, Nature. 466 (2010) 267–271. https://doi.org/10.1038/nature09145.

[304] R.W. Bradley, B. Wang, Designer cell signal processing circuits for biotechnology, N Biotechnol. 32 (2015) 635–643. https://doi.org/10.1016/j.nbt.2014.12.009.

[305] M.G. Dorrington, I.D.C. Fraser, NF-κB signaling in macrophages: Dynamics, crosstalk, and signal integration, Front Immunol. 10 (2019). https://doi.org/10.3389/fimmu.2019.00705.

[306] N. Paterson, T. Lämmermann, Macrophage network dynamics depend on haptokinesis for optimal local surveillance., Elife. 11 (2022). https://doi.org/10.7554/eLife.75354.

[307] J. Huang, M. Brameshuber, X. Zeng, J. Xie, Q. jing Li, Y. hsiu Chien, S. Valitutti, M.M. Davis, A Single peptide-major histocompatibility complex ligand triggers digital cytokine secretion in CD4+ T Cells, Immunity. 39 (2013) 846–857. https://doi.org/10.1016/j.immuni.2013.08.036.

[308] T. Starr, T.J. Bauler, P. Malik-Kale, O. Steele-Mortimer, The phorbol 12-myristate-13-acetate differentiation protocol is critical to the interaction of THP-1 macrophages with Salmonella Typhimurium, PLoS One. 13 (2018) 1–13. https://doi.org/10.1371/journal.pone.0193601.

[309] S. Tedesco, F. de Majo, J. Kim, A. Trenti, L. Trevisi, G.P. Fadini, C. Bolego, P.W. Zandstra, A. Cignarella, L. Vitiello, Convenience versus biological significance: Are PMA-differentiated THP-1 cells a reliable substitute for blood-derived

macrophages when studying in vitro polarization?, Front Pharmacol. 9 (2018) 1–13. https://doi.org/10.3389/fphar.2018.00071.

[310] R. Trikha, D. Greig, B. V. Kelley, Z. Mamouei, T. Sekimura, N. Cevallos, T. Olson, A. Chaudry, C. Magyar, D. Leisman, A. Stavrakis, M.R. Yeaman, N.M. Bernthal, Inhibition of Angiotensin Converting Enzyme Impairs Anti-staphylococcal Immune Function in a Preclinical Model of Implant Infection, Front Immunol. 11 (2020) 1–14. https://doi.org/10.3389/fimmu.2020.01919.

[311] G. Vazeux, J. Cotton, P. Cuniasse, V. Dive, Potency and selectivity of RXP407 on human, rat, and mouse angiotensin-converting enzyme, Biochem Pharmacol. 61 (2001) 835–841. https://doi.org/10.1016/S0006-2952(01)00550-0.

[312] V. Dive, J. Cotton, A. Yiotakis, A. Michaud, S. Vassiliou, J. Jiracek, G. Vazeux, M.-T. Chauvet, P. Cuniasse, P. Corvol, RXP 407, a phosphinic peptide, is a potent inhibitor of angiotensin I converting enzyme able to differentiate between its two active sites, Proceedings of the National Academy of Sciences. 96 (1999) 4330–4335. https://doi.org/10.1073/pnas.96.8.4330.

[313] M.J. Maxwell, N. Srivastava, M.Y. Park, E. Tsantikos, R.W. Engelman, W.G. Kerr, M.L. Hibbs, SHIP-1 deficiency in the myeloid compartment is insufficient to induce myeloid expansion or chronic inflammation, Genes Immun. 15 (2014) 233–240. https://doi.org/10.1038/gene.2014.9.

[314] S.D. Pauls, A.J. Marshall, Regulation of immune cell signaling by SHIP1: A phosphatase, scaffold protein, and potential therapeutic target, Eur J Immunol. 47 (2017) 932–945. https://doi.org/10.1002/eji.201646795.

[315] K. Kohlstedt, C. Trouvain, D. Namgaladze, I. Fleming, Adipocyte-derived lipids increase angiotensin-converting enzyme (ACE) expression and modulate macrophage phenotype, Basic Res Cardiol. 106 (2011) 205–215. https://doi.org/10.1007/s00395-010-0137-9.

[316] X.Z. Shen, H.D. Xiao, P. Li, S. Billet, C.X. Lin, S. Fuchs, K.E. Bernstein, Tissue specific expression of angiotensin converting enzyme: a new way to study an

old friend., Int Immunopharmacol. 8 (2008) 171–6. https://doi.org/10.1016/j.intimp.2007.08.010.

[317] S.M. Danilov, S.I. Tovsky, D.E. Schwartz, R.O. Dull, ACE Phenotyping as a Guide Toward Personalized Therapy With ACE Inhibitors, J Cardiovasc Pharmacol Ther. 22 (2017) 374–386. https://doi.org/10.1177/1074248416686188.

[318] S.M. Danilov, O. V. Kurilova, V.E. Sinitsyn, A.A. Kamalov, J.G.N. Garcia, S.M. Dudek, Predictive potential of ACE phenotyping in extrapulmonary sarcoidosis, Respir Res. 23 (2022). https://doi.org/10.1186/s12931-022-02145-z.

[319] S.M. Danilov, R. Metzger, E. Klieser, K. Sotlar, I.N. Trakht, J.G.N. Garcia, Tissue ACE phenotyping in lung cancer., PLoS One. 14 (2019) e0226553. https://doi.org/10.1371/journal.pone.0226553.

8. Appendix

8.1. Bio-Rad Bradford Rapid Quantification Standard Curve

A standard curve was plotted to determine protein concentration of cell lysate and precipitated proteins.

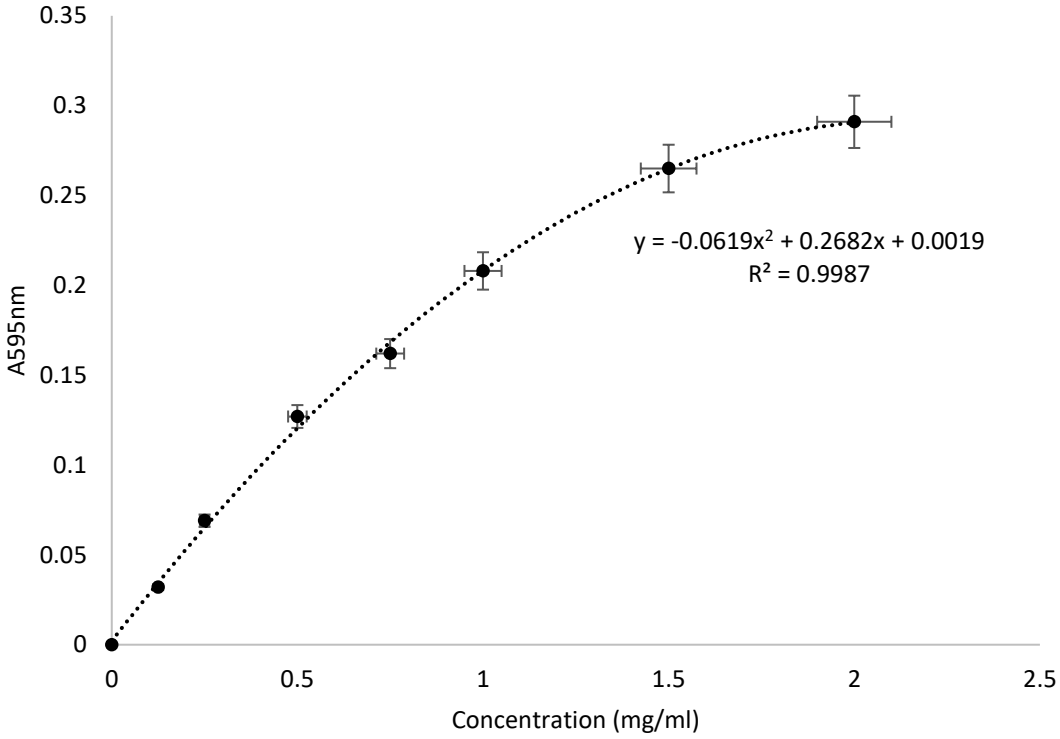

Figure 8.1: BSA Standard Curve used for mass spectrometry protein sample quantification. Curvilinear regression (second order polynomial) was used in the Bradford protein quantification assay ranging from 0 – 2.5 mg/ml BSA.

8.2. Mouse Proteomic & Phosphoproteomic Analysis

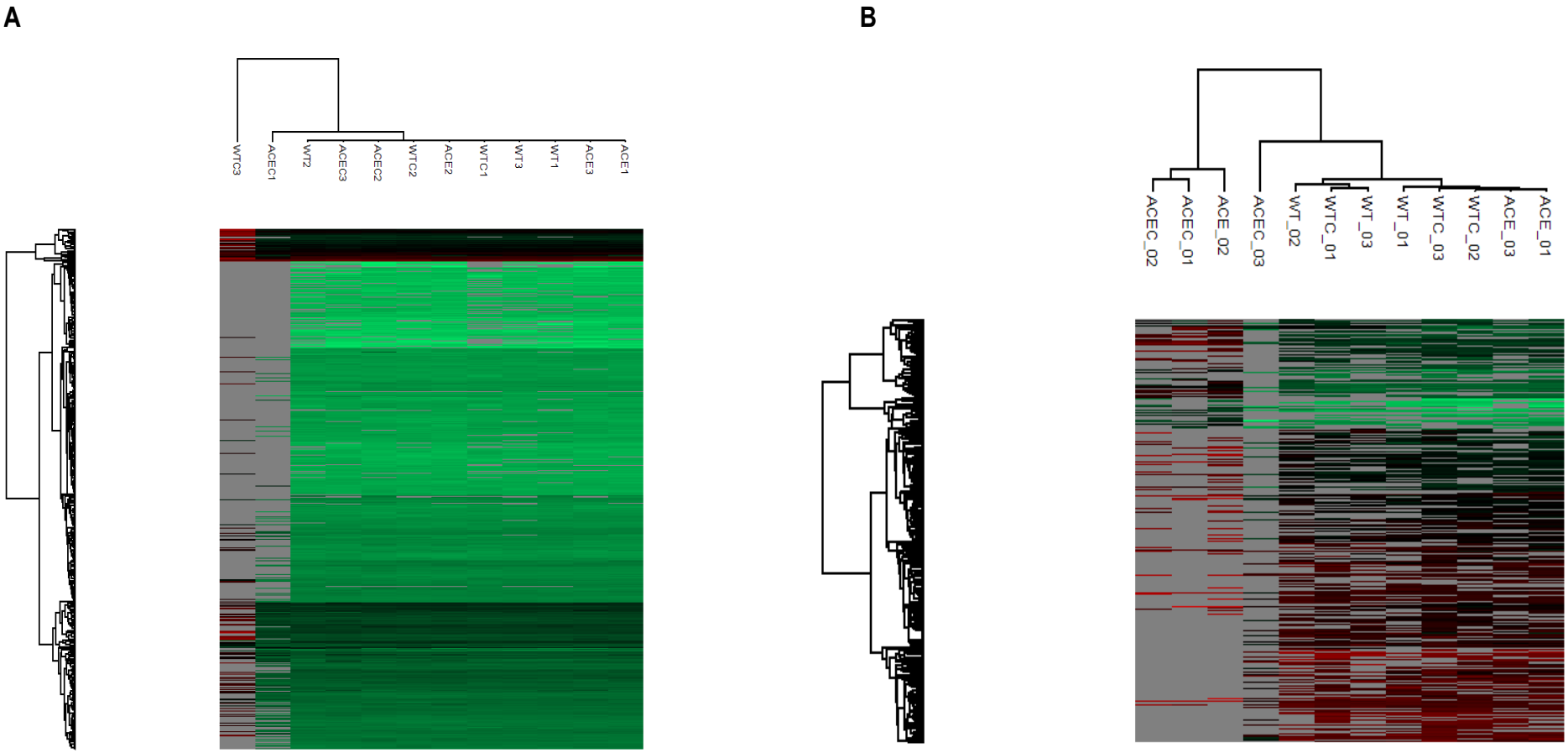

Figure 8.2: Hierarchical clustering analysis of (A) TTOF proteome and (B) QE phosphoproteome. Proteome samples WTC3 and ACEC1, and ACE_02 in the phosphoproteome were excluded from further analysis. The ACEC phosphoproteome group was retained.

Table 8.1: Identified PhosphoSitePlus (PSP) phosphorylation sites and their corresponding kinases within the differentially expressed phosphoproteins of ACE 10/10 and WT TPM lysates.

Protein	*Gene*	*PhosphoSitePlus window*	*PhosphoSitePlus kinase*	*PhosphoSitePlus kinase uniprot*	*Phospho (STY) Probabilities*
Prelamin-A/C;Lamin-A/C	Lmna	EEERLRLsPsPtsQR	CDK1	P06493	LRLS(1)PSPTSQR
DENN-domain-containing protein 4C	Dennd4c;Dennd4c	DSEDKLFsPVISRNL	ERK2	P63085	TSDSEDKLFS(1)PVISR
Cytoplasmic dynein 1 light intermediate chain 1	Dync1li1	VsPttPtsPtEGEAs	ERK2	P63085	KPASVSPTTPT(0.024)S(0.975)PT(0.001)EGEAS
Unconventional myosin-IXb	Myo9b;Myo9b	RATGAALtPTEERRI;RATGAALtPtEERRI	ERK2	P63085	ATGAALT(1)PTEER
Sorting nexin 2	Snx2	sPAVtPVtPttLIAP	ERK2	P63085	ELILSSEPSPAVTPVT(0.992)PT(0.006)T(0.002)LIAPR
Heterogeneous nuclear ribonucleoprotein H2	Hnrnph2	LKHtGPNsPDtANDG	ERK2;P38A	P63085;P47811	HTGPNS(1)PDTANDGFVR
Lymphocyte-specific protein 1	Lsp1	KLADRTEsLNRsIKK	MAPKAPK2	P49137	LADRT(0.002)ES(0.998)LNR
Rab11 family-interacting protein 5	Rab11fip5	LTHKRtysDEAsQLR	NDR1	Q91VJ4	TYS(1)DEASQLR
Phosphatidylinositol 3,4,5-trisphosphate 5-phosphatase 1	Inpp5d	PPsQPPLsPKKFsSS	PKA	P17612	GEGPPTPPSQPPLS(1)PK
		RLFDQQLsPGLRPRP	PKA	P17612	LFDQQLS(1)PGLRPR
Vimentin	Vim	GQVINEtsQHHDDLE	PLK1	P53350	DGQVINET(0.018)S(0.982)QHHDDLE

8.3. HL Standard Curve – ACE Activity Assay

An HL standard curve was plotted to determine ACE activity of cell lysate samples using the ZFHL assay.

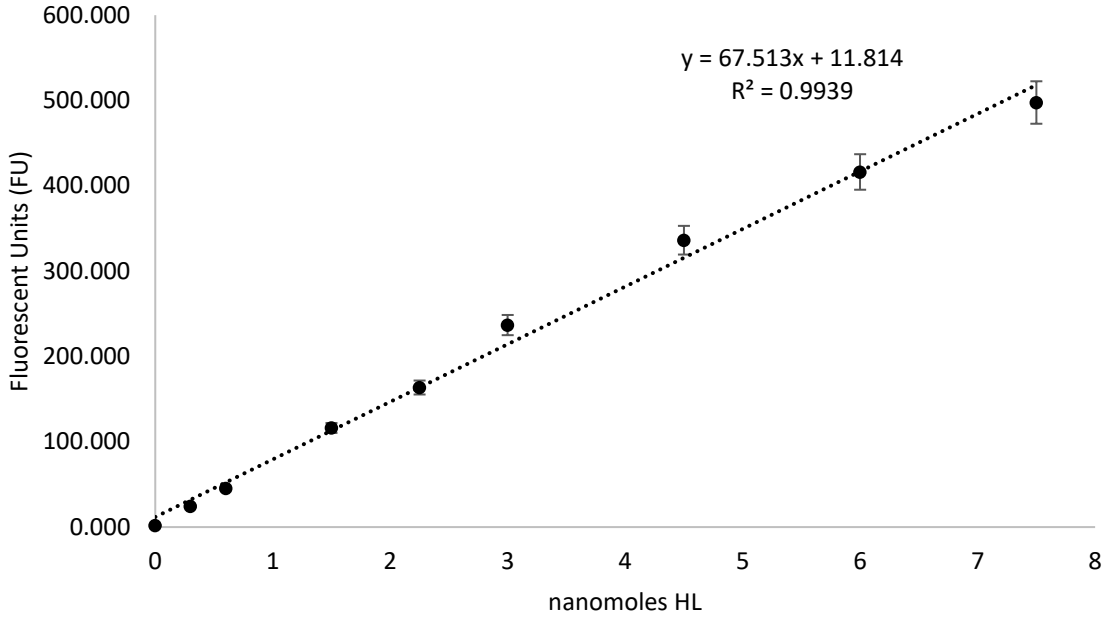

Figure 8.3: HL Standard Curve used to calculate ACE activity.

8.4. Triple-TOF SWATH-MS of Human ACE Overexpressing & WT THP-1 Macrophages

8.4.1. Hierarchical Clustering Output

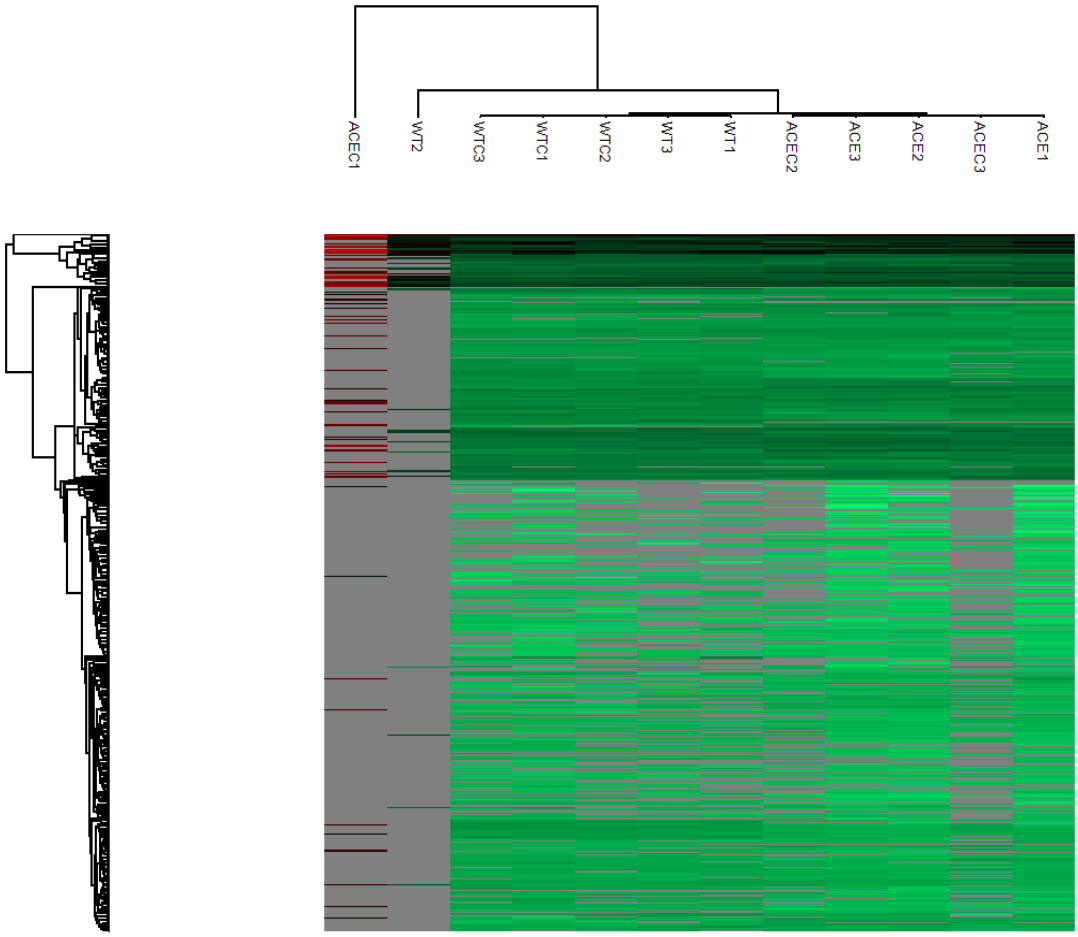

Figure 8.4: Hierarchical Euclidean clustering of human macrophage proteomic samples. ACEC1 and WT2 were excluded from analysis.

8.4.2. ACE Overexpression Confirmation

Western blot and ACE activity confirmation of ACE overexpression in ACE +/+ THP-1 macrophages.

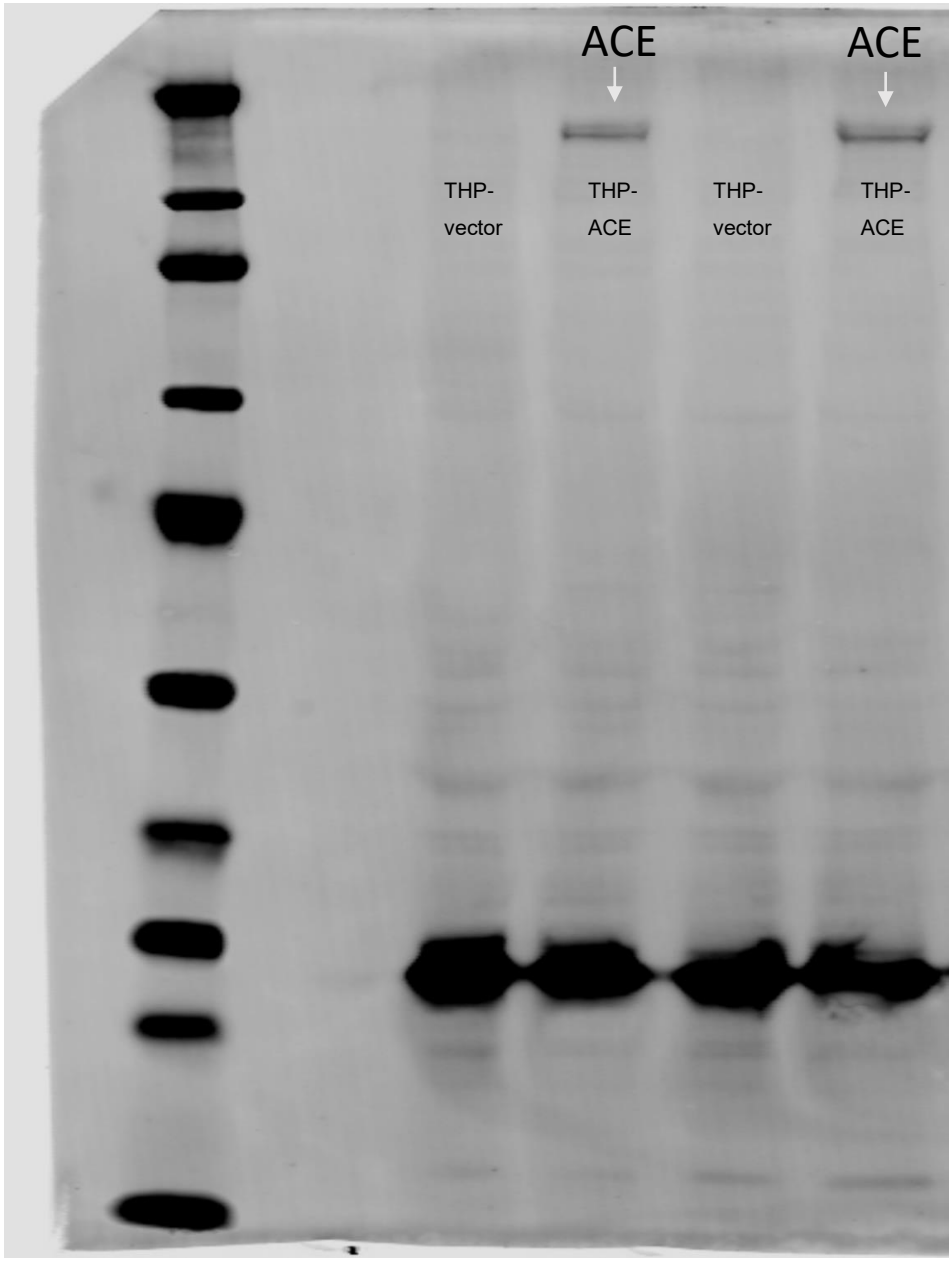

Figure 8.5: ACE overexpression in ACE +/+ THP-1 macrophages after PMA treatment and before cell lysate harvest. Increased ACE expression is recorded in ACE +/+ THP-1 macrophages as detected using polyclonal CD143/ACE antibody (R&D Systems). Western blot provided by Dr Duo-Yao Cao (Bernstein Lab, Cedar-Sinai, USA).

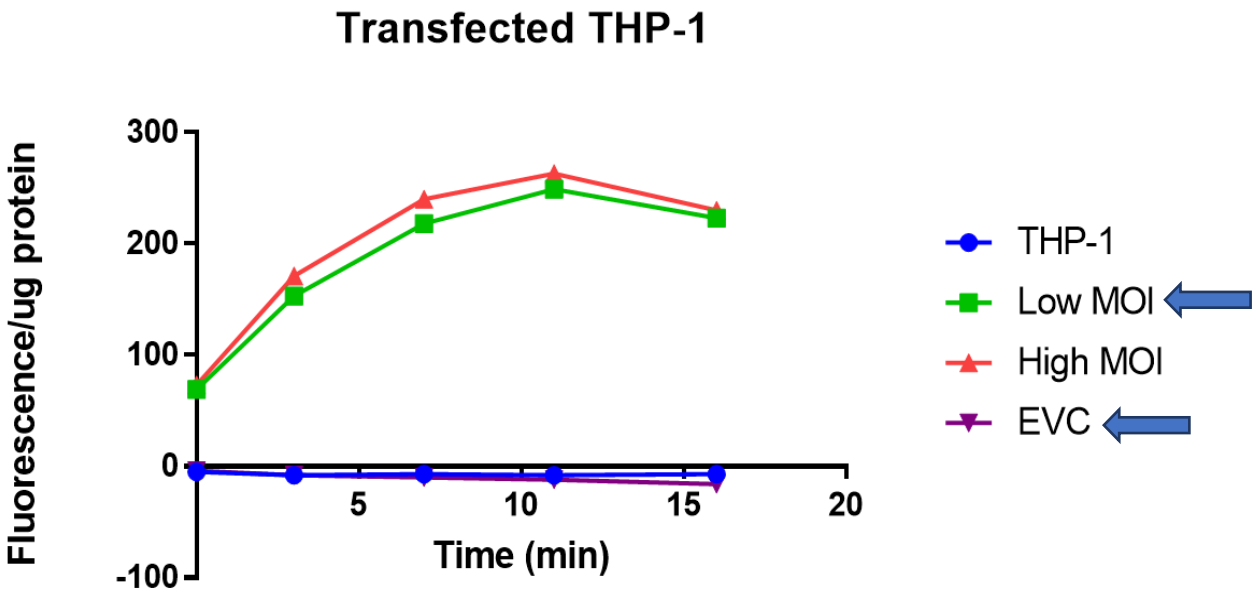

Figure 8.6: ACE activity results of monocytic state ACE +/+ THP-1 macrophages. Increased ACE activity was recorded in transfected ACE +/+ THP-1 microphages, denoted as either high or low MOI (red and green curves) whilst no activity was recorded in the empty vector control (EVC, purple curve) and WT THP-1 monocytic cell line (THP-1, blue curve). Provided by Dr Luciana Veiras (Bernstein lab, Cedar-Sinai, USA).